1

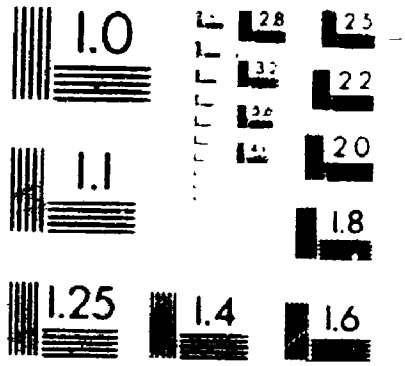

MicroD

STRATIGRAPHY, STRUCTURE AND METAMORPHISM OF THE NORTH FLANK OF THE MONASHEE COMPLEX, SOUTHEASTERN BRITISH COLUMBIA: A RECORD OF PROTEROZOIC EXTENSION AND PHANEROZOIC CRUSTAL THICKENING

by

ROBERT JOHN SCAMMELL, B.Sc.

A thesis submitted to the Faculty of
Graduate Studies and Research in partial fulfillment
of the requirements for the degree of
Master of Sciences, Department of Geology

Carleton University
Ottawa, Ontario

November, 1986

ISBN 0-315-35853-X

The undersigned hereby recommend to the Faculty of Graduate Studies and Research acceptance of the thesis "Stratigraphy, Structure and Metamorphism of the North Flank of the Monashee Complex, Southeastern British Columbia: A Record of Proterozoic Extension and Phanerozoic Crustal Thickening" submitted by Robert John Scammell, B.Sc., in partial fulfillment of the requirements for the degree of Master of Sciences

Thesis Supervisor

Chairman, Department of Geology

Carleton University

November 20, 1986

ABSTRACT

The Monashee complex affords a rare view of a Late Proterozoic rift sequence in the Cordillera. Mantling gneisses, which lie unconformably on Early Proterozoic core gneisses, are interpreted to have been deposited on continental crust that initially experienced broad, relatively stable subsidence, and was later affected by the Monashee Extensional Disturbance. Throughout most of the complex, this syndepositional disturbance is first marked by a laterally extensive (>100 km) stratiform pyroclastic carbonatite believed to be part of an episodic (long-lived?) alkaline event. The alkaline nature and timing of this event (U-Pb zircon, 746 +40, -39 Ma) make it unique in the Cordillera. It is later characterized at the north end of the complex by immature siliciclastic sediments intercalated with ultramafic and mafic sills and flows, plus minor felsic pyroclastic deposits. This evolution is characteristic of passive asymmetric rifting, and suggests mechanisms similar to those operative in the Phanerozoic. Extension recorded by the mantling gneisses is believed to be a regional component of broad protracted Late Proterozoic rifting that culminated with deposition of deep water Windermere Supergroup clastic sediments.

An erosional window through the Selkirk allochthon exposes the complex and its tectonic boundary, the Monashee decollement. This boundary is marked at the north end of the complex by a melt-softened detachment which truncates lower-plate stratigraphy and structures, and records high-pressure, east-verging overthrusting. Formation of mylonitic rocks and melt-softened shears, in both plates and along the detachment, are major mechanisms by which shear strain was accommodated. Lower-plate rock geometry at this location is controlled by three sets of folds: (i) pre- to early metamorphic, overturned, south-southeast-verging, km-scale folds (Sibley Creek Syncline-Anticline pair) which control map-scale (1:15000) geometry, (ii) overprinting syn-metamorphic, east-verging drag folds and reclined, tight to isoclinal, generally north-verging buckle folds with fold axes sub-parallel to a penetrative west-trending mineral stretching lineation, and (iii) rare weakly developed, post-metamorphic, west-trending upright warps. Brittle deformation has played a minor role. Recognized upper-plate folds are similar in style to phase II lower-plate folds. Fold mechanisms and microfabrics are consistent with high-grade ductile deformation. Metastable pelitic mineral assemblages record two distinct syn-kinematic metamorphic episodes: M1-parageneses indicate high-temperature (640-679°C), high-pressure (6.4-7.1 kb), minimum peak physical conditions which locally outlasted shearing; later syn-kinematic M2-parageneses define an inverted metamorphic gradient generated during a low-pressure (2.0-3.4 kb), high-temperature (615-678°C) event believed to be related to later thrusting along a splay in the Monashee decollement outside the map area to the northwest. These thermo-structural observations and inferences are most compatible with a previously proposed model of compression-induced, (Mesozoic) crustal imbrication, and subsequent (Cenozoic) uplift and unroofing.

ACKNOWLEDGEMENTS

Financial support for this study was provided by the Natural Sciences and Engineering Council of Canada in the form of operating grant A2693 to R.L. Brown, and a post-graduate scholarship to the author. I would like to thank G. Skippen and V. Trommsdorf for their thoughts on the metamorphic aspects of this thesis, and K. Bell, T. Hoy and J. Pell for informative discussions concerning carbonatites. T. Hoy is thanked for providing a draft of an in prep. paper. R. Taylor prepared thin sections, J. Stevenson provided XRF analyses and R. Conlon performed XRD analyses. D. Bethune, D. Murphy and C. Rees are thanked for their most capable assistance in the field. A. MacKean is thanked for typing and proof-reading parts of the manuscript. Invaluable insights were provided by Cordilleran co-workers: M. Bardoux, S. Carr, L. Lane, D. Murphy, C. Rees and C. Roots. I gratefully acknowledge R. Parrish for stimulating discussions and providing unpublished radiometric dates. I extend my gratitude to R. L. Brown for suggesting the topic, and providing patient supervision. Many thanks to M. Journeay for enlightening discussions, and providing a guiding light in the form of an early draft of his Ph. D. thesis. Last, but certainly not least, I extend very special thanks to D. MacKean (whose name should be on this thesis) for her endless support.

TABLE OF CONTENTS

LIST OF FIGURES

LIST OF TABLES

LIST OF PHOTOGRAPHIC PLATES

LIST OF APPENDICES

INTRODUCTION

1.1 PREAMBLE

Metamorphic core complexes of the North American Cordillera (Crittenden et al. 1978, 1980; Coney 1979, 1980; Davis & Coney, 1979; Armstrong, 1982) are elongate structural domes composed of uplifted metamorphic rocks. These domes, lying in a narrow winding belt extending from southern British Columbia to northwestern Mexico, are significant in their potential to provide information regarding tectonic processes operative during the entire evolution of the orogen. Their uniqueness lies in an inherent capacity to provide information concerning relatively older, deeper level tectonic processes; information not readily accessible outside the complexes. Multiple deformation and polymetamorphism are basic traits reflecting the complexity of these tectonic processes, and are the source of considerable controversy centering on their age and tectonic significance (cf. Davis & Coney, 1979, 1980; Coney, 1980; DeWitt, 1980; Brown & Read, 1983; Coney & Harms, 1984; Price, 1985). Based on data collected at the north end of the Monashee complex (Fig. 1, Plate 1A) this thesis examines: (1) characteristics of Proterozoic extension, and their implications for the early evolution of the western North American continent-ocean interface, and (2) the effects of Phanerozoic crustal thickening, and their implications for Mesozoic-Cenozoic tectonic models.

1.2 REGIONAL GEOLOGIC SETTING

The Monashee Complex is one of several core complexes that lie within the Omenica Belt (inset Fig. 1), a major structural and metamorphic zone

that straddles the paleocontinental margin of North America and allochthonous terranes that were accreted during Early Jurassic to mid-Cretaceous time (Monger, 1977; Mongér & Price 1979, 1981; Monger et al. 1982). The complex, exposed through a window in the Selkirk Allochthon, is interpreted to be an antiformal duplex of basement cored horses bounded above by the Monashee decollement, a westerly rooted, mylonitic roof thrust (Brown 1980, 1981; Read & Brown 1981; Brown & Read 1983; Journeay 1983, 1985, 1986; Journeay & Brown 1985; Monger et al. 1985; Brown et al. 1986).

Wheeler (1965) first recognized broad mappable lithostratigraphic units in the vicinity of Frenchman Cap dome. Continued detailed investigations have corroborated, refined and extended these subdivisions south to Thor-Odin dome (Fyles, 1970a, b; Reesor, 1970; Reesor & Moore, 1971; McMillan, 1970, 1973; Hoy, 1979, 1980, 1982a; Hoy & McMillan, 1979; Wanless & Reesor, 1975; Psutka, 1978; Brown & Psutka, 1979; Brown, 1980, 1981; Hoy & Brown, 1981; Read 1979a, b, 1980; Read & Klepaki, 1981; Parrish & Armstrong, 1983; Duncan, 1978; Scammell, 1985; Journeay, 1981, 1982, 1986). Tectono-stratigraphic assemblages within the complex comprise para- and granitic ortho-gneisses of the core (assumed to be of North American continental crust affinity), and an unconformably overlying mantling gneiss sequence composed of dominantly platform-like metasedimentary rocks, with minor intrusive and extrusive rocks.

Structures documented within the Monashee complex have been described briefly by Fyles (1970a), Brown and Psutka (1979), Brown (1980), Hoy (1979, 1980, 1982), Hoy and McMillan (1979), Read (1979a, b, 1980), Read and Klepaki (1981), Scammell (1985), and Brown et al. (1986). Detailed descriptions are given by Jones (1959), McMillan (1969, 1970, 1973), Reesor and Moore (1971), Fyles (1970b), Psutka (1978), Duncan (1984) and Journeay

(1981, 1986). A general sequence involving four phases of folding has emerged, with up to six phases interpreted at the south end of the complex (Duncan, 1984; questioned by Van Den Driessche, 1986).

The most prominent structures in the complex are large-scale (km-scale amplitudes and limb lengths), pre- to early metamorphic folds. These overturned isoclinal structures which are generally north-trending and east-verging, include the Sibley Creek Syncline, Kirbyville Anticline, Grace Mountain-Pingston Syncline and Hall Mountain Anticline (see Journeay, 1986). They are associated with low-angle thrust faults that predate the peak of regional metamorphism. An axial-planar foliation is locally preserved in their hinge zones. These folds are refolded by two types of synchronous syn-metamorphic structures. They are east-verging sheath folds and asymmetric, dcm- to 10 m-scale buckle folds which are commonly reclined about hinges sub-parallel to a penetrative east-west mineral stretching lineation, and axial surfaces which dip moderately to the west. All of these structures are overprinted by post-metamorphic north-trending, open upright to tight east-verging folds, and a weaker set of west-trending upright warps. A north-trending system of late normal faults, conjugate shear fractures and tension fractures, plus a northeast-trending set of tension fractures cut the above structures.

Within the Selkirk allochthon the earliest record of deformation is found in the Kootenay Arc where west-verging recumbent isoclinal folds and associated thrust faults predate a Devonian-Mississippian erosional unconformity (Read & Wheeler, 1976). To the east of the complex Brown and Tippett (1978) document isoclinal folds that pre-date the Middle Jurassic peak of regional metamorphism in the central and northern Selkirk Mountains. These folds are interpreted to be west-verging (Brown & Lane,

in prep.). Second phase, predominantly west-verging folds are pre- to syn-Middle Jurassic regional metamorphism, and form a structural fan in this region (Wheeler, 1965; Simony et al. 1980; Brown & Tippett, 1978; Tippett, 1976; Perkins, 1983). Both of these pre- to syn-metamorphic folds are overprinted by post-metamorphic east-verging folds. Approximately 25 km to the north of the complex a southwest-verging, pre- to early metamorphic recumbent fold with an overturned limb length in excess of 50 km has been mapped (Scrip Nappe; Simony et al. 1980; Raeside & Simony, 1983). Synmetamorphic, tight northeast-verging folds refold the nappe. Post-metamorphic northeast-verging buckle folds overprint these structures at this location.

The Monashee decollement is a fundamental regional tectonic boundary. It was initially mapped by Wheeler (1965) as a lithologic boundary marking the limit of a highly pegmatized zone. Subsequent studies (Brown & Psutka, 1978; Read, 1977, 1979a, b, 1980; Read & Brown, 1981; Brown, 1980, 1981; Brown & Murphy, 1982; Lane, 1984b, c; Scammell, 1985; Journeay, 1986) reveal it to be a mylonitic crustal-scale shear zone, which records easterly directed motion of the upper-plate. It forms the upper boundary of the Monashee complex, and truncates structures, isograds and lithostratigraphic units in both plates. Recent work by Journeay (1983, 1985, 1986) and Journeay & Brown (1986) shows that it records early high-pressure and later low-pressure displacements (designated MD1 and MD2 respectively).

Other major tectonic boundaries include (1) an east-dipping and rooting, mainly brittle normal fault, marked by the Columbia River fault zone (Read & Brown, 1981; Lane 1981, 1983, 1984a) which overprints the Monashee decollement on the east side of the complex between Upper Arrow

Lake and Hoskins Creek, and (2) the low-angle, west-dipping Eagle River detachment and related splays to the west of, and crosscutting the complex (Journeay & Brown, 1986).

Selkirk allochthon rocks have been the subject of numerous detailed metamorphic studies (see Read & Brown, Fig. 6, 1981, for a summary). In a region 100 to 200 km north and east of the map area several detailed studies completed at Carleton University and the University of Calgary (e.g. Leatherbarrow, 1981; Raeside, 1982; Simony et al. 1980; see selected bibliography) document Barrovian-type mineral assemblages, and an increase in grade towards a metamorphic culmination in the vicinity of Adams River. High-pressure assemblage zones can be traced across the Columbia River south of Mica Dam, and are truncated at the base of the allochthon by the Monashee Decollement. On the west side of the complex melt phases form large composite plutons (Wheeler, 1965; Journeay & Brown, pers. comm. 1985).

Detailed metamorphic studies within the Monashee complex are few (McMillan, 1973; Reesor & Moore, 1971; Psutka, 1978; Journeay, 1983, 1985, 1986). Of these, Journeay (1986) has provided the most comprehensive study based on observations in the northern west-central part of the complex (south of the map area). At this location metastable pelitic mineral assemblages record two distinct syn-kinematic metamorphic episodes. The first (M1) is characterized by a high-pressure sequence of Barrovian-type assemblage zones that range from lower granulite facies within the core of the dome, to middle-amphibolite facies along the flanks, and are synchronous with second-phase folding. The second (M2) is a low-pressure event that defines an inverted, Buchan-type sequence of assemblage zones that range from upper-amphibolite facies in the upper carapace to greenschist in the

core of the dome, and are coeval with third-phase folding.

1.3 GEOCHRONOLOGY

Six sets of ages are critical to the construction of comprehensive tectonic models. These comprise the ages of the protoliths of rocks within the complex, metamorphic events, displacive events along the Monashee decollement, uplift, cooling, and unroofing. Constraints on these six sets of ages are summarized below.

Past speculations on the ages of rocks which comprise the Monashee complex span a range from pre-Beltian to Paleozoic (see Okulitch, 1984, and Journeay, 1986 for reviews). Constraints are now provided by radiometric studies: core gneisses, which unconformably underlie mantling gneisses, range from ca. 2.8 to 1.96 Ga (2.8 +/-0.2 Ga Rb-Sr whole rock date on paragneisses, Duncan, 1978; U-Pb zircon dates on orthogneisses intruding paragneisses, 2.0-2.1 Ga Parrish & Armstrong, 1983, and 1960 +35, -45 Ma Wanless & Reesor, 1975). Nepheline syenite intrusions (near Mount Copeland) which crosscut basement and part of the autochthonous mantling gneiss sequence have a preliminary date of ca. 773 Ma (+280, -218 Ma, U-Pb zircon Okulitch et al. 1981). Recent U-Pb zircon data from the same body yields a date of 746 +40, -39 Ma (Parrish, unpublished data 1986). This date is based on zircons hand picked by the author. The zircon population consisted of several varieties including clouded (interpreted to be of magmatic origin), clear (interpreted to be of metamorphic origin), and varieties with clouded cores and clear rims. Graphical representation of their analyses results in a discordia line. Parrish (pers. comm. 1986) interprets the upper intercept to be the age of the clouded zircons (i.e. the age of emplacement of the syenite; 746 +40, -39 Ma), and the lower

intercept to be the age (60 +/-2 Ma) of the clear zircon. Lead-loss is not thought to have occurred. Hence the age of mantling gneisses intruded by nepheline syenite must be between ca. 2100 and 750 Ma, and those overlying could be younger. The tectonic significance of the ca. 60 Ma age for the metamorphic zircons presently remains unknown.

The absolute ages of metamorphic and deformational events within the Monashee complex are currently unknown. High-pressure assemblage zones and isograds within the Selkirk allochthon are interpreted to have quenched in the Middle Jurassic based on geochronometry of crosscutting igneous bodies (e.g. 180-160 Ma, Armstrong, 1982; K-Ar and U-Pb zircon 166-156 Ma Archibald et al. 1983; U-Pb zircon 173 +4, +5 Ma, Parrish & Wheeler, 1983; U-Pb zircon 165 +/-4 Ma, Shaw, 1980). At the southeast corner of the Monashee complex the Monashee decollement is crosscut by the Galena Bay stock which yields a Rb-Sr whole-rock isochron of 157, +/-2 Ma (Armstrong, 1981, quoted as pers. comm. in Brown & Read, 1983). Journeay and Brown (1986) use the above data, plus the inference that high-pressure M1 assemblage zones crosscut MD1, to infer that M1 isograds within the complex were quenched between 157 and 155 Ma, and that early displacements along MD1 occurred between 165 and 155 Ma. A problem with this line of reasoning is the uncertainty regarding the relationship of the Galena Bay Stock to displacements on the Monashee decollement (Parrish, pers. comm. 1986). An argument which does not rely on the Galena Bay stock (Brown, pers. comm. 1986) is that syn-kinematic high-pressure and temperature M1 mineral assemblages that grew in the shear zone also grew in both plates of the Monashee decollement. These assemblages in the upper-plate were quenched by ca. 165 Ma. If one believes that this quenching was a result of ramping on the Monashee decollement then M1 mineral assemblages in the shear zone

must be at most 165 Ma old. The general time frame (Jurassic or younger) is most likely correct since the collision of allochthonous terranes from early Jurassic time onward (Monger et al. 1982) was most certainly accompanied by extensive crustal thickening and metamorphism.

Journeay (1986) suggests reactivation of the Monashee decollement along MD2 is no older than 80 to 95 Ma. This estimate is based on geochronometry of mid-Jurassic and mid-Cretaceous plutons, their levels of emplacement (Archibald et al. 1983), and inferred rates of uplift. The youngest age for the M2-MD2 event is constrained by conventional K-Ar mica cooling dates to between 40 and 60 Ma.

Arguments presented later in this thesis (section 3.2.5) constrain phase one folding to younger than 746 +40, -39 Ma, and older than the age of the early high-pressure M1 metamorphic peak.

Mafic dykes which intrude brittle extension fractures yield K-Ar mineral cooling dates of ca. 40 Ma (Wheeler, 1965; Lane, 1984b). This date provides an approximate minimum age for brittle deformation, and presumably approximates the age of final uplift, cooling and unroofing of the complex.

1.4 PREVIOUS WORK IN THE MAP AREA

Reconnaissance mapping by Wheeler (1965), Brown (1980) and Scammell (1985) comprises all previous work in the map area ~~at the~~ north end of the Monashee complex. Brown (1980) determined the area to be underlain by rocks of the Monashee complex, Selkirk allochthon, and intervening Monashee decollement. Brown (1980) documented the existence of the Sibley Creek Syncline, a major large-scale, overturned structure with a fold axis plunging moderately to the west-southwest, and an axial surface dipping to the northwest, away from the dome. The decollement at this location has

recently been interpreted by Journeay and Brown (1986) to be MD1, an early high-pressure zone of shear that was later overprinted by a low-pressure displacement designated MD2. Intervening arching resulted in their coincidence on the west side, and splays at the northwest and southwest corners of the complex (see Fig. 10.2 of Journeay & Brown, 1986). In this interpretation MD2 lies and dips to the northwest of the map area. Brown (1980) interprets rocks of the upper-plate to be of probable Horsethief Creek Group affinity.

1.5 STUDY OBJECTIVES

The aims of this study were:

(1) To determine the stratigraphic sequence; in particular the sequence of mantling gneisses, and attempt to determine their relationships within the complex, and tectonic significance regarding the Proterozoic evolution of the western North American continent-ocean interface.

(2) To investigate the effects of Phanerozoic crustal thickening; specifically the structural, kinematic and metamorphic evolutions of rocks at the north end of the Monashee complex, and their implications for thermotectonic models.

Data were collected during the snow-bound and relatively snow-free summers of 1984 and 1985 respectively (Fig. 2, in back pocket), and in the lab during the intervening time from fall 1984 to summer 1986. The following chapters summarize observations and interpretations relevant to the above objectives.

LITHOSTRATIGRAPHY: ITS RELATIONSHIP TO PROTEROZOIC RIFTING OF THE WESTERN NORTH AMERICAN MARGIN

2

2.1 INTRODUCTION

Direct evidence for early continental attenuation is generally deeply buried along passive margins, but can be found in rare exposures created through later orogenesis (Bott, 1982b; Bally, 1982). In the western Cordillera of North America, the Monashee complex (Fig. 1) is one of few such exposures revealing information that concerns the early evolution of late Proterozoic rifting which initiated and geometrically controlled miogeoclinal sedimentation.

This chapter has two goals. The first is to present new data collected from the mantling gneisses, an extensive, dominantly metasedimentary succession within the Monashee complex. These data are interpreted as evidence for a syndepositional tectonic disturbance initiated at ca. 750 Ma. The second aim of this chapter is to investigate the significance of mantling gneisses in terms of the paleo-environment. In order to achieve this, the above data are integrated with information gathered elsewhere within and outside the complex. Discussion centers on: (1) sedimentary environment, (2) evidence for syndepositional tectonic activity, encompassing synsedimentary, intrusive and extrusive, alkaline, mafic and felsic rocks, (3) broad-scale regional correlation based on the timing of this tectonic event, and (4) possible theoretical tectonic processes which can account for the features observed in and outside the complex.

2.2 LITHOSTRATIGRAPHY

At the north end of the Monashee Complex, a lithostratigraphic succession in the amphibolite-grade mantling gneisses has been established on the basis of typical associations, the local preponderance of certain rock types, observed facies relationships, and the presence of laterally persistent marker horizons. Twelve composite lithostratigraphic units have been delineated (Figs. 3 p. 109 & 4 in back pocket). Contacts are gradational, interlayered and abrupt, and are considered conformable. Attenuation of large-scale, early fold limbs (D1) has resulted in considerable thinning of the stratigraphy. Later buckle folding (D2), flattening and shearing have further thickened and thinned local sections; hence the original stratigraphic thickness is unknown. Estimated stratigraphic thicknesses were arrived at by assuming the dominance of flexural flow folding where thicknesses measured in the hinges of large-scale folds are nearest to original values. The geometry and exposure of units 1 to 5 (inclusive) allowed measurement only along the attenuated limbs of folds. Therefore thicknesses of these units, shown in Figure 3, are considered average minimums. These calculations render a total exposed thickness of slightly greater than 2 km. Correlation of lithostratigraphic units within the complex (Fig. 5), indicates that the north end of the Monashee Complex exposes rocks at a higher stratigraphic level than have been previously mapped (as noted by Read & Brown, 1981). Therefore the interpretation of this sequence is significant in that it contains data pertinent to the mantling gneisses but unexposed elsewhere in the complex. Brief descriptions and interpretations of all units mapped at the north end of the Monashee complex can be found in Figure 3, Plates 2 and 3, and in the following section.

2.2.1 MONASHEE COMPLEX

2.2.1.1 CORE GNEISSES

Unit 1

In the south part of the map area scattered sub-tree line exposures reveal a very coarse-grained kyanite-garnet-biotite-muscovite schist, structurally underlain by a thinly layered biotite-quartz-feldspar gneiss. These rocks are basement (Brown 1980), and considered correlative with undifferentiated paragneisses mapped to the south (Journeay, 1986; Hoy, 1979) and to the southeast (Psutka, 1978; Brown & Psutka, 1979).

2.2.1.2 MANTLING GNEISSES

Basement/Cover Contact

The basement/cover contact has not been observed by the writer. Exposures of this contact to the south of the map area display gradational, sharp and sheared relationships (Wheeler, 1965; McMillan, 1969; Fyles, 1970a, b; Hoy, 1979; Psutka, 1978). Journeay (1986) has interpreted this contact as an erosional unconformity.

Unit 2

This laterally persistant unit, informally known as the "basal quartzite", was observed in the south part of the map area where it is greater than 30 m thick. Metapelitic partings define a gross cm- to m-scale bedding which thickens towards the lowest exposure. These beds of meta-arenite are composed of cm-scale parallel laminated, well sorted quartzite with minor arkosic, subarkosic and micaceous layers.

Unit 3

The lower part of this 100 to 300 m thick unit is composed of coarse-grained, kyanite-garnet-biotite-muscovite-bearing pelitic and semipelitic (>50% mica) schists (ca. 70%), which are interbedded with quartzo-feldspathic gneisses (ca. 30%), and capped by a 2 to 3 m thick white quartzite which forms an excellent marker horizon. This is overlain by pelitic and semipelitic schists which are interbedded with quartzo-feldspathic gneisses (meta-arenites), the later increasing in volume (up to 40%) at the top of the unit, which is marked by the first appearance of interbedded quartzite.

Unit 4

The base of unit 4 is marked by the appearance of quartzites. It forms an excellent marker horizon 20 to 70 m thick. Micaceous partings define 0.5 to 3 m thick quarzite layers which are finely layered and contain up to 20% feldspar, muscovite, hornblende and/or pyroxene. Feldspathic subunits are most common towards the contacts of the unit, while purity and thickness increase towards its center. The uppermost contact is interbedded in the south, and sharp in the north.

Unit 5

This 10 to 60 m thick unit is characterized by a succession of interbedded coarse-grained kyanite-sillimanite-andalusite-bearing pelitic and semipelitic schists with subordinate hornblende- and biotite-bearing gneisses and garnet-bearing amphibolites. In the south part of the map area, the base of the unit displays a flaggy parting with up to 50% quartzo-feldspathic gneiss. This gneiss component is absent in the north.

Unit 6

Unit 6 is a widespread heterogeneous unit characterized by calc-silicate gneisses, impure marbles and carbonatite, and is the most distinctive in the map area. Four of five subunits are gradational into each other with carbonate content increasing upwards. The lowermost subunit (6i) is 0 to 50 m thick, and composed of a medium- to coarse-grained hornblende gneiss with cm- to dcm-scale layering. Banded coarse-grained diopside, scapolite-, garnet- and biotite-bearing calc-silicate gneisses form subunit 6ii, 0 to 50 m thick. Hietenan (1967) argues that scapolite-bearing layers in the Belt Supergroup were originally deposited in a restricted saline environment. It is possible that similar scapolite-bearing layers in the map area were originally deposited in this type of environment. A 20 to 50 m thick sequence of cm- to dcm-scale bedded cyclic impure carbonates with siliciclastic bases constitute subunit 6iii. Subunit 6iv is the most unusual map unit. Discontinuous, faintly laminated, and ranging from 2 to 10 m thick where present, it is characterized by 2 mm to 1 m diameter randomly oriented, dispersed lithic and crystal fragments, which comprise 5 to 30% of the unit (Plate 2A & B). Well rounded to sharp and irregularly shaped fragments are composed of layered fine-grained plagioclase and biotite, massive biotite, feldspar, and irregular (flamme-like) fine-grained melanocratic material. Some of these lithic fragments are brecciated (Plate 2B). Crystal fragments are dominantly 0.1 to 2 cm long plagioclase grains and biotite up to 10 cm in diameter. The matrix is composed of coarse-grained ferroan calcite and plagioclase with a wide array of accessory minerals. Those identified include apatite, muscovite, sphene and amphibole. Unidentified iron-oxides are common accessory minerals. Preliminary geochemical analyses (XRF 3000-4000 ppm total

strontium) indicate that these rocks are of carbonatitic affinity (K. Bell, pers. comm. 1986). Ancient and modern eruptive carbonatite lavas, tuffs and agglomerates are present throughout the world (e.g. Dawson et al. 1968; Hay & O'Niel, 1983; Deans & Roberts, 1984). Pyroclastic carbonatites display similar fragmented textures, areal extents, layering and mineralogy (ref. op. cit.). On this basis this subunit is herein interpreted to be stratiform block-lapilli carbonatite tuff (Schmid, 1981). This origin is discussed later in section 2.3.2. The sequence is capped by subunit 6v, a discontinuous 2 to 3 m thick quartzite present only in the north.

Unit 7

Unit 7 is 3 to 40 m thick, and composed dominantly of coarse-grained, rusty weathering, sillimanite-kyanite-andalusite-garnet-biotite bearing schist. At the base of the unit in the north part of the map area, there is a 1 to 2 m thick, discontinuous, relatively pure graphite-phlogopite-bearing white marble thought to be correlative with the "virgin marble" (informal name; unit 4m Brown, 1980; Hoy and Brown, 1980) mapped throughout the region to the south. Quartzo-feldspathic gneisses and amphibolites become interlayered at the top.

Unit 8

This 60 to 300 m thick unit is lithologically the most heterogeneous, being composed of a complete spectrum of rock types including amphibolite, hornblendite, various gneisses, quartzites, pelitic and semipelitic schists, and rare carbonate rocks. It is subdivided into two broad subunits: (1) 8G, is dominated by amphibolites and hornblende gneisses (Plate 2C & D), and constitutes the majority of the unit; (2) 8P, found in

the north part of the map area, has kyanite-sillimanite-andalusite-bearing schists and semipelites as its major constituents. Near the top of the unit is a 1 to 3 m thick, poorly sorted orthoconglomerate with a framework of angular clasts composed of fine-grained quartz and feldspar, and minor rounded quartzite clasts, set in a matrix of hornblende, biotite and garnet (Plate 2E). This layer is interpreted to be of an epiclastic origin.

Unit 9

This sequence is marked by a dominance of quartzite with interlayered amphibolite, hornblendite, ultramafic rocks, quartzo-feldspathic gneiss, pelitic and semipelitic schists, and rare calcareous rocks. Both primary sedimentation and later strain have produced a marked range in thickness from 12 m in the south to 800 m along the east flank of the map area. Discordant ultramafic units composed dominantly of orthoamphibole and minor garnet, kyanite, andalusite, quartz and phlogopite, are found in the lower half of the sequence (Plate 2F). It contains both discordant and concordant amphibolite throughout (Plates 2G & H, 3A, C & D), and discordant muscovite schist dykes in the upper part (Plate 3B). Meta-arenites include arkosic, subarkosic, hornblende- and diopside-bearing varieties with quartz-arenite being dominant. Preserved festooned crossbedding (Plate 3C), graded bedding and scours provide stratigraphic facing directions for the whole cover sequence. This unit is interpreted to be a metamophosed interlayered sequence of quartz arenites, arkoses and subarkoses, mafic and ultramafic sills and/or flows, mudstones and possibly dolomarls, and is best described as a mafic sill-sediment complex, possibly generated in the same manner as similar complexes in the Gulf of California (see section 2.3.2). It is believed that the emplacement of the mafic and

ultramafic sills and/or flows, plus related tectonic activity, caused instability in the sedimentary pile and contemporaneous intrusion of pelitic dykes.

Unit 10

This ca. 500 m thick unit consists of dominantly amphibolite and aluminosilicate-deficient pelitic and semipelitic schists (subunit 10AP), interlayered quartzites (subunits 10Q), and kyanite-sillimanite-andalusite-bearing migmatitic schists (subunit 10P). Hornblendite and quartzo-feldspathic gneisses are common throughout subunit 10AP. Several unique layers are present within subunit 10AP that are believed indicative of ancient volcanic processes. These include: (1) several 2 to 3 m thick ash-flow-like metaconglomerate subunits with a dispersed framework of felsic to mafic clasts set in a felsic matrix (Plate 3E & F), and (2) a remarkable discontinuous fine-grained, friable felsic unit that resembles air-fall material. Unit 10 is thought to have been deposited in a low energy clastic sedimentary environment periodically disrupted by both mafic and felsic volcanic deposits, and higher energy clastic deposits.

Unit 11

This 120 to 210 m thick unit is composed of dominantly aluminosilicate-rich, coarse-grained pelite with interbedded semipelite, quartzo-feldspathic gneisses and minor amphibolites, and hornblendites, which comprise subunit 11P, ca. 90% of the unit. Subunit 11MQ is a 4 to 6 m thick discontinuous quartzite and calc-silicate horizon; subunit 11H is a 200 by 300 m pod of hornblendite (Plate 3G), interpreted as mafic flows with minor interflow sediments, and subunit 11G is a flaggy biotite-

hornblende gneiss unit. Unit 11 is believed to represent a low energy environment periodically disrupted by higher energy conditions and mafic volcanic activity.

Unit 12

Unit 12 is lithologically a complex heterogeneous sudivision which displays numerous facies changes, and forms the uppermost exposure of the mantling gneiss sequence. Ground cover hindered the accurate identification and delineation of subunits. The base of the sequence is marked by up to 100 m of amphibolite, hornblendite and minor calcareous biotite schist which together comprise subunit 12i. This is overlain by 50 to 100 m of kyanite-sillimanite-andalusite-bearing schists interbedded with amphibolite and various gneisses (subunit 12ii), in turn overlain by a discontinuous pod up to 50 m thick, of hornblendite (subunit 12iiiH) interpreted to be mafic flows (pillows?) and interflow sediments (Plate 3H). Overlying rocks are difficult to differentiate, but do contain all of the above rock types. Subunits identified comprise amphibolite (12iiiA), and biotite-, garnet- and hornblende-bearing quartzo-feldspathic gneisses and quartzites (12iiiQF). Unit 12 is interpreted to have been dominantly mafic volcanic related deposits intercalated with a wide array of siliciclastic sediments.

Syenite Intrusive Rocks

Biotite-bearing syenite gneiss crosscuts the upper part of unit 6 in the northern part of the map area. This white, irregularly weathering unit is calcite-bearing. In the middle of unit 9, a small m-scale pod of white orthoamphibole-bearing syenite is intimately associated with an ultramafic

orthoamphibole sill.

2.2.2 SELKIRK ALLOCHTHON

Upper-plate rocks in the area mapped comprise a sequence of highly migmatized and pegmatized pelites, semipelites, quartzo-feldspathic gneisses, minor quartzite, amphibolite and calcareous rocks. Pelitic and semipelitic schists dominate the sequence. Sillimanite is very common, muscovite is present only at the base, and kyanite is present only as anhedral remnants which become rarer as one traverses into the upper-plate. Tonalitic pegmatite is very common and can comprise up to 50% of the upper-plate (see section 3.4.5). These upper-plate rocks are interpreted to be a metamorphosed clastic sequence dominated by chemically mature mudstones and interbedded immature arenites. They are inferred to be correlative with Horsethief Creek Group rocks (Brown, 1980). Further discussion of the Selkirk Allochthon can be found in Read and Brown (1979), Brown and Read (1983), and Journeay and Brown (1986).

2.2.3 SUMMARY

The map area is underlain by dominantly siliciclastic and relatively minor carbonate metasedimentary rocks which comprise core gneisses, mantling gneisses and rocks of the Selkirk allochthon. Observed facies relationships and the presence of laterally persistent marker horizons have enabled subdivision of the mantling gneisses into 11 composite lithostratigraphic units. Anomalous units include: (1) stratiform carbonatite, (2) mafic, ultramafic and syenite sills and/or flows, (3) immature mafic arenites, (4) aluminosilicate-deficient pelite, and (5) volcaniclastic deposits; all occurring above unit 6iii as extensive

deposits. These observations are indicative of a typical shallow water platform-like environment (units 2-6iii), which evolved into an environment strongly influenced by extension related igneous and volcanic activity (units 6iv-12), with the initial disturbance recorded by a pyroclastic carbonatite (unit 6iv).

2.3 MANTLING GNEISSES: INTERPRETATION

Problems in the interpretation of tectono-stratigraphic components of the Monashee complex revolve in particular around three issues: their age, affinities, and paleotectonic significance. Constraints on their ages are summarized in section 1.3. Despite high-grade metamorphism and deformation, well displayed primary features of the mantling gneisses, described in the preceeding sections and elsewhere (ref. op. cit.), supply rare information on the latter two issues regarding the early evolution of the western North American Proterozoic margin. This section attempts an integration of these data, and an analysis of their implications.

2.3.1 METASEDIMENTARY ROCKS & DEPOSITIONAL ENVIRONMENT

Regionally metamorphosed, upper amphibolite-grade, polydeformed mantling metasedimentary rocks are composed of siliciclastic and carbonate sequences unconformably overlying core gneisses. Most common are metamorphosed equivalents of quartz and quartz-feldspar arenites, pelites, and impure carbonate rocks, all occurring as laterally extensive horizons. Less common metasedimentary units include a basal quartz-pebble conglomerate, stratabound lead-zinc deposits and impure scapolite-bearing marbles. Stratigraphic contacts, which are generally gradational and less commonly abrupt, are considered conformable. Preserved thicknesses range

from ca. 750 m (Fig. 5; Mt. McPherson, Read, 1980; Cotton Belt, Hoy, 1979, 1982a) to greater than 2000 m (Fig. 5; Journeay, 1986; this study). Structural thinning and thickening has been recognized but there is little difficulty in establishing the stratigraphic succession.

Informal stratigraphic subdivisions have been established at several locations around Frenchman Cap and Thor-Odin domes, with relatively local correlations suggested for interdomal regions (Read, 1980), along the west flank to the southeast corner of Frenchman Cap (Hoy & McMillan, 1979; Hoy, 1982a), along the west flank over to the east flank (Psutka, 1978; Journeay, 1986), and to the north flank (this study, Fig. 5). Examination of proposed subdivisions and revisions reveal broadly homotaxial successions within which two laterally persistent, regionally significant horizons occur: a basal quartzite, and a calc-silicate/marble/carbonatite horizon (units 2 & 6 respectively in Figure 3; units 3 & 4iv respectively in Brown, 1980 and Hoy & Brown, 1980). Based on the presence of these two horizons a compilation uniting the proposed correlations and stratigraphic columns has been constructed (Fig. 5) which clearly demonstrates complications due to facies changes.

The presence of quartzite and local quartz-pebble conglomerate at the base of the succession indicates a transgressive phase, while restricted circulation is suggested by stratabound lead-zinc deposits (Hoy, 1979), and impure scapolite-bearing marbles (Hoy & Kwong in press; this study). Chemically and texturally immature siliciclastic (Plate 2C) and epiclastic sediments (Plate 2E), and clastic dykes at the north end of the complex (Plate 3B, see also Fig. 3) are indicative of a tectonic disturbance at this location. High-grade metamorphism and high strain, which have not erased all primary structures (e.g. cross bedding, graded bedding, scours,

and primary contact types), do preclude the acquisition of detailed sedimentological data from which one might be able to propose a well supported facies model.

All Monashee complex research (references cited in chapter 1) supports the proposition that the mantling gneisses comprise a platform sequence. Whether they comprise a continental margin platform sequence remains very speculative since there is no evidence of oceanic crust within the complex. The most convincing data are that they constitute a laterally extensive sequence of shallow water siliciclastic and carbonate sediments, with minor intercalated intrusive and extrusive deposits, similar to Phanerozoic continental margin platform sequences; and they rest upon older Aphebian basement believed to have been in the vicinity of the paleocontinental margin of North America. Evidence presented in section 2.2.1.2 and discussed in section 2.3.2 also suggests that some mantling gneisses may represent a sill-sediment complex (Einsele, 1986), which further suggests accumulation during the transitional stage between continental stretching and accretion of oceanic crust.

Although a continental margin platform model does explain the observed facies assemblages, vertical and lateral sequences, and apparent tectonic setting of the mantling gneisses, other sedimentary environments (e.g. lacustrine, foredeep, epeiric sea etc.) cannot be dismissed for the following reasons. Continental shelf environments are extremely complicated and presently not well understood (e.g. Walker, 1984; Montadert et al. 1979); consequently present day shelf sedimentation models applicable to ancient shelf sequences are rare. Criteria most reliable for recognition of ancient shallow marine deposits, features controlled by salinity and water depth (e.g. marine fossils, trace elements and certain

authigenic minerals, Johnson, 1978; Reinick & Singh, 1980), are nonexistent for the mantling gneisses. Geochemical and sedimentological data for the mantling gneisses are extremely poor and are not in themselves diagnostic of a continental margin platform sedimentary environment. Various stratigraphic analytical approaches yield subdivisions of documented mantling gneiss sequences into innumerable combinations of asymmetric and/or symmetric cycles which can be interpreted as products of such processes as transgression, regression and progradation. Again, there does not exist enough sedimentological data, especially with regards to contact relationships, to determine exactly which processes were operative. Therefore some of these cycles may have no sedimentological significance. In short, the causative mechanisms of sedimentation for sediments which now comprise the mantling gneisses are currently unknown.

2.3.2 MAGMATIC EVIDENCE FOR COEVAL TECTONIC ACTIVITY

ALKALINE MAGMATISM

Nepheline syenite gneisses mapped along the west and south flanks of Frenchman Cap dome (Fyles, 1970a, b; Currie, 1976b; McMillan & Moore, 1974; Pell, 1986b; Journeay, 1981, 1986) and stratiform carbonatite mapped and described along the west and north flanks (McMillan, 1970, 1973; McMillan & Moore, 1974; Hoy, 1979; Hoy & Brown, 1980; Read, 1980; Hoy & Pell, 1986a, b; Hoy & Kwong in press; Journeay, 1986; this study) lie within the Cordilleran Alkaline Province (Currie, 1976a; White, 1985; Pell, 1986a, b, c, d). Aside from their unique mineralogy (McMillan, 1973; McMillan & Moore, 1974; Currie, 1976b; Hoy & Pell, 1986a, b), chemical compositions (Currie, 1976b; Hoy & Pell, 1986a, b; Hoy & Kwong in press; Pell, 1986d), and economic importance (Fyles, 1970a; Currie, 1976a), these volumetrically

insignificant rocks are of great paleotectonic significance.

The stratiform fragmental carbonatite horizon, recently interpreted as carbonatitic pyroclastic deposits laid down in a carbonate environment (Hoy & Pell, 1986a, b; Hoy & Kwong in press; this study), is the most extensive indicator of syndepositional tectonic activity in the Monashee complex. This interpretation is based on comparison of observations made of rare ancient and modern eruptive carbonatite lavas, tuffs and agglomerates present throughout the world (e.g. Dawson et al. 1968; Hay & O'Niel, 1983; Deans & Roberts, 1984), with those observations made in the Monashee complex (ref. op. cit., and this study), which leave little doubt that this horizon is pyroclastic in origin. A low energy carbonate environment, as indicated by the host calc-silicate/carbonate horizon (Figs. 3 & 5), is a favourable location for preservation of highly erodible pyroclastic deposits extruded from a carbonatitic volcano. Diffuse boundaries of the unit with impure marbles which lack fenitization haloes, suggests mixing of pyroclastic carbonatite and unconsolidated carbonate sediment. Its large areal extent (>100 km), fragmental nature, and intercalation with metasedimentary rocks are difficult to explain otherwise.

There are several mechanisms capable of dispersing carbonatitic material over a wide area. One is the occurrence of violent eruptions. The synsedimentary characteristics of the stratiform carbonatite are suggestive of a water saturated paleohydrogeological condition (a condition not fully appreciated by experimental petrologists in consideration of violent eruptions, Fisher & Schminke, p. 44, 1984). Phreatomagmatic activity could give rise to violent explosions (e.g. Lorenz, 1980) and subsequent widespread deposition of hydroclastic deposits. Carbonatitic maar volcanoes do occur (Dawson, 1964a, b; Lorenz, 1980), and although not

yet identified, may be present within the mantling gneiss sequence. Other mechanisms invoked to explain wide lateral extents of fragmental carbonatite deposits, which may have played depositional roles in the Monashee complex, include avalanches, mudslides and pyroclastic flows (cf. Hay, 1978, 1983; Silva et al. 1981).

Presently there exists no direct proof that the stratiform carbonatite and dated intrusive nepheline syenite gneisses lower in the sequence (Fig. 5) are comagmatic. Such a relationship is reasonable considering that: (1) intrusive carbonatite associated with nepheline syenite has been documented in the complex (McMillan, 1973; McMillan & Moore, 1974; Hoy & Pell, 1986a), (2) an association of carbonatite with alkaline igneous rocks including pyroxenites, peridotites, ijolites, nepheline syenites and fine-grained equivalents is well documented throughout the world (e.g. Le Bas, 1977), and (3) possible autoliths within the stratiform carbonatite are nepheline syenite clasts documented by Hoy and Pell (1986a, b).

Petrological affinities of unusual ultramafic and syenite rocks which occur above the stratiform carbonatite (Fig. 3; Journeay, 1986) are not presently known. Considering the second point in the paragraph above, and that Currie (1976b) has documented alkaline amphibolite associated with nepheline syenite at the Mount Copeland locality, it is possible that they are genetically related to alkaline activity. The occurrence of possible syngenetic igneous rocks, coupled with the recent discovery of the intrusive Ren carbonatite (see Hoy & Pell, 1986a, b), both higher in the mantling gneiss sequence, is suggestive of periodic (long-lived?) alkaline activity during a major part of the time span that sediments which now comprise the mantling gneisses were deposited. The timing and alkaline nature of this event makes it unique in the Cordillera.

Carbonatite has not been recognized on the east side of the complex, while the calc-silicate/carbonate horizon which contains the carbonatite on the west and north flanks of the complex, is present (Fig. 5, column 8; Psutka, 1978; Brown & Psutka, 1979). Hoy and Pell (1986a, b) document several eruptive deposits on the west flank. Large lithic clasts up to 1 m in diameter dispersed within the stratiform carbonatite at the north end of the complex (e.g. Plate 2B), and those ca. 5 km to the south (Hoy & Pell pers. comm. 1986; note >5 km if unfolded), are thought to be indicative of proximal deposits to separate vents. These data suggest an ancient sedimentary basin or platform with several active alkaline volcanic centers possibly located within rocks of the complex (e.g. Mt. Copeland?), and/or north, west and south of the exposed part of the platform, periodically erupting carbonatitic material into a low energy carbonate environment.

Although generally associated with cratonic rifts in regions of unusually high heat flow (Bailey, 1974; Gittins, 1986), carbonatites are found in other tectonic settings (e.g. oceanic crust, Silva et al. 1981; Black et al. 1985; convergent and divergent plate boundaries, Woolley, 1986). Rift systems occasionally evolve into ocean basins with passive margin sequences which contain alkaline deposits (e.g. Tertiary evolution of east Greenland, Neilsen, 1985). Mantling gneisses may have formed the base of such a passive margin sequence, in which case the alkaline magmatic event may prove to be a useful factor in evaluating possible distal detached continental fragments.

MAFIC & FELSIC MAGMATISM

Figure 5 demonstrates that higher stratigraphic levels of the mantling gneisses are preserved in the map area than elsewhere. It is from

this most complete section (column no. 10) that further evidence for a syndepositional tectonic disturbance has been compiled (this study). Collectively the 12 units mapped at this location point to a shallow water platform-like environment (units 2-6iii), which evolved into a setting strongly influenced by extension-related igneous and volcanic activity (units 6iv-12), with the initial disturbance being recorded by the deposition of pyroclastic carbonatite (unit 6iv).

Post-carbonatite mafic magmatism and minor felsic volcanic activity documented at this location are similar to some plutonic/volcanic sequences and associations observed in parts of the East Africa rift (e.g. King et al. 1972; Baker et al. 1972) and continental rifts in general (Bailey, 1983; Giret & Lameyre, 1985). Units 8 to 12 (Fig. 3) are composed of metasedimentary rocks which host syndepositional mafic and ultramafic sills and flows, and in this respect are similar to published descriptions of basaltic sill-sediment complexes documented at young oblique spreading centers in the Guaymas Basin of the Gulf of California (see Einsele, 1986). These complexes form through an interplay of sedimentation rates, spreading rates, and timing of magmatic pulses during the transitional stage between continental attenuation and accretion of new oceanic crust (Einsele, 1986). This suggests an extensional environment with like sediment/magmatic processes during deposition of the mantling gneisses, but not necessarily a similar tectonic setting (i.e. oceanic spreading centers). High sedimentation rates and contemporaneous mafic magmatic pulses could produce a sequence similar to units 8 and 9. Units 10 and 11 may reflect decreasing and fining sedimentation due to faster spreading, basin subsidence, starving of the basin or a change in sedimentary processes. This could result in eventual extrusion of subaqueous mafic magmas (e.g.

units 11H and 12iiiH).

This scenario, which may not have resulted in formation of normal oceanic crust, portrays a period of rifting similar to other Proterozoic rift assemblages of the Canadian Shield where lower clastic assemblages are overlain by thick mafic sill-sediment complexes thought to be related to incipient crustal extension, aborted rifting, and the possible formation of narrow oceanic rifts (see Easton, 1983). In terms of the regional stratigraphic framework, evidence for other plutonic/volcanic activity exists in Late Proterozoic to early Paleozoic rocks of the Selkirk Allochthon (e.g. Brown et al. 1978; Simony et al. 1980). Although these sequences have possibly been transported as much as 80 km to the east, relative to the Monashee complex (Brown & Read, 1983; Brown et al. 1986), this region appears to have experienced long-lived, episodic Proterozoic to Paleozoic volcanic activity.

2.3.3 REGIONAL CORRELATION

Evenchick et al. (1984) have emphasised that many Precambrian gneiss exposures within the Omenica Belt are overlain by successions consisting of pure or feldspathic quartzite, marble, amphibolite and schists. Although their lithological characteristics and sequences are similar, correlating mantling gneisses of the Monashee complex with the above rocks remains difficult and uncertain due to the lack of chronometric data, time markers, unique and major events. Much of the following centers on the most reasonable assumption that the nepheline syenite body, dated at ca. 750 Ma, and the synsedimentary stratiform carbonatite are cogenetic (discussed in section 3.3.2).

Possible correlatives to the south, in the vicinity of the Kettle

Dome, are rocks of the Tenas Mary Creek sequence (Cheney, 1980; Parker & Calkins, 1964; equivalent to the Grand Forks Group of Preto, 1970). The age of this sequence is poorly constrained to older than late Paleozoic; a Precambrian age for both is favoured by Cheney (1980). Paragneisses of uncertain origin documented within the Valhalla complex (Carr, 1986) may also be correlatives. Correlation of basal quartzites overlying basement gneisses ca. 200 km to the north of the Monashee complex (i.e. the Malton Gneiss), in the vicinity of the Rocky Mountain Trench (Morrison, 1982; Simony et al. 1980; McDonough & Simony, 1984; among others), is attractive but tenuous since basement/cover contacts are apparently tectonic at this location (ref. op. cit.).

Stratigraphy at the north end of the Monashee complex has some elements in common with those in the Deserters Range, ca. 750 km to the north, where a basal quartzite and quartz-feldspar pebble conglomerate nonconformably overlie a gneissic granite dated at 728 +8, -7 Ma (U-Pb zircon Evenchick et al. 1984; Evenchick, 1983b). In particular both sequences comprise siliciclastic rocks with intercalated mafic volcanic rocks (cf. figure 3, and Evenchick, 1982, 1983b), which when coupled with the radiometric data indicates that they are at least temporal correlatives which display similar environments of deposition. Correlation with similar Proterozoic strata in the Sifton Range (Evenchick et al. 1984; Evenchick, 1983a, 1984) ca. 850 km to the north is not warranted since basement/cover relationships are not known.

Proterozoic stratigraphy lying between basement rocks of the North American craton (>1600 Ma), and early Paleozoic miogeoclinal rocks (<570 Ma), comprises three major time/rock assemblages separated by two major tectonic disturbances (for summaries see Young et al. 1979; Eisbacher,

1981; Young, 1981). The oldest assemblage, greater than 1200 Ma in age is represented by the Wernecke Supergroup and Belt-Purcell Supergroup (or parts thereof, see Whipple & Balla, 1986) in the north and central parts of the Cordillera, the Unkar Group in the Grand Canyon, and scattered equivalents throughout the southwestern U.S.; the middle assemblage, ca. 1200 to 800 Ma, is represented by the shallow marine Pinguicula Group and Mackenzie Mountain Supergroup in northwest Canada, a hiatus in the central Cordillera, Chuar Group rocks in the Grand Canyon, and equivalents in California and Utah; the uppermost assemblage comprises a predominantly clastic succession lying between crystalline basement of the North American craton or the above two assemblages, and the base of lower Cambrian quartzites, includes the Windermere Supergroup and equivalent rocks from the Yukon to Sonora.

Several lines of reasoning suggest mantling gneisses are not pre- or syn-Belt-Purcell, but may be part of one of other thick Proterozoic sequences postulated by Evenchick et al. (1984) to lie directly upon granitic basement without intervening Belt-Purcell strata. Mantling gneisses are relatively shallow water siliciclastic and carbonate platform-like sediments with sedimentological attributes unlike regional Belt-Purcell strata (e.g. McMechan, 1981; Hoy, 1982b), or late Aphebian to Helikian sedimentary successions of the Canadian Shield (e.g. Fraser et al. 1970). They do not display any evidence of pre-Mesozoic compression, regional metamorphism or granitic intrusion, which could be correlated with the East Kootenay or Racklan orogenies (1300-1350 Ma, McMechan & Price, 1982; ca. 1200 Ma, Young et al. 1979, respectively) which terminated Belt-Purcell and Wernecke sedimentation. These arguments may not be considered conclusive but they certainly favour a post-Belt-Purcell age for the

mantling gneisses.

Evidence presented in this chapter suggests that mantling gneisses were most likely deposited during crustal attenuation. If one accepts the assumption of syenite/carbonatite cogenesis, then the synsedimentary disturbance in the Mohashee complex occurred at ca. 750 Ma, and is broadly coeval with other synsedimentary extensional events recorded throughout the Cordillera at this time (Table 1). Some or all of the stratigraphy lower in the sequence may be older. Several possiblities exist: (1) this lower stratigraphy could all be Belt-Purcell (>1350 Ma), in which case a hiatus of at least 600 Ma would be required in the sequence, (2) it is possible that some stratigraphy is Belt-Purcell, and some 1350 to 750 Ma old, which requires extremely slow sedimentation rates, or one or more hiatuses, or both, and (3) all lower stratigraphy could be part of the 1350 to 800 Ma assemblage filling, in part or whole, the hiatus in the sedimentary record of southeastern British Columbia.

There is no evidence of any breaks in the mantling gneiss sequence, and its characteristics suggest continuous rapid sedimentation in an extensional environment, similar to that in the Gulf of California. It is therefore proposed that the whole mantling gneiss sequence is earliest Windermere in age, and that they record the extensional episode initiating sedimentation of the western North American miogeocline. This implies temporal correlatives in Greenland, the Arctic islands, northwestern Canada, British Columbia, Idaho, Montana, northern Utah, the Grand Canyon and Death Valley regions (see Young, 1981 for a review).

Working in a time/orogeny framework, breakdowns of supracrustal sequences in the manner of Young et al. (1979), Young (1981), and Eisbacher (1981), plus correlation of broadly coeval orogenies or disturbances (ref.

op. cit., McMechan & Price, 1982; Elston & McKee, 1982) are useful as preliminary working frameworks. Consideration of more detailed studies can create problems if these events become boundaries between which strata must be sorted (i.e. "any dates or facies which pass into an interorogenic gap run the risk of being enticed into the rocks of the nearest defined orogenesis", Nisbet, 1985). It is thus proposed that the extensional/magmatic event recorded in the mantling gneisses of the Monashee complex be referred to as the Monashee Extensional Disturbance.

2.5.4 RIFT STRUCTURES, MODELS AND MECHANISMS

Although a great deal more research is required before comprehensive comparisons can be made with proposed models of passive margin types and evolution, enough is now known to allow some preliminary conclusions to be drawn regarding applicable models and operative mechanisms for the Late Proterozoic evolution of the western North American margin. Extensional tectonics is suggested by volcanogenic and plutonic rocks observed within the Monashee complex, while syndepositional extensional structures (e.g. listric normal faults, Bally et al. 1981) have yet to be documented. Paucity of extensional structures suggest either one or a combination of broad-scale downward lithospheric flexure similar to that documented during the early evolution of the Bay of Biscay (Montadert et al. 1979), large-scale block faulting characteristic of upper-plate passive margin sequences underlain by a master detachment fault dipping toward the continent (Lister et al. 1986a), or the non-attenuated side of a rift (Bally & Oldow, 1986).

Deep-rooted, long-lived high-angle normal faults are believed to have been active during Belt-Purcell and Windermere sediment accumulation (e.g. references in Table 1). These faults are poorly understood and warrant a

great deal more research. It can be argued that these faults were active in southeastern British Columbia outside the Monashee complex, producing subsidence and accumulation of all mantling gneiss sediments during initial Windermere rifting and sedimentation, and that the earliest magmatic manifestations of this activity in the mantling gneiss sequence are carbonatite/nepheline syenite deposits.

In direct contrast to the above evolution, synsedimentary normal faulting, carbonate, evaporite and red bed sequences of the MacKenzie Mountain Supergroup and Coates Lake Group in the MacKenzie Mountains (e.g. Jefferson & Ruelle in press; Ruelle, 1982; Aitken, 1982), and equivalent rocks which fill half-grabens in the Ogilvie Mountains (Thompson, 1986) of northwest Canada, are suggestive of lower-plate passive margin geometry and sedimentation (Lister et al. 1986a). These structural and lithological observations support a Proterozoic western North American passive margin with alternating upper-plate and lower-plate geometries and lithologic sequences (cf. Bally, 1981, 1982; Lister et al. 1986a), terminating against unidentified transfer faults (Gibbs, 1984; Lister et al. 1986a, b; Bosworth, 1986) which accommodate their different motions.

The asymmetry of continental margins in general (see Bally, 1982), and the observation that opposing margins of rifted continents are usually dissimilar (e.g. matching margins of the Atlantic Ocean, Wilson & Williams, 1979), can be accounted for in models based on low-angle detachments (Bally, 1981, 1982; Bally & Oldow, 1986; Lister et al. 1986a). The inference that these models are applicable to the Late Proterozoic margin of North America implies that the structure and stratigraphy of distal candidates for the opposing margins of the rift (should they exist, cf. Badham, 1978; Sears & Price, 1978; Young et al. 1979; Jefferson, 1978;

Bell, 1986a, b; Piper, 1982; Bond et al. 1984; Young, 1984) be dissimilar and of a complementary asymmetry.

Suggestions that the Monashee complex may have been part of a passive margin basement high (Hoy & McMillan, 1979; Brown, 1981) can be accommodated by two general models, in part accounting for the absence of typical rift phase structures and rock types. The first, using models presented by Gibbs (1984) and Lister et al. (1986a), proposes that core gneisses may have been part of a marginal plateau or continental ribbon created through multiple detachment systems (cf. Brown, 1981). McDonough & Simony (1984, 1986) present sedimentological arguments for an ancient basement high (Malton Gneiss) ca. 200 km to the north. Such a plateau or ribbon may have been the focus for large broad structural highs that evolved during later orogenesis.

A second model suggests core gneisses may have been part of a transverse basement high. Lithologic sequences and radiometric dating, although not extensive, appear to support the proposition that Windermere rifting produced depocenters at different places and times along the rifting margin resulting in a wide range in age of initial miogeoclinal deposits (Labotka & Albee, 1977; Evenchick et al. 1984), and that the rate of continental separation was spacially and temporally variable (Stewart, 1976; Pell, 1983). This is typical of rift localization (McKenzie, 1986; Courtillot, 1982) and continental rift propagation (Vink, 1982; Courtillot, 1982), where continent/ocean boundaries are not isochrons (Vink, 1982). Such an early evolution would result in a chain of restricted depocentres bound by basement faults and highs similar to Mesozoic rift phase structural configurations of the Atlantic margin (e.g. Sheridan, 1976; Grow, 1981; Manspeizer, 1981).

Proposed ages for block faulting, mafic volcanism and deposition of glacial diamictites, which characterize the commencement of Windermere and miogeoclinal sedimentation, are not precisely constrained, and range from ca. 800 to 900 Ma (Stewart, 1972, 1976; Burchfiel & Davis, 1975; Miller et al. 1973; Dickinson, 1977; Young et al. 1979; Eisbacher, 1981; McMechan & Price, 1982). Quantitative subsidence analyses yield ages between 555 and 650 Ma for the final phases of rifting, continental separation and the initiation of sea-floor spreading (Stewart & Suczek, 1977; Bond & Kominz, 1984, and references cited therein). It has been pointed out that the above ages, encompassing 900 to 555 Ma, imply an episodic rifting event of long duration (at least 150 Ma) prior to sea-floor spreading (Stewart, 1978; Bond & Kominz, 1984; Devlin et al. 1985), and cast some doubt on when true continental separation occurred. A solution supported by this study (if one accepts the age of ca. 750 Ma for the Monashee Extensional Disturbance), would be that mafic volcanism and coeval block faulting which initiated Windermere sedimentation, represent episodic or aborted rifting, and that continental separation occurred later at ca. 600 Ma as indicated by thermal subsidence studies. Such long pre-oceanic rifting (ca. 200 Ma) is not uncommon during passive margin genesis elsewhere (e.g. the Adelaide Rift of southern Australia, Von der Borch, 1980; the Garder igneous province in south Greenland, Upton & Blundell, 1978; the Atlantic margin of northwest Europe and the Indian Ocean margin of western Australia, see references cited in Bond & Kominz, 1984). Such a scenario supports proposals that Proterozoic rifting and passive margin formation processes were similar to those operative in the Phanerozoic, but protracted and aborted rifting, plus greater intracratonic activity and the development of small ocean basins were more common (Hynes, 1982; Easton, 1983; Young,

1984; Von der Borch, 1980).

Deep structure, geometry and paleodynamics of the lithospheric plate involved are believed to be controlling factors affecting proposed primary mechanisms of alkaline magma generation: focussed decompressive melting (see Black et al. 1985; Bailey, 1983; and Woolley, 1986), and shear heating (De Gruyter & Vogel, 1981). All of these factors likely played roles of varying importance in accounting for the generation, long-lived nature, and repetition (Pell, 1985, 1986b) of regional alkaline events. For example, alkaline magmatism in the Monashee complex may be indicative of a zone of weakness (transfer fault?, Gibbs, 1984; Lister et al. 1986a, b; Bosworth, 1986). Such zones have been proposed to account for documented continental alkaline complexes found in linear arrays along the Atlantic margins, apparently associated with major oceanic transform faults (e.g. Bailey, 1978; Sykes, 1980). It is also possible that this alkaline magmatism is a reflection of localized igneous underplating predicted to be concentrated at the base of continental crust forming an upper-plate margin (Lister et al. 1986a).

In consideration of active or passive mechanisms of rifting (Sengor & Burke, 1978; Baker & Morgan, 1981), there is a paucity of supportive evidence for the former, where thermal energy in the form of mantle plumes (Morgan, 1971) impinges upon the base of the lithosphere causing a surficial doming-volcanism-rifting sequence. Doming at different scales is typical of East African, within-plate alkaline magmatism (Bailey, 1974; Le Bas, 1980) and active rifting (Sengor & Burke, 1978). With renewed sedimentation these vertical movements should be reflected by unconformities. Unconformities within the mantling gneisses have not been observed, while minor doming may be reflected by deposition of higher

energy deposits above the stratiform carbonatite.

It is more likely that rifting was produced through a passive mechanism caused by a tensile stress system in the lithosphere. Various sources of tension (see Bott, p. 364, 1982a) result in rifting along pre-existing lines of weakness (Bailey, 1978; Sykes, 1980) and diapiric upwelling of upper mantle material producing a rifting-(doming?)-volcanism sequence (Sengor & Burke, 1978). Support for this mechanism is found in the lack of direct evidence for doming, and the fact that observed volcanism occurs high in the sedimentary sequence. A pre-existing zone of structural weakness is implied by the broad subsidence which led to the accumulation of mantling gneisses. This points to lithospheric control on the location of magmatic activity, and suggests that passive rather than active rift mechanisms were responsible for the accumulation of the mantling gneiss sequence. Bedard (1985) and Smedley (1986) have applied similar arguments for passive rifting to the Jurassic eastern North American passive margin sequence, and the Carboniferous rift sequence in the Midland Valley of Scotland, respectively. Worldwide late extrusive-intrusive activity in rifts and rifted margins (Eldholm & Montadert, 1981; Bedard, Table I, 1985), is also believed to be associated with late phase rifting and early phase sea-floor spreading (Eldholm & Montadert, 1981).

It therefore appears that a model of passive asymmetric rifting is most applicable to the mantling gneiss sequence in the Monashee complex of southeastern British Columbia. It may also have played a role in the Late Proterozoic evolution of other parts of the western North American margin. In the Monashee complex it accounts for several features including the paucity of extensional structures, an evolution of sediment accumulation followed by syndepositional magmatic activity, and the alkaline nature of

some of these magmatic deposits. This model, rift localization, rift propogation and episodic rifting account for apparent geochronological discrepancies for the initiation of rifting and continental drift along the length of the Cordillera.

2.4 SYNTHESIS

Mantling metasedimetary rocks of the Monashee complex comprise a conformable sequence of platform-like, shallow-water siliciclastic and carbonate metasedimentary rocks deposited on core gneisses composed of possible North American continental crust. Core gneisses were part of large subsiding blocks of continental crust, possibly constituting either a margin plateau or continental ribbon, a transverse zone separating early localized depocenters, or part of a relatively unstructured upper-plate passive margin. The subsidence mechanism was most likely passive asymmetric rifting, where attenuation was accommodated by motion on major crustal-scale normal faults, and an unexposed low-angle detachment dipping towards the continent in southeastern British Columbia.

The dominant aspect of the lower part of the succession is that of a slowly subsiding relatively stable basin, while rocks in the upper part of the succession display several features indicative of the onset of less stable tectonic conditions. Evidence for a syndepositional extensional event is first recorded throughout most of the complex by pyroclastic carbonatite extruded during explosive (phreatomagmatic?) eruptions from several vents within and outside the complex, deposited in a low energy carbonate environment, and most likely comagmatic with a large intrusive body of nepheline syenite dated at 746 +40, -39 Ma. Later intrusive ultramafic, syenite and carbonatite suggest a periodically active (long-

lived?) alkaline center, perhaps related to lithospheric structures (transfer faults?) or plate paleodynamics. The alkaline nature and timing of this event makes it unique in the Cordillera.

At the north end of the complex alkaline volcanism was followed by syndepositional mafic and minor felsic intrusive and extrusive deposits, resulting in a sequence similar in character to: (1) the geochemical evolution of continental rift sequences, (2) other Proterozoic successions in that magmatic activity occurs later in the evolution, and (3) actively forming mafic sill-sediment complexes in the Gulf of California. The latter suggests proximity to a continent-ocean interface formed by mafic sill-sediment interactions and rift processes similar to those operative today, and suggests high sedimentation rates. Magmatic events recorded in the Monashee complex are only part of the documented regional Late Proterozoic to early Paleozoic magmatic activity reflecting protracted episodic rifting.

3 DEFORMATION, FABRIC GENERATION AND METAMORPHISM

3.1 INTRODUCTION

A study of the interactions and relationships between deformation, deformation processes, fabric generation and metamorphic recrystallization and neomineralization is fundamental to understanding the dynamothermal evolution of rocks in polydeformed and multi-metamorphosed terranes. In southeastern British Columbia the Monashee complex and Selkirk allochthon are two such terranes separated by a major regional tectonic boundary, the Monashee decollement. The map area of this study straddles this boundary (Fig. 1), and has the potential of providing information regarding the dynamothermal evolution of the Monashee complex. The goals of this chapter are: (1) to document the structures of rocks in both upper- and lower-plates of the decollement, and assess their relationship to structures mapped elsewhere, (2) to describe the characteristics of the decollement and related mylonitic rocks, and attempt to determine their kinematic significance, deformation processes and physical conditions of deformation, and (3) in light of these data and interpretations, to evaluate models proposed to account for the Monashee complex.

3.2 FOLDING AND RELATED STRUCTURES

3.2.1 INTRODUCTION

This section summarizes the styles, hierarchy, and related structures and fabrics of folds in both lower- and upper-plates. Lower-plate rocks are deformed by three phases of folding (Fig. 6 in back pocket). Phase I are pre- to early-metamorphic, overturned structures which dominate the

map-scale distribution of lithologic units. They comprise the previously mapped Sibley Creek Syncline and a newly mapped structure, the Sibley Creek Anticline. Syn-metamorphic phase II structures comprise sheath and buckle folds which overprint the above structures and dominate at the outcrop-scale. Phase III deformation comprises post-metamorphic, west-trending warps which weakly overprint earlier structures. Upper-plate structures are similar in style to phase II structures of the lower-plate. A penetrative west-trending mineral stretching lineation (Figures 7 & 8, both in back pocket) and boudinage are characteristic of both plates.

3.2.2 LOWER-PLATE

PHASE I STRUCTURES (D1)

The Sibley Creek Syncline (SCS) and its structurally overlying anticlinal mate (SCA) are overturned nonplane folds with moderately dipping (ca. 20-30 degrees) periclinal axial surfaces, and fold axes which plunge (ca. 10-25 degrees) towards west-southwest (Fig. 7). They are well defined by an upright-inverted-upright sequence of established stratigraphy (chapter 2) which can be walked around both closures. Stratigraphic facing directions in unit 9 clearly corroborate the existence of SCS whose fold closure can be seen in the 7900 ft. peak to the east. In cross-section (Fig. 9 in back pocket) these folds have limb lengths of ca. 6.5 km.

The upright limb of the SCS displays high attenuation of lithologic units relative to the core (especially unit 9). The shared overturned limb of the anticline-syncline pair shows a lower degree of attenuation. Stratigraphically higher units in the core of SCA are eroded and covered in a creek valley, while units 3 to 11 (inclusive) at the north end of the map area are clearly truncated by a detachment surface. The upright limb of

the SCA shows extreme attenuation and truncation by the detachment. These folds are overprinted by M1 metamorphism (section 3.4.7).

Minor structures and fabrics associated with this phase of folding have mostly been obliterated and transposed during later high-grade metamorphism, folding and shear strain. Axial planar S1 foliations are rarely preserved as a biotite schistosity at moderate angles to the compositional layering (S0), folded around the noses of D2 folds, and preserved as inclusions of quartz and biotite in porphyroblasts of garnet (Fig. 11C). Delineation of D1 minor structures in the field was difficult due to the intensity and dominance of mesoscopic phase II structures. Phase I minor structures were mapped in the core of SCA below the detachment (Fig. 10C), in the northwest corner, and in the core of SCS (Fig. 10B). These 10-meter scale structures fold S0 and have the expected vergence relative to the axial surfaces of the respective phase I structures. Based on these minimal observations they are interpreted as phase I structures. Considering the problems associated with vergence in multiply deformed terranes (Bell, 1981; Weijermars, 1982, 1985), it is most probable that some m-scale folds of wrong vergence are of D1 origin.

Minor structures to SCS-SCA are typically tight and reclined with thickened hinge zones which have been rotated parallel to the regional stretching lineation. Limbs display moderate to extreme attenuation. The relative rarity of these structures on the upright limbs of SCS and SCA compared to the good preservation on the shared limb, is believed to be due to post-D1 flattening.

No axial planar foliations were observed in hinge zones indicating pre-metamorphic folding, while folded and crenulated biotite schistosities, assumed to be axial planar to D1 folds on their limbs, indicate early-

metamorphic folding. These folds are therefore inferred to be pre- to early-metamorphic. Rare rootless folds with attenuated limbs and intrafolial thickened hinges are inferred to be of D1 origin (Fig. 10A & D).

Qualitative observations of folded mutilayers reveal thickened hinges, thinned limbs, and thicknesses measured parallel to the axial surfaces that are nearly constant. This suggests either flexural flow or slip fold mechanisms (Ramsay, 1967, p. 432). Evidence that these are pre- to early-metamorphic folds suggests both mechanisms were operative. Later metamorphism and D2 flexual flow folding have erased any early evidence, such as slickenslides and stretching lineations, which could provide evidence for differentiation of these mechanisms.

Phase I SCA-SCS structures are designated the earliest structures by the fact that they are overprinted by phase II structures. Phase I structures control the distribution of rock types at the macroscopic scale, while both phase II, and to a lesser extent phase I, control distribution at the mesoscopic-scale, causing difficulty in differentiation of D1 and D2 structures at the later scale. Suggestions that this order is reversed (Brown, 1980, originally mapped SCS as an F3 structure) can be discounted by the fact that D2 axial surfaces are not folded around D1 hinges.

PHASE II STRUCTURES (D2)

Structures and fabrics developed during the second phase of deformation are the most penetrative in the map area, and dominate outcrop-scale geometry (Fig. 10E-G, 11A-G). These syn-metamorphic structures comprise two sets of folds, axial planar fabrics, co-linear stretching and colour streaking lineations (LS).

One set of syn-metamorphic folds are drag folds (for definition see Suppe, p. 342 1985; Fig. 11C-F) which have occasionally developed into non-cylindrical sheath folds (Quinquis et.al. 1978; Cobbold & Quinquis, 1980). These folds are similar in geometry and fabric relationships to the set described below. They are rare and have developed in zones of high shear strain. Observed on a dcm- to m-scale they have curvilinear hinge lines that range from parallel to perpendicular with the mineral stretching lineation, and display eye-shaped fold structures in cross-sections perpendicular to the lineation.

Another set of syn-metamorphic folds are much more penetrative, and are typically asymmetric, dominantly northerly-verging, overturned and reclined (Fig. 10E-F, 11A, B, & G). In profile they comprise multilayers of alternating curved and angular nonparallel (i.e. class 3 and 1c of Ramsay, 1967), tight to isoclinal folds which are locally disharmonic. Axial planes (S2) dip to the west, while hinge lines (L2) are nearly always co-axial with a penetrative west-trending mineral stretching lineation, LS (Fig. 7; cf. Wust, 1986).

This mineral stretching lineation is defined by the preferred dimensional orientation of inequant metamorphic minerals which include garnet, kyanite, sillimanite, hornblende and feldspar, and elongate mineral aggregates composed of the above minerals plus biotite and muscovite. Pressure shadows composed of quartz, feldspar and phyllosilicates also contribute to the definition of the mineral stretching lineation. Paracrystalline boudinage with fractures perpendicular to LS is common. This west-trending mineral lineation is invariably parallel to a strong colour streaking defined by the intersection of D2 crenulation axial planes and SO in the hinges of D2 folds.

Axial planar synmetamorphic fabrics are defined by a weakly developed biotite foliation observed in the hinge zones of semipelitic and quartzo-feldspathic layers (Fig. 10G). Crenulation of pelitic foliations is characteristic of pelitic layers (Fig. 11G; Plate 12H). Although these aspects suggest that the folds developed during the waning stages of metamorphism when the rocks were still ductile (cf. Snoke, 1980), they are also analogous to flexural flow folds formed during amphibolite-grade metamorphism in the Grenville Province of the Canadian Shield (cf. Wynne-Edwards, 1963).

Observations which suggest that these are early to peak metamorphic structures are as follows. Limbs of these folds display intense flattening which has transposed early S0 and S1 foliations into orientations sub-parallel with S2, and have been mimetically overgrown (Hobbs et al. 1976, p. 249; Williams, 1985) by higher-grade minerals of biotite, muscovite, plagioclase, garnet and kyanite. Close examination of fold hinges and thin section studies display the same overgrowth fabric indicating mimetic high-grade fabric growth suggesting possible early metamorphic folding. This explains the difficulty experienced in the field in differentiating between pre- and syn-peak metamorphic fabrics (i.e. S1 and S2 respectively).

In addition, the near-co-axial nature of the fold hinges, colour streaking lineation, and penetrative syn-metamorphic mineral stretching lineation suggest that peak-metamorphic mineral growth occurred with long axes sub-parallel to their present orientations (Journeay, 1986). Journeay (1986) points out that extremely large shear strains could produce a penetrative stretching lineation through rigid body rotation, but dismisses this proposition since this mechanism would not likely result in a regional consistent pattern, and also requires extreme magnitudes of shear strain

for this volume of rock (Skjernaa, 1980). These folds also deform, and are crosscut and truncated by sheared pegmatite coeval with the peak metamorphic assemblages (Fig. 11F).

Using geometrical descriptions of flexural and passive flow folds, and their mechanisms of formation (Donath & Parker, 1964; Wynne-Edwards, 1963) as analogies, D2 folds in the map area are interpreted to be products of a combination of passive and flexural flow folding, and indicative of relatively high-temperature conditions at the time of deformation. Phase II folds and associated mineral stretching lineations are inferred to be pre- to syn-peak (M1 see section 3.4.7) metamorphic structures.

Rare refolding of syn-metamorphic D2 folds by similar syn-metamorphic folds results in type 3 interference patterns (Fig. 11B; Thiessen & Means, 1980) viewed perpendicular to LS and SO. This interference pattern coupled with straight foliations in sections perpendicular to SO and parallel to LS indicate true type 3 fold interference produced by co-axial refolding (Thiessen & Means, 1980). These later syn-metamorphic folds are inferred to be a product of co-axial refolding during one deformation phase (cf. Duncan, 1984 and Van Den Driessche, 1986), and are considered analogous to high-grade structures described by Wynne-Edwards (1963).

Syn-metamorphic D2 deformation has modified earlier D1 folds in two ways. First, they have rarely been observed to interfere in a non-coaxial manner. At one location (Fig. 11A) they produce type 2 interference patterns where D1 fold axes and axial planes are folded by D2 (Thiessen & Means, 1980). Secondly, it appears to have transposed D1 minor structures on the upright limbs of SCA-SCS.

Although D2 fold axes (L2) are generally parallel with LS, at rare locations there exist an acute angle of relatively high magnitude (up to 30

degrees) with folds verging to the northeast. Although a progressive rotation of fold axes into colinearity with LS within any particular fold train was not documented, the above observations suggest D2 reclined asymmetric folds were originally verging somewhere east of north, and have subsequently been rotated into their present westerly trends. These northeasterly verging folds tend to be preserved in more competent quartzo-feldspathic layers that have suffered less shear strain relative to mica-rich layers which have only west-trending folds. Journeay (1986) describes similar reorientation plus tightening of D2 structures as the decollement is approached to the south. Such a minor reorientation of linear fabric elements is consistent with strain-induced passive rotation towards the finite stretching direction in a shear couple with upper member motion to the east or west (Skjernaa, 1980), and is not an uncommon development in zones of shear strain elsewhere (e.g. Sanderson, 1973; Ramsay & Sturt, 1973; Bryant & Reed, 1969; Escher & Watterson, 1974; Bell, 1978; Quinquis et al. 1978).

PHASE III STRUCTURES (D3)

Only at one location (station 84-RS195) is a third phase of folding well developed. They are m-scale warps (Fig. 11H) with vertical axial planes and west-trending hinge lines. These warps have no fabric associated with them, and they deform earlier peak metamorphic fabrics.

3.2.3 UPPER-PLATE STRUCTURES

Observed upper-plate structures comprise two sets of folds. One set includes syn-metamorphic dcm- to dm-scale sheath folds (Brown, pers. comm. 1985). The other set are tight to isoclinal reclined m-scale folds folded

around northwesterly dipping axial planes (Fig. 7) and fold axes which sub-parallel a penetrative west-, to west-northwest-trending mineral stretching lineation. These folds deform compositional layering which is thickened in hinge zones and attenuated along limbs. They are commonly truncated and disrupted by sub-axial planar, layer-parallel sheared pegmatites. Consequently vergence is difficult to determine. Dm-scale, rootless, reclined, isochnal folds observed at one station (84-RS210) suggest an earlier folding event. Since this is a zone of high shear strain they could also be flattened and transposed folds of the above sets. Their presence at only one location does not warrant designation of an earlier deformation event. The penetrative mineral stretching lineation is completely analogous to the lineation in the lower-plate. Although the fold sets and lineations in the upper-plate are nearly identical to D2 folds and mineral stretching lineations in the lower-plate, they cannot be correlated across the detachment surface where sheared pegmatite is highly concentrated and not folded.

3.2.4 BOUDINAGE

In the map area, boudinage of amphibole-rich lithologic units can be very spectacular. Boudinage is a common structure in ductiley deformed terranes throughout the world, and is believed to be a direct consequence of layer-parallel extension of layers with different rheology (see Ramsay, 1982). Long axes of boudins can be found both perpendicular and parallel to the regional stretching lineation. Those perpendicular are interpreted as products of extension associated with west-over-east shearing on the detachment, and are discussed in section 3.4.3. Those parallel to LS are believed to be products of flattening and extension which accompanied both

D1 and D2 folding. They show a variety of forms (Fig. 12) similar to those described by Rast (1963) and Ramsay (1982).

Boudins range from dcm- to 10 m-scale, with amphibolites and orthoamphibole boudins generally being the largest. Incipient boudinage is marked by mm-scale tension fractures perpendicular to LS. These are infilled with chlorite, epidote and actinolite, and are inferred to be late-stage brittle structures (see section 3.3). Boudinage is a structure formed during all stages of deformation. Those boudins associated with D1 and D2 folding are the most spectacular qualitative indicators of high strain (cf. Hanmer & Lucas, 1985) in the map area.

3.2.5 REGIONAL RELATIONSHIPS

Comparison of the deformation hierarchy and their respective structures shows that structures of the map area are in complete accord with those mapped elsewhere in the complex (ref. op. cit.). Journeay (1986) has interpreted the SCS and structurally underlying Kirbyville Anticline (KA, Brown, 1980) to be parasitic structures on the short overturned limb of the Grace Mountain Syncline (GMS) mapped to the south. The SCA (this study) may be another parasitic fold to the GMS. Alternatively this allows the interpretation that the KA is the major structure to which the SCS-SCA are parasitic.

Based on fold and associated fault styles, and stratigraphic arguments, Journeay (1986) favours correlation of this major structure with an unnamed isoclinal-syncline mapped above the Bews Creek Fault at the south end of Frenchman Cap dome. If this correlation proves accurate then the SCS-SCA are the structurally highest structures mapped in the north end of the Monashee Complex.

Okulitch (1984) has suggested that these structures may have been generated during one of three pre-Mesozoic events: (1) deformation associated with the Hudsonian Orogeney in the Canadian Shield, (2) the Proterozoic East Kootenay orogeney (ca. 1350-1300 Ma, McMechan & Price, 1982), and (3) post-early Cambrian, pre-Carboniferous orogenesis in the Kootenay Arc (Read & Wheeler, 1976). Mapping at the south end of Frenchman Cap dome (Fyles, 1970a, b; Hoy & McMillan, 1979) reveals that the Mount Copeland nepheline syenite gneiss and related deposits (e.g. carbonatite) are involved in this phase of early folding. If one accepts the U-Pb zircon radiometric dates, 773 +280, -218 Ma (Okulitch et al. 1981) and 746 +40, -39 Ma (Parrish, unpublished data 1986), as the approximate age of magmatic crystallization of this body, then D1 folding must be later than ca. 750 Ma which discounts the first two of the above options. Further geochronologic data is required in order to constrain the age of these folds.

To the south in the vicinity of Ratchford Creek, Journeay (1986) notes that syn-metamorphic D2 cross-folds can be traced into deeper structural levels where they are part of a northeasterly-verging set of asymmetric km-scale folds. These folds extend south to Thor-Odin dome and appear to be kinematically linked with syn-metamorphic thrust faults at the south end of the complex (Duncan, 1984). On the basis of radiometric data and crosscutting relationships determined elsewhere in the Omenica Belt (see section 1.3), Journeay (1983, 1986) and Journeay & Brown (1986) infer that these structures formed during the late Middle Jurassic. D2 structures in the map area are interpreted to be part of this fold set.

Third phase folds are believed to be part of a set of west-trending post-metamorphic folds which weakly overprint all other folds to the south

(Journeay, 1986). They are thought to have developed during late stage uplift, transpression and flexure that produced the Monashee Antiform (Journeay, 1986).

Characteristics of upper-plate structures in the map area are consistent with D2 folds of Journeay (1986) mapped to the south, and are herein interpreted to be part of that set. Journeay (1986) proposes two possible relationships. First, based on vergence and stratigraphic arguments, is that they may be high-order parasitic structures on southwest-verging recumbent structures with limb lengths of >50 km, similar to the Scripp Nappe to the north of the complex (Raeside & Simony, 1983). Second, is that they may have originally been south-southeasterly-verging folds that were rotated to their present orientation during overthrusting on the Monashee decollement.

3.3 BRITTLE DEFORMATION

All structures and fabrics formed by ductile processes are overprinted by four sets of brittle features. They have had little influence on the overall structural geometry of rocks in the map area relative to those to the south. These comprise a north-trending set of down to the west normal faults, a set of conjugate shear fractures, and two sets of extension fractures. A systematic detailed study of these features was not undertaken. The following summary is based on few detailed measurements and numerous qualitative field observations.

NORMAL FAULTS

North-trending, high-angle normal faults with down to the west displacements are late-stage features of local importance only. Ranging in

width from mm- to m-scale and lengths from m- to km-scale, only two were of sufficient scale to be mapped (Fig. 6 in back pocket). One lies in the north-central part of the map area while the other lies in the central part. Several other zones of fracture and brecciation with characteristics similar to the normal faults are believed to be associated, and are also of sufficient scale to be mapped. These zones of fracture have vertical to steep westerly dips, are 1 to 20 m wide, and can be traced along strike for distances ranging from 100 m to several kilometers. They are marked by brecciated fault wall rocks. In some cases fault wall breccia is supported in a matrix of fine-grained fault gouge. Some zones are chloritized and silicified, some silicified, others bleached, and some not affected by these processes.

A fault in the central part of the map area is tentatively marked as a normal-type. This vertical to steeply dipping zone is up to 20 m wide, and marked by a mixture of chloritized and silicified gouge. It truncates metamorphic fabrics and compositional layering dipping moderately to the south, and shows an apparent left lateral displacement of ca. 25 m. This apparent displacement can be explained by four single motion fault types which include: (1) strike-slip, (2) reverse dip-slip, (3) a combination of (1) or (2), or (4) scissor-type normal motion with greater displacement at its south end. Multiple displacements cannot be ruled out. Scissor-type normal faults of much larger scale are known to the south, (Journeay, 1986) and for this reason option (4) is favoured.

Normal faults and related fractures in the map area are interpreted to be associated with major north-trending scissor-type normal faults that lie within the Monashee complex to the south. These are the Englishman Creek and Perry River structues, the latter of which can be traced for >30 km

from Kirbyville Creek in the north, where displacements are minimal, to Bews Creek in the south, where displacments are in the order of several hundred meters (Wheeler, 1965; Fyles, 1970b; Hoy & Brown, 1980; Journeay, 1986). This fault is believed to extend into the Eagle River detachment (Journeay & Brown, 1986). These brittle faults and others are interpreted by Journeay and Brown (1986) to represent a break-away zone for the Okanagan Shear zone to the southwest, which was active in the Eocene (Bardoux, 1985, 1986; Templeman-Kluit & Parkinson, 1986).

CONJUGATE SHEAR FRACTURES

Conjugate shear fractures are best exposed in rock faces parallel to the regional stretching lineation and perpendicular to compositional layering, and are most commonly developed in competent units. One set strikes between 350 and 010 degrees and dips between 90 and 50 degrees to the east. The second set has a similar strike but dips 70 to 90 degrees to the west. These shears display thicknesses and displacements in the mm-scale and often show no displacements. These are interpreted to be second-order fractures associated with larger shears displaying m-scale displacements mapped to the south (Journeay, 1986).

EXTENSION FRACTURES

Two sets of extension fractures are present in the map area. The first set are best developed and comprise mm-scale fractures oriented perpendicular to the mineral stretching lineation, and mark incipient boudinage of selected layers. They measure 1 to 3 mm wide. In vertical cross-section, parallel to the west-trending mineral stretching lineation they are 1 to 5 cm high. In layer parallel cross-section they range from 1

to 30 cm long. A second set, sporadically developed, strike at ca. 065 and dip 80 to 90 degress to the southeast. Only one, in the northwest corner of the map area, was of sufficient scale to map with an extension displacement of ca. 2 m (Fig. 6 in back pocket). Both sets of extension fractures are developed in competent units. These sets of extension fractures are believed to be second-order structures associated with similarily oriented extension fractures, commonly filled with 1 to 3 m thick pegmatite and lamprophyre dykes, mapped to the south (Wheeler, 1965; Journeay, 1986)

REGIONAL RELATIONSHIPS

Applying Anderson's theory of faulting (see Suppe, p. 292-295, 1985) the orientations of the principal stresses prior to fracture can be estimated. In the map area, the north-striking extension fractures and conjugate shears imply a vertical to steeply easterly-plunging principal stress, north-trending near-horizontal intermediate stress, and a west-trending principal extension axis. Similar orientations have been inferred to the south where larger-scale joint sets, commonly filled with mafic or pegmatite material, are interpreted to have accommodated a maximum of 500 m extension (Journeay, 1986). The relationship between northeast- and north-striking extension fractures is not known in the map area. To the south, where they are conjugate, the northeast-striking set are inferred to have formed during a component of northeast extension (Journeay, 1986).

Brittle features within and flanking the Monashee complex are believed indicative of second-order processes produced through compression-induced uplift and denudation of the Monashee complex during Late Cretaceous to early Tertiary time (Brown & Journeay, 1985; Journeay & Brown, 1986;

Journeay, 1986). This interpretation is based on: (1) K-Ar data which indicates Eocence cooling ages for mafic dykes infilling extension fractures (Wheeler, 1965; Lane, 1984b), (2) orientation of principal stresses prior to fracture (Journeay, 1986), (3) estimated amounts of extension which are far less then those expected in models of lithospheric megaboudinage or dextral strike-slip faulting (Journeay, 1986), and (4) the presence of brittle, high-angle normal faults that root to the east on the east side (Columbia River fault; Read & Brown, 1981; Lane, 1984 a, b), and root to the west on the west side (Eagle River detachment; Journeay & Brown, 1986) of the complex.

3.4 MONASHEE DECOLLEMENT AND RELATED MYLONITIC ROCKS

3.4.1 INTRODUCTION

In the northwest corner of the map area a northwest-dipping zone of detachment truncates stratigraphy and structures of the footwall (Fig. 3 & 6). Most rocks of the hanging and footwalls are mylonitic (see Appendix 2). Fabrics and structures believed to have been generated during shearing along the detachment under amphibolite-grade conditions include: S-C tectonites (Lister & Snoke, 1984) which display a strong mineral stretching lineation, variably developed mylonitic foliations and microstructures typical of strain softening, D2 folds, boudinage and rotational normal faults in competent lithologies, plus melt softened shears. The following sections describe these features, attach a kinematic significance to them, summarize a preliminary analysis of the variation in strain, strain rate and deformation paths as revealed in thin section, analyse strain softening mechanisms, and attempt to determine the physical conditions under which they formed.

3.4.2 MACRO- & MESOSCOPIC DISCONTINUITIES

In the northwest corner of the map area a zone of detachment is marked by a ca. 100 m thick melange composed of up to 50% concordant and subconcordant sheared pegmatite and intercalated disrupted pelitic, semipelitic and quartzo-feldspathic rocks with minor quartzite and amphibolite (Plate 1B & C). This distinctive zone, clearly visible from a distance, is best exposed in inaccessible south- and east-facing cliffs. "Hands on" experience was acquired through inclined traverses up the >8100 ft., unnamed peak at the north end of the map area. Detailed mapping reveals a low-angle truncation of folded footwall stratigraphy in the core of the Sibley Creek Anticline, and along its upright limb to the west of the icefield (units 3 to 11).

As one approaches the detachment from within the footwall an increase in strain is indicated by attenuation and thinning of lithologic units (especially along the upright limb of the Sibley Creek Anticline), the overturning and tightening of second phase folds, and the increased sugary and vitreous appearance of mylonitic quartzite near the detachment. Within the lower- and upper-plates, sub-axial planar, relatively thin mm- to m-scale, pegmatitic shears commonly truncate D2 folds. Notable are mm- to cm-scale shears marked by biotite-sillimanite intergrowths and pulled-apart, lineated parallel to LS, sillimanite sheets up to several square meters in size (Plate 12C & D), which also truncate D2 structures and fabrics.

3.4.3 KINEMATICS

Meso- and microscopic observations of both upper- and lower-plate rocks reveal fabrics and structures believed to be useful as kinematic

indicators; structures "resulting from flow, whose geometry is indicative of the progressive rotation of the principal axes (stretches) of the kinematic framework and/or the shear plane of the deformation" at the scale of observation (Hanmer, 1984b, 1986). Their kinematic significance is based upon proposed testable hypotheses (see Hanmer, 1984b, 1986 and references cited therein). Only where a structural assemblage of mechanically independent kinematic indicators (two of more) were observed, was a kinematic significance allocated (Fig. 8 in back pocket). Kinematic indicators that were most useful in determining sense of shear were S-C foliations (Berthe, et al. 1979), and shear bands (Platt & Vissers, 1986). Other less common but useful kinematic indicators were sheath folds (Cobbold & Quinquis, 1980), rotation of axial planes (Hanmer & Lucas, 1985; Hanmer, pers. comm. 1986), rotated porphyroclasts (Ghosh & Ramberg, 1976; Hanmer, 1984b; Simpson & Passchier, 1985), and rotated listric normal faults.

Rocks in the map area are S-C tectonites (Lister & Snoke, 1984) which display a penetrative mineral stretching lineation, herein assumed to define the direction of principal finite extension. Kinematic indicators were best observed for their kinematic significance on rock faces, and in thin sections, oriented perpendicular to the foliation and parallel to the mineral stretching direction. The dominant sense of shear is west-over-east (i.e. the upper member of the shear couple was displaced eastward). Local zones of opposite shear sense are present and explanations for this are offered at the end of the section. The following describes the most significant kinematic indicators in the map area, their proposed mechanisms of formation and kinematic interpretation.

S-C FOLIATIONS

Mylonitic S-C foliations have recently been used extensively as shear sense indicators (e.g. Berthe et al. 1979; White et al. 1980; Brown & Murphy, 1981; Simpson & Schmidt, 1983; Lister & Snoke, 1984). They form in zones of non-coaxial strain (Berthe et al. 1979; Lister & Snoke, 1984). C-foliations are interpreted as discrete shear domains that commonly define a compositional layering parallel to the walls of the shear zone, and are therefore assumed to define the bulk plane of shear (cf. Passchier, 1986). The presence of rigid porphyroclasts commonly causes a deflection of these planes. S-foliations are a second set of flattening foliations defined by flattened and foliated mineral aggregates and elongate minerals which initially form an acute angle of ca. 45 degrees to the C-foliation. This foliation contains the maximum extension direction, and is assumed to approximate the XY-plane of the finite strain ellipsoid. In ideal progressive simple shear the principal axis of finite extension, initially oriented at 45 degrees to the shear plane, rotates towards the shear plane with continued shear strain (Hobbs et al. 1976). In this manner S-foliations rotate towards the C-foliations with accumulated shear strain. The sense of displacement across the zone of shear, and to a lesser extent the magnitude (Ramsay & Graham, 1970) of shear strain, can be determined through recognition of the facing direction of the acute angle between C- and S-foliations, and its magnitude.

According to Berthe et al. (1979) it is important that these two foliations develop synchronously, a specification that is generally difficult to determine (Lister & Snoke, 1984). In mylonitic rocks of the study area no unequivocal timing relationships could be established, and they are assumed to have been generated simultaneously.

Meso- and microstructural observations reveal C-foliations parallel to compositional layering (SO1; Plate 4). They are discrete, continuous and discontinuous shear domains composed of heterogeneous quartz most commonly in the form of ribbons, plastically and brittely deformed feldspar, biotite-sillimanite intergrowths and foliated phyllosilicate-rich segregations. Although generally planar, they do wrap around broken porphyroclasts and foliation fish which define flattening foliations.

Flattening fabrics define S-planes which form acute angles of less than 45 degrees with the C-planes. They are well defined by the long axes of grains of kyanite, sillimanite, feldspar, garnet and quartz, some displaying paracrystalline boudinage with pull-aparts perpendicular to the stretching lineation. Mica and foliation fish composed of foliated aggregates of any or all of the above minerals, plus recrystallized polymineralic pressure shadows, also contribute to the definition of S-planes.

In the field, these fabric elements are often difficult to differentiate. This is probably due to mimetic metamorphic fabrics overgrowing a foliation which approximates the shear-surface (C-foliation), and in other cases may be due to a high value of finite shear strain which would rotate S-planes into C-planes. C-foliations and rotated S-foliations characteristically wrap around more rigid porphyroclasts resulting in an anastomozing foliation parallel to the compositional layering. Where S-foliations do not parallel the C-foliation, they are most commonly inclined to the east indicating a west-over-east sense of shear.

SHEAR BANDS

Shear bands are very useful kinematic indicators in the map area.

These structures and their kinematic significance have been discribed by White et al. (1980), Platt and Visser (1980), Platt (1984), Harris (1983), Harris and Cobbold (1983), Passchier (1984) and Gapais and White (1982), and have been used extensively in recent studies as indicators of shear sense (see references cited in previous section and selected bibliography).

These secondary penetrative cleavages, or ductile shear bands, form in the late stages of shear zone development as conjugate, multiple and single sets oriented oblique (<45 degrees, typically ca. 30 degrees) to the C-foliations which they overprint. They are believed to develop when bulk flow in shear zones is spatially partitioned (Lister & Williams, 1979, 1983) such that it deviates from simple shear (Platt & Visser, 1980; Platt, 1984). This is probably due to the anisotropy developed through the intensification of primary foliation (White et al. 1980; Gapais & White, 1982; Platt, 1984). Care must be taken to determine which set(s) are present (Harris, 1983; Harris & Cobbold, 1985). Single sets of shear bands oriented at a low angle, and displaying a synthetic shear sense, to the bulk flow plane can be used as kinematic indicators (White et al. 1980; Platt & Visser, 1980; Platt, 1984).

In the map area shear bands are most common in pelitic rock types, and best displayed on rock faces and in thin sections cut perpendicular to the foliation, and parallel to the stretching lineation. Both conjugate sets and single sets are present, and crosscut S-C foliations. Originating and ending in C-foliations they are sigmoidal in cross-section, and form maximum angles ranging from 10 to 30 degrees with the C-foliations (Plate 4). They also occur as discrete extensional shears at the ends of foliation fish, porphyroclasts and mafic boudins, where they lie in the "pinches" between these asymmetric features (cf. Hanmer, 1986). "Swells",

internal foliation, and pressure shadows are deflected into single sets of shear bands. In thin section they clearly crosscut earlier fabrics and are commonly marked by relatively fine-grained phyllosilicates and opaque oxides. Of the phyllosilicates, biotite is the most common. Recrystallized pressure shadows also define these extensional shears. Single sets of shear bands dip to the east at 10 to 45 degrees relative to the C-foliation, and are inferred to record west-over-east senses of shear.

ASYMMETRIC PULL-APARTS AND FOLIATION FISH

Boudinage is a common structure in the more competent mafic layers. Boudins with long axes parallel to the stretching lineation are believed contemporaneous with the generation of D1 and D2 folds, and are described in section 3.2.2. Boudins perpendicular to the stretching lineation are products of shear strain associated with the detachment. They have a wide variety of shapes (Fig. 12), presumably reflecting contrasting competences of the enclosing layers and boudinaged layer (Ramsay, 1982; Hanmer, 1984b, 1986) and the effects of internal anisotropy (Hanmer, 1984b, 1986).

Hanmer (1984b, 1986) has described asymmetrical pull-aparts and foliation fish, plus their kinematic significance based on a mechanical model. In the presence of angular corners the competency/viscosity ratio controls the response of the boudin to layer parallel shear. Corners that lie within the extensional quadrants of the instantaneous strain ellipsoid develop maximum mean stress and flow towards the lower pressure interboudin gaps (type 1 asymmetrical pull-apart). Internal anisotropy controls the response of pinch and swell structures in the absence of angular corners. Depending upon the orientation of the internal anisotropy to the bulk flow

plane the canalizing effect of the anisotropy to maximize slip along these planes causes deviations in the local shear regime. The "swells" will deform either: (1) to produce apparent back rotation, (2) by back rotation of the internal anisotropy but not the principal geometric plane, or (3) back rotate the internal anisotropy and principal geometric plane (Type 2A, Fig. 12E & F). Antithetic rotation of "swells" can also be a result of displacement along discrete extension shears, analogous to shear bands, located between the "swells" (Type 2B, Fig. 12C & D). In well foliated rocks where competent layers are absent, foliation fish can develop. These structures are geometrically analogous to Type 2 asymmetrical pull-aparts. All of the above structures are present but not common in the map area. The majority (ca. 10:2) were interpreted to indicate west-over-east senses of shear.

FOLDS

Sheath folds and their use as kinematic indicators have been described by Quinquis et al. (1978) and Cobbold and Quinquis (1980). They are not common in the map area. Where present their cross-sections display a typical eye shape pattern (Fig. 11E), or vergence reversals looking down the lineation (Fig. 11F). Where the direction of closure can be determined they give a west-over-east sense of shear.

Axial planes of dcm-scale and micro-scale drag folds (for definition see Suppe, p. 342, 1985), in a given fold train or as one approaches the closure of a given fold, have been observed in cross-sections to rotate toward the bulk shear plane in such a manner that the magnitude of dip of west-dipping axial planes decreases (Fig. 11C). These observations can be used to determine shear sense which is interpreted to be synthetic with the

sense of rotation indicated by the change in orientation of the the axial planes (Hanmer & Lucas, 1985; Hanmer, pers. comm. 1986). The above observations indicate a west-over-east shear sense. Fault propogation folds (for definition see Suppe, p. 398, 1985) have also been observed in vertical east-west cross-sections (Fig. 11D). They are interpreted to indicate a west-over-east sense of shear.

ROTATIONAL NORMAL FAULTS

Sets of planar rotational normal faults localized in more competent mafic lithologies are a common feature observed in rock faces parallel to the stretching lineation, and perpendicular to the foliation (Plate 5). Trains of rotated blocks, usually with dimensions longer perpendicular than parallel to the compositional layering, have been rotated along essentially planar synthetically rotated, consistently west-dipping shears, some of which root in leucocratic segregations.

A number of recent publications illustrate similar structures observed in the field (e.g. Borradaille et al. 1982, plates 74, 75; Davis, 1980, Figs. 9 & 20; Rehrig & Reynolds, 1980, Fig. 3f; Bally et al. 1981, Fig. 1 and references cited therein) and as fault block models (e.g. Wernicke & Burchfiel, 1982; Brun & Choukrone, 1983; Gibbs, 1984; Nur et al. 1986). This phenomena is well illustrated by analogy with a sheared stack of dominos, books or cards (Fig. 13A & B).

In a general progressive deformation where layer parallel progressive simple shear is dominant, a layer normal progressive pure shear strain component may manifest itself in extension fractures perpendicular to bedding, or shear fractures inclined to bedding. The progressive simple shear strain component may also be responsible for the tension fractures.

Using the analogy of fibre loading (White et al. 1980), tangential stresses applied to the surface of the competent layer by ductiley flowing bounding layers may be balanced by layer parallel tension in the competent layer, resulting in tension fractures perpendicular to the layering. Once these fractures are formed, tangential stresses cause rotation of the blocks and faults synthetic with the flow. The more ductile bounding layers serve as a cushion and fill the spaces (see fault block models ref. op. cit., Plate 5A) created by rotation of the fault blocks. Those fractures that are not inclined in the direction of flow may undergo folding as they rotate and enter the compression field of the strain ellipsoid (Fig. 13C).

Davis (1980) suggests that similar structures in core complexes in the southern Basin and Range province indicate a dominance of flattening, and are indicators of a regional system of extension deformation. In a progressive pure shear model these faults should rotate in the direction of their initial inclination to the compression axis. If these fractures originate as extension fractures they theoretically will have no inclination and should not rotate. Perturbations developed through strain partitioning, and inclinations due to anisotropy, can cause rotation, but over a large area no preferred orientation should be expected. If there is a component of progressive simple shear in the general progressive deformation then the fractures become faults and rotate with the same sense of vorticity as the progressive simple shear strain component, resulting in a preferred orientation. The problem in the latter case is that it does not reveal which two components, progressive simple shear strain or progressive pure shear strain, in a general progressive deformation are dominant over the other. As noted by Gibbs (1984) large layer parallel extensions and boudin rotations are required before appreciable thinning of

a mutilayer sequence can take place.

The above theoretical model is used to interpret such structures observed in the field. In the map area, both fault planes and blocks are inferred to have rotated clockwise looking north perpendicular to the lineation, and are interpreted to indicate a west-over-east sense of shear. Further support for this interpretation is found in the ductile boundin g layers which synchronously fill the gaps created. These layers have penetrative mylonitic fabrics (S-C foliations and shear bands) which indicate equivalent senses of shear to the above interpretation (Plate 5A), and are believed to indicate the dominance of progressive simple shear strain.

At one locality (station 85-R167) rotational normal faults dissected a boudin in such a way as to indicate a north-over-south sense of shear (Plate 5C). This observation, coupled with the observations of boudins parallel to the stretching lineation, are indicative that the strain was heterogeneous and typically partitioned (Lister & Williams, 1979, 1983).

DISCUSSION

Kinematic indicators observed in the map area display a dominant west-over-east shear sense, as opposed to east-over-west shear sense (40:9, Fig. 8 in back pocket). The latter occur in a cluster in the north central part of the map area. Kinematic indicators in this zone display the same relationships to deformation and metamorphism as those elsewhere in the field area. This zone must therefore represent a volume of antithetic flow within the zone of high shear strain associated with the Monashee decollement. There are several possible explanations for the presence of this zone.

Folding of mylonitic rocks around fold axes parallel to the mineral stretching lineation could produce a reversal in the sense of shear. This mechanism is unlikely in the map area since west-trending, reclined, isoclinal post-metamorphic folds have not been recognized, and no such structures are present anywhere in the complex.

This zone may reflect strain partitioning (Lister & Williams, 1979, 1983) throughout the entire zone of shear. In this case, strain was partitioned in such a way to cause a zone of antithetic shear. Similar arguments have been made by Bouchez et al. (1983) to account for reversals in quartz petrofabric asymmetry in the Cabo Creus shear zone. This suggestion cannot presently be tested.

Sanderson (1982) presents a theoretical model in which shear strain within a thrust sheet experiences a reversal in shear sense on leaving a ramp. At present this suggestion also cannot be tested, but fits proposals by Journeay (1986), Journeay and Brown (1985), Brown and Journeay (1985), Brown et al. (1986), Brown and Journeay (1985) and Brown and Read (1983) that the complex is the exposed upper-horse of an east-verging antiformal duplex.

Other possible models which fit a model of duplex building for the Monashee complex (references cited above) are presented by Law et al. (1984). These are variations of strain partitioning in a thrust sheet. One model portrays thinning of a lower thrust sheet at a ramp when an overlying, more competent thrust sheet, resists deformation as it moves over the ramp. A second model involves thinning of a thrust sheet as other thrust sheets are loaded on top of it. A third model involves thinning of a thrust sheet due to gravity spreading. All of these models could explain the relatively small zone of sense of shear reversal, but none can be tested.

3.4.4 MICROFABRICS AND MINERALOGY

Studies of polyphase mylonitic rocks show that mineralogy, internal structures, and microfabrics can record the operation of a range of deformation and metamorphic processes, and the conditions under which they operated (e.g. Vernon, 1976; Hobbs et al. 1976; White, 1977; Kerrich & Allison, 1978; Schmid, 1982; White et al. 1982; Knipe & Wintsch, 1984). The presence or absence of various internal optical strain features (e.g. kinks, deformation bands, undulatory extinction, etc.) records the active interplay of deformation, recrystallization and neomineralization. These microstructures are relatively easily identified and can be used in conjunction with porphyroblast-matrix microstructural criteria in determining the chronological relationships between mineral growth and deformation (e.g. Spry, 1963; Zwart, 1960a, b, 1963; Bell, 1985; Bell et al. 1986; Vernon, 1976, 1977b, 1978). Most chronological inferences rely upon interpretations of porphyroblast-matrix relationships, most of which are clearly ambiguous and subject to several interpretations (Vernon, 1977b, 1978; Bell et al. 1986). Other useful criteria include inferred reactions and their mechanisms, microstructures, and inferred conditions of deformation. In consideration of the above, the mineralogy and microstructures of pelitic and quartzo-feldspathic rocks, plus quartzite, were studied in thin section, and a chronological analysis was made with extreme care and is summarized in Table 2. A summary of the mineralogy present in thin sections studied is presented in Appendix 3. The following sections summarize the optical strain features and microstructures of the main mineral components as typified in mylonitic rocks of the map area.

QUARTZ

The quartz phase of the mylonitic foliations displays a range of shapes. In phyllosilicate-rich domains quartz grains tend to be elongate parallel to the foliation, with smooth to extremely irregular grain boundaries. Quartz ribbons are composed of inequant and amoeboid shaped grains, and are commonly wrapped around rigid porphyroclasts (Plate 6C). Some are elongate with aligned grain boundaries, imparting a weak foliation inclined to the quartz ribbon boundaries. Quartzites are composed of inequant irregular grains. Some grain boundaries appear to be pinned by aligned micas (Plate 6A & B), maintaining the foliation. Others have grown to enclose micas and other quartz grains. A preferred crystallographic fabric is indicated by observations with a lambda plate. All quartz grains throughout the map area display weak to moderate undulose extinction. Subgrains and deformation bands are present, but not well developed.

Microstructural features produced in quartz through natural and experimental deformation, recovery and recrystallization have been the subject of several papers (e.g. Vernon, 1976; Wilson, 1973, Marjoribanks, 1976; White, 1973, 1976, 1977; Lister & Hobbs, 1980; Lister et al. 1978; Bouchez et al. 1983). Comparison with the above work suggests that quartz in the map area has deformed in a ductile manner, generating fabrics entirely consistent with quartz microstructures formed during amphibolite-grade, dynamic recovery and recrystallization (see Wilson, 1973).

Further proof of syntectonic (i.e. syn-shearing) quartz growth is its presence in pressure shadows and in fractures between porphyroclasts. This quartz was most likely crystallized from solution. Post-ductile shearing quartz is evidenced by its existence in viens crosscutting the mylonitic fabric elements.

FELDSPAR

Both plagioclase and K-feldspar are present in a variety of forms. Where polysynthetic twinning was present, optically determined plagioclase compositions range from An15 to An30 (oligoclase). Lack of twinning and its resemblance to recrystallized quartz made optical identification of K-feldspar difficult. Staining of rock slabs corroborated its existence in some pelitic specimens. Feldspar porphyroclasts are equant to elongate with well defined lobate, smooth, and rare embayed grain boundaries, some marked by a yellow alteration. Some porphyroclasts display core and mantle structures, sweeping extinction, and less commonly microfracturing, and often form augen elongate parallel to the foliation. These porphyroclasts are both twinned (polysynthetic) and untwinned, and display evidence of strain in the form of bent and sheared twins, narrow needle-shaped twins terminating inside grains, and undulatory extinction. Both feldspars commonly coexist with quartz, forming spindle-shaped aggregates. Mutual boundaries are usually lobate. Individual grains of these aggregates show weak undulatory extinction and are most commonly untwinned.

Dynamically recrystallized grains can be found as mantles around larger augen and along shear planes within larger crystals. They have slightly equant to elongate shapes with smooth curved and lobate grain boundaries. Locally they form low energy equilibrium microstructures. Most are untwinned with weak sweeping extinction.

Myrmekite intergrowths are common along mutual boundaries between plagioclase and K-feldspar, and along the margins of both feldspar porphyroclasts (Plate 6D). These myrmekitic intergrowths resemble those in upper-amphibolite grade mylonitic rocks described by Hanmer (1982) and Simpson (1985). Both researchers suggest strain enhanced diffusion as a

process for its formation in mylonitic rocks. A review of possible mechanisms of formation is summarized by Phillips (1974). Recognized metamorphic myrmekite-forming processes are retrograde, and include exsolution from, and replacement of K-feldspar. Ashworth (1986) has recently described myrmekite interpreted to have formed by prograde replacement of albite. The relationships and textures of myrmekite observed in the map area suggest that all of the above processes were active.

Experimentally and naturally deformed feldspars, which display a wide variety of microstructures (e.g. White, 1975; Vernon, 1975a, 1976; Debat et al. 1978; Lister & Price, 1978; Berthe et al. 1979; Hanmer, 1982; Tullis, 1983; Jensen & Starkey, 1985), are poorly understood in terms of deformation mechanisms. Comparison of microstructures observed in rocks of the map area, with those of the above studies, suggest that >60% of the feldspar has deformed ductiley, and dynamically recrystallized via bulge nucleation and subgrain rotation mechanisms (White, 1975; Vernon, 1975a; Jensen & Starkey, 1985) under amphibolite-grade conditions. Brittle fractures are interpreted to be a consequence of lower-grade deformation, or higher strain rates, or both.

All feldspar appears to be syn-shearing as evidenced by internal strain features and their morphology. Some syn-tectonic porphyroblasts of plagioclase overgrow earlier S1 biotite fabrics and are intergrown with syn-tectonic biotite and/or sillimanite in its pressure shadows (Plate 6E & F). The presence of plagioclase in pressure shadows of kyanite and garnet is also indicative of a syntectonic origin. Some rare grains show oscillatory zoning. This suggests that partial melting occurred at these location.

PHYLLOSILICATES

Deformation and recrystallization processes, and associated optical features, of naturally and experimentally deformed biotite and muscovite have been investigated by relatively few workers (e.g. Etheridge et al. 1973; Etheridge & Hobbs, 1974; Vernon, 1976, 1977a; Wilson & Bell, 1979; Bell, 1979; Behrmann, 1984; Lister & Snoke, 1984; Bell et al. 1986). Biotite, muscovite and chlorite are ubiquitous in pelitic rocks of the map area. Summarized below are their optical strain features and fabric relationships which indicate the existence of several generations, and conditions under which they deformed and recrystallized.

Biotite

Fine- to coarse-grained biotite occurs in several different forms indicating the operation of several deformation processes. The first consists of relatively large porphyroclasts analogous to type I grains of Wilson and Bell (1979). They are usually deformed, displaying variations from gentle bending indicated by sweeping extinction and bent cleavage planes, to sharp kinks (Plate 7A). Kinks generally do not penetrate across grains, are commonly localized along broad warps, and have shapes ranging from discrete lenses to zones of multiple kinks. Kink band boundaries are planar and irregular, and commonly displace (001) cleavage. These grains can be folded and display slip and segmentation along the (001) cleavage. Where grains are in mutual contact, serrated grain boundaries indicate either biotite dissolution (Wilson & Bell, 1979), or migration processes (Etheridge & Hobbs, 1974). These grains commonly form foliation and mica fish defining S-foliations (Berthe et al. 1979, see section 3.4.3).

A second type of biotite is analogous to type II grains of Wilson and

Bell (1979). These grains usually occur in narrow aggregates of aligned grains, and are commonly intergrown with quartz, plagioclase, and sillimanite. Together with rotated type I grains, they contribute to the definition of the mylonitic C-foliation (see section 3.4.3 and Berthe et al. 1979). They are usually less deformed than type I grains. Type I grains, occasionally occurring within type II aggregates, are gradational into type II grains. Some grains in the type II aggregates are extremely ragged with undulose extinction. At higher grades type II grains are intergrown with sillimanite.

A third type of biotite is found in very fine-grained aggregates which form discontinuous mantles around both type I and type II grains. These recrystallized grains are analogous to those described in rocks deformed under amphibolite-grade conditions (Bell, 1979).

The above microstructures are indicative of strain through kinking, lattice bending, recovery and recrystallization processes. Accompanied by other textural criteria, they indicate at least three generations of biotite growth. Relatively rare first generation pre-shearing biotites define a flattening foliation (S1) axial planar to D1 folds. These grains are commonly overprinted and transposed into the S2 foliation. Remnants can be recognized as ragged grains with undulatory extinction within aggregates of type II biotite, or as aligned inclusions within porphyroblasts of garnet, plagioclase and kyanite (Plates 6E, 7D, 8A). Pre- to syn-shearing biotites comprise all three microstructural types described above. They define the mylonitic foliation, some are axial planar to D2 folds, and others have mimetically overgrown a crenulated foliation in D2 hinges. Some are intergrown with porphyroblasts of kyanite, garnet, muscovite and plagioclase, and grow in their pressure

shadows (e.g. Plate 8A). The youngest biotite grains occur as laths which grew across the mylonitic fabrics (Plate 7B), and as alteration products associated with chlorite found along fractures in garnet.

Muscovite

Microstructures of muscovite are completely analogous to those of biotite. Inferred processes of deformation include bending of the lattice, kinks, recovery and recrystallization indicating a wide range of metamorphic conditions.

First generation muscovites overgrow earlier biotite, lie in the mylonitic foliation, and appear to be pre- to syn-shearing (Plate 6G & H) and axial planar to D2 folding. Porphyroblasts of kyanite, garnet and plagioclase commonly overgrow these grains. A second generation of muscovite growth is evidenced by laths which have overgrown and crosscut the mylonitic fabric, enclose kyanite (Plate 9F), and grow within aluminosilicate pull-aparts (Plates 6C, 9G & H). The latest generation of muscovite appears as fine-grained laths associated with biotite and chlorite in garnet fractures, as sericite alteration of feldspars, and as fine-grained mats which have altered biotite-sillimanite intergrowths.

Chlorite

Chlorite is a retrograde late stage product. It can be found in radiating clusters (Plate 4B), in fractures of garnet associated with biotite and opaque oxides (Plate 7C), and as mimetic alterations of older biotite grains. No syn-kinematic chlorite was observed.

GARNET

Garnet is present in most rock types throughout the map area (Plate 7C-H). Porphyroblasts are equant to oblate spheroids with long axes parallel to the regional stretching lineation (Plate 12B). In thin section they do not display any features indicative of ductile intracrystalline strain. Formation of brittle fractures perpendicular to the mineral stretching lineation is most common. The few desriptions of oblate garnets in mylonitic rocks (Dalziel & Bailey, 1968; Ross, 1973) corroborate an interpretion of syn-tectonic crystallization under amphibolite-grade conditions.

Two generations of garnet are recognized. The first are poikioblastic, with inclusions of quartz, plagioclase and biotite which occasionally define a foliation. Some garnets display rotation relative to the external fabric about axes both parallel to the mineral stretching lineation (Plate 12A), and perpendicular to this lineation (Plate 7E), parallel to the compositional layering. They are subhedral to anhedral and ragged when not overgrown by second stage garnet. On rare occasions kyanite was observed to be intergrown with these garnet porphyroclasts (Plate 7F).

A second stage of garnet growth is inferred by the presence of relatively inclusion free subhedral porphyroclasts, and subhedral to anhedral rims around earlier garnets (Plate 7G). Minor inclusions include biotite, quartz and sillimanite (Plate 7D-G). On rare occasions sillimanite-biotite intergrowths were noted to grow out of these garnets.

Garnet porphyroclasts generally form rigid grains around which the mylonitic foliation is flattened. Quartz, biotite and plagioclase pressure shadows, the inclinations of elongate porphyroblasts, and tension fractures

within them, contribute to the definition of the S-foliation (see section 3.4.3 and Berthe et al. 1979) in these mylonitic rocks (Plate 4).

ZEOLITES

Minerals of the zeolite group are rare in the map area. Those identified by X-ray diffraction analysis are mesolite and natrolite. They occur as random sprays in late brittle fractures, and are interpreted to have been deposited by hydrothermal fluids.

ALUMINOSILICATE RELATIONSHIPS

The three aluminosilicate polymorphs are widespread throughout the map area. They form mineral components in a range of rock types including most metapelites, semipelites, quartzo-feldspathic rocks, orthoamphibole-rich rocks, quartz-sweats and tonalitic pegmatites. They are noteably absent, or low in concentration, in muscovite-rich pelitic rocks (most common within unit 10). Aluminosilicates are spectacular in the forms, grain-size, textures and colours they display. Microstructural observations of these phases are very important in understanding the deformational environment of the map area, especially its thermotectonic evolution. While experimental plastic deformation of aluminosilicates has been described by Menard et al. (1979), Doukhan and Paquet (1982), and Doukhan and Christie (1982), deformation mechanisms in general have received scant attention in the literature.

Kyanite is ubiquitous in the lower-plate and restricted to the lower 100 m of the upper-plate (Appendix 3). It displays a wide variety of colours including emerald-green, deep-blue, grey and colourless. Coarse-grained laths characteristically lie in the plane of flattening parallel to

compositional layering. They are often pulled apart with lower grade minerals (e.g. andalusite, muscovite, biotite) crystallized in the pull-aparts (e.g. Plates 10, 11 & 12E), and invariably subparallel to the D2 fold hinges contributing to the definition of the mineral stretching lineation. Poikiolitic varieties contain inclusions of garnet, biotite, muscovite, quartz, feldspar, apatite and opaque oxides (Plate 8A). In the lower-plate, with proximity to the detachment surface, kyanite is commonly enveloped in muscovite (Plate 9F). This texture is also present in the lower part of the upper-plate. Proceeding up into the upper-plate, kyanite becomes more ragged and eventually disappears. Varieties with sweeping extinction, kinks and folds are present (Plate 8C & D).

These observations suggest that kyanite crystallized during D2 folding (see section 3.2.2), and is pre- to syn-shearing. In the field, rare dcm-scale localities display random kyanite porphyroblasts. Since the enclosing rocks are mylonitic, it is unlikely they escaped reorientation due to shear strain. Random kyanite is also common in quartz sweats and tonalitic pegmatites (Plate 12G). These observations suggest conditions for kyanite growth locally out lasted shearing.

Andalusite is found almost exclusively in the lower plate (one location in the upper-plate, see Appendix 3). Most common in kyanite-bearing pelitic rocks (Plate 12E), it also can be found in aluminosilicate-bearing quartz sweats and pegmatite. Although found as single grains and massive aggregates in a quartz vein at one locality (station 85-R215), it is characteristically found as a replacement of kyanite (Plates 8EF, 9ABC, 10 & 11). Two types of replacements are recognized. The first appears to be an intergrowth with kyanite and is not associated with pull-apart fractures in kyanite (Plate 11B). This texture is believed to indicate

replacement of kyanite under static conditions. The second, more common form, is found along the pulled apart margins of kyanite (Plates 10 & 11A). This andalusite is commonly pulled apart, with lower-grade minerals (biotite, muscovite, chlorite) infilling the pull-aparts, and is interpreted to be syn-kinematic.

All andalusite observed in thin section displays small, slightly misoriented subgrains (Plate 8E & F). Replacements at the ends of kyanite laths commonly display a V-like pattern into the kyanite with a planar discontinuity bisecting the V. This discontinuity resembles a kink plane separating slightly elongate andalusite subgrains. These subgrains have a dimensionally preferred orientation on either side of this plane which defines a complementary V-pattern. The origin of these subgrains and pattern is not known. It is proposed that the greater unit cell volume of andalusite over kyanite (Winter & Ghose, 1979) results in this pattern as andalusite crystallizes.

Sillimanite is present throughout both upper- and lower-plates. It is the only aluminosilicate in the upper part of the upper-plate. It occurrs as large pulled apart mats along discrete D2 sub-axial planar shears which truncate D2 folds and related fabrics (Plate 12D), and as fibrolitic intergrowths with biotite in phyllosilicate-rich discrete shear domains (Plates 8F & 9E). It is always aligned parallel to D2 fold axes, and contributes to the definition of the mineral stretching lineation. Fibrolitic growths, mats and coarser prismatic crystals lie in the plane of flattening and are commonly pulled apart with fractures perpendicular to the mineral stretching lineation, and infilled with biotite and/or muscovite. Intergrowths in shear domains commonly display a sweeping extinction, and form a foliation which wraps around rigid porphyroclasts of

kyanite, andalusite, garnet and feldspar. No reaction textures were observed when in contact with earlier prograde muscovite. The above sillimanite is interpreted to be syn-kinematic. Less common very fine grains of sillimanite form random clusters completely enclosed in quartz, muscovite, plagioclase (Plate 8G) and garnet (Plate 7H). These are interpreted to be post-kinematic. Sillimanite in the upper-plate is commonly folded and axial planar to these folds (Plate 8H).

In most thin sections sillimanite is not in contact with either of the other two polymorphs. The development of mylonitic fabrics further hinders a chronological analysis. Observations which suggest, but do not prove that sillimanite is the youngest polymorph are: (1) sillimanite-biotite intergrowths which wrap around the other polymorphs, (2) the relative low internal strain of sillimanite, and (3) sillimanite mats occurring on discrete shear surfaces which truncate D2 folds and related fabrics. A key observation is that in some thin sections sillimanite has crystallized on, and replaced the edges of both kyanite and andalusite (Plate 9A-D). This sillimanite "flows" into the sillimanite-biotite shear domains (C-folations). These observations lead to the conclusion that some sillimanite post-dates both kyanite and andalusite.

From the above, the inferred sequence of aluminosilicate crystallization is, kyanite-andalusite-sillimanite. The possibility that this is a direct prograde sequence is unlikely because equilibria metamorphic assemblages associated with kyanite (see section 3.4.7) indicate kyanite grew at temperatures higher than those which occur at the aluminosilicate triple point. Two further points suggest some sillimanite post-dates kyanite and is older than andalusite. First, the presence of sillimanite in aluminosilicate-bearing tonalitic pegmatites inferred to

have been generated during peak metamorphic conditions prior to andalusite growth (M1 metamorphism section 3.4.7). Secondly, the presence of random sillimanite within quartz, plagioclase and muscovite grains suggest that these are post-kinematic. By analogy to random kyanite this suggests conditions for sillimanite growth outlasted shearing. Static conditions for sillimanite growth appear to have only occurred at or after M1 peak metamorphism. Fibrous sillimanite in muscovite generated during M2 metamorphism (section 3.4.7) and coeval shearing are invariably aligned in the mineral lineation, indicating that shearing occurred throughout M2 silliminite-forming conditions. The local nature and relative rarity of the above two observations weakens the credibility, but does not negate the proposal for post-kyanite, pre-andalusite sillimanite growth. The sequence of aluminosilicate growth is therefore inferred to be kyanite-sillimanite-andalusite-sillimanite. A similar ordering of aluminosilicate growth has been proposed by Journeay (1985, 1986) for mylonitic footwall rocks in the Monashee complex to the south, and by Rhodes (1986) for mylonitic footwall rocks of the Spokane Dome, south of the international border.

This sequence of aluminosilicate crystallization, their fabric relationships, plus the interpretation that some kyanite, sillimanite and andalusite grew in static conditions implies two syn-shearing metamorphic peaks; the first accompanied by kyanite growth and the second accompanied by sillimanite growth. These peaks were separated by an intervening static period during which some kyanite, sillimanite and andalusite grew. Further refinement of the P-T path is based upon interpreted mineral parageneses, and the identification of a metamorphic field gradient described in section 3.4.7.

3.4.5 MIGMATITES AND PEGMATITES

Rocks of the map area display a protracted history of deformation and metamorphism which has given rise to a complex suite of migmatites. In this section migmatite nomenclature follows that of Ashworth (1985). Coarser leucosomes, or veins, which display a large grain-size contrast of >1 order of magnitude with the mesosome, are termed pegmatitic or pegmatites after Ashworth and McLellan (1985). Inferences regarding timing of migmatization and pegmatite development require care (see above references). Based on relationships relative to detachment-related shearing fabrics, and synchronous D2 folding, a crude separation was made in a manner similar to that of Barr (1985), into two broad catagories that include early and late leucosomes. Early leucosomes, which are invariably deformed and most common, include quartz veins, quartz veins with aluminosilicates or hematite, discordant and concordant pegmatites. Late leucosomes are pegmatites which display igneous textures or are weakly deformed.

Early leucosomes in the form of discontinuous layer-parallel quartz veins are well developed throughout the map area. They are folded around D2 fold hinges, and display coeval flattening fabrics along their limbs. Some of the most spectacular kyanite and andalusite occurs in these quartz segregations (Plate 12C). Although some kyanite grains are aligned in the mineral stretching direction, most have grown in a random fashion parallel to the compositional layering, indicating local static conditions during neomineralization in the kyanite field of stability. Locally these quartz sweats can contain up to 40% massive specular hematite. Other secondary minerals include black dravite and blue dumortierite.

Amphibolitic and pelitic metatexites are also common throughout the

map area (Plate 12C). They display early stromatic leucosomes that are thin-banded (1-10 mm), discontinuous, and composed of both quartz and tonalite (Streckeisen, 1976). Tonalitic leucosomes commonly occur as deformed, mm- to cm-scale, augen-shaped pods. Biotite selvages are common in pelitic rocks. Accessory minerals in tonalitic leucosomes include biotite, hornblende, kyanite, sillimanite and garnet.

Early leucosomes of sheared pegmatite display a variety of crosscutting relationships and mineralogy. These pegmatites are least common deep in the footwall. Their abundance increases dramatically at the zone of detachment where they compose up to 50% of the exposure (Plate 1C). Along the limbs of D2 folds, and at the detachment zone, they are concordant to subconcordant with compositional layering. They can be folded about D2 fold hinges but most commonly truncate D2 structures in their hinge zones, similar to "syn-slide" leucosomes of Barr (1985). Mylonitic fabrics usually give ambiguous senses of shear. They are of tonalite and granite compositions, with the latter being subordinate in volume. Secondary minerals include garnet, kyanite, andalusite, sillimanite, biotite, muscovite and tourmaline. Retrograde phases of chlorite, epidote and sericite are also present.

Late leucosomes are all highly discordant, dilational pegmatite dykes. These pegmatites which are clearly subordinate in numbers to earlier pegmatites appear to slightly increase in numbers as the detachment is approached from within the footwall. Granitic varieties are most common. They contain biotite and muscovite as secondary phases. These granitic pegmatites are also the coarsest-grained, some K-feldspar reaching 30 cm in length, and muscovite crystals up to 15 cm in diameter (station 85-R143). Tonalitic varieties are subordinate. Locally these pegmatites contain

extremely coarse grains of tourmaline, and agmatize the host metasedimentary rocks.

A great deal more work is required before well supported propositions can be put forth concerning the relative importance of active migmatization processes. From the above preliminary observations it is clear that partial melting and melt injection are two processes that were operative in producing some migmatites in the map area. The roles of metasomatism and metamorphic differentiation remain to be investigated.

3.4.6 DEFORMATION PROCESSES

Shear zones in deep crustal rocks are important focuses of strain softening and deformation, in which the formation of mylonite and ductile flow can accommodate large displacements (White et al. 1980; Ramsey, 1980). Microstructures and fabrics of mylonitic rocks are products of both the spacial and temporal variation of strain softening mechanisms (see Poirier, 1980, White et al. 1980), finite strain, strain rate, and strain path (Knipe & Wintsch, 1984). Determination of operative strain softening mechanisms has the potential of providing general information on the conditions of deformation. Descriptions of observed microstructures (section 3.4.4) indicate the operation of a wide range of deformation mechanisms incuding cataclasis, intracrystalline plasticity, and diffusive mass transfer, all of which operated at some time contributing to the final fabric. This range of deformation mechanisms is attributed to the different responses of various rock forming minerals under different environments of deformation. On a granular-scale brittle processes are subordinate to ductile responses, resulting in mesoscopic ductile deformation.

Although a more rigorous microstructural analysis is required, some preliminary statements can be made concerning the interpretation of preserved microstructural domains, plus macro- and mesoscopic structures, in terms of the variation in strain, strain rate, strain paths and softening mechanisms.

Individual domains in the mylonitic fabric may indicate a variation in the finite strain. For example, those domains which define the S-foliation at relatively high angles to the C-foliation are interpreted to record less finite strain than those at a lower angle. This variation can be explained in terms of the "lifetime" of the domains and a variation in strain rate (Knipe & Wintsch, 1984). It is also possible that some domains that define the S-foliation are strain-insensitive domains (Means, 1981; Hanmer, 1984a).

Strain rate variation may be due to a change in strain rate across the whole shear zone, or local variations brought about by changing conditions, and therefore rheology. Fractured feldspar could be the result of localized increases in strain rate. Compositional differences in these S-C tectonites have induced, and reflect variations in strain rate. For example, large porphyroblasts in those domains which define S-foliations generate local high strain rates in the adjacent enveloping C-foliations where phyllosilicates recrystallize and are concentrated.

Preserved microstructures also indicate a variation in strain paths. The inferred overall strain path of S-C tectonites in the map area is one dominated by progressive simple shear parallel to the compositional layering with a west-over-east sense of shear. Deviations are recorded by the microstructures. The presence of micro-drag folds indicates the heterogeneous distribution of strain on a granular-scale. Concentrations

of phyllosilicates in C-foliations, and quartzo-feldspathic phases in pressure shadows, is indicative of local syntectonic volume changes, and demonstrates a variation in strain path.

Domains of deformation mechanisms exist which reflect the dominant minerology of those domains. For example, quartz ribbons appear to have deformed by the ductile processes of dynamic recovery and recrystallization, perhaps reflecting lower strain rates but high finite strains. Phyllosilicate-rich domains deform by recrystallization, kinking, lattice bending and grain boundary sliding. Kyanite, sillimanite and garnet deform primarily by fracturing, possibly producing or reflecting higher strain rates. The removal of quartz from phyllosilicate-rich domains indicates another deformation mechanism, diffusion mass transfer. The kinetics of this process is dependent upon the rate of dissolution of quartz.

The observed textures of quartz in quartzites, especially the preferred crystallographic orientation, is indicative of geometrical softening (see Schmid, 1982; White et al. 1982). During this process flow stresses for intracrystalline slip drop to a minimum. This is a result of increased average resolved shear stress on one or a few slip systems as they rotate into parallelism with the shear zone boundaries, and as the slip direction rotates into parallelism with the stretching lineation (ref. op. cit.). The reorientation of the lattice is commonly assisted by continual dynamic recrystallization.

Softening by strain-induced changes in deformation mechanisms can be an effective mechanism of deformation (see Schmid, 1982; White et al. 1980). Dynamic recrystallization generally results in a reduced grain size and the possibility of changing deformation regimes (e.g. power-law creep

to superplastic flow, see ref. op. cit.). Microstructural observations indicate that dynamic recrystallization has not resulted in extensive grain-size reduction and is consistent with microstructures formed at high temperatures (cf. Wilson, 1973), where a change from power-law creep to superplastic flow is unlikely (Schmid, 1982). Therefore, changes in deformation mechanism are not likely to have enhanced strain softening.

Reaction softening is enhanced ductility due to metamorphic reactions, (e.g. White & Knipe, 1978; Poirier, 1980; White et al. 1980; Williams & Dixon, 1982; Dixon & Williams, 1983; Rubie, 1983; Brodie & Rutter, 1984). Softening may be a result of fluid release during dehydration reactions, or the result of the production of strain-free neoblasts which are more easily deformed than the original grains, or both. Both of these mechanisms, and in particular the production and accumulation of melt, are believed to have been very effective strain softening mechanisms in the map area.

The presence of sheared melt and high-grade synkinematic minerals along discrete shears which cut fabrics and folds throughout the map area, and the high concentration of sheared pegmatite at the zone of detachment, are suggestive of a relationship between shear strain associated with the detachment, and the production and accumulation of melt phases.

The production and accumulation of melt can have a dramatic effect on rock rheology (e.g. Arzi, 1978), and can cause strain softening by at least two mechanisms associated with increasing pore fluid pressure. The first is through the accumulation of melt along a pre-existing shear zone. This would cause a reduction in the effective normal shear stress and resistance to sliding. The second mechanism is similar to the first except the accumulation of the melt phase promotes the formation of the shear zone. In this case the melt reduces the effective normal stress in the rock body,

which effectively reduces the resistance to shear fracture, promoting failure. The "pore fluid pressure can be thought of as having a lubricating effect on faults in the sense that it reduces the frictional resistance to movement, but it does not have a lubricating effect in the sense that the coefficient of internal friction is changed by the pore pressure" (Hobbs et al. p. 320, 1976). Although both mechanisms probably operated in the map area, the extent to which they operated, relative to each other, is not presently known. The field data do indicate that melt played a major rôle in the accumulation of shear strain.

This form of strain softening is a hybrid of two strain softening processes, reaction softening and pore fluid effects, and is herein referred to as melt softening. Melt softening clearly enhances strain softening (cf. melt-enhanced deformation of Crawford & Hollister, 1986; Hollister & Crawford, 1986). Characteristics of this process (Hollister & Crawford, 1986) include: localization of melt along shear zones, juxtaposition of rocks across the shear zone that formed at different crustal levels, and the preservation of high T-P metamorphism and textures, all characteristics of the Selkirk allochthon, Monashee decollement and Monashee complex (Journeay, 1983, 1985, 1986; this study).

In summary, ductile flow in the polyphase mylonitic rocks studied, was achieved through the operation of a wide range of deformation and metamorphic processes. The microstructures preserved in microstructural domains show evidence for different finite strains, strain rates, and strain paths. Geometrical softening, continual recrystallization, reaction softening and melt softening are believed to be major strain softening processes operative in rocks in the map area, and are indicative of relatively high temperatures of deformation.

2

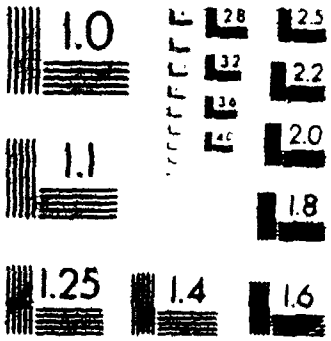

MicroD

3.4.7 METAMORPHISM DURING MYLONITIZATION

With the aim of determining metamorphic conditions during mylonitization, this section attempts to relate naturally occurring metamorphic mineral assemblages, in both upper- and lower-plates, to the experimentally determined P-T conditions of their stability. Descriptions in section 3.4.4 indicate metastable mineral assemblages, equilibria, disequilibria and deformation textures developed during a complex thermotectonic history. Establishment of equilibrium metamorphic assemblages based on textural interpretations, is both hindered and enhanced by the coeval development of syn-metamorphic mylonitic fabrics.

Criteria used to differentiate and determine equilibrium assemblages coeval with multiple episodes of high-temperature recrystallization and neomineralization, and later retogression, are based on various textural criteria proposed in the literature (e.g. Carmicheal, 1969; Vernon, 1975b, 1976, 1977b; Vernon & Flood, 1977), compatibility with known mineral reactions in the pelitic system (e.g. Thompson, 1976; Carmicheal, 1969), and timing of mineral growth (ref. op. cit.). It is the interpretation of textures that is used herein to establish reaction schemes and estimate conditions of metamorphism.

Keys to understanding the thermotectonic evolution of rocks in the map area are: (1) the determination of the order of aluminosilicate crystallization, which is interpreted to be kyanite-sillimanite-andalusite-sillimanite (section 3.4.4), and (2) recognition of two distinct peak syn-shearing metamorphic events (M1 & M2) which affected rocks in both upper- and lower-plates. This section describes these two metamorphic events and attempts to define peak metamorphic conditions and a P-T path. To facilitate this a petrogenetic grid for the system SiO_2-Al_2O_3-FeO-MgO-Na_2O-

K_2O-H_2O compiled by Journeay (1986, modified after Carmicheal, 1978) is used. This also aids comparison with observations and interpretations made by Journeay (1986), the most comprehensive study in Frenchman Cap dome region. A summary of mineral symbols used can be found in Appendix 1.

The determination of physical conditions during metamorphism was done with some hesitancy. Conditions for metamorphic reaction equilibria are greatly influenced by many factors, other than pressure and temperature, which have not been investigated to determine the degree and manner they influence mineral transformations in rocks of this study (e.g. cation, disorder, presence of fluids, deformation, etc., see Carpenter & Puthis, 1984; Rubie & Thompson, 1984; Brodie & Rutter, 1984). Consequently, determined pressures and temperatures of metamorphism are considered to be only first approximations based on the assumption that ambient P-T conditions were the principal controls of metamorphic grade achieved.

M1 METAMORPHISM

Textures and mineralogy described in sections 3.4.4 and 3.4.5 suggest that mylonitic pelitic rocks of the map area preserve metastable mineral assemblages indicative of an early high-pressure and high-temperature peak metamorphic event. Peak equilibrium parageneses observed are interpreted to be quartz $\pm$ plagioclase $\pm$ biotite $\pm$ muscovite $\pm$ garnet $\pm$ kyanite $\pm$ sillimanite $\pm$ tonalitic melt. Varietal minerals include tourmaline, zircon, apatite and opaque oxides. This mineral assemblage shows evidence of recrystallization during, and subsequent to an early shearing event (see section 3.4.4), and is widespread throughout the lower-plate.

Envelopes of muscovite around kyanite (Fig. 9F), observed to be more abundant with proximity to the detachment in both upper- and lower-plates,

are interpreted to be prograde products of later M2 metamorphism. Kyanite in the lower part of the upper-plate is so strongly affected by this later event that it disappears higher in the plate. The presence of equivalent mineral parageneses and textures in both upper- and lower-plates strongly suggests, but does not prove, that the divariant field representing peak metamorphic conditions crossed the detachment.

Metastable parageneses Ms ± Qtz ± Bt ± Grt ± As may be related to the discontinuous reaction:

St + Ms + Qtz = Bt + Grt + As + water (1)

or any of the following divariant reactions:

(Bt) St + Qtz = Grt + As + water T Mg > T Fe (2)

(Grt) St + Ms + Qtz = Bt + As + water T Fe > T MG (3)

(As) St + Bt + Qtz = Grt + Ms + water T Mg > T Fe (4)

(St) Grt + Ms = Bt + As + Qtz T Fe > T MG (5)

(see McLellan, 1985; Thompson, 1976; Pigage, 1982)

The paucity of staurolite and mineral chemistry data for these rocks precludes differentiation of these reactions. The absence of aluminosilicates in some pelitic units (mostly in unit 10) may be the result of reaction (4), indicating iron-rich rocks (Fe-enrichment would be in accord with the volcanogenic nature of subunits within unit 10; see section 2.2.1.2). This mechanism has been used by McLellan (1985) to account for the absence of aluminosilicates in some pelitic rocks of the Barrovian type area. Reaction (1) is believed responsible for similar assemblages to the south (Journeay, 1986).

Parageneses Bt - Grt - As - tonalitic melt are interpreted to reflect peak metamorphic conditions. Tonalitic leucosomes are common in pelitic rocks. Of the possibilities for their origin summarized by Ashworth

(1985), their textures and compositions point to an anatectic origin. The above parageneses are interpreted to reflect the anatectic reaction

Kf + Ms + Pl + Qtz + water = melt + As

and to have been generated within the range necessary for anatectic melts of this composition (ca. 700°C, see Johannes, 1985; Winkler, 1979).

Assuming that sillimanite and/or kyanite plus tonalitic melt are the products of peak metamorphic conditions, then peak conditions lie at least within bathozone 5 (Fig. 14; Carmicheal, 1978). Minimum pressure is constrained to range from ca. 6.4 kb, the pressure at which the Ky = Sil and Qtz + Ms + Pl + v = As + melt reaction curves intersect assuming water saturation, to ca. 7.1 kb, the maximum pressure boundary of bathozone 5. Kyanite and tonalitic melt can coexist at pressures well beyond the above values. It is the presence of both kyanite and sillimanite in tonalitic melt that indicates that M1 metamorphism peaked between ca. 6.4 and 7.1 kb since 7.1 kb is the maximum pressure for the generation of the assemblage sillimanite-tonalitic melt (assuming aH2O=1). Using the above constraints and arguments these reaction curves and bathograd limit the peak temperature to range from at least ca. 640 to 679 degrees celcius. Therefore, M1 peak metamorphic conditions are inferred to lie in the range 640 to 679 degrees celcius and 6.4 to 7.1 kb, approximating crustal depths of 22 to 25 km (assuming a pressure gradient of ca. 0.3 kb/km).

It should be pointed out that these temperatures and pressures are minimums based on the assumption that the activity of water is 1. Decreased water activity causes the Qtz + Ms + Pl + v = As + melt reaction curve to translate into the higher temperature region. This would increase both T and P at the intersection point of the Ky = Sil and Qtz + Ms + Pl + v = As + melt reaction curves. It is most probable that these rocks were

at higher temperatures and pressures prior to quenching. Therefore the above T-P estimates for M1 peak metamorphic conditions are considered minimum values.

Textural relationships between prograde minerals biotite, muscovite, quartz, plagioclase, kyanite and sillimanite are often identical to those described by Carmicheal (1969). These textures are believed to indicate cation exchange diffusion processes whose net result is the polymorphic inversion Ky = Sil (Carmicheal, 1969). These mechanisms were most likely active during both M1 and M2 metamorphism, and development of related shearing fabrics, consequently assignment of timing of growth is most often ambiguous.

After peak metamorphic conditions these rocks followed a P-T path into the andalusite stability field. This is interpreted to indicate uplift to crustal depths of ca. 13 km, assuming the aluminosilicate triple point occurs at 3.76 kb (Holdaway, 1971), and a pressure gradient of ca. 0.3 kb/km. Retrograde sillimanite appears to be rare, while evidence for a Sil=And reaction was never observed. The former can be explained by the fact that retrograde reactions are characteristically sluggish, and the latter requires Al-Si diffusion inhibiting this process (Winter & Ghose, 1979). A petrogenetic grid applicable to this system is presented in Figure 14. This figure shows the divariant fields indicated by peak metamorphic and retrograde parageneses, the order they were entered, and a possible P-T path for the M1 metamorphic event.

M2 METAMORPHISM

Microstructures and mineralogy described in section 3.4.4 indicate that M1 metamorphic parageneses are overprinted by a syn-shearing M2

metamorphic event. Three low-pressure assemblage zones and associated isograds (Fig. 15) define a metamorphic field gradient that crosses the detachment surface. On the basis of leucosome distribution and intensity, this gradient is inferred to be inverted with northwesterly dipping isograd surfaces. Key prograde mineral assemblages which overgrow earlier M1 mineral assemblages and define these zones in increasing metamorphic grade are: andalusite-muscovite+/-sillimanite, sillimanite-muscovite and sillimanite-K-feldspar-granitic melt. Secondary retrograde phases which have crystallized in all rocks of the map area are chlorite, biotite, muscovite, epidote and actinolite.

The andalusite-muscovite+/-sillimanite zone is restricted to the lower-plate. Mineral textures indicate that M1 metamorphism retrogressed into the andalusite stability field prior to shearing coeval with M2 metamorphism. It was in this stability field that andalusite initially replaced kyanite under static conditions. This was followed by low-pressure M2 metamorphism and associated shearing. Shearing began in the andalusite field as evidenced by pulled apart kyanite grains with andalusite replacing kyanite along the pull-apart margins. Andalusite was subsequently pulled apart during retrogression as indicated by muscovite, biotite and chlorite which crystallized in the pull-aparts.

Sillimanite in this zone is most commonly intergrown with biotite making differentiation from M1 sillimanite difficult. It is rarely in contact with andalusite displaying post-andalusite growth relationships. This suggests cation exchange diffusion processes similar to those proposed for the Ky=Sil inversion by Carmichael (1969) may have been the mechanism for the And=Sil inversion noted in this zone. This zone covers most of the lower-plate indicating that the And-Sil transition is a broad zone.

Sillimanite could also be a product of any one of reactions (1), (2), (3), and (5) (see M1 metamorphism). These reactions could have exhausted any remaining staurolite and also account for the co-existence of sillimanite and muscovite in this zone. This zone is bound in the northwest corner by an ill-defined andalusite-out isograd.

The ca. 200 m thick sillimanite-muscovite zone, straddling the detachment, is bound by the muscovite-kyanite-out and andalusite-out isograds. All minerals and textures are similar in appearance to those in the andalusite-sillimanite-muscovite field except andalusite is absent, and prograde muscovite is less common and more ragged. M1 prograde kyanite is present in both plates in this zone, and typically enveloped in prograde muscovite. Inclined traverses into the upper-plate reveal that both kyanite and muscovite become more ragged and disappear (Appendix 3).

Kyanite-out and muscovite-out isograds appear to coincide in the field defining the lower boundary of the sillimanite-k-feldspar-granite melt zone. This boundary is interpreted to represent the reaction

$$\text{Qtz} + \text{Ms} + \text{Pl} = \text{Kfs} + \text{As} + \text{melt}.$$

Sillimanite, K-feldspar and granitic pegmatite are inferred to represent the peak M2 metamorphic assemblage. Although the muscovite-out isograd appears to be relatively sharp in the field, combinations of the assemblage Ms-Bt-Grt-Qtz-Pl-Kfs-Ky-And-Sil is sporadically developed in the lower-plate, indicating that this reaction occupies a diffuse zone throughout the map area. Observations that leucosome development increases parallel the northwest-dipping detachment suggests that the isograds are inverted and dip in a similar orientation.

Retrograde Chl, Bt, Ms, Ep and Act are widespread in the map area. The phyllosilicates appear as random laths (Plate 7B), pseudomorphic

replacements and sericitization of feldspars in thin section. In the field, late brittle mm-scale extension fractures, perpendicular to the compositional layering and mineral stretching lineation, are infilled with chlorite, epidote and actinolite.

The above progression of assemblage zones represents a low-pressure reheating of rocks in both upper- and lower-plates. The physical conditions under which the sequence of assemblage zones andalusite-muscovite+/-sillimanite, sillimanite-muscovite and sillimanite-K-feldspar-granitic melt could develop are low-pressure and increasing temperature (Fig. 16). The transition from the sillimanite-muscovite field to the sillimanite-K-feldspar-granitic melt field is bound by bathograds 3a/3b and 1/2, which are infuenced by the coeffient of water activity. A water activity of less than one will displace bathograd 3a/3b to higher pressures and increase the range of temperatures under which sillimanite, K-feldspar and granitic melt are stable. Assuming a water activity of one provides a minimum temperature and pressure range of ca. 615 to 678 degrees celcius and 2.0 to 3.4 kb, approximating crustal levels of 7 to 12 kilometers. In Figure 16 a possible P-T path for the M2 metamorphic event is shown cutting through the divariant fields indicated by the M2 mineral parageneses.

DISCUSSION

Barrovian and Buchan metastable mineral assemblages in rocks of the map area respresent two distinct metamorphic events. Earliest M1 peak metamorphic conditions are inferred to have at least ranged from 640 to 679 degrees celcius and 6.4 to 7.1 kb, indicating maximum depths of burial of 22 to 25 km. These conditions are believed to have existed in both upper- and lower-plates (i.e. across the shear zone) and to have locally outlasted

early shear strain along the detachment surface. Recrystallization, neomineralization and fabric development associated with M1 metamorphism has erased any evidence for an earlier thermal event, if there was one.

Later syn-shearing M2 metamorphism defines an inverted low-pressure metamorphic gradient that decreases from upper- to lower-plate. Inferred peak metamorphic conditions are estimated to lie in the range 615 to 678 degrees celcius and a minimum pressure range of 2.0 to 3.4 kb, approximating crustal levels of 7 to 12 km.

These syn-kinematic metamorphic peaks were separated by a static period within the kyanite, sillimanite and andalusite stability fields, respectively. Similar metamorphic histories have been proposed for footwall rocks of the Ratchford Creek area in the Monashee complex (Journeay, 1985, 1986), and the southern Priest River complex (Rhodes, 1986).

Absolute ages of these thermal events are unknown. A summary of proposals and age constraints can be found in section 1.3. Using arguments presented by Journeay (1986), Journeay & Brown (1986), Brown et al. (1986) and Rhodes (1986) a general P-T-t path has been constructed (Fig. 17). M1 peak metamorphism is assumed to have quenched in the Late Jurassic. M2 peak metamorphism is assumed to be a Late Cretaceous event.

3.5 INTERPRETATION AND MODEL EVALUATION

Several tectonic processes have the ability to generate a structural culmination with the dimensions of the Monashee complex (3600 sq. km.). These include: (1) diapiric upwelling, (2) interference of crustal-scale folds, (3) crustal megaboudinage, (4) crustal attenuation accompanied by crustal-scale low-angle normal faults, and (5) crustal-scale duplex

formation in response to compression. All but (4) have been proposed to account for the origin of the Monashee complex. The first four mechanisms and the premises for their rejections are summarized below. The fifth mechanism is the basis of the comprehensive model proposed by Journeay (1985, 1986). This model is summarized in relatively more detail than the first four. Evaluation in light of data and conclusions presented in this thesis lend further support to this model.

Diapiric upwelling and lateral spreading of hot mobile gneissic rocks from a deep-seated infrastructure was (Price & Mountjoy, 1970; Reesor & Moore, 1971) and still is (Van Den Driessche, 1986) a popular proposition. Read (1980) points out that it is highly unlikely that upwelling material would stop at precisely the same horizon, the base of the basal quartzite, throughout the entire complex. Comparisons made between regional strain patterns and those predicted by diapir modeling (e.g. Dixon, 1975) show no correspondence, and thus the unlikeliness of this mechanism (Journeay, 1986; Duncan, 1984). This mechanism was also proposed to be the driving mechanism of foreland thin-skinned shortening (Price & Mountjoy, 1970; Price, 1973). Recognition that deformation and metamorphism of the hinterland preceded foreland shortening (Brown & Tippett, 1978) casts further doubt on the operation of this mechanism (Brown, 1978).

The superposition of north-trending crustal-scale buckle folds on north-verging nappes creating domal interference patterns has been proposed to account for the Monashee complex, and its second-order culminations, Frenchman Cap and Thor-Odin domes (Read & Klepaki, 1981; Duncan, 1984). Journeay (1986) provides structural arguments which negate this proposition. Buckle folding should produce structural vergence towards the centre of the dome. Instead late structures of the northern Monashee

Complex are consistently northeast-verging, indicating northeast directed shear; observations incongruous with a buckle fold origin.

The structural culmination of the Monashee complex has been interpreted to be a result of increased heat flow (Price et al. 1981), resulting in east-west ductile crustal stretching, necking and unroofing in a manner similar to megaboudinage of Davis & Coney (1979). Again the consistent northeasterly- to east-vergence of minor structures and kinematic indicators on all flanks of the dome discounts this proposition (Journeay, 1986).

Displacements of large magnitudes on crustal-scale low-angle normal faults could generate a structural culmination the dimensions of the Monashee complex (Spencer, 1984; Wernecke, 1985). The northeast- to east-vergence of minor structures implies an easterly rooting normal fault. In contrast a folded westerly-rooted low-angle thrust fault is suggested by the emplacement of higher grade over lower grade rocks on the west side of the dome (Journeay, 1986, this study), and the geometry of isobars and isotherms in the complex (Journeay 1986, to be discussed). The absence of a brittle-ductile transition during displacement along the Monashee decollement (Brown & Murphy, 1981; Lane, 1984a, 1984b; Journeay, 1986; this study), does not support genesis through low-angle, crustal-scale normal faulting.

The above propositions are general hypotheses based upon a limited data base. The most comprehensive model to date is that proposed by Journeay & Brown (1985), Journeay (1985, 1986), Brown & Journeay (1985), Brown et al. (1986) and Journeay & Brown (1986). In this model the culmination and second-order domes are essentially a product of fault-bend folding over a non-planar fault surface. A description of this model and

the details upon which it is based can be found in the above work, and is summarized below.

This model proposes that the Monashee complex is the exposed uppermost horse in an east-verging antiformal duplex composed of basement-cored horses and bound above by the Monashee decollement. It was generated in response to tectonic suturing of allochthonous terranes in the Early to Middle Jurassic, and forms the west part of an eastward tapering deformational wedge which tapers into the foreland.

The Monashee decollement is interpreted to be a westerly-rooted crustal-scale thrust that originated at crustal levels >25 km, and records two displacive events, designated MD1 and MD2. During the early evolution of the decollement (MD1) it formed a floor thrust at the base of the Selkirk allochthon. Evidence for its thrust nature can be found in reconstructions of M1 isobaric and isothermal surfaces within the complex which reveal a ramp-flat thrust geometry at this time (Journeay, 1985, 1986).

Prior to renewed thrusting, metastable mineral assemblages indicate the complex was uplifted 10 to 12 km. Footwall ramp collapse and incorporation of deep-level horses into the duplex is inferred to be the uplift mechanism. Renewed thrusting along the decollement (MD2) resulted in emplacement of hotter over colder rocks, and an inverted low-pressure metamorphic sequence (M2) overprinting earlier M1 metastable assemblages. Both MD1 and MD2 are coincident on the west flank of the complex and diverge along north and south margins due to pre-MD2 arching of MD1. Kinematic indicators consistently give west-over-east shear senses for both displacements. This data forms the basis for the proposition that the decollement acted as a kinematic link between crustal shortening in the

hinterland and thin-skinned thrusting and folding in the foreland (Brown et al. 1986). Brittle features within, bounding and outside the complex, plus Eocene K-Ar dates, are interpreted to reflect final quenching and uplift-induced denudation.

The structural-metamorphic data and inferences of this study can most easily be interpreted in light of the above model. The M1 P-T path presented in Figure 14 for rocks in both upper- and lower-plates of the map area is identical to that proposed by Journeay (1986) for rocks of the lower-plate to the south. The geometry of M1 isograds to the south has allowed the construction of an east-west P-T profile through the dome displaying the two-dimensional geometry of isograds, isobars and isotherms (see Fig. 18B and Journeay, 1986). An ideal P-T profile displaying these surfaces prior to duplex formation is shown in Figure 18A. This profile is implied by Journeay (1986) to be applicable as a general profile cut at any vertical orientation through the centre of Frenchman Cap dome. Metastable pelitic mineral assemblages believed to have been generated during peak M1 metamorphic conditions in the map area lie in the field indicated. Therefore, interpreted M1 peak metamorphic assemblages in the map area appear to support the three dimensional geometry of peak M1 isograds, isobars and isotherms proposed by Journeay (1985, 1986).

Detailed mapping of this study clearly documents a detachment surface and a footwall cut-off. This surface was originally recognized during reconnaissance mapping by Brown (1980) who designated it to be the northern extension of the Monashee decollement. Recent reconnaissance work by Journeay and Brown (1986) has led them to the conclusion that it is MDI. Comparison of detailed observations related to the detachment in this study and observations to the south by Journeay (1986), plus the fact that

regional reconnaissance mapping (Wheeler, 1965; Brown, 1980) indicates upper-plate rocks are correlative with Selkirk allochthon Horsethief Creek Group strata, leads the author to the conclusion that this detachment surface is MD1. The presence of relict kyanite in the upper-plate of the map area also corroborates the unsupported assertion (Journeay & Brown, 1986) that M1 metamorphic zones overprint MD1 at this location.

Journeay (pers. comm. 1985) has mapped a metamorphic and lithologic boundary designated as MD2 to the northwest of the map area (see Journeay & Brown, 1986). At this boundary, along the west flank of Frenchman Cap dome, Selkirk allochthon rocks containing assemblages which equilibrated at peak conditions of >7.1 kb and temperatures between 650 to 750 degrees celcius are thrust against lower-grade assemblages of M1 metamorphism in the Monashee complex (Journeay, 1986). Downward heat flow from the allochthon is believed to have resulted in the inverted M2 metamorphic sequence documented in the lower-plate to the south (Fig. 18C; Journeay, 1986), and is herein inferred to have been responsible for the inverted M2 metamorphic sequence in both upper- and lower-plates in the map area. It therefore appears that the structural-metamorphic data and interpretations, documented at the north end of the Monashee complex, support tectonothermal models and evolutions (ref. op. cit.) based on fault bend folding and reactivation of major crustal-scale thrust faults.

3.6 SYNTHESIS

Rocks throughout the map area display a wide spectrum of structures indicative of both ductile and brittle behaviour, contrasting rheological properties, and strain partitioning on a variety of scales.

The present geometry of lithological units in the footwall is a

product of three phases of folding. Phase I structures, the Sibley Creek Syncline and previously unmapped anticlinal mate, control the map-scale geometry of lithologic units. These pre- to early metamorphic, south-southeast-verging, overturned structures have hinges which plunge to the west-southwest and limb lengths of several kilometers.

Phase I structures are refolded and transposed by two sets of phase II structures. They comprise east-verging drag folds and reclined, tight to isoclinal generally north-verging buckle folds. The later have hinge lines which are sub-parallel to a penetrative syn-metamorphic west-trending mineral stretching lineation. Phase II structures are inferred to have been generated during peak conditions of an early high-pressure and high-temperature metamorphic event (M1). The penetrative mineral stretching lineation was generated during both M1 and a later low-pressure reheating event, M2. Rare post-metamorphic west-trending upright warps comprise phase III deformation.

All folds are dissected by late brittle deformation which includes down to the west high-angle normal faults, east- and west-dipping conjugate shear fractures, and two sets of near vertical north- and northeast-striking extension fractures. The effects of brittle deformation are relatively minimal at this location in the Monashee complex.

Two phases of folding in the upper-plate are similar in style, but not necessarily correlative with phase II structures in the lower-plate.

All rocks display effects of flattening and shear strain associated with ductile thrusting along both the detachment surface at the northwest corner of the map area, inferred to be MD1, and MD2 just outside the map area to the northwest. MD1 is a zone of high strain marked by a ca. 100 m thick melange of various rock types set in a matrix of sheared pegmatite

which truncates footwall stratigraphy and structures. Kinematic indicators give west-over-east shear senses throughout most of the map area.

Observed microfabrics are consistent with fabrics generated during high-temperature deformation. Ductile deformation was achieved through a combination of intracrystalline plasticity and diffusive mass transfer processes, kinking, plus subordinate cataclasis. These processes contributed to geometrical softening, continual recrystallization, reaction softening and melt softening. The latter process was extremely effective in the accommodation of shear strain through the development of melt-softened shears.

Metastable mineral assemblages in the map area record two distinct syn-shearing metamorphic events. The earliest metamorphism (M1) produced peak mineral assemblages indicative of minimum physical conditions ranging from 6.4 to 7.1 kb, (Bathozone 5), and 640 to 679 degrees celcius. The second metamorphic episode (M2) produced an inverted metamorphic sequence with minimum peak physical conditions ranging from 2.0 to 3.4 kb (Bathozones 2 & 3a), and 615 to 678 degrees celcius. These two peaks were separated by static conditions within the kyanite, sillimanite and andalusite stability fields, respectively. This metamorphic evolution indicates that these rocks were buried to crustal depths of ca. 22 to 25 km, uplifted to a depth of ca. 13 km, reheated (and buried?), and finally uplifted and unroofed.

The above observations are consistent with proposed thermotectonic models based on fault-bend folding, reactivation of the Monashee decollement, and the generation of a crustal-scale duplex.

SUMMARY OF CONCLUSIONS

4

This study has documented and attempted analyses of geological features believed to have been generated during activity of Proterozoic divergent, and later Phanerozoic convergent dynamic tectonic systems along the western continent-ocean interface of North America. The following is a summary of conclusions reached in this study.

(1) The Monashee complex affords a view of a Late Proterozoic rift sequence (mantling gneisses).

(2) Mantling gneisses are composed of thick (>2000 m) and laterally extensive (ca. 150 km) shallow water, continental margin platform-like metasedimentary rocks locally intercalated with minor intrusive and extrusive phases.

(3) The succession was deposited on continental crust (core gneisses) that initially experienced broad, relatively stable subsidence, and was later affected by the Monashee extensional disturbance.

(4) Throughout most of the complex, this syndepositional disturbance is first marked by a laterally extensive (>100 km) stratiform pyroclastic carbonatite, part of an episodic (long-lived?) alkaline event which is unique in the Cordillera at this time (U-Pb zircon 746 +40, -39 Ma). It is later characterized at the north end of the complex by immature siliciclastic sediments intercalated with ultramafic and mafic sills and flows, plus minor felsic pyroclastic deposits.

(5) The evolution of the mantling gneisses is consistent with characteristics predicted by models of passive asymmetric rifting.

(6) This evolution is similar to: (i) other North American Proterozoic

rift successions, (ii) general geochemical evolutions of continental rifts, and (iii) actualistic models of rifting in the Gulf of California, supporting proposals that rift processes have been similar during Proterozoic and Phanerozoic time.

(7) Extension recorded by the mantling gneisses is believed to be a regional component of broad protracted Late Proterozoic rifting that culminated with deposition of deep water Windermere Supergroup clastic sediments.

(8) The geometrical distribution of rocks in the footwall of the Monashee decollement, at the north end of the complex, is controlled by three phases of folding which include: (i) the Sibley Creek Syncline-Anticline pair which are km-scale, overturned, south-southeast-verging, pre- to early metamorphic structures controlling the map-scale (1:15000) geometry, (ii) overprinting syn-metamorphic east-verging drag folds and reclined, tight to isoclinal, north-verging buckle folds with fold axes generally parallel to a penetrative, west-trending, mineral stretching lineation, and (iii) rare, weakly developed, post-metamorphic, west-trending upright warps.

(9) Brittle deformation has had relatively little effect on the distribution of map units.

(10) Recorded upper-plate structures are analogous in style to phase II structures in the lower-plate, but cannot be correlated across the detachment.

(11) The Monashee decollement, marked by a ca. 100 m thick melange of various rock types supported by a matrix of sheared pegmatite, truncates lower-plate structures and stratigraphy, and is a manifestation of early high-pressure, west-over-east displacement (MD1).

(12) Mylonite formation and the development of melt-softened shears, in both upper- and lower-plates, and along the detachment surface, are the major mechanisms by which shear strain accumulated.

(13) At a granular-scale, intracrystalline plasticity and diffusive mass transfer, plus subordinate cataclasis, contributed to ductile deformation and the formation of microfabrics suggestive of high-temperature shearing.

(14) Metastable pelitic mineral assemblages record two distinct syn-kinematic metamorphic episodes. The earliest (M1) parageneses indicate minimum peak physical conditions of 6.4 to 7.1 kb (22-25 km) and 640 to 679 degrees celcius, which locally outlasted shearing. Later syn-kinematic metamorphism (M2) defines a low-pressure, inverted metamorphic gradient, believed to be related to later thrusting along a splay in the Monashee decollement to the northwest of the map area. Inferred peak conditions are estimated to have been 2.0 to 3.4 kb (7-12 km), and 615 to 678 degrees celcius.

(15) The above structural and metamorphic inferences are most compatible with a previously proposed model which comprises building of an east-verging, crustal-scale, antiformal duplex accompanied by uplift-induced denudation.

FIGURE 1: REGIONAL GEOLOGY AND LOCATION MAP

Regional geology (modified after Journeay and Brown 1986). Faults marked in heavy lines: thrust faults (**barbs**) and normal faults (**dots**) with notation on hanging walls, include the Monashee decollement (MD), the Rocky Mountain Trench (RMT), the Columbia River Fault Zone (CRFZ) and the Eagle River detachment (ERD). Map units are upper Proterozoic and Mesozoic rocks of uncertain provenance (**blank**), Proterozoic and lower Paleozoic continental margin sequence of the Selkirk allochthon (**light stipple**), Proterozoic Belt-Purcell Supergroup (**horizontal dashes**), the Monashee complex (MC) composed of mantling gneisses (**medium stipple**) and core gneisses (**dark shading**), undifferentiated Paleozoic plutonic rocks (**single random dashes**), Middle Jurassic to lower Cretaceous plutonic rocks (**paired random dashes**), and undifferentiated Cenozoic plutonic and related volcanic rocks (**crosses**). Miogeoclinal rocks northeast of the RMT are not patterned. The map area is outlined at the north end of the Monashee complex. FCD = Frenchman Cap dome, TOD = Thor-Odin dome. Inset map outlines the region's location relative to the five geological belts of the Canadian Cordillera: the Foreland Thrust and Fold Belt (1), Omenica Belt (2), Intermontane Belt (3), Coast Plutonic Belt (4), and Insular Belt (5).

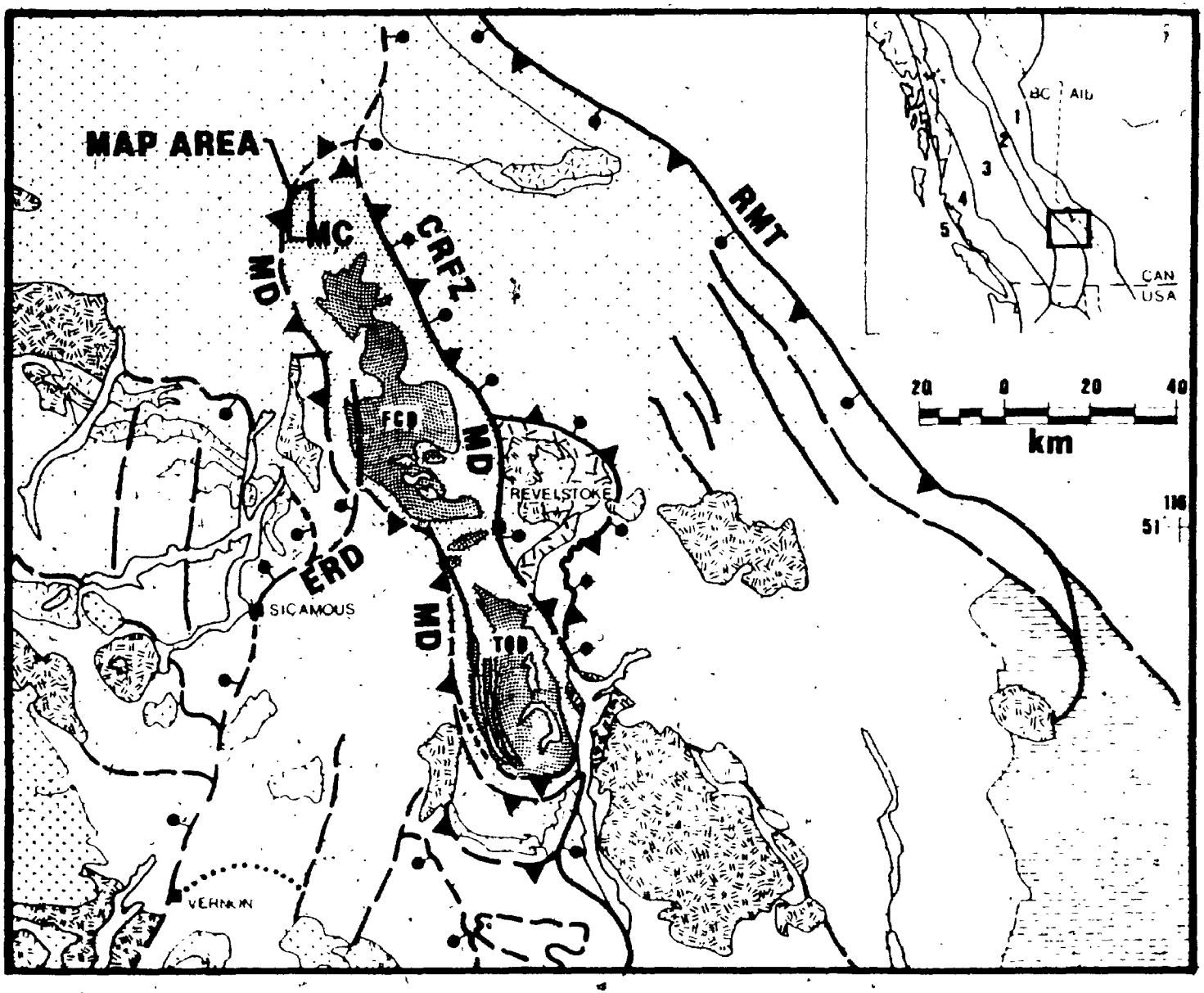
MAP AREA
MC
MD
CRFZ
RMT
FCD
MD
REVELSTOKE
ERD
SICAMOUS
MD
TCD
VERNON
BC
Alb
1
2
3
4
5
CAN
USA
20
0
20
40
km
116
51

FIGURE 3: Stratigraphic column, descriptions and interpretations of gneisses between Sibley and Kirbyville creeks at the north end of the Monashee complex.

For summary of lithofacies symbols used see figure 5. Lower case roman numerals and arabic numerals imply stratigraphic order. No stratigraphic order is implied by the position of the Monashee decollement which cross-cuts units 5 to 12. Qtz = quartz, Fsp = feldspar, Bt = biotite, Grt = garnet, Hbl = hornblende, And = andalusite, Sil = sillimanite, Ky = kyanite. Arrow indicates stratigraphic facing direction determined from primary sedimentary structures.

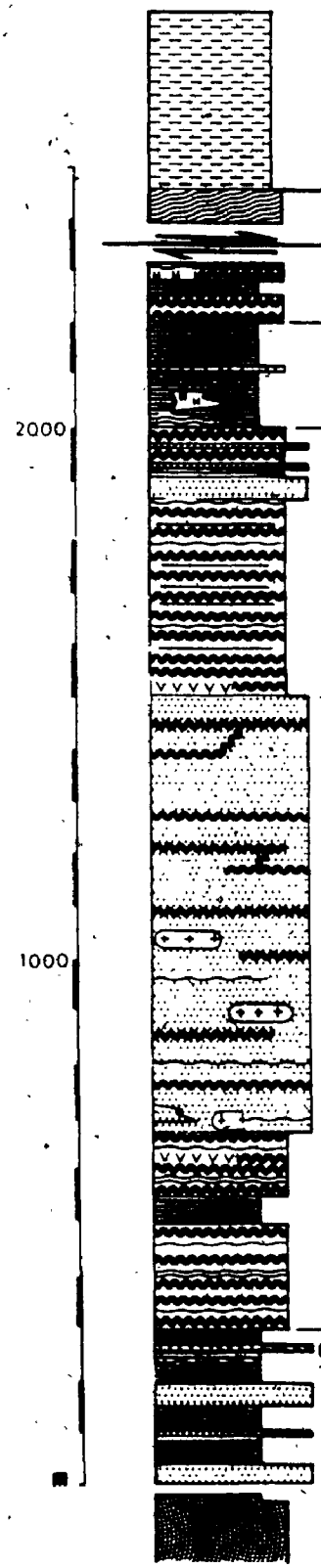

UNIT	DESCRIPTION	PROBABLE PROTOLITHS
	SELKIRK ALLOCHTHON	
SA	Dominantly pelitic & semipelitic schists interlayered with Qtz Fsp gneiss, quartzite and minor amphibolite pegmatite locally composes ca. 25%	Chemically mature mudstones immature arenites, quartz arenites
	MONASHEE DECOLLEMENT	
MD	Melange of various schists, gneisses, quartzites and calc-silicates in a matrix of up to 50% pegmatite a high strain zone	
	MANTLING GNEISSES	
[illegible]	Undifferentiated amphibolites gneisses pelitic schists and hornblendite	See below
[illegible]A	Amphibolite	Mafic flows, immature arenites and possibly dolo-marls
[illegible]QF	Bt-Grt Hbl-Qtz Fsp gneiss	Immature arenites
[illegible]H	Hornblendite with subordinate Hbl gneiss	Subaqueous mafic flows interflow sediments
[illegible]	Pelitic schist and amphibolite interbedded with Qtz Fsp gneiss and hornblendite	Chemically mature mudstones, mafic flows immature arenites and possibly dolo-marls
	Amphibolite hornblendite, Bt & Hbl gneisses interbedded with minor calcareous Bt schist	Mafic flows, immature arenites and dolo-marls
[illegible] P	Dominantly pelitic and semipelitic schists interlayered with Qtz Fsp gneiss and subordinate amphibolite and hornblendite	Chemically mature mudstones and Qtz Fsp arenites with minor immature mafic arenites and mafic flows
MQ	Interbedded impure marble calc-silicate and quartzite	Cyclic impure siliceous limestones and Qtz arenite
H	Hornblendite with subordinate Hbl gneiss	Mafic flows and interflow sediments
G	Flaggy Bt-Hbl-Qtz-Fsp gneiss	Immature arenites
10 AP	Amphibolite and Al-deficient pelitic and semi pelitic schists interlayered with subordinate hornblendite quartzite Qtz-Fsp gneiss and metaconglomerate	Chemically immature mudstones, mafic flows and tuffs Qtz and Qtz Fsp arenites, volcaniclastic and/or epiclastic rocks
[illegible]	And-Sil-Ky-Grt-Qtz Fsp schists	Chemically mature mudstones
Q	White quartzite	Qtz arenites
9	Dominantly quartzite with concordant and discordant amphibolite, minor pelitic schists ultramafic and syenite rocks, interlayered Hbl- & Grt-bearing meta-arkose & subarkose	Qtz arenite mafic sills, dikes and possibly flows minor ultramafic sills and/or flows chemically mature mudstones and Qtz-Fsp arenites
QF	Hbl- & Grt bearing pink meta-arkose	Arkose
8 G	Amphibolite and flaggy Hbl gneiss interbedded with minor quartzite various gneisses carbonate rocks and metaconglomerate	Mafic sills and/or flows mafic arenites and tuffs, Qtz arenite dolo-marls and epiclastic rocks
[illegible]	Dominantly pelitic and semipelitic schist interlayered with subordinate amphibolite hornblendite and various gneisses	Chemically mature mudstones immature mafic siliciclastic rocks and mafic flows and/or sills
[illegible]	Pelitic schist with minor interbedded white marble and calc silicate at the base and Qtz Fsp gneiss and amphibolite at the top	Chemically mature mudstones, limestone siliceous limestone Qtz Fsp and mafic arenites
6 [illegible]	Quartzite	Qtz arenite
[illegible]	Stratiform fragmental carbonatite	Carbonatite pyroclastic deposits
[illegible]	Banded impure marble	Cyclic impure limestone with siliciclastic bases
	Banded calc silicate gneiss	Cyclic calcareous siliciclastic marls with impure mafic bases
	Banded Hbl gneiss	Dolo-marls
[illegible]	Pelitic schist interlayered with subordinate amphibolite and Qtz Fsp gneiss	Chemically mature mudstones mafic arenites and Qtz-Fsp arenites
4	Quartzite and feldspathic quartzite with minor pelitic schist partings	Qtz and Qtz Fsp arenites interlayered with minor chemically mature mudstone
3 P	Pelitic schist with minor interlayered Qtz Fsp gneiss and quartzite	Chemically mature mudstones Qtz Fsp arenites and Qtz arenite
2	Quartzite	Qtz arenite
2	Quartzite with pelitic schist partings	Qtz arenite and chemically mature mudstones
	Marble not observed unconformable to the [illegible]	
	CORE GNEISSES	
	[illegible] Bt schist and Bt Qtz Fsp gneiss	Chemically mature mudstone and immature arenite

FIGURE 5: Correlation of mantling gneiss sequences about Frenchman Cap and Thor-Odin domes.

Columns 1 to 3 after Read (1980), 4 after Fyles (1970b) and Hoy and McMillan (1979), 5 after Hoy (1982a), 6 after McMillan (1969) and Hoy and McMillan (1979), modified by Journeay (1986), 7 after Journeay (1986), 8 after Psutka (1978), modified by Journeay (1986), 9 after Hoy (1979), 10 this study. Correlation between columns 1 to 3 after Read (1980), 4, 5 and 6 after Hoy and McMillan (1979), 6, 7, and 8 after Journeay (1986). All other correlations are based on the presence of basal quartzite and the calc-silicate/marble/carbonatite horizons. The date in column 4 (746 +40, -39 Ma, U-Pb zircon, Parrish, unpublished data 1986) is from nepheline syenite gneiss near Mount Copeland. The stratiform carbonatite horizon is used as a chronostratigraphic marker (dash-dot line) where present, and assumed to be the calc-silicate/marble horizon, which usually hosts the stratiform carbonatite, where absent. Stratigraphic facing directions for each column have been regionally established (see references cited above). The stratigraphic duplicating effects of pre- to early-metamorphic low-angle thrust faults have been recognized and removed in columns 5 and 7 (ref. op. cit.). One of these faults is shown in column 6 (after Journeay, 1986).

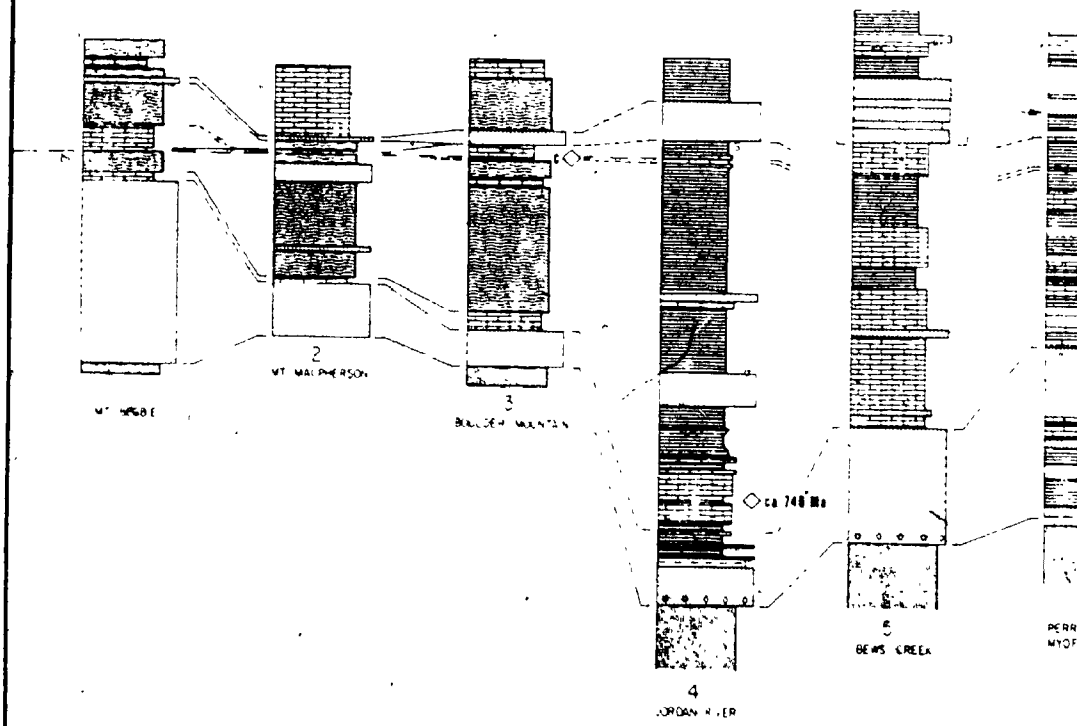

LEGEND

- QUARTZITE, META-ARKOSE & METASUBARKOSE
- QUARTZ PEBBLE CONGLOMERATE
- PELITIC SCHIST
- SEMIPELITIC SCHIST
- MARBLE, IMPURE MARBLE
- CALC - SILICATE CALCAREOUS SCHIST
- BIOTITE - & HORNBLENDE-BEARING QUARTZ-FELDSPAR GNEISS
- NEPHELINE SYENITE & SYENITE GNEISSES
- AMPHIBOLITE
- HORNBLENDITE
- VOLCANICLASTIC and/or EPICLASTIC DEPOSIT
- CARBONATITE
- META-ULTRAMAFIC
- SULPHIDE LAYERS
- CORE GNEISSES

LOCATION MAP

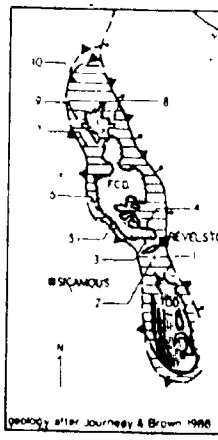

geology after Journeay & Brown 1986

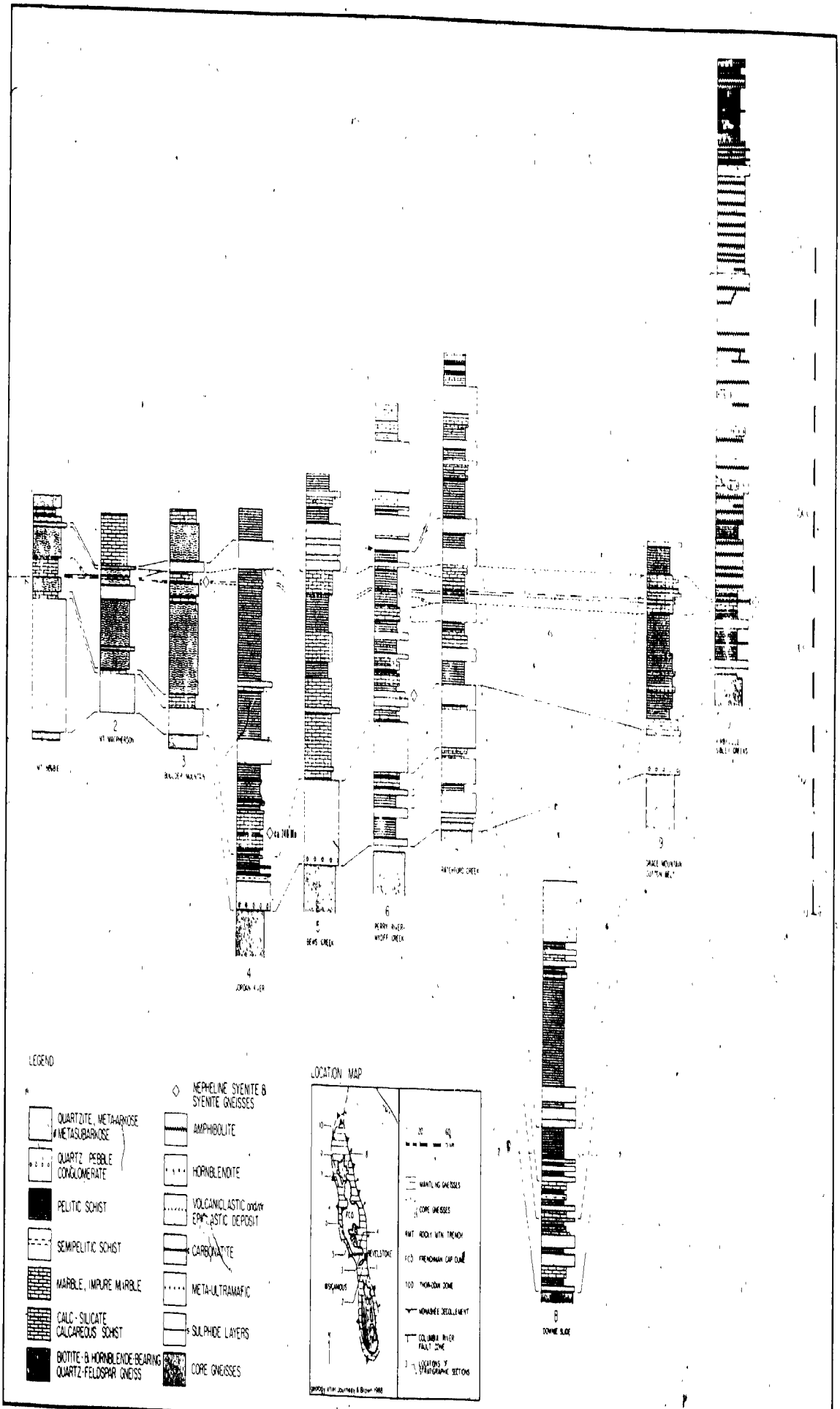
2
3
4
5
6
8
9
LEGEND
QUARTZITE, META-ARKOSE & METASUBARKOSE
QUARTZ PEBBLE CONGLOMERATE
PELITIC SCHIST
SEMIPELITIC SCHIST
MARBLE, IMPURE MARBLE
CALC-SILICATE CALCAREOUS SCHIST
BIOTITE- & HORNBLENDE-BEARING QUARTZ-FELDSPAR GNEISS
NEPHELINE SYENITE & SYENITE GNEISSES
AMPHIBOLITE
HORNBLENDITE
VOLCANICLASTIC and/or EPICLASTIC DEPOSIT
CARBONATITE
META-ULTRAMAFIC
SULPHIDE LAYERS
CORE GNEISSES
LOCATION MAP
MANTLING GNEISSES
CORE GNEISSES
FCD FRENCHMAN CAP DOME
100 THOR-ODIN DOME
MONASHEE DECOLLEMENT
COLUMBIA RIVER FAULT ZONE
LOCATIONS OF STRATIGRAPHIC SECTIONS
DOME SLIDE

TABLE 1 SUMMARY OF EVIDENCE FOR LATE PROTEROZOIC TECTONIC ACTIVITY IN THE NORTH AMERICAN CORDILLERA

LOCATION	STRATIGRAPHY	EVIDENCE	DATING METHODS	KEY REFERENCES
1. S.W. Rocky Mtns. B.C.	Belt Purcell Supergroup Windermere Supergroup	Great Rift Dyke (c. 800-900 Ma) [illegible] faulting and low grade metamorphism	Stratigraphic correlation with [illegible] dated sequences (e.g. [illegible])	[illegible]
2. Dorsetshire, Ogilvie & Mackenzie Mtns. Yukon & N.W.T.	Windermere, Mackenzie Mtns. & Windermere Supergroup [illegible]	Sturtian (Rapitan) (c. 800 Ma) [illegible] faulting and basin subsidence [illegible]	Stratigraphic correlation with [illegible] dated sequences [illegible]	[illegible]
3. Mackenzie Mtns. Yukon & N.W.T.	Mackenzie Mtns. Supergroup Tsezotene Formation	[illegible]	[illegible]	[illegible]
	Little Dal Group	[illegible] normal faulting	[illegible]	[illegible] Hoffman & Aitken [illegible] Aitken et al. [illegible] Aitken [illegible] Park & Aitken [illegible] Eisbacher [illegible]
	Coates Lake Group	Synsedimentational normal faulting and abrupt thickness and facies changes	[illegible]	Jefferson & Rigby [illegible] Rainbird [illegible] Eisbacher [illegible]
4. Ogilvie Mtns. Yukon	Windermere Supergroup	Mount Harper volcanic complex and synsedimentational normal faulting	U-Pb zircon 777 ± [illegible] Ma on felsic extrusives	Roots in prep. Thompson [illegible] Roots & Thompson [illegible]
5. Eastern Alaska	Tindir Group	Mafic pillowed volcanics and synsedimentational faulting implied by the presence of clasts of lower units in higher units	Stratigraphic similarity with Mackenzie and Ogilvie dated sequences	Young [illegible]
6. Monashee Mtns. Southern B.C.	Monashee Complex (Windermere Supergroup)	Monashee Paroxysmal (Disturbance) synsedimentational alkalines, mafic and felsic intrusive and extrusive deposits	Unconformably overlies c. 2.1 Ga basement dated from alkaline intrusive rocks: U-Pb zircon 773 +280 -218 Ma and 746 ± 60 -19 Ma	[illegible] Parrish unpublished data [illegible]
7. Purcell Mtns. Southern B.C.	Windermere Supergroup	Synsedimentational normal faulting	Unconformably overlies Belt Purcell and unconformably underlies Cambrian strata	[illegible]
8. Southern B.C. & northern Washington	Windermere Supergroup Huckleberry Formation	Lowest mafic volcanics at the base of the sequence	K-Ar whole rock & mineral separate dates 827-918 Ma (evidence for Rift disturbance therefore K-Ar dates is suspect see Devlin et al. 1985)	Miller et al. [illegible]
9. Utah & S.E. Idaho	Pocatello Formation	Thermal mafic volcanics and synsedimentational faulting implied by abrupt facies changes and clasts of lower units in higher units	Limited radiometric dating, stratigraphic similarity with dated sequences (e.g. [illegible])	[illegible] 1983 Harper & [illegible] 1984
10. Grand Canyon, Arizona	Grand Canyon Supergroup	Grand Canyon (Disturbance) c. 825 Ma mafic flows and synsedimentational normal faulting	K-Ar 930-[illegible] 825-[illegible] 26 Ma, inferred to be reset dates, paleomagnetic & paleontological studies, stratigraphic correlation with similar dated sequences (e.g. [illegible])	Fillon & [illegible] 1982
11. East California	Kingston Group Kingston Peak Formation	Synsedimentational faulting implied by buried faults, abrupt thickness changes interbedded pillowed flows and strata deposited on variable substrate	Unconformably overlies rocks intruded by alkaline rocks c. 1400 Ma and paleontological data, and stratigraphic correlation with similar dated sequences (e.g. [illegible]) suggest c. 1200-800 Ma age	Miller 1983 Miller et al. 1984

FIGURE 10: FOLD CHARACTERISTICS

A. Intrafolial rootless phase I folds. Station 85-R231.

B. Reclined isoclinal phase I fold in the core of the Sibley Creek Syncline. Station 85-R231.

C. Disharmonic phase I folds in the core of the Sibley Creek Anticline looking west down the mineral stretching lineation. Station 84-RS37.

D. Reclined isoclinal phase I fold looking west down the mineral stretching lineation. Station 85-R193.

E. Reclined phase II flexural flow folds. Station 85-R136.

F. A discrete pegmatitic shear which truncates the lower limb of a 10m-scale phase II fold. Phase II drag folds are present in the lower-plate of this shear. Station 84-RS25.

G. Reclined tight phase II folds looking west down the lineation. Note that the axial planar fabric in one layer is defined by biotite. Station 84-RS105.

H. Reclined phase II passive flow folds. Station 85-R113.

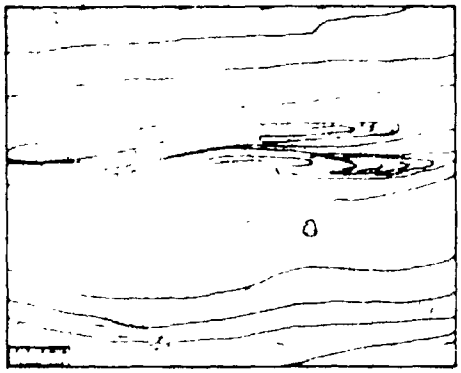

A

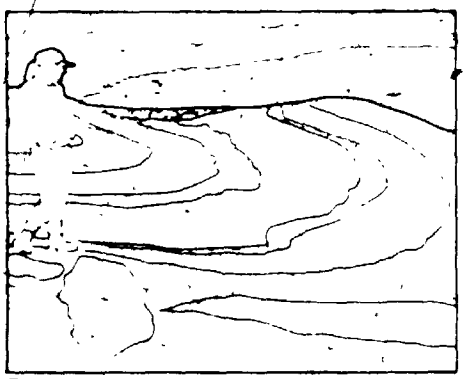

B

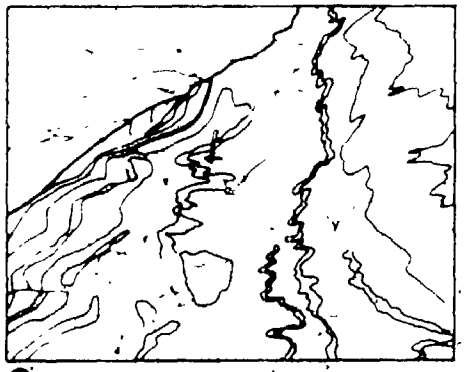

C

D

E

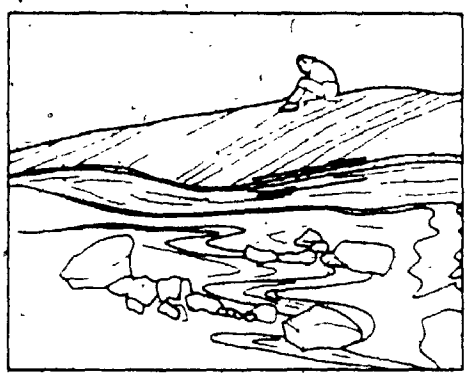

F

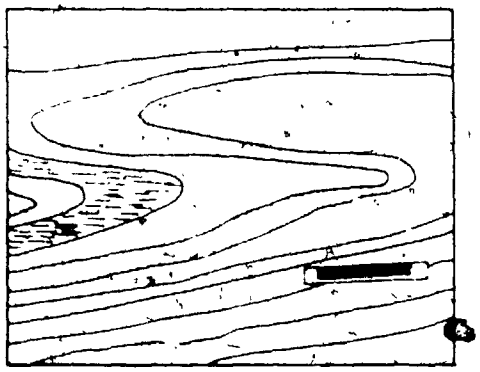

G

H

FIGURE 11: FOLD CHARACTERISTICS

A. Type 2 interference pattern (Thiessen & Means, 1980) produced by interference of phase I and II folds. Station 84-RS119.

B. Type 3 interference pattern (Thiessen & Means, 1980) produced by interference of phase II folds. Station 85-R20.

C. Phase II drag folds in profile parallel to the mineral stretching lineation and perpendicular to the foliation. Note that the axial planes become more reclined to the east along the fold train and towards the fold closures of the individual folds. These observations are believed to indicate that the upper-plate of the shear couple moved to the east. Station 85-R21.

D. Phase II fault propogation folds in profile parallel to the mineral stretching lineation and perpendicular to the foliation. These structures are interpreted to indicate that the upper-plate of the shear couple moved to the east. Station 85-R21.

E. An oblique profile of a phase II sheath fold which closes to the east. The pen held in the hand points down the westerly trending mineral stretching lineation. These relationships are interpreted to indicate that the upper member of the shear couple moved in an easterly direction. Station 85-R3.

F. A view looking to the west down the mineral stretching lineation at a profile of a phase II sheath fold. The sense of shear cannot be determined. Note the vergence reversal. Station 85-R37.

G. A profile of a phase II fold closure. Note the kinked foliation and the internal foliation within the garnets which also define the fold. Station 85-R36.

H. Phase III upright warps in profile looking east. Station 84-RS195.

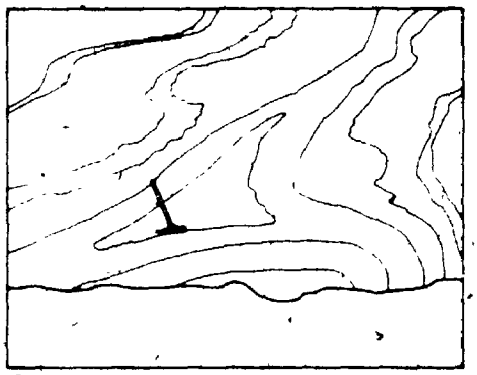

A

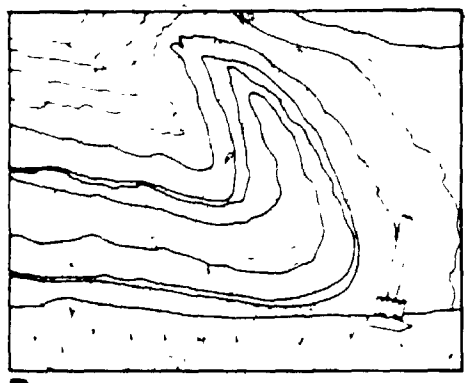

B

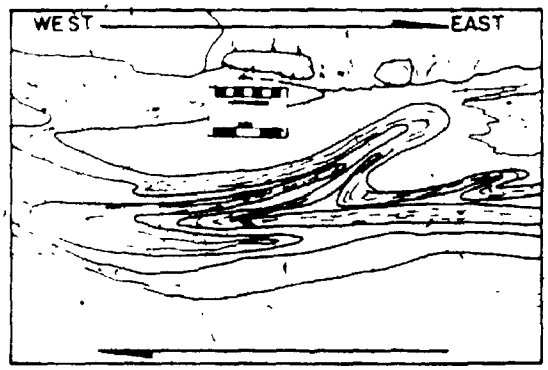

C

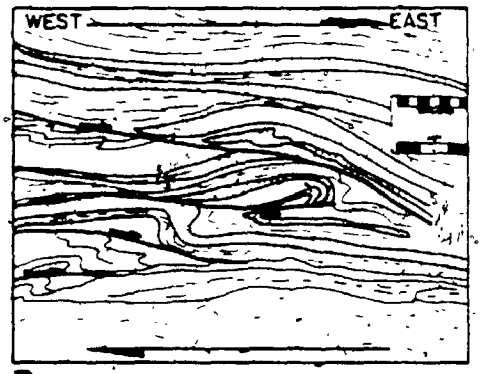

D

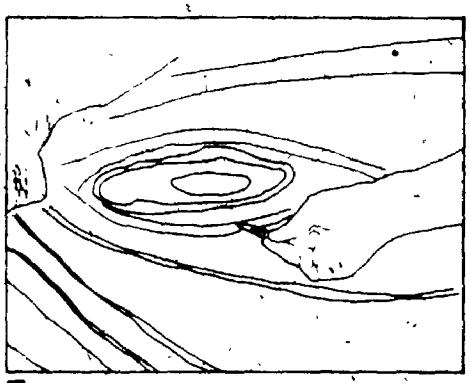

E

F

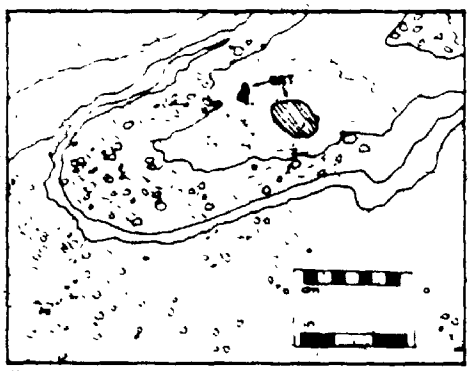

G

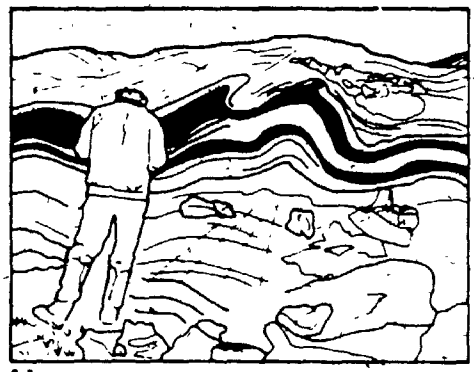

H

FIGURE 12: PULL-APART STRUCTURES

A. The only remnants of this mafic layer in the immediate vicinity, these m-scale boudins are interpreted as qualitative indicators of high strain. Station 85-R152.

B. Blocky boudins indicative of layer parallel extension. Station 84-RS153.

C. Type 2B asymmetrical pull-aparts (Hanmer, 1986) interpreted to indicate that the upper member of the shear couple moved to the west. Station 84-RS143.

D. Type 2B asymmetrical pull-aparts (Hanmer, 1986) interpreted to indicate that the upper member of the shear couple moved to the east. Station 85-R12.

E. Type 2A asymmetrical pull-apart (Hanmer, 1986) interpreted to indicate that the upper-plate of the shear couple moved to the west. Station 84-RS129.

F. Type 2A asymmetrical pull-aparts (Hanmer, 1986) interpreted to indicate that the upper member of the shear couple moved to the east. Station 85-R167.

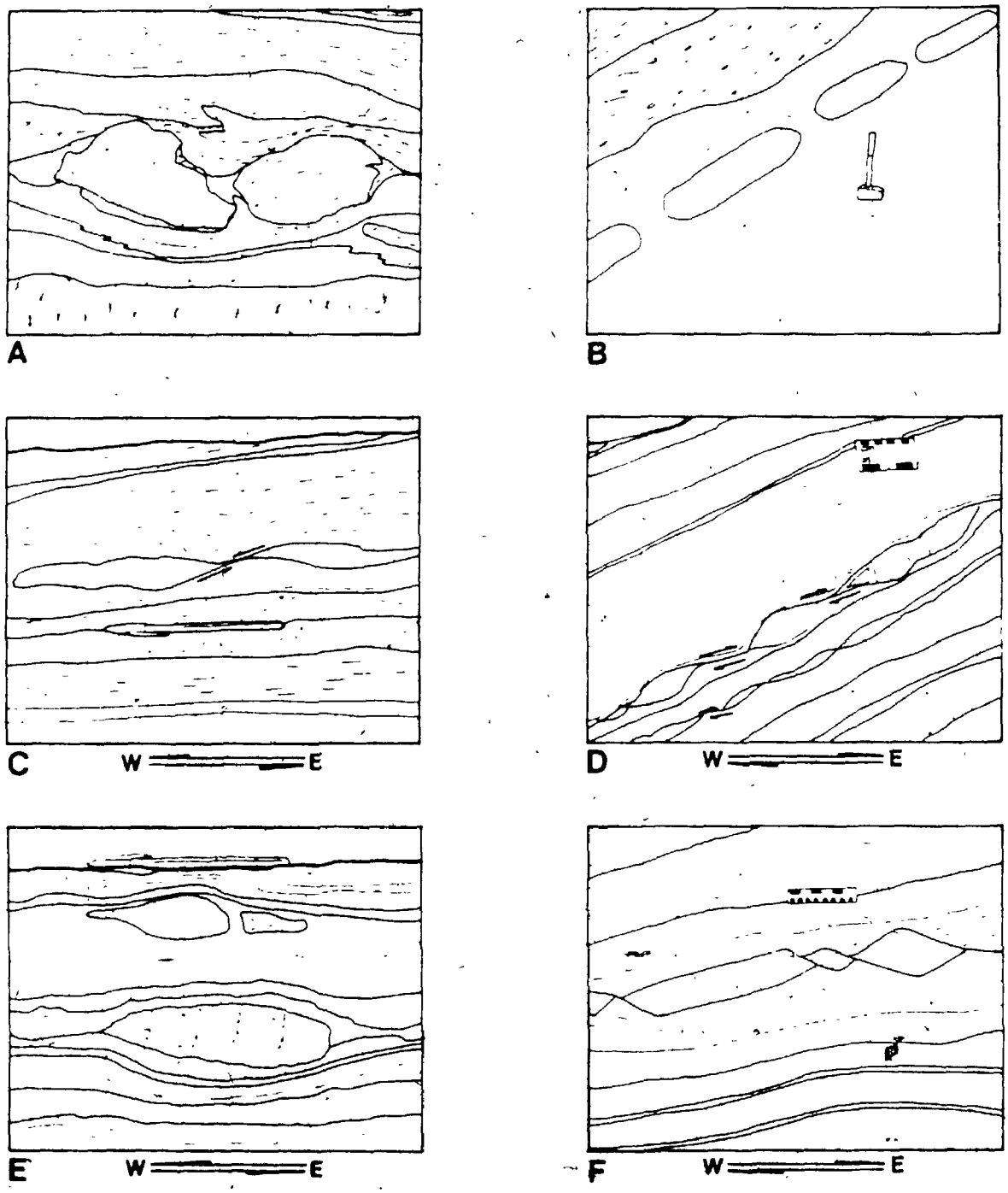
A
B
C
W
E
D
W
E
E
W
E
F
W
E

FIGURE 13: Rotational normal faults as kinematic indicators

A. Possible initial configuration with vertical extension fractures, and an inclined shear fracture. The thick black line represents compositional layering.

B. Rotation of blocks and faults with progressive simple shear strain.

C. A configuration similar to A but the end blocks were confined between the dashed lines and assumed to deform in part by ductile flow. This section is balanced.

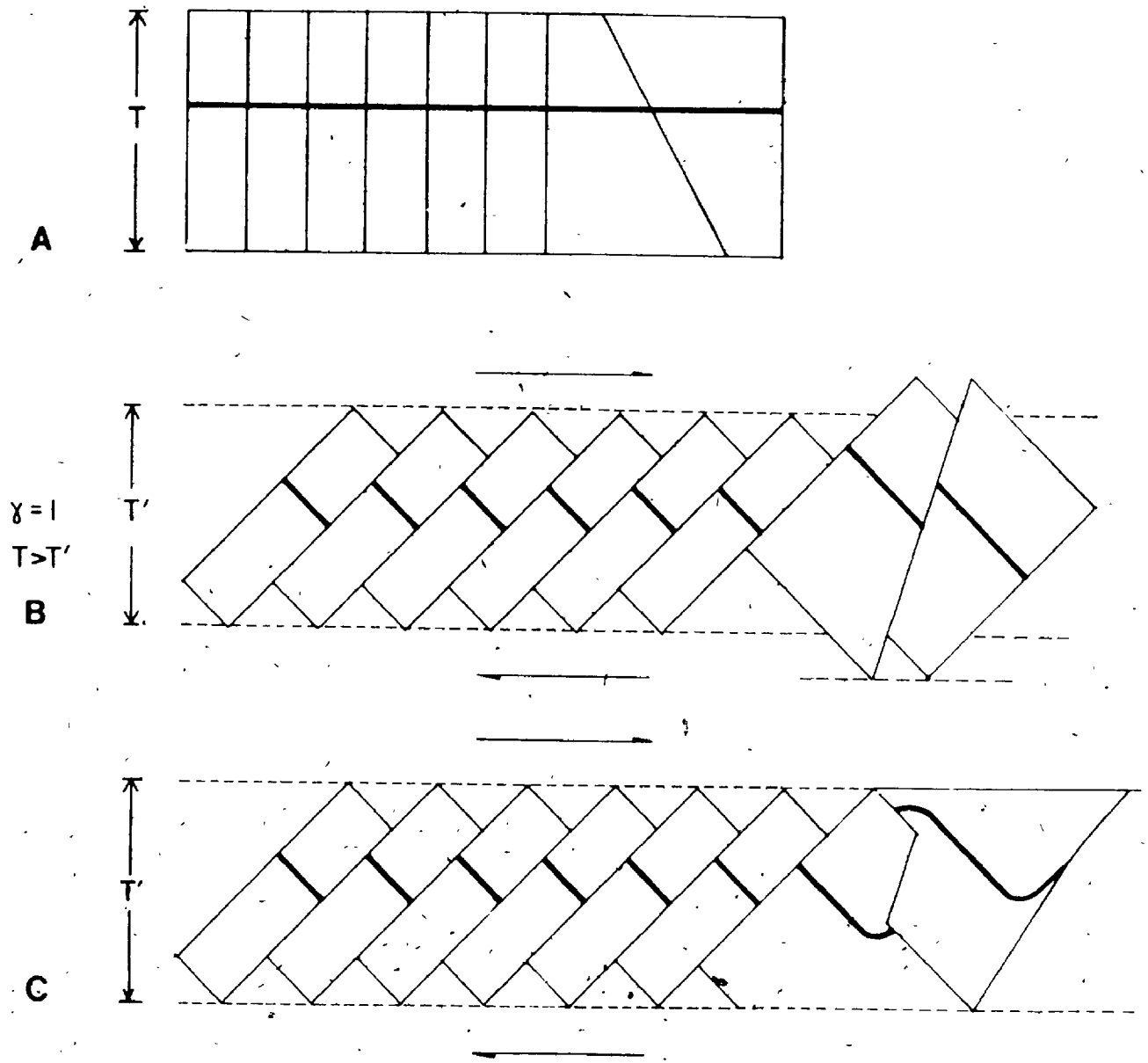
A
T
γ = 1
T>T′
T′
B
T′
C

TABLE 2 . RELATIONSHIPS BETWEEN DEFORMATION, NEOMINERALIZATION AND MELT GENERATION

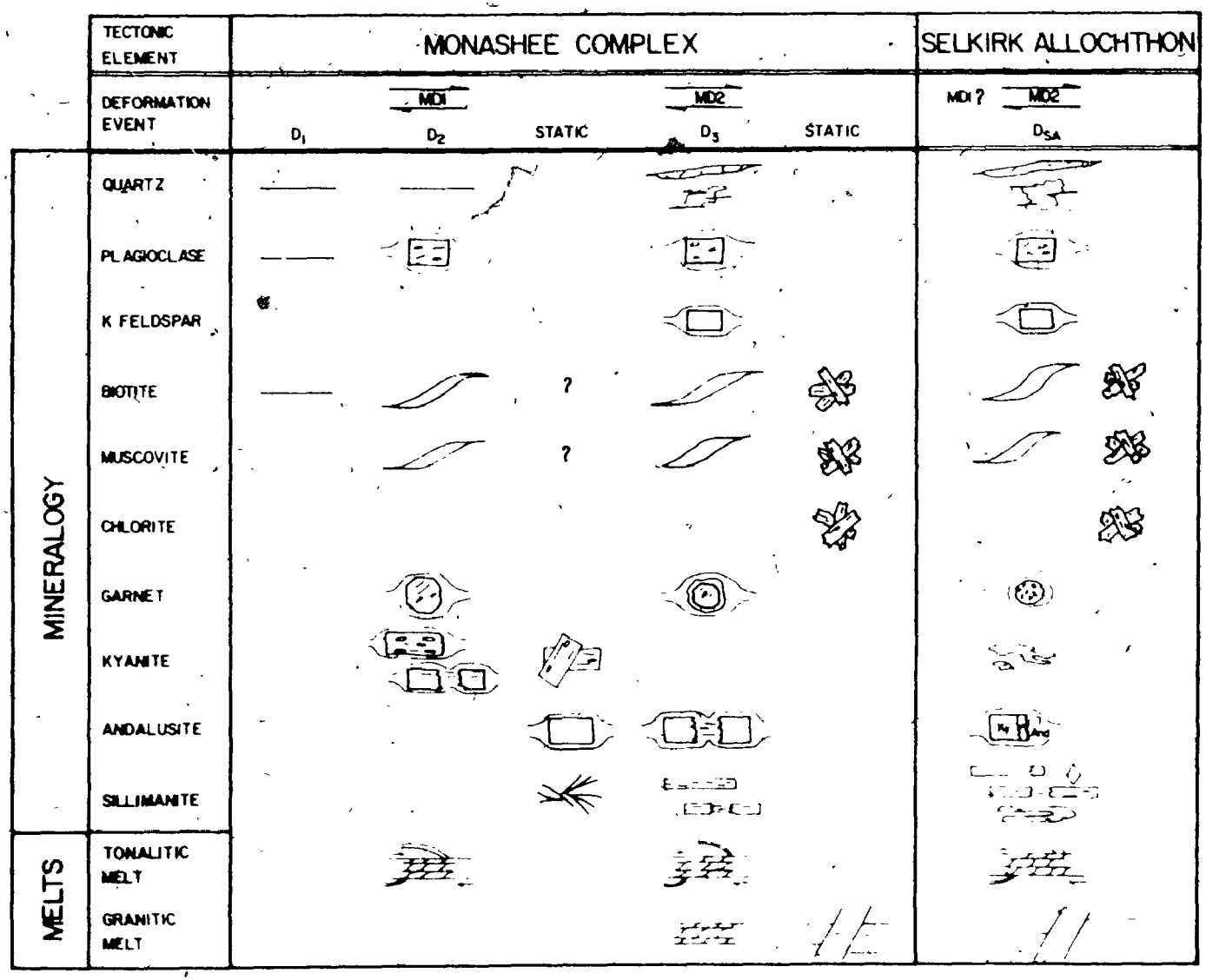

FIGURE 14: M1 P-T Path

Divariant P-T fields entered as indicated by textural interpretations of M1 mineral parageneses. Their order of progression is indicated by the boxed numbers. A possible P-T path for M1 metamorphism in the map area is indicated by the double line. The P-T diagram is after Carmicheal (1978) and modified by Journeay (1986). See text for discussion.

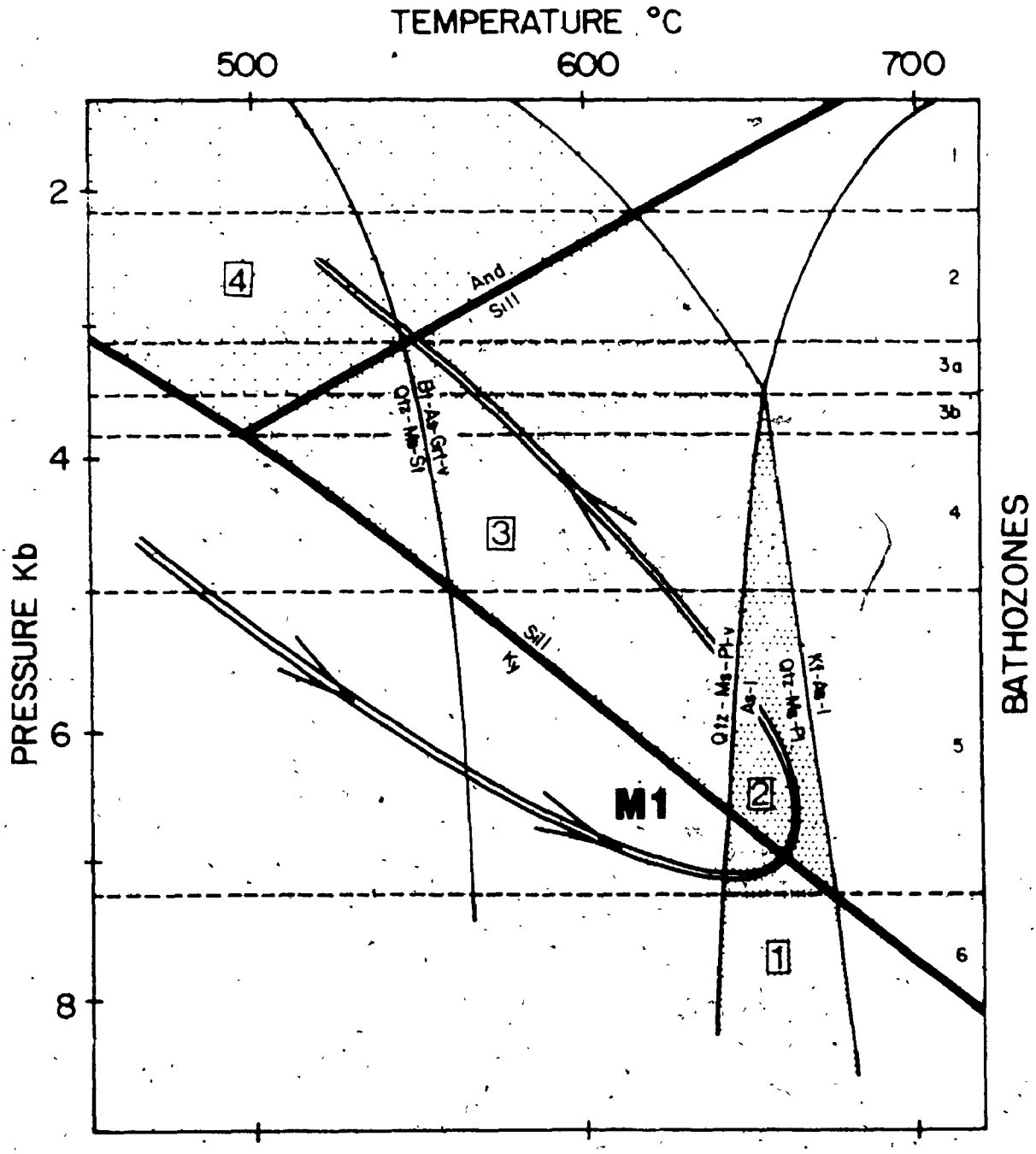
TEMPERATURE °C
500
600
700
PRESSURE Kb
2
4
6
8
BATHOZONES
1
2
3a
3b
4
5
6
And.
Sill
Ky
Sill
Bt-Ab-Grt-V
Qtz-Ma-St
Qtz-Ma-Pl-V
Ab-I
Qtz-Ma-Pl
Ki-Ab-I
M1
1
2
3
4

FIGURE 15: ALUMINOSILICATE ASSEMBLAGE ZONES

Aluminosilicate assemblage zones Sil-Kfs, Ky-Sil and Ky-And+/-Sil, plus intervening isograds, Ky-Ms-out and And-out isograds, respectively, are readily identified in the field. Thin section studies reveal remnants of Ky and And in the Sil-Kfs zone, and And in the Ky-Sil zone. Ky is interpreted to be a remnant of M1 metamorphism, and was not observed in the field to the northwest of the Ky-out isograd, which coincides with the Ms-out isograd. M1 assemblages are overprinted by M2 Sil-Kfs-granitic melt, Sil-Ms and And-Ms+/-Sil zones, (the latter two being equivalent to the Ky-Sil and Ky-And+/-sil zones respectively). These zones are bound by the Ms-out and And-out isograds which are interpreted to reflect the reactions Qtz + Ms + Pl = Kfs + As + melt and And = Sil respectively. These data and inferrences, plus the observations that leucosome development increases as one approaches the upper-plate, and forms a pegmatized zone that dips to the northwest, are used to infer the existence of an inverted metamorphic gradient, with reaction isograds dipping to the northwest.

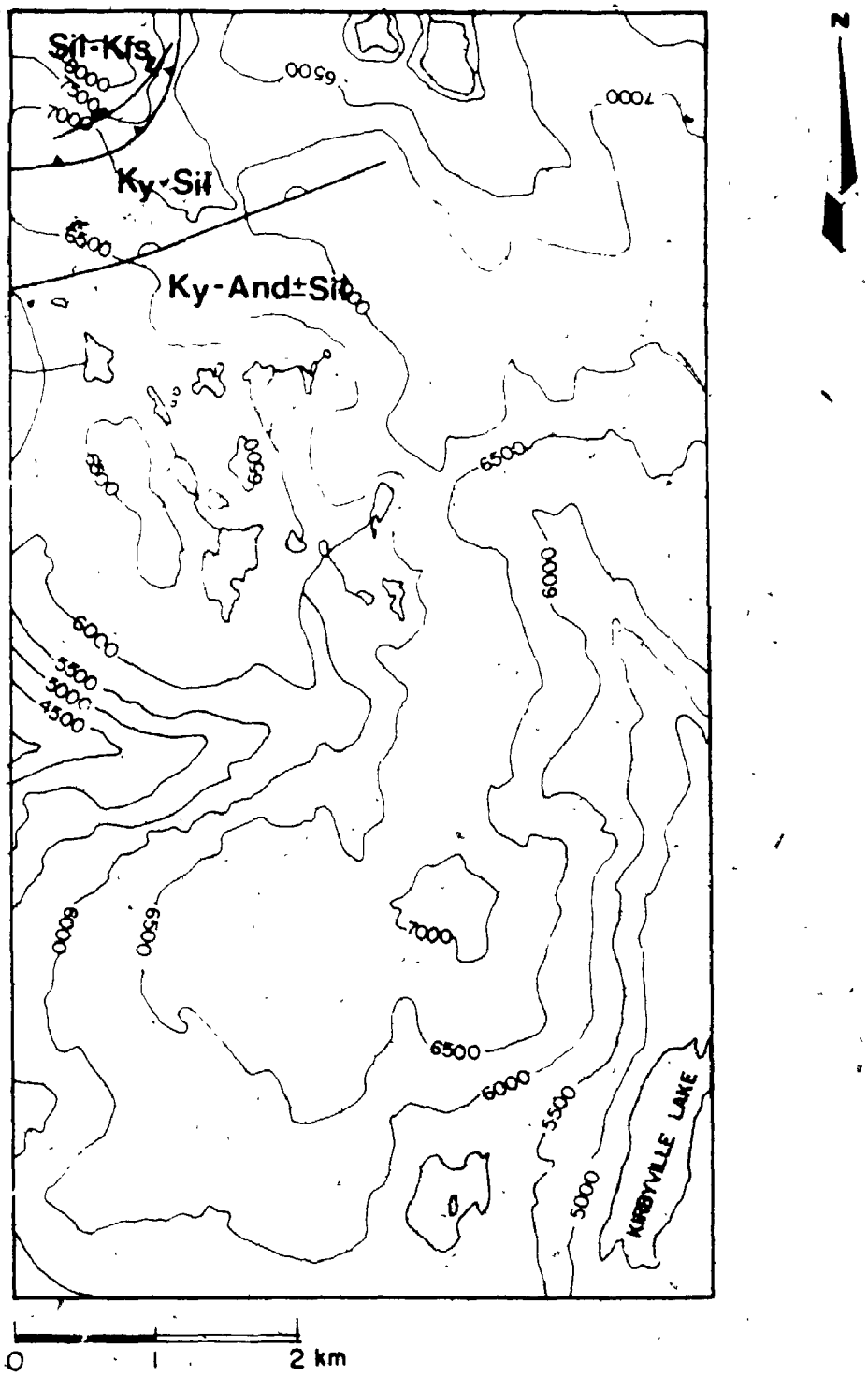

6000 Elevation contour in feet above sea level

Monashee decollement

Andalusite-out isograd

Kyanite- and muscovite-out isograd

FIGURE 16: M2 P-T Path

Divariant P-T fields entered as indicated by textural interpretations of M2 mineral parageneses. Their order of progression is indicated by the boxed numbers. The double line represents a qualitative P-T path for M2 metamorphism in the map area. The P-T diagram is after Carmicheal (1978) and modified by Journeay (1986). See text for discussion.

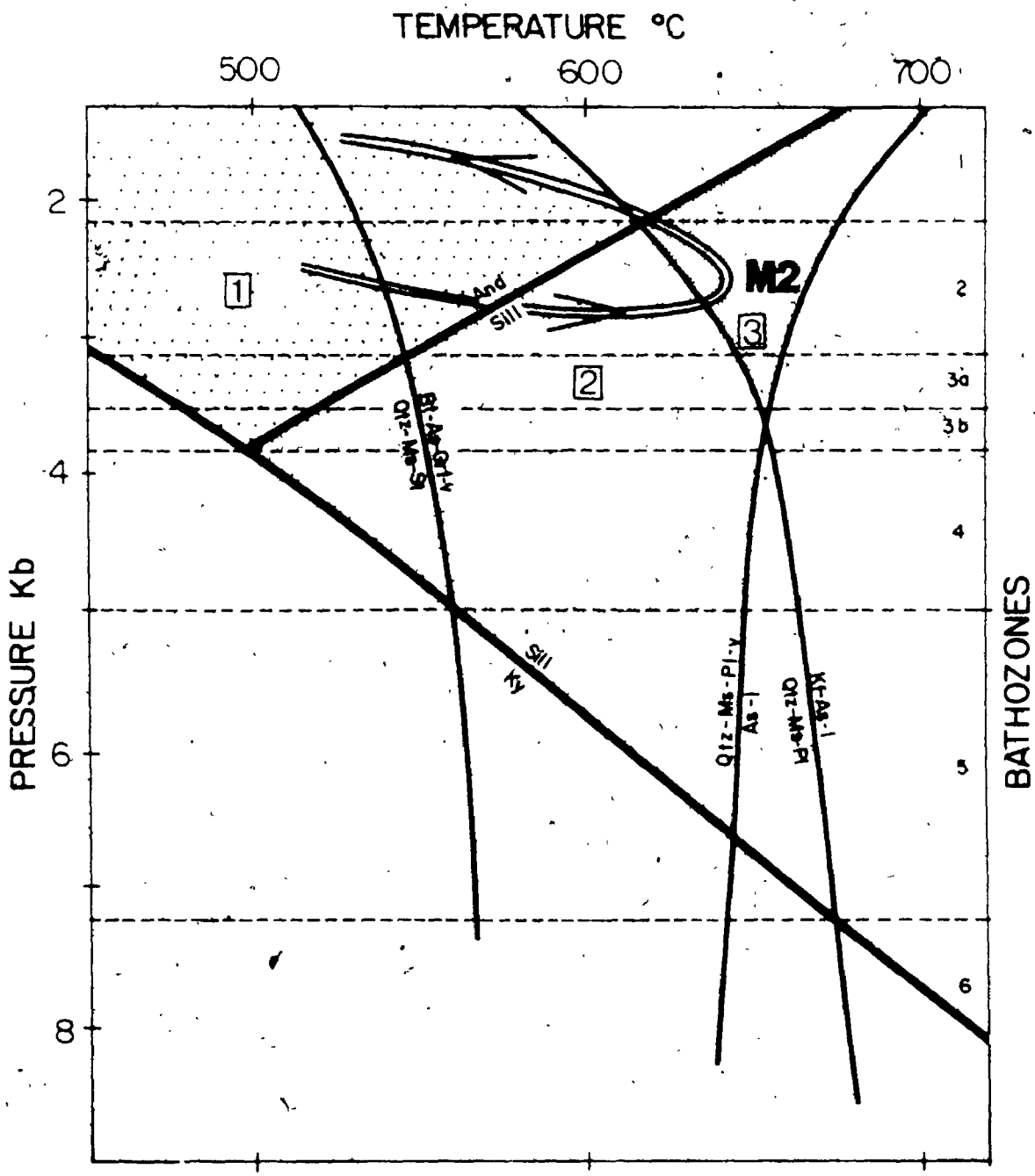
TEMPERATURE °C
500
600
700
PRESSURE Kb
2
4
6
8
BATHOZONES
1
2
3a
3b
4
5
6
1
2
3
M2
And
Sill
Ky
Sill
Bt-Ab-Qtz-V
Qtz-Ms-Sil
Qtz-Ms-Pl-V
As-I
Qtz-Ms-Pl
Kf-Ab-I

FIGURE 17: P-T-t PATH

A possible P-T-t path for rocks at the north end of the Monashee complex. See text for discussion.

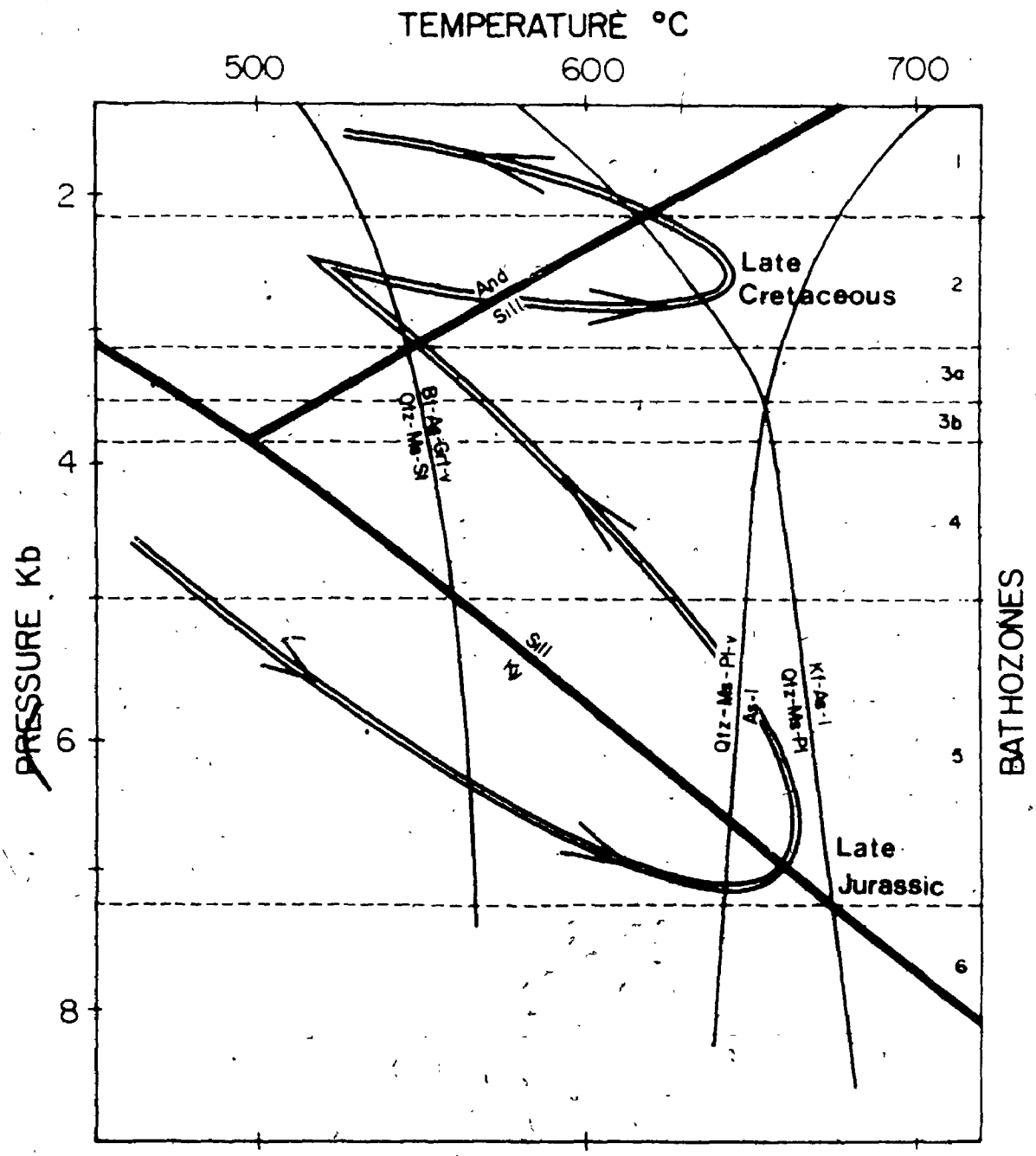
TEMPERATURE °C
500
600
700
PRESSURE Kb
2
4
6
8
BATHOZONES
1
2
3a
3b
4
5
6
Late Cretaceous
Late Jurassic
And
Sill
Sill
Qtz-Ms-Sp
Bi-Ab-Grt-v
Qtz-Ms-Pl-v
Ag-l
Qtz-Ms-Pl
Kl-Ab-l

FIGURE 18: P-T PROFILES

A. Ideal P-T profile through the Monashee complex prior to arching of the Monashee decollement (after Journeay, 1986). M1 parageneses at the north end of the complex indicate peak metamorphic conditions in the shaded region.

B. Reconstructed M1 P-T profile through the Monashee complex in the vicinity of Ratchford Creek (after Journeay, 1986). M1 parageneses at the north end of the complex indicate peak metamorphic conditions on the shaded region.

C. Reconstruction of M2 P-T profile at the same location as A (after Journeay, 1986). M2 parageneses at the north end of the complex indicate metamorphic conditions spanned the shaded fields.

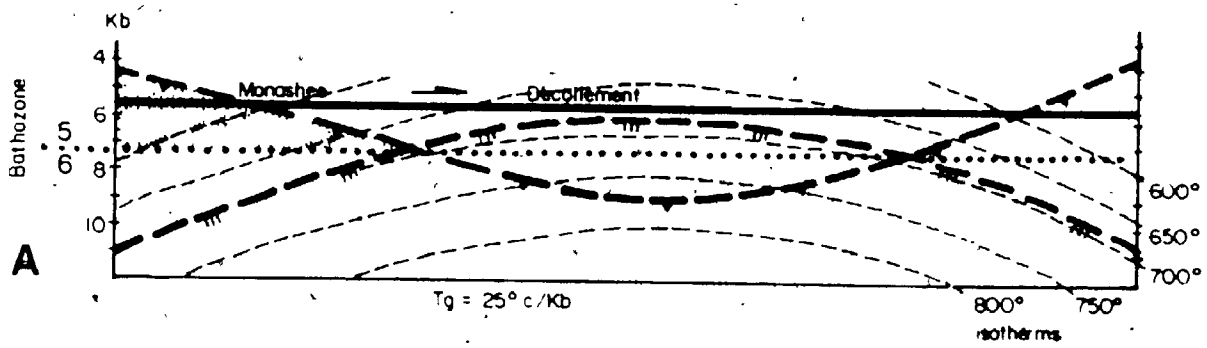

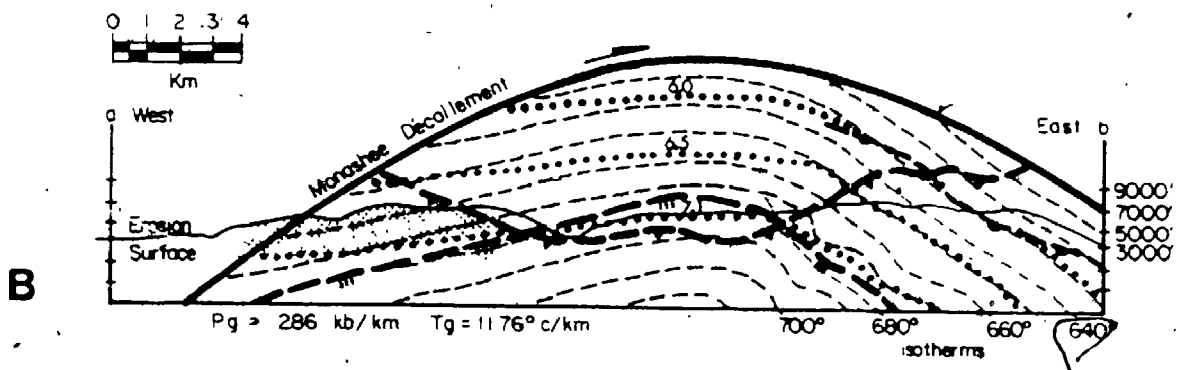

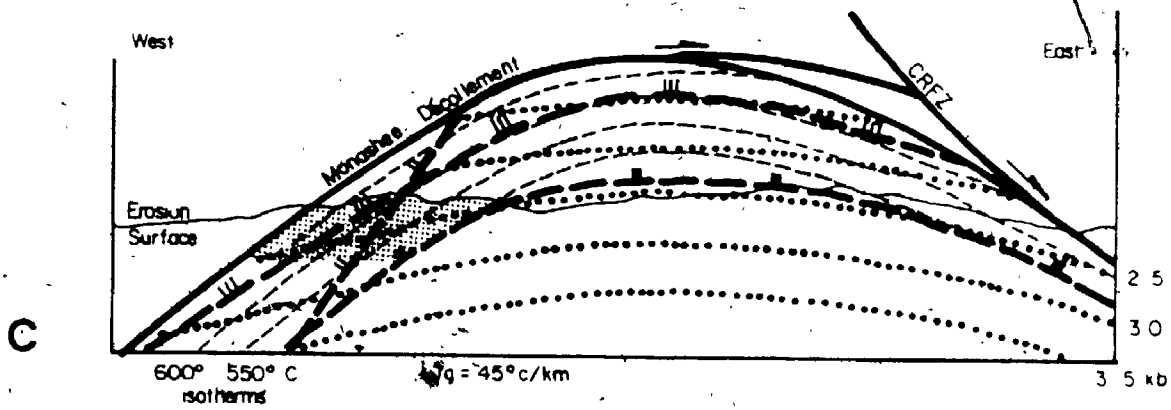

KEY

ISOGRADS:

St + Ms + Qtz ⟶ Ky + Grt + Bt + H_2O

Ky ⟶ Sil

And ⟶ Sil

Qtz + Ms + Pl ⟶ As + Kfs + l

Grt + Chl ⟶ As + Grt + v

Ornamentation on high temperature side of isograds

isobars

isotherms

PLATE 1: Overviews

A. Panorama looking in a southerly direction over the field area in the northern Monashee complex. Taken from station 85-R211.

B. Panorama looking in a northerly direction at the Monashee decollement in the north part of the map area. Taken from station 85-R96.

C. Zone of detachment marked by a melange of pegmatite and various gneisses. Taken near station 85-R206.

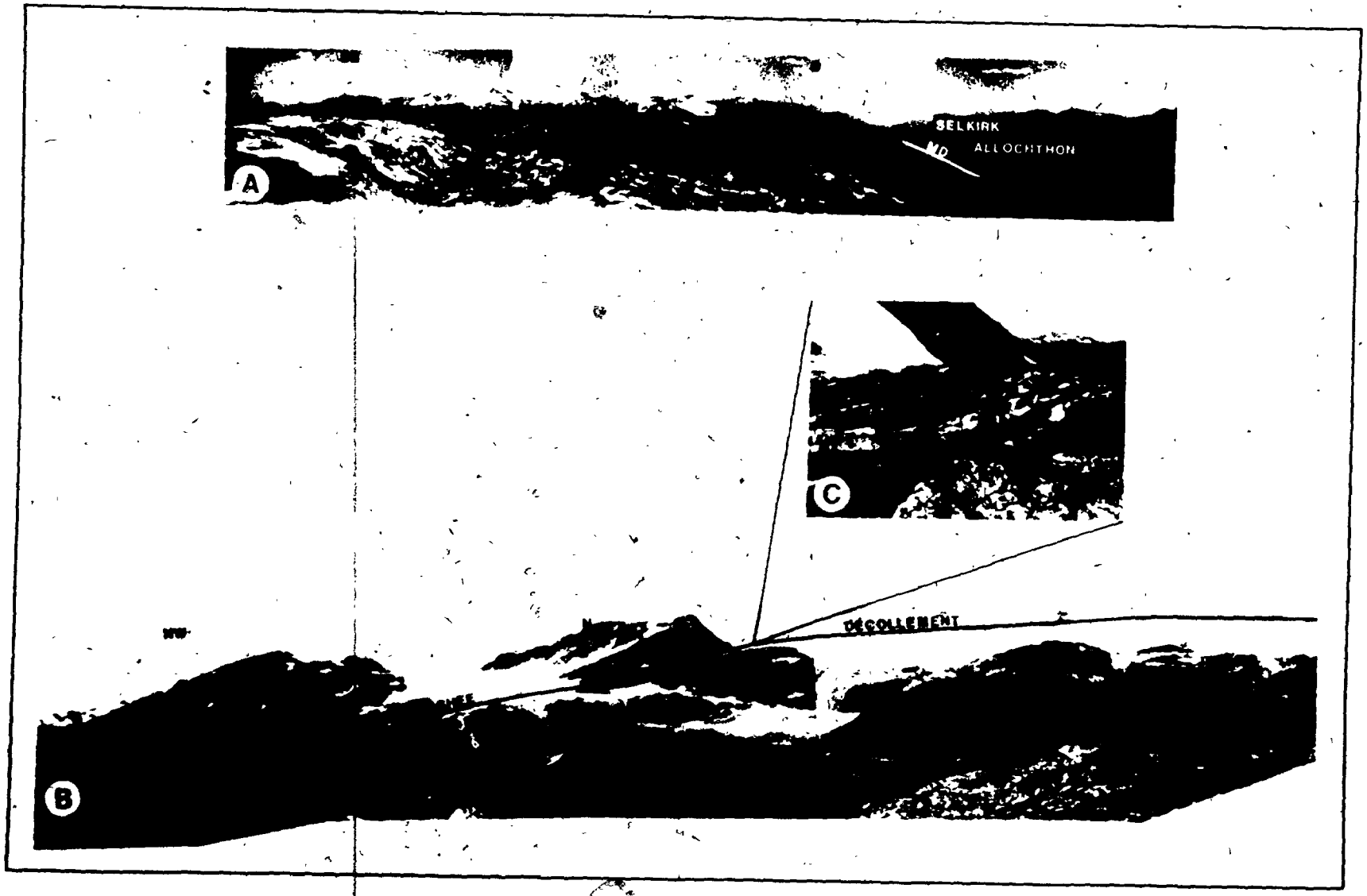
A
SELKIRK
ALLOCHTHON
C
DÉCOLLEMENT
B

PLATE 2: Evidence for a syndepositional tectonic disturbance

A. In situ eroded blocks of pyroclastic carbonatite (unit 6iv). Note the faint compositional layering (S01, primary or secondary?) and the pebble- to cobble-size lithic fragments. Station 85-R17.

B. An unusually large brecciated fragment supported by a carbonatite matrix (unit 6iv). It is composed of alternating layers of fine-grained albite(?) and biotite. Note the black fragment to the left is an aggregate of biotite. Station 85-R18.

C. Interlayered amphibolites (mafic flows and/or sills) and hornblende gneisses (immature arenites), unit 8G. Station 85-R151.

D. Mafic sill with feeder dyke cross-cutting compositional layering (S0) in metasedimentary rocks. Station 85-R148.

E. Deformed conglomerate composed of leucocratic clasts set in a mafic matrix (unit 8G). This conglomerate is interpreted to represent an epiclastic deposit interlayered with mafic flows and immature mafic sediments. Station 85-R150.

F. Discordant contact between a meta-ultramafic sill (composed of orthoamphibole) and quartzite, unit 9. Station 85-R269.

G. Discordant cross-cutting mafic dykes, unit 8. Station 85-R147.

H. Folded discordant and bedding-parallel amphibolite sills(?) layered with quartzite, unit 9. Station 85-R267.

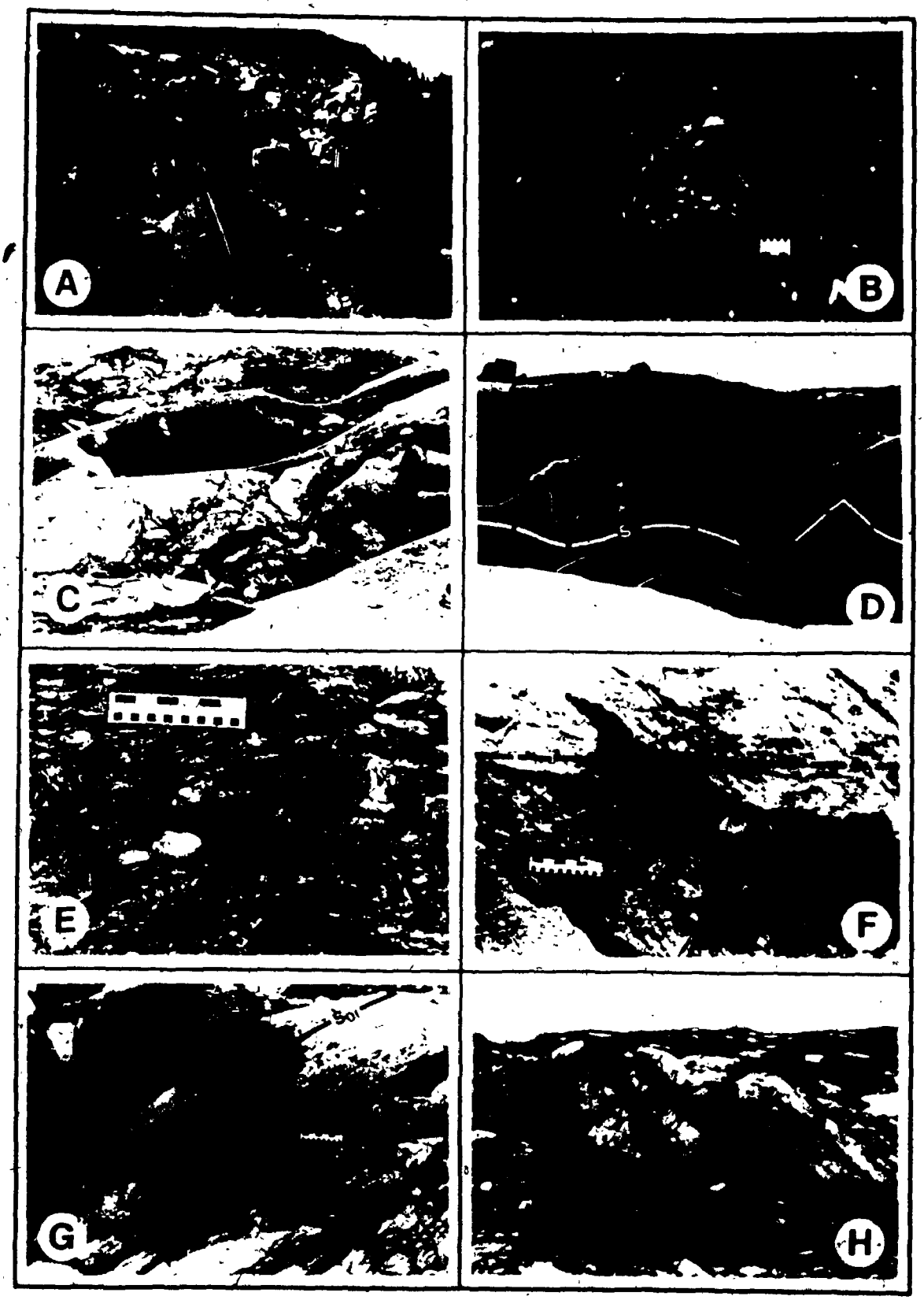
A
B
C
D
E
F
G
H

PLATE 3: Evidence for a syndepositional tectonic disturbance

A. High-angle discordant mafic dyke cross-cutting compositional layering (S0) in quartzite of unit 9. Station 85-R267.

B. High-angle discordant pelitic dyke cross-cutting compositional layering (S0) in meta-subarkose and quartzite, unit 9. Emplacement of mafic dykes plus associated tectonic activity are believed to have produced instability in the sedimentary pile, and subsequent injection of pelitic units along fractures in the arenite units. Station 84-R6152.

C. Low-angle discordant amphibolite interlayered with meta-subarkose and quartzite, unit 9. Note the overturned crossbeds in layers to the left, emphasised in black. Station 84-RS8.

D. Amphibolite sills and dykes interlayered with meta-subarkose and quartzite, unit 9. Station 84-RS144.

E. Deformed felsic volcaniclastic breccia, unit 8. Near station 85-R123.

F. A fragmental bed interpreted to be a pyroclastic deposit (ash flow?), unit 10. Station 85-R113.

G. Typical hornblendite of unit 11H. Note the thin white layer which may be interflow sediments separating large mafic flows. Station 85-R172.

H. Irregular bulbous hornblendite and hornblende gneiss, unit 12iiiH. This unit may represent subaqueous mafic flows and interflow sediments. Station 85-R62.

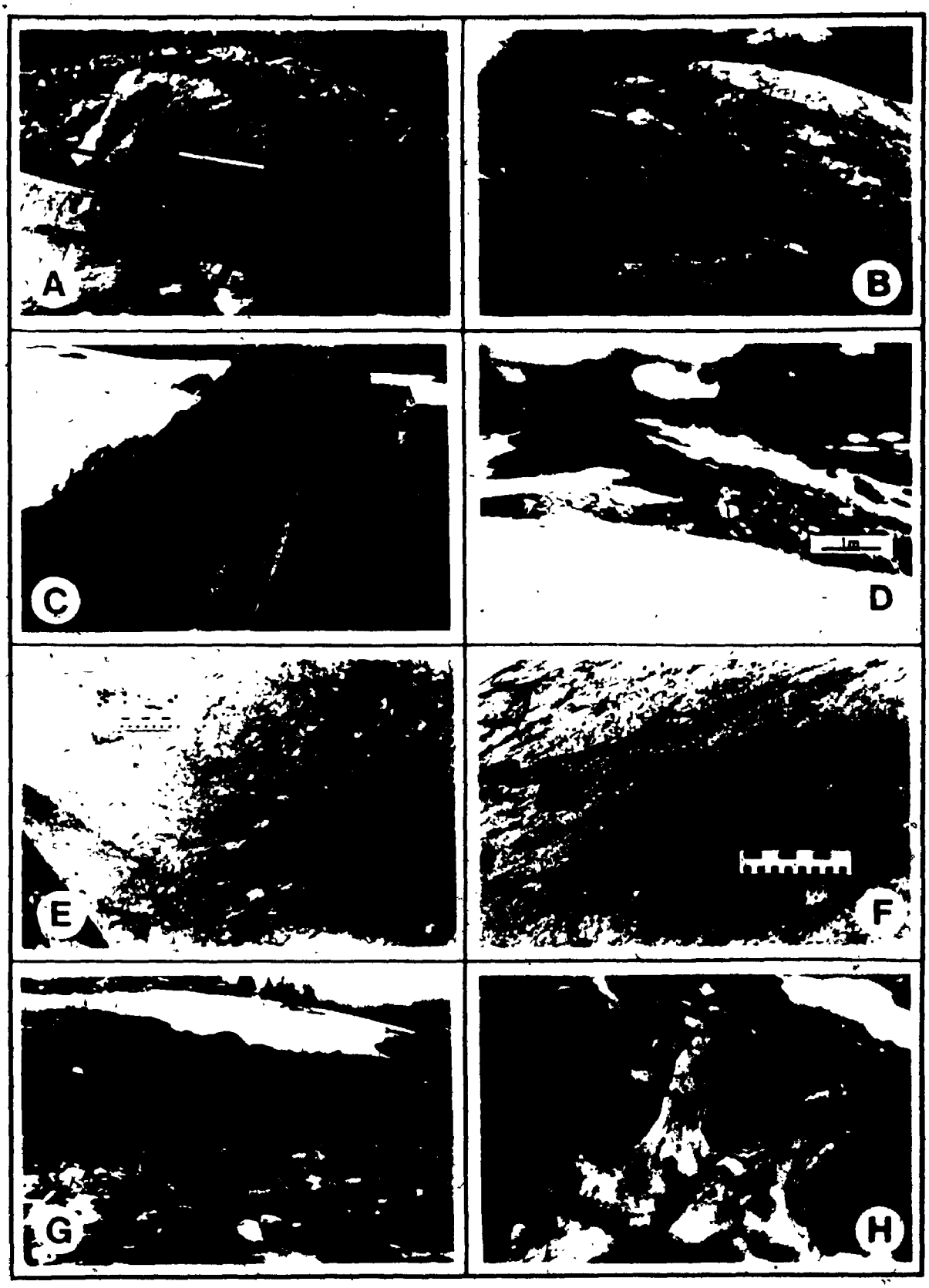
A
B
C
1m
D
E
F
G
H

PLATE 4: Photomicrographs of S-C and shear band fabrics

A. Upper-plate sillimanite-biotite schist displaying S-C and shear band (SB) fabrics. Photograph is looking north parallel to the mineral stretching lineation and perpendicular to the foliation. These fabric elememts are interpreted to indicate that the upper member of the shear couple moved to the east. Specimen 85-R212-4.

B. Lower-plate sillimanite-kyanite-garnet-muscovite-biotite schist displaying S-C and shear band (SB) fabrics. Photograph is looking south parallel to the mineral stretching direction and perpendicular to the foliation. These fabrics are interpreted to indicate that the upper member of the shear couple moved to the west. Specimen 85-R216-1.


A


B
C

PLATE 5: Kinematic indicators - rotational normal faults

A. Rotational normal faults, rooting in a pegmatite zone, are interpreted to indicate that the upper member of the shear couple moved east (see text section 3.4.3). Note that although most of these faults are planar some have been folded in a manner similar to that shown in Figure 13. Stations 84-RS87, 85-R99.

B. Folded rotational normal faults interpreted to indicate that the upper member of the shear couple moved to the east. Station 84-RS162.

C. An elliptical boudin dissected by rotational normal faults which are interpreted to indicate that the upper member of the shear couple moved to the south. Station 85-R168.

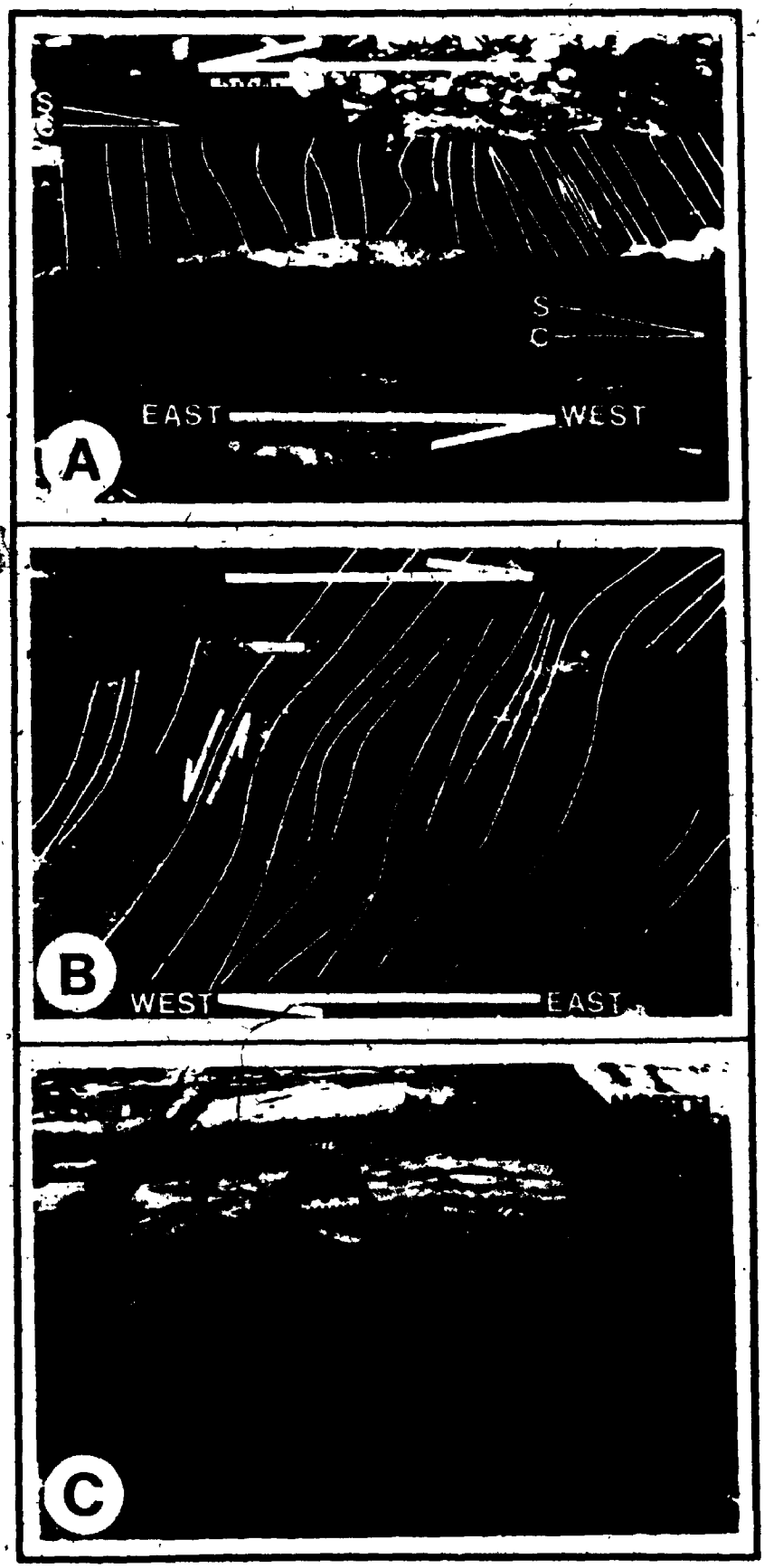
S
S
C
EAST
WEST
A
B
WEST
EAST
C

PLATE 6: Photomicrographs - all with crossed nicols

A. Typical exaggerated quartz grain growth preserved in mylonitic quartzite. Based on studies by Wilson (1973) these fabrics are believed indicative of syn-shearing sillimanite zone physical conditions. Specimen 84-RS206-1.

B. Typical exaggerated quartz grain growth interpreted in the same manner as (A) above. Note that some grains are "pinned" by micas. Specimen 84-RS106-3.

C. Quartz ribbons. Note the crossed kyanite grains in the center of the photograph. These are believed indicative of the existence of static conditions during some kyanite nucleation. Specimen 84-RS162-2.

D. Plagioclase grain enclosed and partly replaced by myrmekite. Specimen 84-RS208-1.

E. Plagioclase porphyroblast with inclusions of biotite (bottom-center), and a pulled apart kyanite grain with muscovite in the pull-apart. Specimen 84-RS182.

F. Plagioclase porphyroblast intergrown with sillimanite on its lower left margin and in its pressure shadow. Specimen 84-RS205.

G. Synkinematic muscovite fish. Specimen 84-RS162-2.

H. A synkinematic muscovite fish intergrown with biotite in its pressure shadow. Specimen 84-RS183.

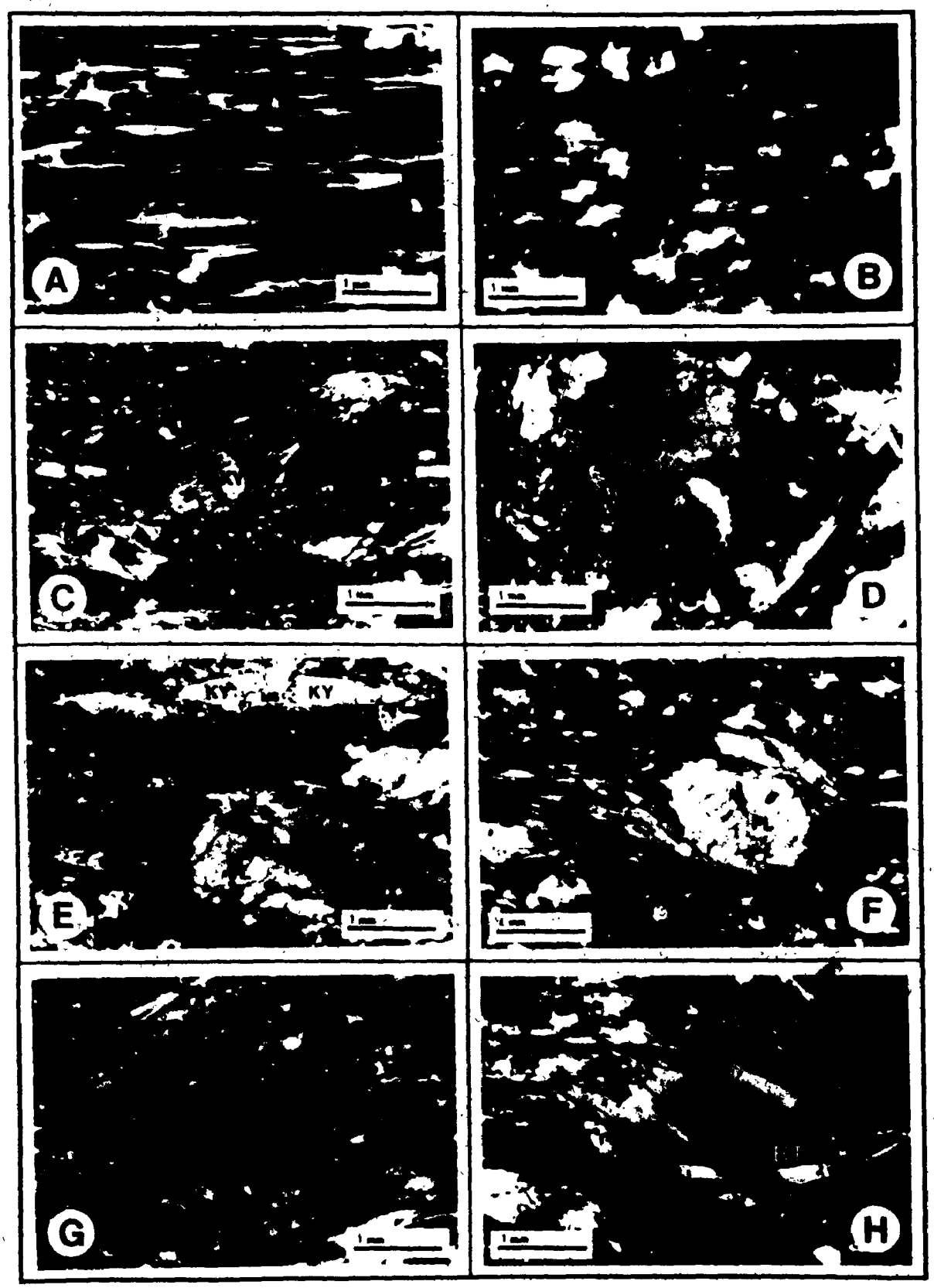
A
B
C
D
KY
KY
E
F
G
H

PLATE 7: Photomicrographs

A. Synkinematic biotite laths. Note the kinked grains in the center of the photograph. Crossed nicols. Specimen 85-R224-1.

B. Late biotite and chlorite laths. Plane polarized light. Specimen 84-RS144.

C. Garnet porphyroblast with biotite pressure shadows and late chlorite-muscovite marking fractures in the grain. Crossed nicols. Specimen 84-RS107-1.

D. Garnet porphyroblast with random inclusions of biotite and quartz. Plane polarized light. Specimen 84-RS205.

E. Garnet with sigmoidal inclusion trails (highlighted in white). This is the only garnet with this type of inclusion pattern observed in thin section. It is not known whether this indicates rotation of either the garnet or external foliation during growth, or that the garnet has overgrown a folded foliation. Crossed nicols. Specimen 85-R141-1.

F. Garnet intergrown with kyanite. Plane polarized light. Specimen 85-R50-2.

G. Garnet displaying two stages of growth. The first stage is marked by inclusions while the second stage is marked by inclusion free ends. Crossed nicols. Specimen 85-R213-3.

H. Garnet with inclusions of quartz, plagioclase and sillimanite intergrown with quartz. Crossed nicols. Specimen 84-RS205.

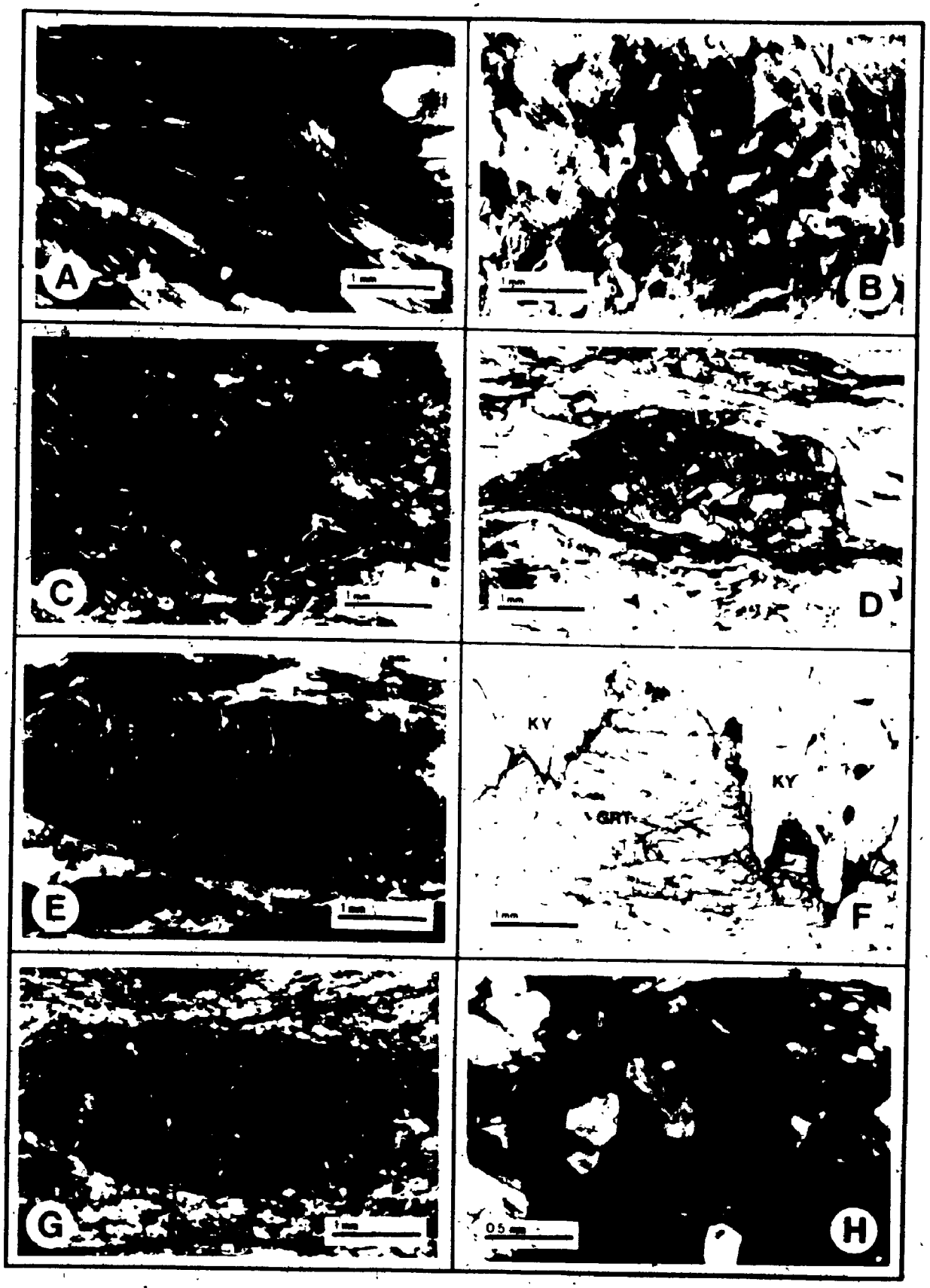
A
1mm
B
1mm
C
1mm
D
1mm
E
1mm
KY
KY
GRT
1mm
F
G
1mm
0.5 mm
H

PLATE 8: Aluminosilicate textures and relationships

A. Kyanite with inclusions of biotite. Crossed nicols. Specimen 84-RS206-1.

B. Kyanite and biotite laths defining a foliation and elliptical pods around which seams of sillimanite-biotite intergrowths anastomose. Plane polarized light. Specimen 84-RS171-2.

C. Multiple kinks in kyanite. Crossed nicols. Specimen 84-RS107-1.

D. Folded kyanite grain. Crossed nicols. Specimen 85-RS97-1.

E. Andalusite replacing kyanite. Note the subgrains in the andalusite. Crossed nicols. Specimen 85-R145-1.

F. Andalusite replacement of kyanite. Note the remnant of kyanite in the upper left corner of the photograph and that the andalusite is enclosed by a sillimanite-biotite seam. Note also that the relationships between subgrains in the andalusite and the sillimanite-biotite seam resemble S-C fabrics. Crossed nicols. Specimen 85-R145-1.

G. Kyanite grain with random sillimanite intergrown with plagioclase along its margin. This sillimanite may have nucleated during static conditions. Crossed nicols. Specimen 85-R168-1.

H. Folded fibrolitic sillimanite in the upper-plate. Some sillimanite is axial planar to the fold. Crossed nicols. Specimen 84-RS107-2.

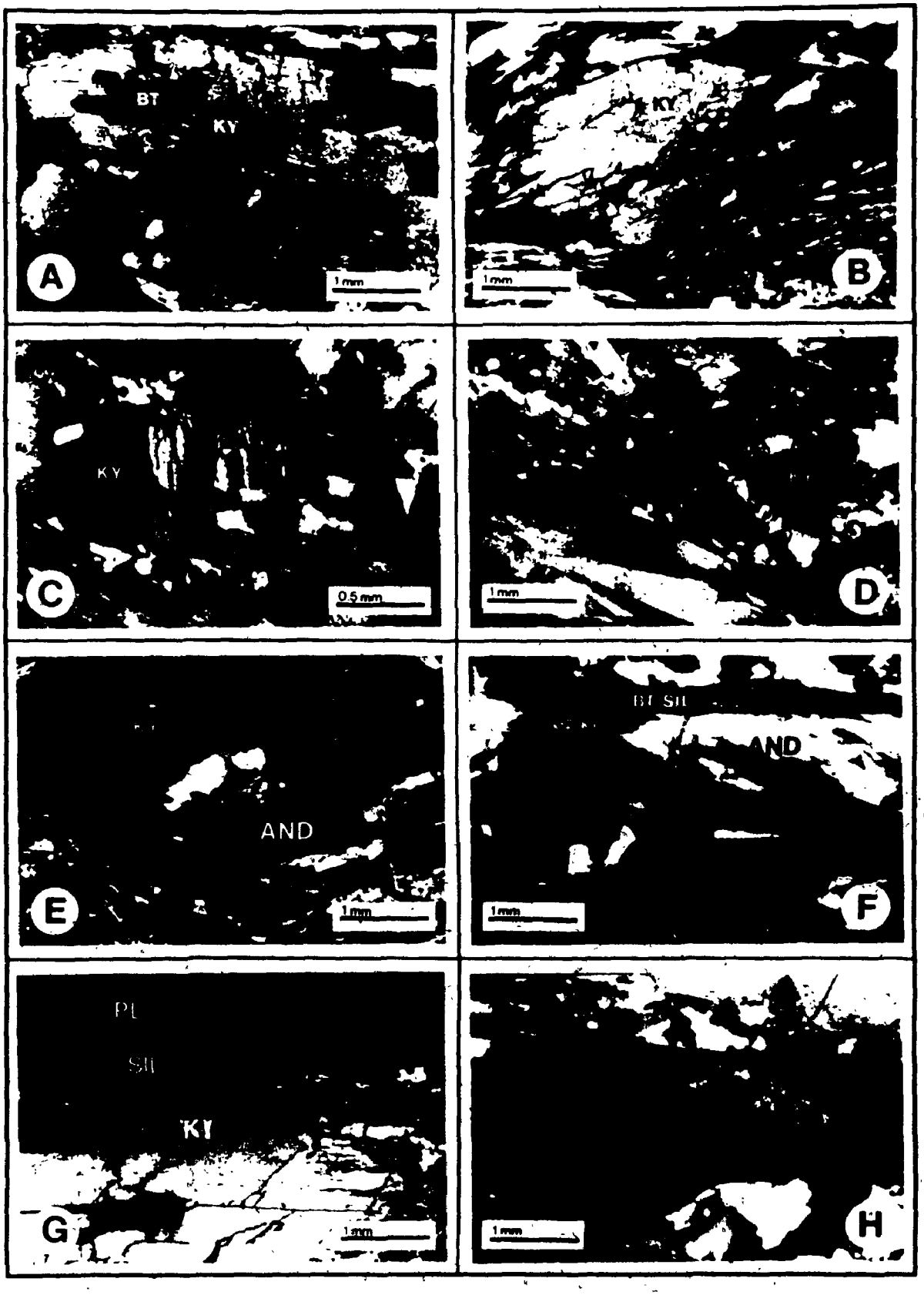
BT
KY
A
1 mm
KY
B
1 mm
KY
C
0.5 mm
D
1 mm
AND
E
1 mm
BT SIL
AND
F
1 mm
PL
SIL
KY
G
1 mm
H
1 mm

PLATE 9: Aluminosilicate relationships - all under plane polarized light

A. Kyanite remnants enclosed in an andalusite replacement which has a sillimanite-biotite intergrowth along its fractured margin. These relationships are interpreted to indicate a Ky -> And -> Sil order of crystallization. Specimen 85-R182-2.

B. Andalusite replacement of kyanite, and repaced by sillimanite. Specimen 84-RS107-2.

C. Kyanite remnant enclosed by an andalusite replacement. Both are replaced by later sillimanite. Specimen 84-RS140-2.

D. Kyanite lath replaced and partly bound by a sillimanite-biotite seam. Specimen 84-RS208-1.

E. A sillimanite-biotite seam, garnet and a kyanite remnant enclosed by later muscovite. This mineral assemblage and textural relationship is typical of the lower-plate near the detachment and of the upper-plate. Specimen 84-RS107-1.

F. Kyanite remnant nearly completely replaced by later muscovite. Specimen 85-R145-1.

G. Pulled apart sillimanite with synkinematic muscovite in the pull-apart. Specimen 85-R145-2.

H. Pulled apart kyanite with synkinematic muscovite in the pull-apart. Specimen 85-R145-2.

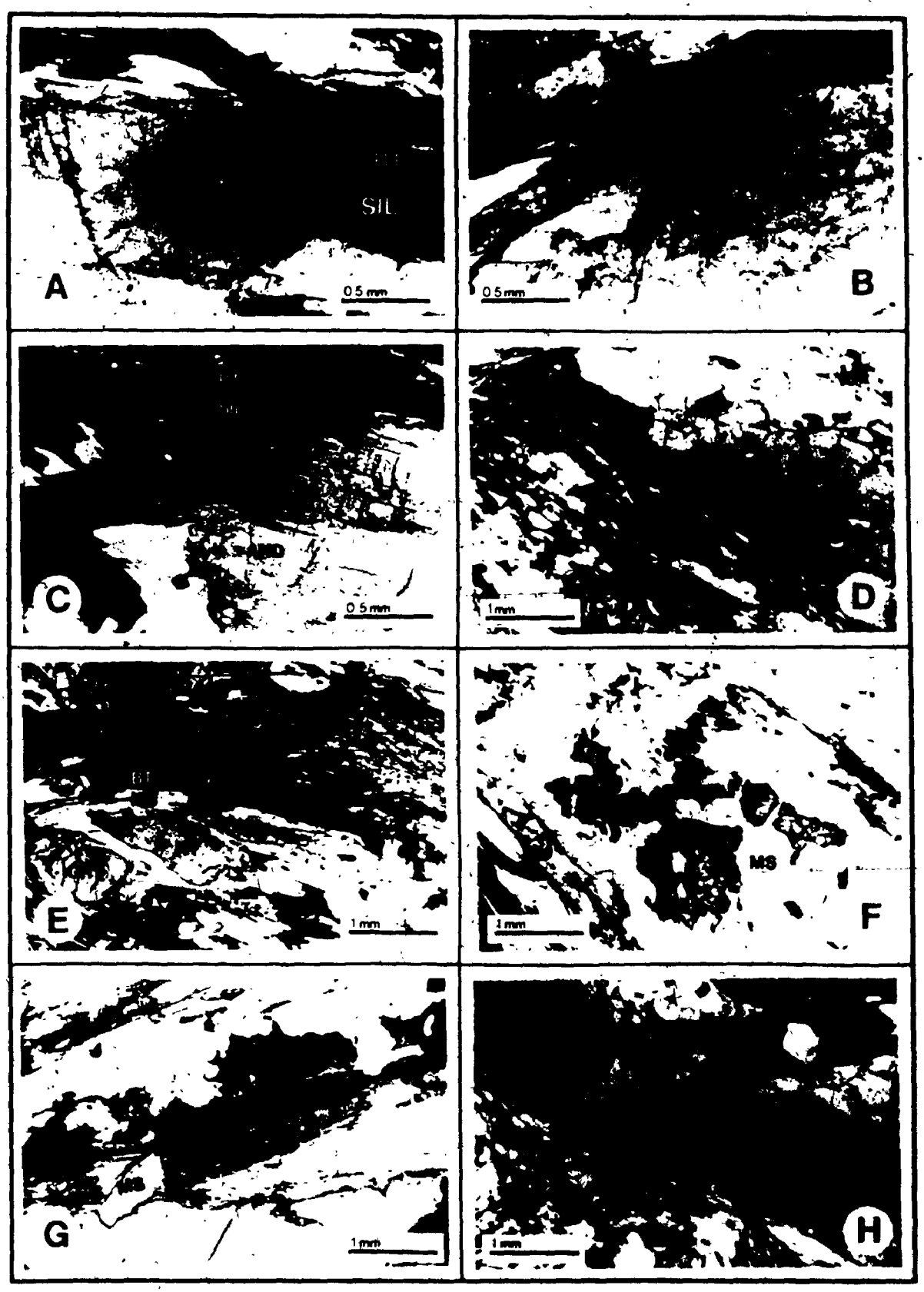
A
SIL
0.5 mm
B
0.5 mm
C
0.5 mm
D
1 mm
E
BT
1 mm
F
MS
1 mm
G
1 mm
H
1 mm

PLATE 10: Aluminosilicate relationships - crossed nicols

A. Kyanite that has been fractured and pulled apart at two locations. Andalusite has replaced kyanite along its rifted margins and in the central part of the photograph. Muscovite has nucleated in the pulled-aparts of andalusite. These relationships are interpreted to indicate a Ky -> And -> Ms order of crystallization. Specimen 84-RS74-5.

B. A pulled apart kyanite grain with andalusite replacement along its rifted margins and muscovite, biotite and opaques growing in the pull-apart. These textural relationships are interpreted to be indicative of a Ky -> And -> Ms-Bt-Op order of crystallization. Specimen 85-R36-1.


KY
KY
A
1mm

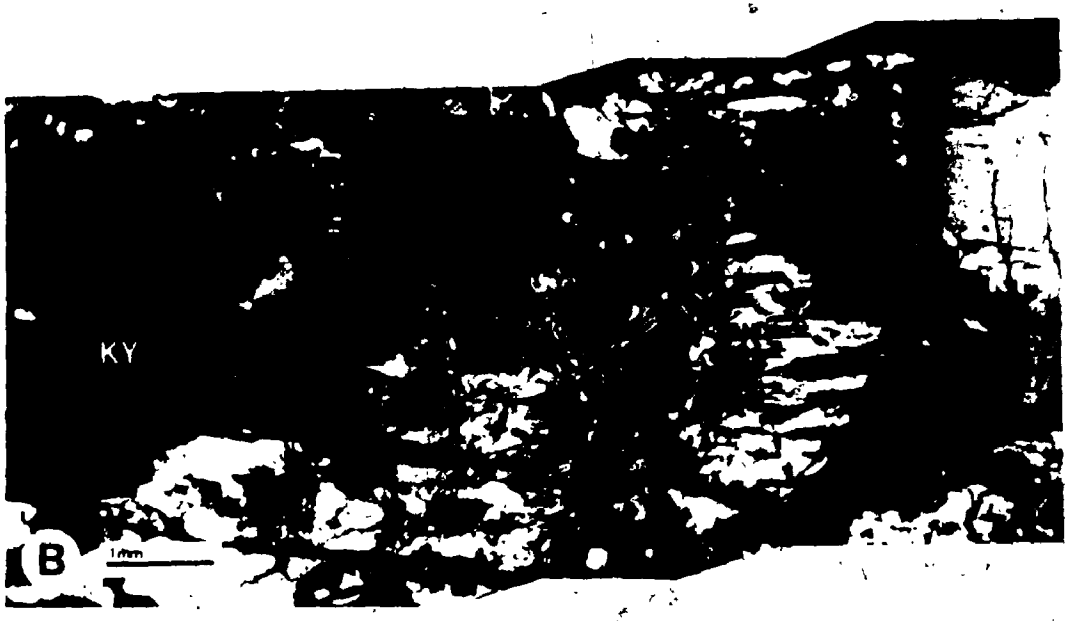
KY
B
1mm

PLATE 11: **Aluminosilicate relationships** - plane polarized light

A. Andalusite replacement of a kyanite grain (left half of the photograph), and a shear band, marked by a sillimanite-biotite intergrowth, along which the fractured Ky-And grain has been displaced. These textural relationships are believed indicative of a Ky -> And -> Sil order of crystallization. Specimen 85-R168-1.

B. Kyanite which has been partly replaced by andalusite. The texture exhibited in this photograph is believed to be indicative of static conditions during replacement, and suggests these static conditions prevailed during the time that the physical conditions (T, P, etc.) for the Ky -> Sil reaction prevailed. Specimen 85-R183-6.

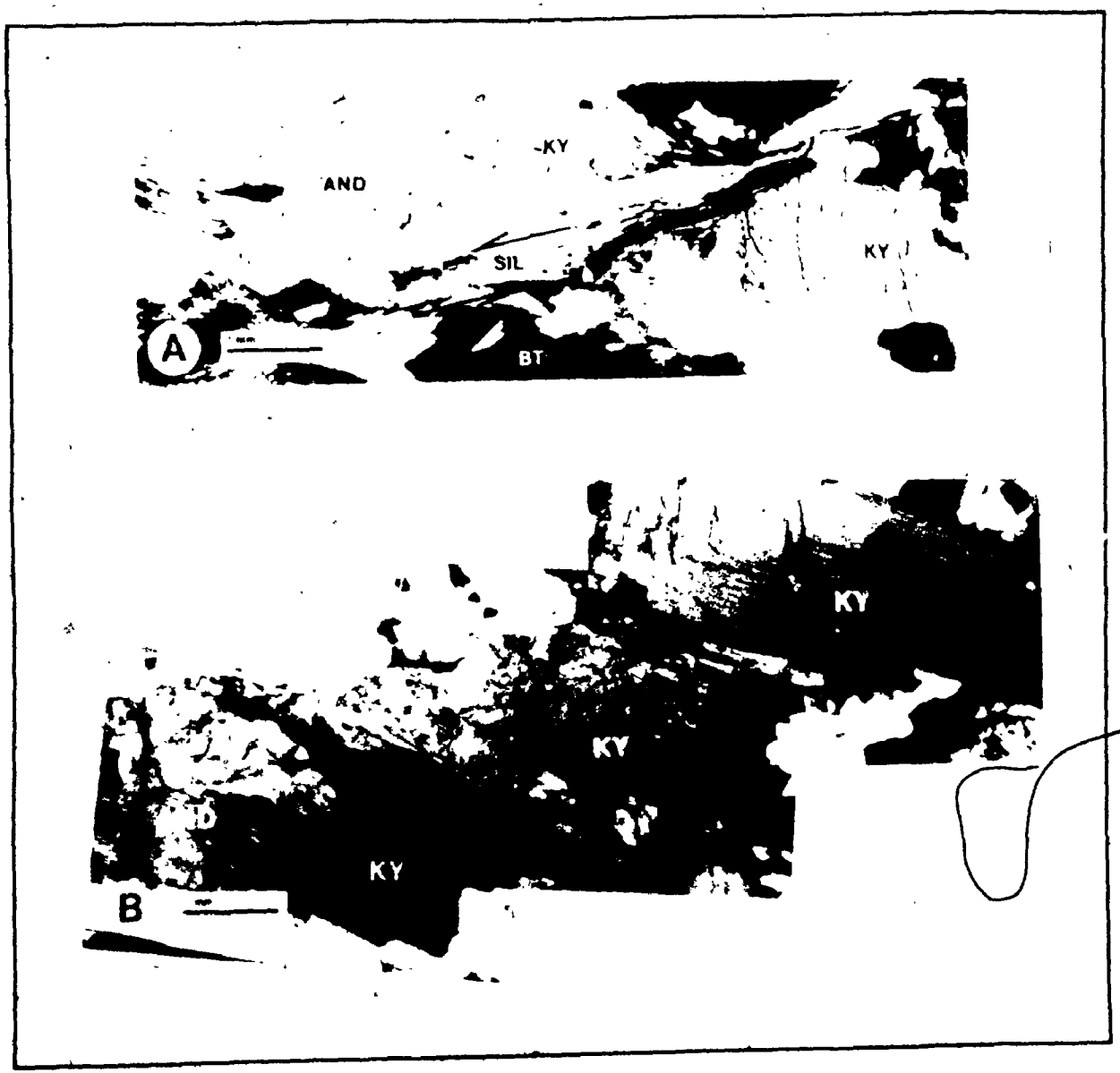
AND
KY
SIL
KY
A
BT
KY
KY
KY
B

PLATE 12: Field photographs

A. Garnets with sigmoidal inclusion trails and plagioclase-quartz pressure shadows looking west down the mineral stretching lineation. Station 85-R97.

B. A view looking down at the foliation surface displaying elongate garnets and quartz-plagioclase pressure shadows at the same location as (A).

C. Stromatic pelitic metatexite that displays a foliation (dipping to the right) that is truncated by a horizontal, layer-parallel (to the lower layers) discrete shear. The surface of shears throughout the field area display lineated and pulled apart sillimanite similar to that shown in (D). Station 85-R178.

D. Typical lineated and pulled apart sillimanite that is localized along discrete shear surfaces (e.g. see C.) throughout the map area. Station 85-R183.

E. Pulled apart kyanite with andalusite-plagioclase in the pull-apart and andalusite pseudomorphing the end of the grain in an andalusite-kyanite-garnet schist at station 85-R168.

F. Meta-ultramafic sill composed of >90%, very coarse-grained, radiating grey-green orthoamphibole laths. Station 85-R215.

G. Stromatic pelitic migmatite with leucosomes composed of quartz-kyanite and tonalite. Station 85-R183.

H. Phase II fold hinge in the lower-plate. Note the thickened hinges and thinned limbs, and the kinked foliation. Sation 85-R136.

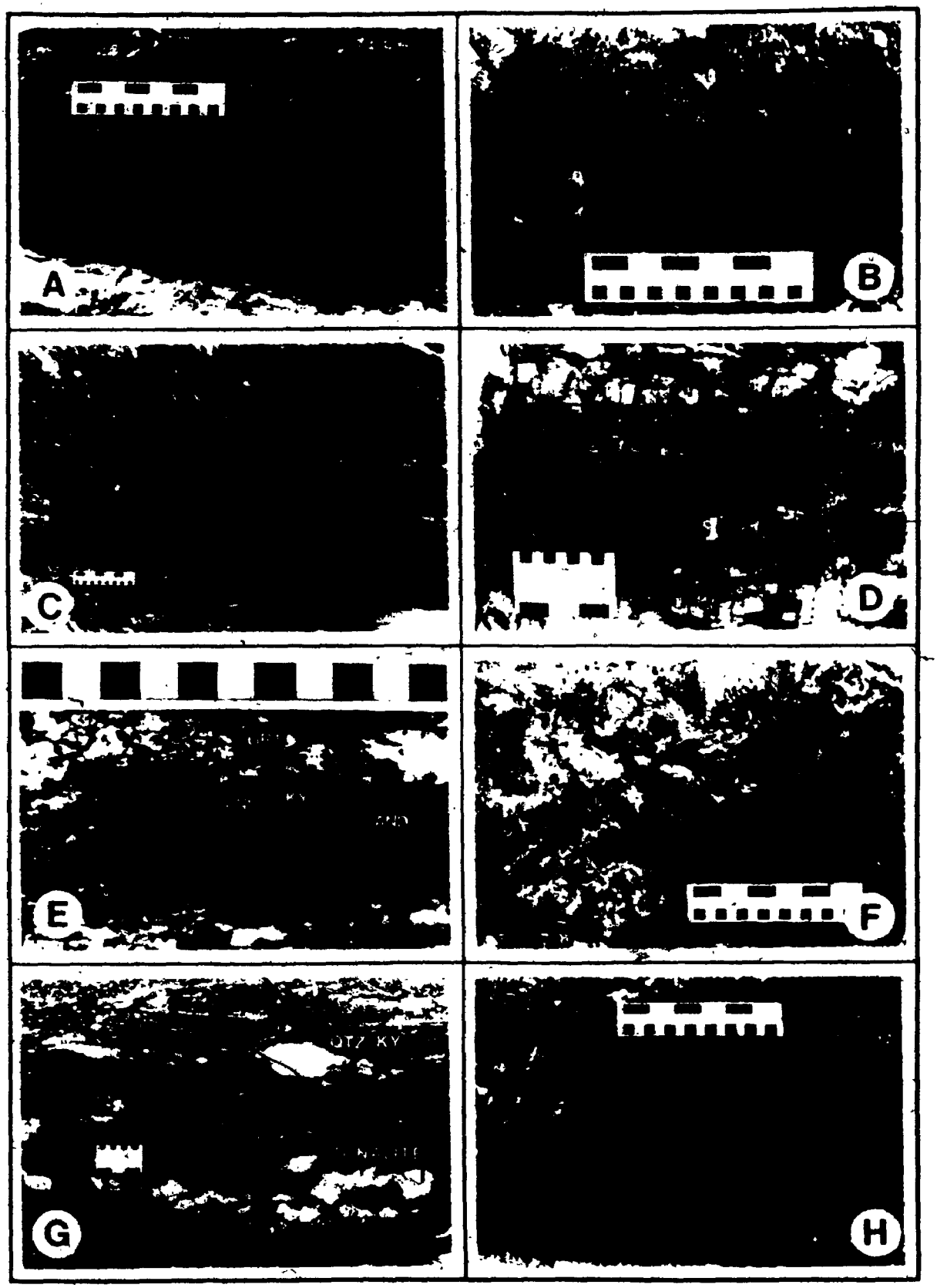
A
B
C
D
E
F
QTZ KY
G
H

APPENDIX I: MINERAL SYMBOLS

Most mineral symbols used in this study are from Kretz (1983). They include:

Act - actinolite
And - andalusite
Ap - apatite
Bt - biotite
Cal - calcite
Chl - chlorite
Di - diopside
Ep - epidote
Grt - garnet
Kfs - K-feldspar
Ky - kyanite
Ms - muscovite
Oam - orthoamphibole
Pl - plagioclase
Qtz - quartz
Scp - scapolite
Sil - sillimanite
Spn - sphene
St - staurolite
Tur - tourmaline
Zrn - zircon

Other symbols include:

As - aluminosilicate
Op - opaque oxide
l - liquid
v - volatiles

APPENDIX 2: A NOTE ON THE TERM MYLONITE

Presently there does not exist a consistent or accepted nomenclature that can be used for the description of coherent fault rocks (cf. e.g. Higgins, 1971; Zeck, 1974; Sibson, 1977; Wise et al. 1984, 1985; Mawer, 1985, 1986; Tullis, 1982; White, 1982; Hanmer & Lucas, 1985). Terms to describe these rocks have been applied inconsistently (see Mawer, 1986; White, 1982). In this study the term mylonitic is used to describe shear zone-related rocks which have deformed without the loss of cohesion under the imposed physical conditions, and display structures and textures characteristic of such rocks as described by Tullis (1982), White (1982), White et al. (1980, 1982), Mawer, (1986), Lister and Snoke (1984), Simpson and Schmidt (1983), Berthe et al. (1979), and Eisbacher (1970), among others. For example, well developed foliations and mineral lineations, and asymmetric structures such as S-C textures, shear bands and rotated porphyroclasts.

APPENDIX 3: MINERALS IDENTIFIED IN THIN SECTION & HAND SPECIMEN

LOWER-PLATE

PELITIC, SEMIPELITIC, QUARTZITE AND QUARTZOFELDSPATHIC ROCKS

SPECIMEN	IDENTIFIED MINERALS													
RS106-3	Qtz	Pl	Kfs							Chl	Zrn	Sph	Cpx?	
RS101-1	Qtz	Pl	Kfs	Bt	Ms	Ky	And	Sil	Grt	Chl				
R7-1	Qtz	Pl	Kfs	Bt	Ms	Ky	And	Sil	Grt	Chl	Zrn	Op		
RS183	Qtz	Pl	Kfs*	Bt	Ms(r)	Ky		Sil	Grt	Chl	Zrn	Tur	Op	Ap
RS182-1	Qtz	Pl	Kfs*	Bt	Ms(r)	Ky		Sil	Grt	Chl	Zrn	Ep?		
RS74-5	Qtz	Pl		Bt	Ms	Ky	And	Sil	Grt	Chl	Zrn	Op	Ap	Ep
RS81-2	Qtz		Kfs*	Bt	Ms	Ky		Sil	Grt	Chl	Zrn	Op		
R224-1	Qtz	Pl	Kfs*	Bt	Ms	Ky	And		Grt	Chl	Zrn	Ep		
R221-2	Qtz	Pl	Kfs*	Bt	Ms	Ky					Zrn	Op		
RS18-2	Qtz	Pl		Bt	Ms	Ky		?	Grt			Ap		
RS140-2	Qtz	Pl		Bt	Ms	Ky				Chl	Zrn	Spn	Op	Ap
RS68-1	Qtz	Pl		Bt	Ms	Ky				Chl	Zrn	Op	Ap	
RS182-2	Qtz	Pl	Kfs	Bt	Ms	Ky		Sil	Grt		Zrn	Spn	Op	Ap
RS18-1	Qtz	Pl		Bt	Ms	Ky				Chl	Zrn	Tur	Op	Ap
RS97-1	Qtz	Pl	Kfs	Bt	Ms	Ky					Zrn	Ap		
RS166	Qtz	Pl	?	Bt	Ms(r)	Ky		Sil		Chl	Zrn	Ap		
RS171-2	Qtz	Pl	?	Bt	Ms	Ky		Sil	Grt		Zrn	Op	Ap	
R216-1	Qtz	Pl	Kfs	Bt	Ms	Ky		Sil	Grt	Chl	Zrn	Op	Ap	
RS163-2	Qtz	Pl	?	Bt	Ms	Ky		Sil		Chl	Zrn	Tur		
RS144-1	Qtz	?		Bt	Ms	Ky	And	Sil		Chl		Op		
RS152-1	Qtz			Bt	Ms					Chl		Op	Ap	
RS140	Qtz		Kfs	Bt	Ms	Ky								
RS113-1	Qtz	Pl	Kfs		Ms(r)	Ky						Hbl	Cpx	
RS136	Qtz		?		Ms									
RS162-1	Qtz	Pl		Bt	Ms(r)							Op		
R145-2	Qtz	Pl	Kfs	Bt	Ms	Ky	And	Sil	Grt	Chl	Zrn	Op		
R145-1	Qtz			Bt	Ms	Ky	And	Sil	Grt	Chl	Zrn	Op		
R145-3	Qtz	Pl	Kfs	Bt	Ms	Ky	And	Sil	Grt	Chl	Zrn	Op		
R154-1		Pl										Cpx		
R154-2	Qtz	Pl		Bt	Ms					Chl		Ap	Oam	
R155-1	Qtz	Pl		Bt	Ms	Ky	And	Sil		Chl	Zrn	Op	Ap	
RS61-1	Qtz	Pl	?	Bt	Ms	Ky		?	Grt	Chl	Zrn	Op		
R136-5	Qtz	Pl	?	Bt	Ms(r)	Ky			Grt	Chl	Zrn	Op		
R141-1	Qtz	Pl	?	Bt	Ms	Ky			Grt	Chl	Zrn	Op	Ap	
R168-1	Qtz	Pl	?	Bt	Ms(R)	Ky	And	Sil		Chl	Zrn	Op		
R168-2	Qtz	Pl	Kfs	Bt	Ms(R)	Ky	And			Chl	Zrn			
R140-1	Qtz	Pl	Kfs	Bt	Ms(R)	Ky	And			Chl	Zrn			
R21-1	Qtz	Pl	Kfs	Bt	Ms	Ky			Grt	Chl	Zrn	Ap		
R23-2	Qtz	Pl	Kfs	Bt	Ms	Ky		Sil		Chl	Zrn	Op	Ap	
R20-2	Qtz	Pl		Bt	Ms	Ky	And	Sil	Grt	Chl	Zrn	Op	Ap	
R50-2	Qtz	Pl	Kfs	Bt	Ms	Ky	And	Sil	Grt	Chl	Zrn	Op		
R50-A	Qtz	Pl	Kfs	Bt	Ms	Ky	And			Chl	Zrn	Op	Ap	
R50-B	Qtz	Pl	Kfs	Bt	Ms(R)	Ky	And	Sil	Grt	Chl	Zrn			
R142-1	Qtz	Pl		Bt	Ms	Ky	And	Sil	Grt	Chl	Zrn	Op		
R36-1	Qtz	Pl	Kfs	Bt	Ms(r)	Ky	And	Sil	Grt	Chl	Zrn	Op		

R36-2A	Qtz	Pl		Bt	Ms	Ky	And	?	Grt	Chl	Zrn	Op	Ap
R36-2B	Qtz	Pl		Bt	Ms	Ky				Chl	Zrn	Op	Ap
R183-6	Qtz	Pl	Kfs	Bt	Ms(R)	Ky	And					Op	
R178-1	Qtz	Pl	Kfs	Bt	Ms	Ky			Grt	Chl	Zrn	Op	Ap
R178-3	Qtz	Pl	?	Bt	Ms	Ky		Sil	Grt	Chl	Zrn	Op	Ap
R51-2	Qtz	Pl	?	Bt	Ms	Ky			Grt	Chl	Zrn	Op	Ap
R66-1	Qtz	Pl		Bt	Ms	Ky			Grt	Chl	Zrn	Op	Ap
R107-1	Qtz	Pl	?	Bt	Ms(R)	Ky		Sil	Grt	Chl	Zrn	Op	Ap

SHEAR ZONE

RS107-2	Qtz	Pl	Kfs*	Bt	Ms(R)			Sil	Grt	Chl	Zrn	Op	Ap
RS205	Qtz	Pl	Kfs*		Ms	Ky		Sil	Grt	Chl	Zrn	Op	Ap

UPPER-PLATE

														ELEVATION
RS205-3	Qtz	Pl	Kfs*	Bt	Ms	Ky		Sil	Grt	Chl	Zrn	Op	Ap	7300 ft.
RS208-1	Qtz	Pl	?	Bt	Ms	Ky		Sil	Grt	Chl	Zrn	Op	Ap	7450
R206-1	Qtz	Pl	?	Bt	Ms(R)	Ky		Sil		Chl		Op		7480
R212-2	Qtz	Pl	Kfs*	Bt	Ms(R)			Sil		Chl	Zrn	Op	Ap	Spn 7750
R212-4	Qtz	Pl	?	Bt	Ms(R)	Ky		Sil	Grt	Chl	Zrn	Op	Ap	7750
RS213-1	Qtz	Pl	?	Bt	Ms(R)			Sil	Grt	Chl	Zrn	Op	Ap	7950
RS213-3	Qtz	Pl	Kfs	Bt	Ms(R)			Sil	Grt	Chl	Zrn	Op		7950
R211-2	Qtz	Pl	Kfs	Bt	Ms(R)			Sil	Grt		Zrn	Op		8000
RS214-1	Qtz	Pl	Kfs	Bt	Ms(R)			Sil	Grt	Chl	Zrn	Op		8050
RS214-2	Qtz	Pl	Kfs*	Bt	Ms(R)	Ky	And	Sil	Grt	Chl	Zrn	Op		8050
M59	Qtz	Pl	Kfs*	Bt	Ms(R)			Sil		Chl	Zrn	Op		?

CALC-SILICATE ROCKS

RS201-2	Di	Scp	Pl	Cal	Grt	Bt	Spn	Op	Chl	Hbl			
R81-1	Di	Scp	Pl	Cal		Bt	Spn	Op	Chl		Qtz(?)	Zrn	
R74-2			Pl		Grt	Bt			Chl	Hbl	Qtz	Zrn	sericite
RS194-4	Di	Scp	Pl			Bt	Spn	Op	Chl	Hbl	Qtz		
RS81-1	Di		Pl	Cal		Bt	Spn	Op	Chl		Qtz	Zrn	
RS194-3	Di	Scp	Pl	Cal		Bt	Spn	Op	Chl		Qtz(?)		graphite
RS74-3	Di	Scp	Pl	Cal			Spn	Op	Chl	Hbl	Qtz(?)		

KEY

(r) = some grains are retrograde
(R) = all grains are retrograde
(?) = not a positive identification in thin section, but most likely present
(*) = K-feldspar identified in thin section, all other K-feldspar identified through Na-cobaltinitrate staining of rock slabs.
See Appendix 1 for mineral symbols

REFERENCES CITED

Aitken, J.D., 1982, Precambrian of the MacKenzie fold belt - a stratigraphic and tectonic overview, in, Hutchinson, R.W., Spence, C.D., and Franklin, J.M., eds., Precambrian Sulphide Deposits: Geological Association of Canada, Special Paper 25, p. 149-161.

Aitken, J.D., Long, D.G.F., and Semikhatov, M.A., 1978, Progress in Helikian statigraphy, MacKenzie Mountains: Geological Survey of Canada, Paper 78-1A, p. 481-484.

Archibald, D.A., Glover, J.K., Price, R.A., Farrar, E., and Carmicheal, D.M., 1983, Geochronology and tectonic implications of magmatism and metamorphism, southern Kootenay Arc and neighbouring regions, southeastern British Columbia. Part I: Jurrasic to mid-Cretaceous: Canadian Journal of Earth Sciences, v. 20, p. 1891-1913.

Armstrong, R.L., 1982, Cordilleran metamorphic core complexes - from Arizona to southern Canada: Annual Review of Earth Sciences, v. 10, p. 129-154.

Armstrong, R.L., Eisbacher, G.H. and Evans, P.D., 1982, Age and stratigraphic-tectonic significance of Proterozoic diabase sheets, MacKenzie Mountains, northwestern Canada: Canadian Journal of Earth Sciences, v. 19, p. 316-332.

Arzi, A.A., 1978, Critical phenomena in the rheology of partially melted rocks: Tectonophysics, v. 44, p. 173-184.

Ashworth, J.R., 1985, Introduction, in, Ashworth, J.R., ed., Migmatites: Blackie & Son Ltd., Glascow, England, p. 1-35.

Ashworth, J.R., 1986, Myrmekite replacing albite in prograde metamorphism: American Mineralogist, v. 71, p. 895-899.

Ashworth, J.R., and McLellan, E.L., 1985, Textures, in, Ashworth, J.R., ed., Migmatites: Blackie & Son Ltd., Glascow, England, p. 180-203.

Badham, J.N.P., 1978, Has there been an oceanic margin to western North America since Archean time? Geology, v. 6, p. 621-625.

Bailey, D.K., 1974, Continental rifting and alkaline magmatism, in, Sorensen, H., ed., The Alkaline Rocks: New York, John Wiley and Sons, p. 148-159.

Bailey, D.K., 1978, Continental rifting and mantle degassing, in, Neuman, E.-R., and Ramberg, I.B., eds., Petrology and Geochemistry of Continental Rifts: D. Reidel Publishing Company, Dordrecht, Holland, p. 1-13.

Bailey, D.K., 1983, The chemical and thermal evolution of rifts: Tectonophysics, v. 94, p. 585-597.

Baker, B.H., Mohr, P.A., and Williams, L.A.J., 1972, Geology of the Eastern

Rift System: The Geological Society of America, Special Paper 136, 67p.

Baker, B.H., and Morgan, P., 1981, Continental rifting: progress and outlook: EOS, v. 62, no. 29, p. 585-586.

Bally, A.W., 1981, Atlantic-type margins, in, Geology of Passive Continental Margins: History, Structure and Sedimentologic Record (With Special Emphasis on the Atlantic Margin), AAPG Eastern Section Meeting and Atlantic Margin Energy Confrence, Education Course Note Series no. 19, p. 1-1 to 1-48.

Bally, A.W., 1982, Musing over sedimentary basin evolution: Philosophical Transcripts of the Royal Society of London, v. A305, p. 325-338.

Bally, A.W., Bernoulli, D., Davis, G.A., and Montadert, L., 1981, Listric normal faults: Oceanologica Acta, Geology of Continental Margins, Proceedings 26th International Geological Congress, p. 87-101.

Bally, A.W., and Oldow, J.S., 1986, Plate tectonics, structural styles and evolution of sedimentary basins, Short Course no. 7: Geological Association of Canada, Cordilleran Section, 238p.

Bardoux, M., 1985, The Kelowna detachment zone, Okanagan Valley, south-central British Columbia: Geological Survey of Canada, Paper 85-1A, p. 333-339.

Bardoux, M., 1986, "Characteristics of the Okanagan Valley shear zone around Kelowna, south-central B.C.": Geological Association of Canada, Program with Abstracts, v.11, p. 43.

Barker, D.S., 1986, Carbonatite emplacement mechanisms: a review: Geological Association of Canada, Program with Abstracts, v. 11, p. 43.

Barr, D., 1985, Migmatites in the Moines, in, Ashworth, J.R., Migmatites: Blackie & Son Ltd., Glascow, England, p. 225-264.

Bedard, J.H., 1985, The opening of the Atlantic, the Mesozoic New England igneous province, and mechanisms of continental breakup: Tectonophysics v. 113, p. 209-232.

Behrmann, J.H., 1984, A study of white mica microstructure and geochemistry in a low grade mylonite: Journal of Structural Geology, v. 6, p. 283-292.

Bell, A.M., 1981, Vergence: an evaluation: Journal of structural Geology, v. 3, p. 197-202.

Bell, R.T., 1986a, Wernecke megabreccias: geological and metallogenic aspects and significance: Geological Survey of Canada, Paper 86-8, p. 2.

Bell, R.T., 1986b, Megabreccias in the northwestern Wernecke Mountains,

Yukon Territory: Geological Survey of Canada, Paper 86-1A, p. 375-384.

Bell, T.H., 1978, Progressive deformation and reorientation of fold axes in a ductile mylonite zone: the Woodroffe thrust: Tectonophysics, v. 44, p. 285-320.

Bell, T.H., 1979, The deformation and recrystallization of biotite in the Woodroffe thrust mylonite zone: Tectonophysics, v. 58, p. 139-158.

Bell, T.H., 1985, Deformation partitioning and porphyroblast rotation in metamorphic rocks: a radical interpretation: Journal of Metamorphic Petrology, v. 3, p. 109-118.

Bell, T.H., Rubenbach, M.J., and Fleming, P.D., 1986, Porphyroblast nucleation, growth and dissolution in regional metamorphic rocks as a function of deformation partitioning during foliation development: Journal of Metamorphic Petrology, v. 4, p. 37-67.

Berthe, D., Choukroune, P., and Jeguzo, P., 1979, Orthogneiss, mylonite and non coaxial deformation of granites: the example of the South Armorican Shear Zone: Journal of Structural Geology, v. 1, p. 31-42.

Black, R., Lameyre, J. and Bonin, B., 1985, The structural setting of alkaline complexes: Journal of African Earth Sciences, v. 3, no. 1/2, p. 5-16.

Bond, G.C., and Kominz, M.A., 1984, Construction of tectonic subsidence curves for the early Paleozoic miogeocline, southern Canadian Rocky Mountains: Implications for subsidence mechanisms, age of breakup, and crustal thinning: Geological Society of America Bulletin, v. 95, p. 155-173.

Bond, G.C., Nickerson, P.A., and Kominz, M.A., 1984, Breakup of a supercontinent between 625 Ma and 555 Ma: new evidence and implications for continental histories: Earth and Planetary Science Letters, v. 70, p. 325-345.

Borradaile, G.J., Bayly, M.B., and Powell, C.McA., 1982, Atlas of deformational and metamorphic rock fabrics: Springer-Verlag, New York, 551p.

Bosworth, W., 1986, Comment on "Detachment faulting and the evolution of passive continental margins": Geology, v. 14, p. 890-892.

Bott, M.H.P., 1982a, The interior of the Earth: its structure, constitution and evolution, second edition: Elsevier, New York, 403p.

Bott, M.H.P., 1982b, The mechanism of continental splitting: Tectonophysics, v. 81, p. 301-309.

Bouchez, J.L., Lister, G.S., and Nicolas, A., 1983, Fabric asymmetry and shear sense in movement zones: Geologische Rundschau, v. 72, p. 401-419.

Brodie, K.H., and Rutter, E.H., 1984, On the relationship between deformation and metamorphism, with special reference to the behavior of basic rocks, in, Metamorphic Reactions: Kinetics, Textures, and Deformation, Advances in Geochemistry, v. 4: Springer-Verlag, New York, p. 138-179.

Brown, R.L., 1978, Structural evolution of the southeast Canadian Cordillera: a new hypothesis: Tectonophysics, v. 48, p. 133-151.

Brown, R.L., 1980, Frenchman Cap dome, Shuswap Complex, British Columbia: a progress report: Geological Survey of Canada, Paper 80-1A, p. 47-51.

Brown, R.L., 1981, Metamorphic complex of southeastern Canadian Cordillera and relationship to foreland thrusting, in, McClay, K. and Price, N.J., eds., Thrust and Nappe Tectonics: Special Publication of the Geological Society of London, no. 9, p. 463-474.

Brown, R.L., and Journeay, M.J., 1985, A duplex model of crustal evolution, Omenica Belt, Southern British Columbia: Geological Associaion of America, Abstracts with Programs, v. 17, no. 6, p. 334.

Brown, R.L., and Lane, L.S., in prep., Backfolding in the Selkirk allochthon of the southern Canadian Cordillera.

Brown, R.L., and Murphy, D.C., 1982, Kinematic interpretation of mylonitic rocks in part of the Columbia River Fault zone, Shuswap Terrane, British Columbia: Canadian Journal of Earth Sciences, v. 19, p. 456-465.

Brown, R.L., and Read, P.B., 1983, Shuswap Terrane of British Columbia: a Mesozoic "Core Complex": Geology, v. 11, p. 164-168.

Brown, R.L., and Tippett, C.R., 1978, The Selkirk fan stucture of the southeastern Canadian Cordillera: Geological Society of America Bulletin, v. 89, p. 548-558.

Brown, R.L., Tippett, C.R., and Lane, L.S., 1978, Stratigraphy, facies changes, and correlations in the northern Selkirk Mountains, southern Canadian Cordillera: Canadian Journal of Earth Sciences, v. 15, p. 1129-1140.

Brown, R.L., Journeay, J.M., Lane, L.S., Murphy, D.C., and Rees, C.J., 1986, Obduction, backfolding and piggyback thrusting in the metamorphic hinterland of the Southeastern Canadian Cordillera: Journal of Structural Geology, v. 8, nos. 3/4, p. 255-268.

Brown, R.L., and Psutka, J.R., 1979, Stratigraphy of the east flank of Frenchman Cap Dome, Shuswap Complex, British Columbia: Geological Survey of Canada, Paper 79-1A, p. 35-36.

Brun, J.P., and Chourkroune, P., 1983, Normal faulting, block titling, and decollement in a stretched crust: Tectonics, v. 2, p. 345-356.

Bryant, B., and Reed, Jr., J.C., 1969, Significance of lineation and minor

folds near major thrust faults in the southern Appalachians and the British and Norwegian Caledonides: Geological Magazine, v. 106, p. 412-429.

Burchfiel, B.C., and Davis, G.A., 1975, Nature and controls of Cordilleran Orogenesis, western United States: extensions of an earlier synthesis: American Journal of Science, v. 275-A, p. 363-396.

Carmicheal, D.M., 1969, On mechanism of prograde metamorphic reactions in quartz-bearing pelitic rocks: Contributions to Mineralogy and Petrology, v. 20, p. 244-267.

Carmicheal, D.M., 1978, Metamorphic bathozones and bathograds: a measure of the depth of post-metamorphic uplift and erosion on the regional scale: American Journal of Science, v. 278, p. 769-797.

Carpenter, M.A., and Putnis, A., 1984, Cation order and disorder during crystal growth: some implications for natural mineral assemblages, in, Thompson, A.B., and Rubie, D.C., eds., Metamorphic Reactions: Kinetics, Textures and Deformation, Advances in Physical Geochemistry, v. 4,: Springer-Verlag, New York, p. 1-26.

Carr, S.D., 1986, The Valkyr shear zone and the Slocan Lake fault: Eocene structures that bound the Valhalla complex, southeastern British Columbia: unpublished M. Sc. thesis, Carleton University, Ottawa, Ontario, Canada, 106p.

Cheney, E.S., 1980, Kettle dome and related structures of northeastern Washington, in, Crittenden, Jr., M.D., Coney, P.J., and Davis, G.H., eds., Cordilleran Meatamorphic Core Complexes: Geological Society of America, Memoir 153, p. 463-468.

Cobbold, P.R., and Quinquis, H., 1980, Develpoment of sheath folds in shear regimes: Journal of Structural Geology, v. 2, p. 119-125.

Coney, P.J., 1979, Tertiary evolution of Cordilleran metamorphic core complexes, in, Armentrout, J.W. et al., S.E.P.M. Pacific Section Symposium; Cenozoic Paleogeography of the western United States, Symposium III, p. 15-28.

Coney, P.J., 1980, Cordilleran metamorphic core complexes: an overview, in, Crittenden, Jr., M.D., Coney, P.J., and Davis, G.H., eds., Cordilleran Metamorphic Core Complexes: Geological Society of America, Memoir 153, p. 4-34.

Coney, P.J., and Harms, T.A., 1984, Cordilleran metamorphic core complexes: Cenozoic extensional relics of Mesozoic compression: Geology, v. 12, p. 550-554.

Courtillot, V., 1982, Propagating rifts and continental breakup: Tectonics, v. 1, no. 3, p. 239-250.

Crawford, M.L., and Hollister, L.S., Melt enhanced deformation - a major tectonic process: Geological Association of Canada, Program with

Abstracts, v. 11, p. 60.

Crittenden, Jr., M.D., Coney, P.J., and Davis, G.H., 1978, Tectonic significance of metamorphic core complexes in the North American Cordillera: Geology, v. 6, p. 79-80.

Crittenden, Jr., M.D., Coney, P.J., and Davis, G.H., 1980, Cordilleran Metamorphic Core Complexes: Geological Society of America, Memoir 153, 490p.

Currie, K.L., 1976a, The Alkaline rocks of Canada: Geological Survey of Canada, Bulletin 239, 228p.

Currie, K.L., 1976b, Notes and petrology of Nepheline gneisses near Mount Copeland, British Columbia: Geological Survey of Canada Bulletin 265, 28p.

Dalziel, I.W.D., and Bailey, S.W., 1968, Deformed garnets from mylonitic rock from the Grenville Front and their tectonic significance: American Journal of Science, v. 266, p. 542-562.

Davis, G.H., 1980, Structural characteristics of metamorphic core complexes, southern Arizona, in, Crittenden, Jr., M.D., Coney, P.J., and Davis, G.H., Cordilleran Metamorphic Core Complexes: Geological Association of America, Memoir 153, p. 35-77.

Davis, G.H., and Coney, P.J., 1979, Geological development of the Cordilleran metamorphic core complexes: Geology, v. 7. p. 120-124.

Davis, G.H., and Coney, P.J., 1980, Comment and reply on "Geological development of the Cordilleran metamorphic core complexes: Geology, v. 8, p. 6-9.

Dawson, J.B., 1964: Carbonatitic tuff cone in northern Tanganyika: Geological Magazine, v. 101, p. 129-137.

Dawson, J.B., Bowden, P., and Clark, C.G., 1968, Activity of the carbonatite volcano Oldoinyo Lengai, 1966: Geologische Rundschau, v. 57, p. 865-879.

Deans, T., and Roberts, B., 1984, Carbonatite tuffs and lava clasts of the Tinderet foothills, western Kenya: a study of calcified natrocarbonatites: Journal of the Geological Society of London, v. 141, p. 563-580.

Debat, P., Soula, J.-C., Kubin, L., and Vidal, J.-L., 1978, Optical studies of natural deformation microstructures in feldspars (gneiss and pegmatites from Occitanie, southern France): Lithos, v. 11, p. 133-145.

De Gruyter, P., and Thomas, A.V., 1981, A model for the origin of the alkaline complexes of Egypt: Nature, v. 291, p. 571-574.

Devlin, W.J., Bond, C., and Bruekner, H.K., 1985, An assessment of the age

and tectonic setting of volcanics near the base of the Windermere Supergroup in northeastern Washington: implications for latest Proterozoic - earliest Cambrian continental separation: Canadian Journal of Earth Sciences, v. 22, p. 829-837.

DeWitt, E., 1980, Comment and reply on 'Geological development of the Cordilleran metamorphic core complexes': Geology, v. 8, p. 6-9.

Dickinson, W.R., 1977, Paleozoic plate tectonics and the evolution of the Cordilleran miogeocline, in, Stewart, J.H., Stevens, C.H., and Fritsche, A.E., eds., Paleozoic Paleogeography of the Western United States, Pacific Paleogeography Symposium 1: Society of Economic Paleontologists and Mineralogists, Los Angeles, California, p. 137-155.

Dixon, J., and Williams, G., 1983, Reaction softening in mylonites from the Arnaboll thrust, Sutherland: Scottish Journal of Geology, v. 19, p. 157-168.

Dixon, J.M., 1975, Finite strain and progressive deformation in models of diapiric structures: Tectonophysics, v. 28, p. 89-124.

Doukhan, J.-C., and Christie, J.M., 1982, Plastic deformation of sillimanite Al2SiO5 single crystals under confining pressure and TEM investigation of the induced defect structure: Bulletin Mineralogie, v. 105, p. 583-589.

Doukhan, J.-C., and Paquet, J., 1982, Plastic deformation of andalusite single crystal Al2SiO5: Bulletin Mineralogie, v. 105, p. 170-175.

Duncan, I.J., 1978, Rb/Sr whole rock evidence for three Precambrian events in the Shuswap Complex, southeastern British Columbia: Geological Association of Canada, Abstracts with Programs, v. 3, p. 392-393.

Duncan, I.J., 1984, Structural evolution of the Thor-Odin gneiss dome: Tectonophysics, v. 101, p. 87-103.

Easton, R.M., 1983, Crustal structure of rifted continental margins: geological constraints from the Proterozoic rocks of the Canadian shield: Tectonophysics, v. 94, p. 371-390.

Einsele, G., 1986, Interaction between sediments and basalt in young Gulf of California-type spreading centers: Geologische Rundschau, v. 75, no. 1, p. 197-208.

Eisbacher, G.H., 1970, Deformation of mylonitic rocks and fractured granite in Cobequid Mountains, Nova Scotia, Canada: Geological Society of America Bulletin, v. 81, p. 2009-2020.

Eisbacher, G.H., 1981, Sedimentary tectonics and glacial record in the Windermere Supergroup, MacKenzie Mountains, northwestern Canada: Geological Survey of Canada, Paper 80-27, 40p.

Eldholm, O., and Montadert, L., 1981, The main types of passive margins: an

introduction: Oceanologica Acta, Geology of Continental Margins, Proceedings 26th International Geological Congress, p. 7-10.

Elston, D.P., and McKee, E.H., 1982, Age and correlation of the late Proterozoic Grand Canyon disturbance, northern Arizona: Geological Society of America Bulletin, v. 93, p. 681-699.

Escher, A., and Watterson, J., 1974, Stretching fabrics, folds and crustal shortening: Tectonophysics, v. 22, p. 223-231.

Etheridge, M.A., and Hobbs, B.E., 1974, Chemical and deformational controls on recrystallization of mica: Contributions to Mineralogy and Petrology, v. 43, p. 111-124.

Etheridge, M.A., Hobbs, B.E., and Paterson, M.S., 1973, Experimental deformation of single crystals of biotite: Contributions to Mineralogy and Petrology, v. 38, p. 21-36.

Evenchick, C.A., 1982, Stratigraphy, structure and metamorphism in Deserters Range, northern Rocky Mountains, British Columbia: Geological Survey of Canada, Paper 82-1A, p. 325-328.

Evenchick, C.A., 1983a, Stratigraphy, structure and metamorphism in the Sifton Ranges, Cassiar Mountains, northern British Columbia: Geological Survey of Canada, Paper 83-1A, p. 221-224.

Evenchick, C.A., 1983b, Nonconformity at the base of upper Proterozoic Misinchinka Group, Deserters Range, northern Rocky Mountains: Geological Survey of Canada, Paper 83-1A, p. 475.

Evenchick, C.A., 1984, Structure and stratigraphy in the hanging wall of the Sifton Fault, Sifton Ranges, northern British Columbia: Geological Survey of Canada, Paper 84-1A, p. 105-108.

Evenchick, C.A., Parrish, R.R., and Gabrielse, H., 1984, Precambrian gneiss and late Proterozoic sedimentation in north-central British Columbia: Geology, v. 12, p. 233-237.

Fisher, R.V., and Sckminke, H.-U., 1984, Pyroclastic Rocks: Springer-Verlag, New York, 472p.

Fraser, J.A., Donaldson, J.A., Fahrig, W.F., and Tremblay, L.P., 1970, Helikian basins and geosynclines of the northwest Canadian Shield, in, Baer, J.A., ed., Symposium on Basins and Geosynclines of the Canadian Shield: Geological Survey of Canada, Paper 70-40, p. 213-238.

Fyles, J.T., 1970a, Structure of the Shuswap metamorphic complex in the Jordan River area, northwest of Revelstoke, British Columbia, in, Wheeler, J.O., ed., Structure of the Southern Canadian Cordillera: Geological Association of Canada Special Paper No. 6, p. 87-98.

Fyles, J.T., 1970b, Jordan River area: British Columbia Department of Mines and Petroleum Resources, Bulletin 57, p. 64.

Gapais, D., and White, S.H., 1982, Ductile shear bands in a naturally deforming quartzite: Textures and Microstructures, v. 5, p. 1-71.

Ghent, E.D., Nicholls, J., Stout, M.Z., and Rottenfusser, B., 1977, Clinopyroxene amphibolite boudins from Three Valley Gap, British Columbia: The Canadian Mineralogist, v. 15, p. 269-282.

Ghosh, S.K., and Ramberg, H., 1976, Reorientation of inclusions by combination of pure and simple shear: Tectonophysics, v. 34, p. 1-70.

Gibbs, A.D., 1984, Structural evolution of extensional basin margins: Journal of the Geological Society of London, v. 141, p. 609-620.

Giret, A., and Lameyre, J., 1985, Inverted alkaline-tholeiitic sequences related to lithosphere thickness in the evolution of continental rifts and oceanic islands: Journal of African earth Sciences, v.3, no. 1/2, p. 261-268.

Gittins, J., 1986, Genesis and evolution of carbonatite magmas: Geological Association of Canada, Program with Abstracts, v. 11, p. 73.

Grow, J.A., 1981, The Atlantic margin of the United States, in, Geology of Passive Continental Margins: History, Structure and Sedimentologic Record (With Special Emphasis on the Atlantic Margin), AAPG Eastern Section Meeting and Atlantic Margin Energy Conference, Education Course Note Series #19, p. 3-1 to 3-41.

Hanmer, S.K., 1982, Microstructure and geochemistry of plagioclase and microcline in naturally deformed granite: Journal of structural Geology, v. 4, p. 197-213.

Hanmer, S.K., 1984a, Strain insensitive foliations in polymineralic rocks: Canadian Journal of Earth Sciences, v. 21, p. 1410-1414.

Hanmer, S.K., 1984b, The potential use of planar and elliptical structures as indicators of strain regime and kinematics of tectonic flow: Geological Survey of Canada, Paper 84-1B, p. 133-142.

Hanmer, S.K., 1986, Asymmetrical pull-aparts and foliation fish as kinematic indicators: Journal of Structural Geology, v. 8, p. 111-122.

Hanmer, S.K., and Lucas, S.B., 1985, Anatomy of a transcurrent shear; the Great Slave Lake Shear Zone, ~~District of Mackenzie,~~ N.W.T. (Preliminary Report): Geological Survey of Canada, Paper 85-1B, p. 7-12.

Harper, G.D., and Link, P.K., 1986, Geochemistry of Upper Proterozoic rift-related volcanics, northern Utah and southeastern Idaho: Geology, v. 14, p. 864-867.

Harris, L.B., 1983, Development of conjugate shear bands by bulk simple shear: a field and experimental study: Terra Cognita, v. 3; p. 248.

Harris, L.B., and Cobbold, P.R., 1985, Development of conjugate shear bands

during bulk simple shearing: Journal of Structural Geology, v. 7, p. 37-44.

Hay, R.L., 1978, Melilitite-carbonatite tuffs in the Laetolil beds of Tanzania: Contributions to Mineralogy and Petrology, v. 67, p. 357-367.

Hay, R.L., 1983, Natrocarbonatite tephra of Kerimasi volcano, Tanzania: Geology, v. 11, p. 599-602.

Hay, R.L., and O'Neil, J.R., 1983, Carbonatite tuffs in the Laetolil beds of Tanzania and the Kaiserstuhl in Germany: Contributions to Mineralogy and Petrology, v. 82, p. 403-406.

Hietanen, A., 1967, Scapolite in the Belt Series in the St. Joe-Clearwater region, Idaho: Geological Society of America, Special Paper 86, 55p.

Higgins, M.W., 1971, Cataclastic rocks: United States Geological Survey, Professional Paper 687, 97p.

Hobbs, B.E., Means, W.D., and Williams, P.E., 1976, An Outline of Structural Geology: John Wiley & Sons, Toronto, 571p.

Hoffman, H.J. and Aitken, J.D., 1979, Precambrian biota from the Little Dal Group, MacKenzie Mountains, northwestern Canada: Canadian Journal of Earth Sciences, v. 16, p. 150-166.

Holdaway, M.J., 1971, Stability of andalusite and the aluminum silicate phase diagram: American Journal of Science, v. 271, p. 97-131.

Holland, C.H., 1986, Does the golden spike still glitter? Journal of the Geological Society, London, v. 143, p. 3-21.

Hollister, L.S., and Crawford, L.S., 1986, Melt-enhanced deformation: a major tectonic process: Geology, v. 14, p. 558-561.

Hoy, T., 1979, Cottonbelt lead/zinc deposit: British Columbia Department of Energy, Mines and Petroleum Resources, Geological Fieldwork, 1978, Paper 1979-1, p. 19-23.

Hoy, T., 1980, Geology of the Bews Creek area southwest margin of Frenchman Cap Dome (82M/2E): British Columbia Department of Energy, Mines and Petroleum Resources, Geological Fieldwork, 1979, Paper 1980-1, p. 17-22.

Hoy, T., 1982a, Stratigraphy and structural setting of stratabound lead-zinc deposits in southeastern B.C.: Canadian Institute of Mining, v. 75, p. 114-134.

Hoy, T., 1982b, The Purcell Supergroup in southeastern British Columbia: sedimentation, tectonics and stratiform lead-zinc deposits, in, Hutchinson, R.W., Spence, C.D., and Franklin, J.M., eds., Precambrian Sulphide Deposits: Geological Association of Canada, Special Paper 25, p. 127-147.

Hoy, T., and McMillan, W.J., 1979, Geology in the vicinity of Frenchman Cap gneiss dome: British Columbia Department of Energy, Mines and Petroleum Resources, Geological Fieldwork, 1979, Paper 1980-1, p. 17-22.

Hoy, T., and Brown, R.L., 1980, Preliminary Map 43, Geology of eastern margin of Shuswap Complex, Frenchman Cap area: British Columbia Ministry of Energy, Mines and Petroleum Resources.

Hoy, T., and Kwong, Y.T.K., in press, The Mount Grace carbonatite - A Nb and LREE-enriched marble of probable pyroclastic origin in the Shuswap Complex, southeastern British Columbia: Economic Geology, v. 81.

Hoy, T., and Pell, J., 1986a, Carbonatites and associated alkalic rocks, Perry River and Mount Grace areas, Shuswap Complex, southeastern British Columbia: British Columbia Ministry of Energy, Mines and Petroleum Resources, Geological Fieldwork, 1985, Paper 1986-1, p. 69-87.

Hoy, T., and Pell, J., 1986b, Intrusive and extrusive carbonatites, southeastern B.C.: Geological Association of Canada, Program with Abstracts, v. 11, p. 83

Hynes, A., 1982, Stability of the oceanic tectosphere - a model for early Proterozoic intercratonic orogeny: Earth and Planetary Science Letters, v. 61, p. 333-345.

Jefferson, C.W., 1978, Correlation of middle and upper Proterozoic strata between northeastern Canada and central Australia: Geological Association of Canada, Abstracts with Programs, v. 3, p. 429.

Jefferson, C.W., and Ruelle, J.C., 1986, The late Proterozoic copper belt, MacKenzie Mountains, N.W.T., in, Morin, J., ed., Mineral deposits of the northern Cordillera: Canadian Institute of Mining and Metallurgy, special volume (in press).

Jensen, L.N., and Starky, J., 1985, Plagioclase microfabrics in a ductile shear zone from Jotun Nappe, Norway: Journal of Structural Geology, v. 7, p. 527-539.

Johannes, W., 1985, The significance of experimental studies for the formation of migmatites, in, Ashworth, J.R., Migmatites: Blackie & Son Limited, London, p. 36-85.

Jones, A.G., 1959, Vernon map-area, British Columbia: Geological Survey of Canada, Memoir 296; 186p.

Journeay, J.M., 1981, Basement-cover relationships and structural evolution of north-central Frenchman Cap dome, Shuswap Complex, southeastern British Columbia: Geological Association of Canada, Programs with Abstracts, p. 29.

Journeay, J.M., 1982, Structural setting along the northwest flank of Frenchman Cap dome, Monashee Complex (82M/7): British Columbia

Ministry of Energy, Mines and Petroleum Resources, Geological Feildwork, 1981, Paper 82-1, p. 187-202.

Journeay, J.M., 1983, Progressive deformation and inverted regional metamorphism associated with Mesozoic emplacement of the Shuswap-Monashee Complexes, S.E. British Columbia: Geological Society of America, Programs with abstracts, v. 15, p. 606.

Journeay, J.M., 1985, Thermo-tectonic evolution of the Monashee Complex: a basement duplex, Omineca Belt, British Columbia: Geological Society of America, Programs with Abstracts, v. 17, p. 364.

Journeay, J.M., 1986, Kinematic and thermo-tectonic evolution of the northern Monashee Complex: a basement duplex, Omineca Hinterland, S.E. British Columbia: unpublished Ph.D. thesis, Queen's University, Kingston, Ontario, Canada.

Journeay, J.M., and Brown, R.L., 1985, Internal strain and kinematic evolution of the Monashee Complex: a basement duplex, Omenica Belt, British Columbia: Geological Society of America, Programs with abstracts, v. 17, p. 364.

Journeay, J.M., and Brown, R.L., 1986, Major tectonic boundaries of the Omenica Belt in southern British Columbia: a progress report: Geological Survey of Canada, Paper 86-1A, p. 81-88.

Kerrich, R., and Allison, L., 1978, Flow mechanisms in rocks: microscopic and macroscopic structures, and their relation to physical conditions of deformation in the crust: Geoscience Canada, v. 5, p. 109-118.

King, B.C., Le Bas, M.J., Sutherland, D.S., 1972, The history of the alkaline volcanoes and intrusive complexes of eastern Uganda and western Kenya: Journal of the Geological Society of London, v. 128, p. 173-205.

Knipe, R.J., and Wintsch, R.P., 1984, Heterogeneous deformation, foliation development, and metamorphic processes in a polyphase mylonite, in, Thompson, A.B., and Rubie, D.C., eds., Metamorphic Reactions: Kinetics, Textures, and Deformation, Advances in Physical Geochemistry, v. 4; Springer-Verlag, New York, p. 180-210.

Labotka, T.C., and Albee, A.L., 1977, Late Precambrian depositional environment of the Pahrump Group, Panamint Mountains, California: California Division of Mines and Geology, Special Report 129, p. 93-100.

Lane, L.S., 1977, Structure and Stratigraphy, Goldstream River-Downie Creek area, Selkirk Mountains, British Columbia: unpublished M. Sc. thesis, Carleton University, Ottawa, Ontario, Canada, 140p.

Lane, L.S., 1981, Brittle features of the Columbia River Fault in a dam site excavation near Revelstoke, British Columbia: Geological Association of Canada, Program with Abstracts, v. 7, p. A33.

Lane, L.S., 1983, Brittle kinematics of the Columbia River fault near Revelstoke, British Columbia: Geological Association of America, Abstracts with Programs, v. 15, no. 5, p. 323.

Lane, L.S., 1984a, Brittle deformation in the Columbia River fault zone near Revelstoke, southeastern British Columbia: Canadian Journal of Earth Sciences, v. 21, p. 584-598.

Lane, L.S., 1984b, Kinematic indicators in mylonites with examples from the Monashee decollement, British Columbia: Geological Association of Canada, Program with Abstracts, v. 9, p. 81.

Lane, L.S., 1984c, Deformation history of the Monashee Decollement and Columbia River Fault zone: unpublished Ph. D. thesis, Carleton University, Ottawa, Ontario, Canada, 218p.

Law, R.D., Knipe, R.J., and Dayan, H., 1984, Strain path partitioning within thrust sheets: Microstructural and petrofabric evidence from the Moine Thrust zone at Loch Eriboll, northwest Scotland: Journal of Structural Geology, v. 6, p.477-497.

Le Bas, M.J., 1977, Carbonatite-nephelinite Volcanism: John Wiley and Sons Ltd., New york, 347p.

Le Bas, M.J., 1980, Alkaline magmatism and uplift of continental crust: Proceedings of the Geological Association, v. 91, p. 33-38.

Link, P.K., 1983, Glacial and tectonically influenced sedimentation in the upper Proterozoic Pocatella Formation, southeastern Idaho, in, Miller, D.M.. Todd, V.R., and Howard, K.A., eds., Tectonics and Stratigraphic Studies in the Great Basin: Geological Society of America, Memoir 157, p. 165-181.

Lis, M.G., Price, R.A., and Glover, J.K., 1975, Late Precambrian (Hadrynian) block faulting across the western margin of the North American craton in southeastern British Columbia: Geological Association of Canada, Program with Abstracts, p. 809-810.

Lister, G.S., and Hobbs, B.E., 1980, The simulation of fabric development during plastic deformation and its application to quartzite: the influence of deformation history: Journal of Structural Geology, v. 2, p. 355-370.

Lister, G.S., Etheridge, M.A., and Symonds, P.A., 1986a, Detachment faulting and the evolution of passive continental margins: Geology, v. 14, p. 246-250.

Lister, G.S., Etheridge, M.A., and Symonds, P.A., 1986b, Reply on "Detachment faulting and the evolution of passive continental margins": Geology, v. 14, p. 890-892.

Lister, G.S., and Price, G.P., 1978, Fabric development in quartz mylonite: Tectonophysics, v. 49, p. 37-38.

Lister, G.S., Paterson, B.E., and Hobbs, B.E., 1978, The simulation of fabric development in plastic deformation and its application to quartzite: a model: Tectonophysics, v. 49, p. 37-78.

Lister, G.S., and Snoke, A.W., 1984, S-C mylonites: Journal of Structural Geology, v. 6, p. 617-638.

Lister, G.S., and Williams, 1979, Fabric development in shear zones: theoretical controls and observed phenomena: Journal of Structural Geology, v. 1, p. 283-297.

Lister, G.S., and Williams, P.F., 1983, The partitioning of deformation in flowing rock masses: Tectonophysics, v. 92, p. 1-33.

Lorenz, V., 1980, Explosive volcanism of alkali basaltic to kimberlitic melts: Lithos, v. 13, p. 217-219.

Manspeizer, W., 1981, Early Mesozoic basins of the central Atlantic passive margins, in, Bally, A.W., ed., Geology of Passive Margins: History, Structure and Sedimentological Record (With Special Emphasis on the Atlantic Margin), American Association of Petroleum Geologists Education Course Note Series #19, p. 4-1 to 4-60.

Marjoribanks, R.W., 1976, The relation between microfabric and strain in progressively deformed quartzite sequence from central Australia: Tectonophysics, v. 32, p. 269-293.

Mawer, C.K., 1985, Comment on "Fault-related rocks: suggestions for terminology: Geology, v. 13, p. 378-379.

Mawer, C.K., 1986, What is a mylonite? Geoscience Canada, v. 13, p.33-34

McDonough, M.R., and Simony, P.S., 1984, Basement gneisses and the Hadrynian metasediments near Bulldog Creek, Selwyn Range, British Columbia: Geological Survey of Canada, Paper 84-1A, p. 99-102.

McDonough, M.R., and Simony, P.S., 1986, Geology of the Selwyn Range, western Main Ranges, Rocky Mountains, British Columbia: preliminary report: Geological Survey of Canada, Paper 86-1A, p. 619-626.

McKenzie, D., 1986, The geometry of propagating rifts: Earth and Planetary Science Letters, v. 77, p. 176-186.

McLellan, E., 1985, Metamorphic reactions in the kyanite and sillimanite zones of the Barrovian type area: Journal of Petrology, v. 26, p. 789-818.

McMechan, M.E., 1981, The middle Proterozoic Purcell Supergroup in the southwestern Rocky and southeastern Purcell Mountains, British Columbia, and the initiation of the Cordilleran miogeocline, southern Canada and adjacent United States: Bulletin of Canadian Petroleum Geology, v. 29, p. 583-621.

McMechan, M.E., and Price, R.A., 1982, Superimposed low-grade metamorphism

in the Mount Fisher area, southeastern British Columbia - implications for the East Kootenay orogeney: Canadian Journal of Earth Sciences, v. 19, p. 476-489.

McMillan, W.J., 1969, West flank, Frenchman's Cap gneiss dome, Shuswap terrane, British Columbia: unpublished Ph. D. thesis, Carleton University, Ottawa, Ontario, Canada.

McMillan, W.J., 1970, West Flank, Frenchman's Cap gneiss dome, Shuswap terrane, British Columbia, in, Wheeler, J.O., ed., Structure of the Southern Canadian Cordillera: Geological Association of Canada, Special Paper no. 6, p. 99-122.

McMillan, W.J., 1973, Petrology and structure of the West Flank, Frenchman's Cap Dome, near Revelstoke, British Columbia: Geological Survey of Canada, Paper 71-29, 87p.

McMillan, W.J., and Moore Jr., J.M., 1974, Gneissic alkalic rocks and carbonatites in the Frenchman's Cap gneiss dome, Shuswap Complex, British Columbia: Canadian Journal of Earth Sciences, v. 11, p. 304-318.

Means, W.D., 1981, The concept of steady-state foliation: Tectonophysics, v. 78, p. 179-199.

Menard, D., Doukhan, J.C., and Paquet, J., 1979, Uniaxial compression of kyanite: Bulletin Mineralogie, v. 102, p. 159-162.

Miller, F.K., McKee, E.H., and Yates, R.G., 1973, Age and correlation of the Windermere Group in Northeastern Washington: Geological Society of America Bulletin, v. 84, p. 3723-3730.

Miller, J.M.G., 1985, Glacial and syntectonic sedimentation: The upper Proterozoic Kingston Peak Formation, southern Panamint Range, eastern California: Geological Society of America Bulletin, v. 96, p. 1537-1553.

Monger, J.W.H., 1977, Upper Paleozoic rocks of the western Canadian Cordillera and their bearing on Cordilleran evolution: Canadian Journal of Earth Sciences, v. 14, p. 1832-1859.

Monger, J.W.H., and Price, R.A., 1979, Geodynamic evolution of the Canadian Cordillera - Progress and Problems: Canadian Journal of Earth Sciences, v. 16, p. 770-791.

Monger, J.W.H., and Price, R.A., 1981, The Canadian Cordilleran Collage: Geological Society of America, Abstracts with Programs, v. 11, no. 7, p. 482.

Monger, J.W.H., Price, R.A., and Templeman-Kluit, D.J., 1982, Tectonic accretion and the origin of two major metamorphic welts in the Canadian Cordillera: Geology, v. 10, p. 70-75.

Monger, J.W.H. (Principal compiler), Woodworth, G.J., Price, R.A., Clowes,

R.N., Riddihough, R.P., Currie, R., Hoy, T., Preto, V.A.G., Simony, P.S., Snavely, P.D., and Yorath, C.J., 1985, Transect B2, Southern Canadian Cordillera, North American continent-ocean transects: Geological Society of America, Decade of North America Program.

Montadert, L., Roberts, D.G., Auffret, G.A., Bock, W.D., Dupeuble, P.A., Hailwood, E.A., Harrison, W.E., Kagami, H., Lumsden, D.N., Muller, C.M., Schnitker, D., Thompson, R.W., Thompson, T.L., Timofeev, P.P., 1979, Initial reports of the deep sea drilling project, v. XLVIII, U.S. Government Printing Office, Washington D.C.

Morgan, W.J., 1971, Convection plumes in the lower mantle: Nature, v. 230, p. 42-43.

Morrison, M.L., 1982, Structure and petrology of the Malton Gneiss Complex: Unpublished Ph.D. thesis, University of Calgary, Calgary, Alberta.

Nielsen, F.D., 1985, Tertiary alkaline magmatism in east Greenland: a review (Abstr.): Journal of the Geological Society of London, v. 142, p. 705.

Nisbet, E.G., 1985, The conceptual framework of Precambrian stratigraphy: a personal opinion: Geological Magazine, v. 122, p. 82-84.

Nur, A., Ron, H., and Scotti, O., 1986, Fault mechanics and kinematics of block rotations: Geology, v. 14, p. 746-749.

Okulitch, A.V., 1984, The role of the Shuswap Metamorphic Complex in Cordilleran tectonism: a review: Canadian Journal of Earth Sciences, v. 21, p. 1171-1193.

Okulitch, A.V., Loveridge, W.D., and Sullivan, R.W., 1981, Preliminary radiometric analyses of zircon from the Mount Copeland Syenite Gneiss, Shuswap Metamorphic Complex, British Columbia: Geological Survey of Canada, Paper 81-1A, p. 33-36.

Park, J.D., and Aitken, J.D., 1986, Paleomagnatism of the Katherine Group in the MacKenzie Mountains: implications for post-Grenville (Hadrynian) apparent polar wander: Canadian Journal of Earth Sciences, v. 23, p. 308-323.

Park, R.G., 1969, Structural correlation in metamorphic belts: Tectonophysics, v. 7, p. 323-328.

Parker, R.L., and Calkins, J.A., 1964, Geology of the Curlew quadrangle, Ferry County, Washington: United States Geological Survey, Bulletin 1169, 95p.

Parrish, R., and Armstrong, R.L., 1983, U-Pb zircon age and tectonic significance of gneisses in structural culminations of the Omenica Crystalline Belt, British Columbia: Geological Society of America, Abstracts with Programs, p. 324.

Passchier, C.W., 1984, The generation of ductile and brittle shear bands in

a low-angle mylonite zone: Journal of Structural Geology, v. 6, p. 273-281.

Passchier, C.W., 1986, Flow in natural shear zones - the consequences of spinning in flow regimes: Earth and Planetary Science Leters, v. 77, p. 70-80.

Pell, J., 1983, Evolution of the western margin of the North American continent in the late Precambrian: Geological Association of Canada, Program with abstracts, v. 8, p. A54.

Pell, J., 1985, Carbonatites and related rocks in British Columbia (82L, 83D, 93I, 93N): British Columbia Ministry of Energy, Mines and Petroleum Resources, Geological Fieldwork, 1984, Paper 1985-1, p. 85-94.

Pell, J., 1986a, Diatreme breccias in British Columbia (82G,J,N; 83C; 94B): British Columbia Ministry of Energy, Mines and Petroleum Resources, Geological Fieldwork, 1985, Paper 1986-1, p. 243-253.

Pell, J., 1986b, Nephiline syenite gneiss complexes in British Columbia (82M,N; 83D; 93I): British Columbia Ministry of Energy, Mines and Petroleum Resources, Geological Fieldwork, 1985, Paper 1986-1, p. 255-260.

Pell, J., 1986c, Carbonatites in British Columbia: The Aley Property (94B/5): British Columbia Ministry of Energy, Mines and Petroleum Resources, Geological Fieldwork, 1985, Paper 1986-1, p. 275-277.

Pell, J., 1986d, Carbonatites in British Columbia: a review: Geological Association of Canada, Program with Abstracts, v. 11, p. 113.

Perkins, M.J., 1983, Structural geology and stratigraphy, Big Bend of the Columbia River, Selkirk Mountains, B.C.: unpublished Ph. D. thesis, Carleton University, Ottawa, Ontario, Canada, 238p.

Phillips, E.R., 1974, Myrmekite - one hundred years later: Lithos, v. 7, p. 181-194.

Pigage, L.C., 1982, Linear regression analysis of sillimanite-forming reactions at Azure Lake, British Columbia: Canadian Mineralogist, v. 20, p. 349-378.

Piper, J.D.A., 1982, The Precambrian paleomagnetic record: the case for the Proterozoic Supercontinent: Earth and Planetary Science Letters, v. 59, p.61-89.

Platt, J.P., 1984, Secondary cleavages in ductile shear zones: Journal of Structural Geology, v. 6, p. 439-442.

Platt, J.P., and Vissers, R.L.M., 1980, Extension structures in anisotropic rocks: Journal of Structural Geology, v. 2, p. 397-410.

Poirier, J.P., 1980, Shear localization and shear instability in minerals

in the ductile field: Journal of Structural Geology, v. 2, p. 135-142.

Preto, V.A., 1970, Structure and petrology of the Grand Forks Group, British Columbia: Geological Survey of Canada, Paper 69-22.

Price, R.A., 1973, Large-scale gravitational flow of supracrustal rocks, southern Canadian Rockies, in, de Jong, K.A., and Scholten, R., eds., Gravity and Tectonics: Wiley, New York, p. 491-502.

Price, R.A., 1985, Metamorphic core complexes or the first and second kind in the cordillera of southern Canada and northern USA: Geological Society of America, Abstacts with Programs, v. 17, no. 6, p. 401.

Price, R.A., Archibald, D., and Farrar, E., 1981, Eocene stretching and necking of the crust and tectonic unroofing of the Cordilleran infrastructure, southeastern British Columbia and adjacent Washington and Idaho: Geological Association of Canada, Program with Abstracts, v. 6, p. 47.

Price, R.A., and Mountjoy, E.W., 1970, Geologic structure of the Canadian Rocky Mountains between Bow and Athabasca Rivers - a progress report, in, wheeler, J.O., ed., Structure of the Southern Canadian Cordillera: Geological Association of Canada, Special Paper no. 6, p.7-25.

Psutka, J.F., 1978, Structural setting of the Downie Slide, northeast flank of Frenchman Cap Gneiss Dome, Shuswap Complex, Southeastern, British Columbia: M.Sc. thesis, Carleton University, Ottawa, Ontario, Canada, 70p.

Quinquis, H., Audren, C., Brun, J.P., and Cobbold, P.R., 1978, Intensive progressive shear in Ile de Groix blueschists and compatibility with subduction or obduction: Nature, v. 273, p. 43-45.

Raeside, R.P., 1982, Structure, metamorphism and migmatization of the Scrip Range, Mica Creek, British Columbia: unpublished Ph. D. thesis, University of Calgary, Calgary, Alberta, Canada, 204p.

Raeside, R.P., and Simony, P., 1983, Stratigraphy and deformational history of the Scrip nappe, Monashee Mountains, British Columbia: Canadian Journal of Earth Sciences, v. 20, p. 639-650.

Ramsey, D.M., and Sturt, B.A., 1973, An analysis of noncylindrical and incongruous fold patterns from the Eo-Cambrian rocks of Soroy, northern Norway. I. Noncylindrical, incongruous, and aberrant folding; II. The significance of synfold stretching lineation in the evolution of noncylidrical folds: Tectonophysics, v. 18, p. 81-121.

Ramsey, J.G., 1967, Folding and Fracturing of Rocks: McGraw-Hill, New York, 568p.

Ramsey, J.G., 1980, Shear zone geometry: a review: Journal of Structural Geology, v. 2, p. 83-99.

Ramsey, J.G., 1982, Rock Ductility and its influence on the development o

tectonic structures in mountain belts, in, Hsu, K.J., ed., Mountain Building Processes: Academic Press, Toronto, p. 111-127.

Ramsey, J.G., and Graham, R.H., 1970, Strain variation in shear belts: Canadian Journal of Earth Sciences, v. 7, p. 786-813.

Rast, N., The origin and significance of boudinage: Geological Magazine, v. 93, p. 401-408.

Read, P.B., 1977, Lardeau map area, British Columbia: Geological Survey of Canada, Paper 77-1A, p. 295-296.

Read, P.B., 1979a, Relationship between the Shuswap Metamorphic Complex and the Kootenay Arc, Vernon east-half, southern British Columbia: Geological Survey of Canada, Paper 79-1A, p. 37-40.

Read, P.B., 1979b, Geology and mineral deposits, eastern part of Vernon east-half, British Columbia: Geological Survey of Canada, Open File 658.

Read, P.B., and Brown, R.L., 1981, Columbia River fault zone: southeastern margin of the Shuswap and Monashee complexes, southern British Columbia: Canadian Journal of Earth Sciences, v. 18, p. 1127-1145.

Read, P.B, and Klepaki, D.W., 1981, Stratigraphy and structure: northern half of Thor-Odin Nappe, Vernon east-half map area, southern British Columbia: Geological Survey of Canada, Paper 81-1A, p. 169-173.

Read, P.B., and Wheeler, J.O., 1976, Geology of the Lardeau west-half map area, British Columbia: Geological Survey of Canada, Open File 432.

Reesor, J.E., 1970, Some aspects of structural evolution and regional settting in part of the Shuswap Complex, in, Wheeler, J.O., ed., Structure of Southern British Columbia: Geological Association of Canada, Special Paper no. 6, p. 73-86.

Reesor, J.E., and Moore, Jr., J.M., 1971, Petrology and structure of Thor-Odin gneiss dome, Shuswap Metamorphic Complex, British Columbia: Geological Survey of Canada, Bulletin 195, 149p.

Rehrig, W.A, and Reynolds, S.J., 1980, Geologic and geochronologic reconnaissance of a northwest-trending zone of metamorphic core complexes in southern and western Arizona, in, Crittenden, Jr., M.D., Coney, P.J., and Davis, G.H., eds., Cordilleran Metamorphic Core Complexes: Geological Society of America, Memoir 153, p. 131-157.

Reineck, H.E., and Singh, I.B., 1980, Depositional Sedimentary Environments: Springer-Verlag, New York, 2nd ed., 549p.

Rhodes, B.P., 1986, Metamorphism of the Spokane dome mylonitic zone, Priest River Complex: constraints on the tectonic evolution of northeastern Washington and northern Idaho: Journal of Geology, v. 94, p. 539-556.

Roots, C.R., 1986, Petrogenetic evolution of the late Proterozoic Mount

Harper Complex, west-central Yukon: Geological Association of Canada, Program with Abstracts, v. 11, p. 121.

Roots, C.R., in prep. Ph. D. Thesis, Carleton University, Ottawa, Ontario, Canada.

Roots, C.R., and Thompson, R.I., 1986, Igneous response to Proterozoic extension faulting of the MacKenzie platform: geological setting of the Mount Harper volcanic complex, Ogilvie Mountains, Yukon: Geological Association of Canada, Program with Abstracts, v. 11, p. 120-121.

Ross, J.V., 1973, Mylonitic rocks and flattened garnets in the southern Okanagan of British Columbia: Canadian Journal of Earth Sciences, v. 10, p. 1-17.

Rubie, D.C., 1983, Reaction enhanced ductility; role of solid-solid univariant reactions in the deformation of the crust and mantle: Tectonophysics, v. 96, p. 331-352.

Ruelle, J.C.L., 1982, Depositional environments and genesis of stratiform copper deposits of the Redstone Copper Belt, MacKenzie Mountains, N.W.T., in, Hutchinson, R.W., Spence, C.D., and Franklin, J.M., eds., Precambrian Sulphide Deposits: Geological Association of Canada Special Paper 25, p. 701-737.

Sanderson, D.J., 1973, The development of fold axes oblique to the regional trend: Tectonophysics, v. 16, p. 55-70.

Sanderson, D.J., 1982, Models of strain variation in nappes and thrust sheets - a review: Tectonophysics, v. 88, p. 201-233.

Scammell, R.J., 1985, Stratigraphy and structure of the northwestern flank of Frenchman Cap Dome, Monashee Complex, British Columbia: preliminary results: Geological Survey of Canada, Paper 85-1A, p. 311-316.

Schmid, R., 1981, Descriptive nomenclature and classification of pyroclastic deposits and fragments: Recommendations of the IUGS Subcommission on the systematics of igneous rocks: Geology, v. 9, p. 41-43.

Schmid, S.M., 1982, Microfabric studies as indicators of deformation mechanisms and flow laws operative in mountain building, in, Hsu, K.J., ed., Mountain Building Processes: Academic Press, Toronto, p. 95-110.

Sears, J.W., and Price, R.A., 1978, The Siberian connection: a case for Precambrian separation of the North American and Siberian cratons: Geology, v. 6, p. 267-270.

Sengor, A.M.C., and Burke, K., 1978, Relative timing of rifting and volcanism on earth and its tectonic implications: Geophysical Research Letters, v. 5, p. 419-421.

Shaw, D.A., 1980, Structural setting of the Adamant Pluton, northern Selkirk Mountains, British Columbia: unpublished Ph. D. thesis, Carleton University, Ottawa, Ontario, Canada, 184p.

Sheridan, R.E., 1976, Sedimentary basins of the Atlantic margin of North America: Tectonophysics, v. 36, p. 113-132.

Silva, L.C., Le Bas, M.J., and Robertson, A.H.F., 1981, An oceanic carbonatite volcano on Santiago, Cape Verde Islands: Nature, v. 294, p. 644-645.

Simony, P.S., Ghent, E.D., Craw, D., Mitchell, W., and Robbins, D.B., 1980, Structural and metamorphic evolution of the northeast flank of the Shuswap complex, southern Canoe River area, British Columbia, in, Crittenden, M.D., Jr., Coney, P.J., and Davis, G.H., eds., Cordilleran Metamphic Core Complexes: Geological Society of America, Memoir 153, p. 445-461.

Simpson, C., 1985, Deformation of granitic rocks across the brittle-ductile transition: Journal of structural Geology, v. 7, p. 503-511.

Simpson, C., and Schmid, S.M., 1983, An evaluation of criteria to deduce the sense of movement in sheared rocks: Geological Society of America Bulletin, v. 94, p. 1281-1288.

Simpson, C., and Passchier, C.W., 1985, Porphyroclast systems as kinematic indicators: Geological Society of America, Abstracts with Programs, v. 17, no. 7, p. 718.

Skjernaa, L., 1980, Rotation and deformation of randomly oriented planar and linear structures in progressive simple shear: Journal of Structural Geology, v. 2, p. 101-109.

Smedley, P.L., 1986, The relationship between calc-alkaline volcanism and within-plate rift volcanism: evidence from Scottish Paleozoic lavas: Earth and Planetary Science Letters, v. 77, p. 113-128.

Snoke, A.W., 1980, Transition from infrastructure to suprastructure in the northern Ruby Mountains, Nevada, in, Crittenden, Jr., M.D., Coney, P.J., and Davis, G.H., eds., Cordilleran Metamorphic Core Complexes: Geological Society of America, Memoir 153, p. 287-333.

Spencer, J.E., 1984, Role of tectonic denudation in warping and uplift of low-angle normal faults: Geology, v. 12, p. 95-98.

Spry, A., 1963, The chronological analysis of crystallization and deformation of some Tasmanian Precambrian rocks: Geological Society of Australia Journal, v. 100, p. 193-208.

Stewart, J.H., 1972, Initial deposits in the Cordilleran geosyncline: Evidence of a late Precambrian (<850 m.y.) continental separation: Geological Society of America Bulletin, v. 83, p. 1345-1360.

Stewart, J.H., 1976, Late Precambrian evolution of North America: plate

tectonics implication: Geology, v. 4, p. 11-15.

Stewart, J.H., 1978, Rift systems in the western United States, in, Ramgerg, I.B., and Neumann, E.R., eds., Tectonics and Geophysics of Continental Rifts, Reidel Publishing Co., Dordrecht, Holland, p. 89-110.

Stewart, J.H., and Suczek, C.A., 1977, Cambrian and latest Precambrian paleogeography and tectonics in the western United States, in, Stewart, J.H., Stevens, C.H., and Fritsche, A.R., eds., Paleozoic Paleogeography of Western United States: Society of Economic Paleontologists and Mineralogists, California, p. 1-18.

Streckeisen, A.L., 1976, To each plutonic rock its proper name: Earth-Science Reviews, v. 12, p. 1-33.

Suppe, J., 1985, Principles of Structural Geology: Prentice-Hall, New Jersey, U.S.A., 537p.

Sykes, L.R., 1980, Earthquakes and the Lithosphere, in, Strangway, D.W., ed., The Continental Crust and its Mineral Deposits: Geological Association of Canada, Special Paper No. 20, p. 215-237.

Tempelman-Kluit, D., and Parkinson, D., 1986, Extension across the Eocene Okanagan crustal shear in southern British Columbia: Geology, v. 14, p.318-321.

Thiessen, R.L., and Means, W.D., 1980, Classification of fold interference patterns: a reexamination: Journal of Structural Geology, v. 2, p. 311-316.

Thompson, A.B., 1976, Mineral reactions in pelitic rocks: I. Prediction of P-T-X(Fe-Mg) phase relations, II.Calculation of some P-T-X(Fe-Mg) phase relations: American Journal of Science, v. 276, p. 425-454.

Thompson, R.I., 1986, Repeated extension on the proto-Pacific margin, west-central Yukon: Geological Survey of Canada, Paper 86-8, p. 11.

Tippett, C.R., 1976, A structural and stratigraphic cross-section through the Selkirk Fan Axis, Selkirk Mountains, southeastern British Columbia: unpublished M. Sc. thesis, Carleton University, Ottawa, Ontario, Canada, 166p.

Tullis, J., 1983, Deformation of Feldspars, in, Ribbe, P.H., ed., Feldspar Mineralogy, 2nd ed.: Mineralogical Society of America, Reviews of Mineralogy, v. 2, p. 297-323.

Tullis, J., Snoke, A.R., and Todd, V.R., 1982, Significance and petrogenesis of mylonitic rocks: Geology, v. 10, p.227-230.

Upton, B.G.J., and Blundell, D.J., 1978, The Gardar Igneous Province. evidence for Proterozoic continental rifting, in, Neumann, E.-R., and Ramberg, I.B., eds., Petrology and Geochemistry of Continental Rifts D. Reidel Publishing Company, Dordrecht, Holland, p. 163-172.

Van den Driessche, J., 1986, Structural evolution of the Thor-Odin gneiss dome - discussion: Tectonophysics, v. 121, p. 351-354.

Vernon, R.H., 1975a, Natural deformation and recrystallization of a plagioclase grain: American Mineralogist, v. 60, p. 884-888.

Vernon, R.H., 1975b, Microstructural mterpretation of some fibrolitic sillimanite aggregates: Mineralogical Magazine, v. 40, p. 303-306.

Vernon, R.H., 1976, Metamorphic Processes: Reactions and Microstuctural Development: Allen & Unwin, London, 247p.

Vernon, R.H., 1977a, Microfabric of mica aggregates in partly recrystallized biotite: Contributions to Mineralogy and Petrology, v. 61, p. 175-185.

Vernon, R.H., 1977b, Relationships between microstuctures and metamorphic assemblages: Tectonophysics, v. 39, p. 439-451.

Vernon, R.H., 1978, Porphyroblast-matrix microstructural relationships in deformed metamorphic rocks: Geologische Rundschau, v. 67, p. 288-305.

Vernon, R.H., and Flood, R.H., 1977, Interpretation of metamorphic assemblages containing fibrolitic sillimanite: Contributions to Mineralogy and Petrology, v. 59, p. 227-235.

Vink, G.E., 1982, Continental rifting and the implications for plate tectonic reconstructions: Journal of Geophysical Research, v. 87, no. B13, p. 10,677-10,688.

Von der Borch, C.C., 1980, Evolution of late Proterozoic to early Paleozoic Adelaide foldbelt, Australia: comparisons with post-Permian rifts and passive margins: Tectonophysics, v. 700, p. 115-134.

Walker, J.D., Klepacki, D.W., and Burchfiel, B.C., 1986, Precambrian tectonism in the Kingston Range, southern California: Geology, v. 14, p. 15-18.

Walker, R.G., 1984, Shelf and shallow marine sands, in, Walker, R.G., ed., Facies Models: Geoscience Canada Reprint Series 1, Second Edition, p. 141-170.

Wanless, R.K., and Reesor, J.E., 1975, Precambrian zircon age of orthogneisses in the Shuswap Metamorphic Complex, British Columbia: Canadian Journal of Earth Sciences, v. 12, p. 326-332.

Weijermars, R., 1982, Vergence boundaries: an extension of the vergence concept: Journal of Structural Geology, v. 4, p. 407-409.

Weijermars, R., 1985, Mapping of major fold closures from minor structures: a review of the relative merits of vergence, facing and S-Z concepts: Geologische Rundschau, v. 74, p. 611-622.

Wernicke, B., 1985, Uniform-sense normal simple shear of the continental

3

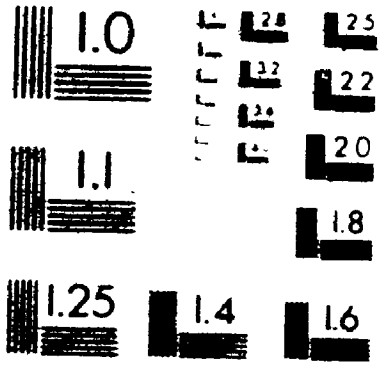

Van den Driessche, J., 1986, Structural evolution of the Thor-Odin gneiss dome - discussion: Tectonophysics, v. 121, p. 351-354.

Vernon, R.H., 1975a, Natural deformation and recrystallization of a plagioclase grain: American Mineralogist, v. 60, p. 884-888.

Vernon, R.H., 1975b, Microstructural mterpretation of some fibrolitic sillimanite aggregates: Mineralogical Magazine, v. 40, p. 303-306.

Vernon, R.H., 1976, Metamorphic Processes: Reactions and Microstuctural Development: Allen & Unwin, London, 247p.

Vernon, R.H., 1977a, Microfabric of mica aggregates in partly recrystallized biotite: Contributions to Mineralogy and Petrology, v. 61, p. 175-185.

Vernon, R.H., 1977b, Relationships between microstuctures and metamorphic assemblages: Tectonophysics, v. 39, p. 439-451.

Vernon, R.H., 1978, Porphyroblast-matrix microstructural relationships in deformed metamorphic rocks: Geologische Rundschau, v. 67, p. 288-305.

Vernon, R.H., and Flood, R.H., 1977, Interpretation of metamorphic assemblages containing fibrolitic sillimanite: Contributions to Mineralogy and Petrology, v. 59, p. 227-235.

Vink, G.E., 1982, Continental rifting and the implications for plate tectonic reconstructions: Journal of Geophysical Research, v. 87, no. B13, p. 10,677-10,688.

Von der Borch, C.C., 1980, Evolution of late Proterozoic to early Paleozoic Adelaide foldbelt, Australia: comparisons with post-Permian rifts and passive margins: Tectonophysics, v. 700, p. 115-134.

Walker, J.D., Klepacki, D.W., and Burchfiel, B.C., 1986, Precambrian tectonism in the Kingston Range, southern California: Geology, v. 14, p. 15-18.

Walker, R.G., 1984, Shelf and shallow marine sands, in, Walker, R.G., ed., Facies Models: Geoscience Canada Reprint Series 1, Second Edition, p. 141-170.

Wanless, R.K., and Reesor, J.E., 1975, Precambrian zircon age of orthogneisses in the Shuswap Metamorphic Complex, British Columbia: Canadian Journal of Earth Sciences, v. 12, p. 326-332.

Weijermars, R., 1982, Vergence boundaries: an extension of the vergence concept: Journal of Structural Geology, v. 4, p. 407-409.

Weijermars, R., 1985, Mapping of major fold closures from minor structures: a review of the relative merits of vergence, facing and S-Z concepts: Geologische Rundschau, v. 74, p. 611-622.

Wernicke, B., 1985, Uniform-sense normal simple shear of the continental

lithosphere: Canadian Journal of Earth Sciences, v. 22, p. 108-125.

Wheeler, J.O., 1965, Big Bend map-area, British Columbia 82 M (east half): Geological Survey of Canada, Paper 64-32, 37p.

White, G.P.E., 1985, Further notes on carbonatites in British Columbia: British Columbia Ministry of Energy, Mines and Petroleum Resources, Geological Fieldwork, 1984, Paper 1985-1, p. 95-100.

White, S.H., 1973, Syntectonic recrystallization and texture development in quartz: Nature, v. 244, p. 276-278.

White, S.H., 1976, The effects of strain on the microstructures, fabrics and deformation mechanisms in quartzites: Philosophical Transcripts of the Royal Society of London, Series A, v. 283, p. 69-86.

White, S.H., 1975, Tectonic deformation and recrystallization of oligoclase: Contributions to Mineralogy and Petrology, v. 50, p. 287-304.

White, S.H., 1977, Geological significance of recovery and recrystalization processes in quartz: Tectonophysics, v. 39, p. 143-170.

White, S.H., 1982, Fault rocks of the Moine Thrust Zone: a guide to their nomenclature: Textures and Microstructures, v. 4, p. 211-221.

White, S.H., Burrows, S.E., Carreras, J., Shaw, N.D., and Humphreys, F.J., 1980, On mylonites in ductile shear zones: Journal of Structural Geology, v. 2, p. 175-187.

White, S.H., Evans, D.J., and Zhong, D.-L., 1982, Fault rocks of the Moine Thrust Zone: microstructures and textures of selected mylonites: Textures and Microstructures, v. 5, p. 33-61.

White, S.H., and Knipe, R.J., 1978, Transformation- and reaction-enhanced ductility in rocks: Journal of the Geological Society of London, v. 135, p. 513-516.

Whipple, J.W., and Balla, J.C., 1986, Proterozoic copper-silver deposits of the Belt Supergroup, Idaho and Montana; Belt and Purcell Supergroups: Regional geology, in, Brown, A.C., and Kirkham, R.V., eds., Proterozoic sediment-hosted stratiform copper deposits of upper Michigan and Belt Supergroup of Idaho and Montana: Geological Association of Canada, Field Trip 1: Guidebook, p. 41-44.

Williams, G., and Dixon, L., 1982, Reaction and geomatrical softening in granitoid mylonites: Textures and Microstructures, v. 4, p. 223-239.

Williams, P.F., 1985, Multiply deformed terrains - problems of correlation: Journal of structural Geology, v. 7, p. 269-280.

Wilson, C.J.L. 1973, The prograde microfabric in a deformed quartzite sequence, Mount Isa, Australia: Tectonophysics, v. 19, p. 39-81.

Wilson, C.J.L., and Bell, T.A., 1979, Deformation of biotite and muscovite: optical microstructure: Tectonophysics, v. 58, p. 179-200.

Wilson, R.C.L., and Williams, C.A., 1979, Oceanic transform structures and the development of Atlantic continental margin sedimentary basins - a review: Journal of the Geological Society of London, v. 136, p. 311-320.

Winkler, J.F., 1979, Petrogenesis of Metamorphic Rocks: Springer-Verlag, New York, 348p.

Winter, J.K., and Ghose, S., 1979, Thermal expansion and high-temperature crystal chemistry of the Al2SiO5 polymorphs: American Mineralogist, v. 64, p. 573-586.

Wise, D.U., Dunn, D.E., Engelder, J.T., Geiser, P.A., Hatcher, R.D., Kish, S.A., Odom, A.L., and Schamel, S., 1984, Fault-related rocks: Suggestions for terminology: Geology, v. 12, p. 391-394.

Wise, D.U., Dunn, D.E., Engelder, J.T., Geisser, P.A., Hatcher, R.D., Kish, S.A, Odom, A.L., and Schamel, S., 1985, Comment and reply on "Fault-related rocks: Suggestions for terminology": Geology, v. 13, p. 378-379.

Woolley, A.R., 1986, Distribution of carbonatites in time and space: Geological Association of Canada, Program with Abstracts, v. 11, p. 147.

Wust, S.L., 1986, Regional correlation of extension directions in Cordilleran metamorphic core complexes: Geology, v. 14, p. 828-830.

Wynne-Edwards, H.R., 1963, Flow folds: American Journal of Science, v. 261, p. 793-814.

Young, G.M., 1981, Upper Proterozoic supracrustal rocks of North America: a breif review: Precambrian Research, v. 15, p. 305-330.

Young, G.M., 1982, The late Proterozoic Tindir Group, east-central Alaska: Evolution of a continental margin: Geological Society of America Bulletin, v. 93, p. 759-783.

Young, G.M., 1984, Proterozoic plate tectonics in Canada with emphasis on evidence for a late Proterozoic rifting event: Precambrian Research, v. 25, p. 233-256.

Young, G.M., Jefferson, C.W., Delaney, G.D., and Yeo, G.M., 1979, Middle and Late Proterozoic evolution of the northern Cordillera and sheild: Geology, v. 7, p. 125-128.

Zeck, H.P., 1974, Cataclastites, hemiclastites, holoclastites, blasto-ditto and myloblastites - cataclastic rocks: American Journal of Science, v. 274, p. 1064-1073.

Zwart, H.J., 1960a, The chronological succession of folding and

metamorphism in the central Pyrenees: Geologische Rundschau, v. 50, p. 203-218.

Zwart, H.J., 1960b, Relations between folding and metamorphism in the central Pyrenees, and their chronological succession: Geologie En Mijnbouw, v. 39, p. 163-180.

Zwart, H.J., 1963, Some examples of the relations between deformation and metamorphism from the central Pyrenees: Geologie En Mijnbouw, v. 42, p. 143-154.

SELECTED BIBLIOGRAPHY

Aitken, J.D., 1980, Sedimentation of the Helikian Little Dal Group, MacKenzie Mountains: Geological Association of Canada, Program with Abstracts, p. 40.

Aitken, J.D., 1981, Stratigraphy and sedimentology of the upper Proterozoic Little Dal Group, MacKenzie Mountains, Northwest Territories: Geological Survey of Canada, Paper 81-10, p. 47-71.

Aitken, J.D., Long, J.D.F., and Semikhatov, M.A., 1978b, Correlation of Helikian strata, MacKenzie Mountains-Brock Inlier-Victoria Island Geological Survey of Canada, Paper 78-1A, p. 485-486.

Aitken, J.D., and Semikhatov, M.A., 1982b, Regional aspects of the Helikian (Precambrian Y) Little Dal Group and Correlatives, Northwestern Canada, in, Reid, R.R., and Williams, G.A., Society of Economic Geologists' Coeur d'Alene Field Conference Idaho - 1977: Idaho Bureau of Mines and Geology, Bulletin 24, 1982, p. 117.

Allsopp, H.L., and Ericksson, S.C., 1986, The Palaborwa Complex: isotope evidence for ancient lithospheric enrichment: Geological Association of Canada, Program with Abstracts, v. 11, p. 40.

Armin, R.A., and Mayer, L., 1983, Subsidence analysis of the Cordilleran miogeocline: Implications for timing of late Proterozoic rifting and amount of extension: Geology, v. 11, p. 702-705.

Armin, R.A., and Mayer, L., 1984, Reply on "Subsidence analysis of the Cordilleran miogeocline: Implications for timing of late Proterozoic rifting and amount of extension": Geology, v. 12, p. 699-701.

Armstrong, R.L., 1983, Cordilleran S- and I-type granites: indicators of lithosphere thickness: Geological Association of Canada, Program with Abstracts, v. 8, p.3.

Anderson, T., and Qvale, H., 1986, Pyroclastic mechanisms for carbonatite intrusion: evidence from intrusives in the Fen complex, SE Norway: Journal of Geology, v. 94, p. 762-769.

Bailey, D.K., 1964, Crustal warping - a possible tectonic control of alkaline magmatism: Journal of Geophysical Research, v. 69, p. 1103-1111.

Bailey, D.K., 1966, Carbonatite volcanoes and shallow intrusions in Zambia, in, Tuttle, O.F., and Gittens J., eds., Carbonatites: Interscience Publishers, John Wiley and Sons, New York, p. 127-154.

Bailey, D.K., 1985, Mantle metasomatism - perspective and prospect (Abstr.): Journal of the Geological Society of London, v. 142, p. 699.

Baker, B.H., Crossley, R., and Goles, G.G., 1978, Tectonic and magmatic evolution of the southern part of the Kenya rift valley, in, Neumann, E.-R., and Ramberg, I.B., Petrology and Geochemistry of Continental

Rifts: D. Reidel Publishing Company, Dordrecht, Holland, p. 29-50.

Baragar, W.R.A., and Scoates, R.F.J., 1981, The circum-superior belt: a Proterozoic plate margin? in, Kroner, A., ed., Precambrian Plate Tectonics: Elsevier, Amsterdam, p. 297-330.

Barker, D.S., 1986, Carbonatite emplacement mechanisms: a review: Geological Association of Canada, Program with Abstracts, v. 11, p. 43.

Bell, I.A., Wilson, C.J.L., McLaren, A.C., and Etheridge, M.A., 1986, Kinks in mica: role of dislocations and (001) cleavage: Tectonophysics, v. 127, p. 46-65.

Bell, K., and Blenkinsop, J., 1986, Carbonatites and subcontinental upper mantle: Geological Association of Canada, Program with Abstracts, v. 11, p. 44.

Bell, T.H., and Etheridge, M.A., 1973, Microstructure of mylonites and their descriptive terminology: Lithos, v. 6, p. 337348.

Bell, T.H., and Etheridge, M.A., 1976, The deformation and recrystallization of quartz in a mylonite zone, central Australia: Tectonophysics, v. 32, p. 235-267.

Bell, T.H., and Hammond, R.L., 1984, On the internal geometry of mylonite zones: Journal of Geology, v. 92, p. 667-686.

Benvenuto, G.L., and Price, R.A., 1979, Structural evolution of the Hosmer thrust sheet, southeastern British Coumbia: Bulletin of Canadian Petroleum Geology, v. 27, p. 360-394.

Berg, R.R., 1975, Depositional environment of upper Cretaceous Sussex sandstone, House Creek Field, Wyoming: American Association of Petroleum Geologists Bulletin, v. 59, no. 11, p. 2099-2110.

Berthe, D., and Brun, J.P., 1980, Evolution of folds during progressive shear in the South Armorican Shear Zone, France: Journal of Structural Geology, v. 2, p. 127-133.

Bond, G.C., and Kominz, M.A., 1982, Evidence for thermal subsidence and eustatic sea level change from the lower Paleozoic miogeocline in western North America: Geological Society of America Abstracts with Programs, v. 14, p. 447.

Bond, G.C., Kominz, M.A., and Devlin, W.J., 1983, Thermal subsidence and eustasy in the lower Palaeozoic miogeocline of western North America: Nature, v. 306, p. 775-779.

Bosworth, W., 1985a, Geometry of propagating continental rifts: Nature, v. 316, p. 625-627.

Bosworth, W., 1985b, Discussion of structural evolution of extensional basin margins: Geological Society of London Journal, v. 142, p. 939-

942.

Bouchez, J.L., 1977, Plastic deformation of quartzites at low temperature in an area of natural strain gradient: Tectonophysics, v. 39, p. 25-50.

Boullier, A.M., 1980, A preliminary study on the Behavoir of brittle minerals in a ductile matrix: examples of zircons and feldspars: Journal of Structural Geology, v. 2, p. 211-217.

Boullier, A.M., 1986, Sense of shear and displacement estimates in the Abeibara-Rarhous late Pan-African shear zone, Adrar des Iforas, Mali: Journal of Structutal Geology, v. 8, p. 47-58.

Bowman, J.R., and Ghent, E.D., 1986, Oxygen and hydrogen isotope study of minerals from metapelitic rocks, staurolite to sillimanite zones, Mica Creek, British Columbia: Journal of Metamorphic Petrology, v. 4, p. 131-141.

Brenner, R.L., and Davies, D.K., 1974, Oxfordian sedimentation in western interior United States: American Association of Petroleum Geologists Bulletin, v. 58, no. 3, p. 407-428.

Brock, R.W., 1903, Preliminary report of the Boundary Creek District, British Columbia: Geological Survey of Canada, Summary Report 1902, p. 92-138.

Brock, R.B., 1934, The metamorphism of the Shuswap terrane of British Columbia: Journal of Geology, v. 42, p. 673-699.

Brown, W.L., Macaudiere, J., Ohnensteter, D., and Ohnenstetter, M., 1980, Ductile shear zones in a meta-anorthosite from Harris, Scotland: textural and compositional changes in plagioclase: Journal of structural geology, v. 2, p. 281-287.

Brunel, M., 1986, Ductile thrusting in the Himalayas: shear sense criteria and stretching lineations: Tectonics, v. 5, p. 247-265.

Burchfiel, B.C., and Davis, G.A., 1972, Structural framework and evolution of the southern part of the Cordilleran orogen, western United States: American Journal of Science, v. 272, p. 97-118.

Burg, J.P., Brunel, M., Gapais, D., Chen, G.M., and Liu, G.H., 1984, Deformation of leucogranites of the crystalline Main Central Sheet in southern Tibet (China): Journal of Structural Geology, v. 6, p. 535-542.

Burke, K., and Dewey, J.F., 1973, Plume-generated triple junctions: Key indicators in applying plate tectonics to old rocks: Journal of Geology, v. 81, p. 406-433.

Byers, C.W., 1982, Stratigraphy - the fall of continuity: Journal of Geological Education, v. 30, p. 215-221.

Cairnes, C.E., 1939, The Shuswap rocks of southern British Columbia:

Proceedings, 6th Pacific Science Congress, 1, p. 259-272.

Carter, N.L., 1976, Steady state flow of rocks: Geophysics and Space Physics Reviews, v. 14, p. 301-359.

Casas, J.-M., 1986, Shear bands and related extensional structures in a mylonitized quartz dyke: Journal of Structural Geology, v. 8, p. 693-699.

Chamberlain, V.E. and Lambert, R. St J., 1985, Cordillera, a newly defined Canadian microcontinent: Nature, v. 314, p. 707-713.

Chamberlain, V.E., and Lambert, R. St. J., 1984, Cretaceous plate tectonics of the Cordillera: the Rocky Mountain Trench as a Mesozoic suture: Geological Society of America, Abstracts with Programs, v. 16, no. 6, p. 467.

Chamberlain, V.E., Lambert, R. St. J., and Holland, J.G., 1980, Petrology and geochemistry of the Archean Rocks of the Malton Gneiss Complex, British Columbia: Precambrian Research, v.11, p. 1-9.

Chamberlain, V.E., Lambert, R. St. J., and Holland, J.G., 1978, Preliminary subdivisions of the Malton Gneiss Complex, British Columbia: Geological Survey of Canada, Paper 78-1A, p. 491-492.

Christie-Blick, N., 1984, Latest Proterozoic and early Cambrian rifting in California, Nevada and Utah: support for early Cambrian continental separation: Geological Society of America, Abstracts with Programs, v. 16, no. 6, p. 471.

Christie-Blick, N., Link, P.K., Miller, J.M.G., Young, G.M., and Crowell, J.C., 1980, Regional geological events inferred from upper Proterozoic rocks of the North American Cordillera: Geological Society of America Abstracts with Programs, p. 402.

Cooper, A.F., Gittins, J., and Tuttle, O.F., 1975, The system Na2CO3-K2CO3-CaCO3 at 1 kilobar and its significance in carbonatite petrogenesis: American Journal of Science, v. 275, p. 534-560.

Craw, D., 1978, Metamorphism, structure and stratigraphy in the southern Park Ranges, British Columbia: Canadian Journal of Earth Sciences, v. 15, p. 86-98.

Crittenden, Jr., M.D., Schaeffer, F.E., Trimble, D.E., and Woodward, L.E., 1971, Nomenclature and correlation of some upper Precambrian and basal sequences in western Utah and Southeastern Idaho: Geological Society of America Bulletin, v. 82, p. 581-602.

Crittenden, Jr., M.D., Stewart, J.H., and Wallace, C.A., 1972, Regional correlation of upper Precambrian strata in western North America: 24th International Geological Congress, 1972, Section 1, p. 334-341.

Crittenden, Jr., M.D., Christie-Blick, N., and Link, P.K., 1983, Evidence for two pulses of glaciation during the late Proterozoic in northern

Utah and southeastern Idaho: Geological Society of America Bulletin, v. 94, p. 437-450.

Daly, R.A., 1915, A geological reconnaissance between Golden and Kamloops, British Columbia, along the Canadian Pacific Railway: Geological Survey of Canada, Memoir 68.

Davy, Ph., and Gillet, Ph., 1986, The stacking of thrust slices in collision zones and its thermal consequences: Tectonics, v. 5, p. 913-929.

Dawson, J.B., 1962a, Sodium carbonatite lavas from Oldoinyo Lengai, Tanganyika: Nature, v. 195, p. 1075-1076.

Dawson, J.B., 1962b, The geology of Oldoinyo Lengai: Bulletin Volcanologique, v. 24, p. 349-387.

Dawson, J.B., 1964, Carbonatitic volcanic ashes in northern Tanganyika: Bulletin Volcanologique, v.27, p. 1-11.

Dawson, J.B., 1966, Oldoinyo Lengai - an active volcano with sodium carbonatite lava flows, in, Tuttle, O.F., and Gittins, J., eds., Carbonatites: Interscience, a division of Wiley, New York, p. 155-168.

Deines, P., 1986, Stable isotope variations in carbonatites: Geological Association of Canada, Program with Abstracts, v. 11, p. 62.

Delany, G.D., Jefferson, C.W., Yeo, G.M., McLennan, S.M., Aitken, J.D., and Bell, R.T., 1982, Some Proterozoic sediment hosted metal occurrences of the northeastern Canadian Cordillera, in, Reid, R.R., and Williams, G.A., eds., Society of Economic Geologists' Coeur d'Alene Field Conference Idaho - 1977: Idaho Bureau of Mines and Geology, Bulletin 24, 1982, p. 97-116.

Devlin, W.J., Bond, G.C., and Kominz, M.A., 1983, Evidence for a rift-drift transition in the latest Precambrian-Early Cambrian Hamill Group, southeatern British Columbia: Geological Association of Canada, Program with Abstracts, v. 8, p. A17.

Devlin, W.J., and Bond, G.C. 1984, Syn-depositional tectonism related to continental break-up in the Hamill Group, northern Selkirk Mountains, British Columbia: Geological Association of Canada, Program with Abstracts, v. 9, p. 57.

Dickinson, W.R., 1981, Plate tectonics and the continental margin of California, in, Ernst, W.G., ed., The Geotectonic Development of California, Rubey Volume I: Prentice-Hall, New Jersey, p. 3-28.

Dimroth, E., 1981, Labradour geosyncline: type example of Early Proterozoic cratonic reactivation, in, Kroner, A., ed., Precambrian Plate Tectonics: Elsevier, Amsterdam, p. 331-352.

Donath, F.A., and Parker, R.B., 1964, Folds and folding: Geological Society of America Bulletin, v. 75, p. 45-62.

Doucet, P., Ghent, E.D., and Simony, P.S., 1985, Metamorphism in the Monashee Mountains east of Blue River, British Columbia: Geological Survey of Canada, Paper 85-1A, p. 69-71.

Du Bois, C.G.B., Furst, J., Guest, N.J., and Jennings, J., 1963, Fresh natro carbonatite lava from Oldoinyo L'engai: Nature, v. 197, p. 445-446.

Edgar, A.D., 1985, Experimental studies pertinent to alkaline rocks: an overview of the last decade (Abstr.): Journal of the Geological Society of London, v. 142, p. 702.

Eggler, D.H., 1986, Peridotite solid and carbonatite melts: a new analysis: Geological Association of Canada, Program with Abstracts, v. 11, p. 66.

Einsele, G., 1982, Mechanisms of sill intrusion into soft sediment and expulsion of pore water, in, Curray, J.R., and Moore, D.G., et al., Initial Reports of the Deep Sea Drilling Project, v. 64, part 2: Washington, D.C., U.S. Government Printing Office, p. 1169-1176.

Einsele, G., 1985, Basaltic sill-sediment complexes in young spreading centers: genesis and significance: Geology, v. 13, no. 4, p. 249-252.

Einsele, G., Gieskes, J.M., Curray, J., Moore, D.M., Aguayo, E., Aubry, M., Fornari, D., Guerrero, J., Kastner M., Kelts, K, Mitchell, L., Matoba, Y., Molina-Cruz, A., Niemitz, J., Rueda, J., Saunders, A., Schrader, H., Simoniet. B., and Vacquier, V., 1980, Intrusion of basaltic sills into highly porous sediments, and resulting hydrothermal activity: Nature, v. 283, p. 441-445.

Eisbacher, G.H., 1976, Proterozoic Rapitan Group and related rocks, Redstone River area, District of MacKenzie: Geological Survey of Canada Paper 76-1A, p. 117-125.

Eisbacher, G.H., 1977, Tectono-stratigraphic framework of the Redstone Copper Belt, Ditrict of MacKenzie: Geological Survey of Canada, Paper 77-1A, p. 229-234.

Eisbacher, G.H., 1978a, Two major Proterozoic unconformities, northern Cordillera: Geological Survey of Canada, Paper 78-1A, p. 53-58.

Eisbacher, G.H., 1979, Comment and reply on "Middle and late Proterozoic evolution of the northern Canadian Cordillera and Shield": Geology, v. 7, p. 329.

Eisbacher, G.H., 1985, Late Proterozoic rifting, glacial sedimentation, and sedimentary cycles in light of Windermere deposition, western Canada: Palaeogeography, Palaeoclimatology, Palaeoecology, v. 51, p. 231-254.

Elston, D.P., 1979, Late Precambrian Sixtymile Formation and orogeny at the top of the Grand Canyon Supergroup, northern Arizona: United States Geological Survey, Professional Paper 1092, 20p.

Elston, D.P., and Bressler, S.L., 1980, Paleomagnetic poles and polarity zonation from the middle Proterozoic Belt Supergroup, Montana and Idaho: Journal of Geophysical Research, v. 85, p. 339-355.

Emeleus, C.H., and Upton, B.G.J., 1976, The Gardar period in southern Greenland, in, Escher, A., and Watt, W.S., eds., Geology of Greenland: Geological Survey of Greenland, p. 153-181.

Emery, K.O., 1968, Relict sediments of continental shelves of the world: American Association of Petroleum Geologists Bulletin, v. 52, p. 445-464.

England, P.C., and Richardson, S.W., 1977, The influence of erosion upon mineral facies of rocks from different metamorphic environments: Journal of the Geological Society of London, v. 134, p. 210-213.

England, P.C., and Thompson, A.B., 1984, Metamorphism I; heat transfer during the evolution of regions of thickened continental crust: Journal of Petrology, v. 25, p. 894-928.

Evans, R., 1978, Origin and significance of evaporites in basins around the Atlantic margin: American Association of Petroleum Geologists Bulletin, v. 62, no. 2, p. 223-234.

Ferguson, C.C., Harte, B., 1975, Textural patterns at porphroblast margins and their use in determining the time relation of deformation and crystallization: Geological Magazine, v. 112, p. 467-480.

Fitton, J.G., and Upton, B.G.J., 1985, Alkaline igneous rocks: a review symposium: Journal of the Geological Society of London, v. 142, p. 697-708.

Fitzgerald, J.D., Etheridge, M.A., and Vernon, R.H., 1983, Dynamic recrystallization in naturally deformed albite: Textures and Microstructures, v. 5, p. 219-237.

Fletcher, J.B., Sbar, M.L., and Sykes, L.R., 1978, Seismic trends and travel time residuals in eastern North America and their tectonic implications: Geological Society of America Bulletin, v. 89, no. 11, p. 1656-1676.

Francheteau, J., and Le Pichon, X., 1972, Marginal fracture zones as structural framework of continental margins in south Atlantic Ocean: American Association of Petroleum Geologists Bulletin, v. 56, p. 991-1007.

Franzen, J.P., 1974, Structural analysis in the Selkirk Fan axis near Argonaut Mountain, southeastern British Columbia: unpublished M. Sc. thesis, Carleton University, Ottawa, Ontario, Canada, 55p.

Friedman, G.M., and Sanders, J.E., 1978, Principles of Sedimentology: John Wiley and Sons, New York, 792p.

Gabrielse, H., 1967, Tectonic evolution of the northern Canadian

Cordillera: Canadian Journal of Earth Sciences, v. 4, p. 271-288.

Gabrielse, H., 1972, Younger Precambrian of the Canadian Cordillera: American Journal of Science, v. 272, p. 521-536.

Gabrielse, H., 1976, Environments of Canadian Cordillera depositional basins, in, Habourty, M.T., Maher J.C., Lian H.M., eds., Circum Pacific Mineral and Energy Resources: American Association of Petroleum Geologists, Memoir 25, p. 492-502.

Gabrielse, H., 1985, Miogeoclines in the early history of the Canadian Cordillera: Geological Society of America, Abstracts with Programs, v. 17, no. 6. p. 355.

Ghent, E.D., Knitter, C.C, Raeside, R.P., and Stout, M.Z., 1982, Geothermometry and geobarometry of pelitic rocks, upper kyanite and sillimanite zones, Mica Creek area, British Columbia: Canadian Mineralogist, v. 20, p. 295-305.

Ghent, E.D., Robbins, D.B., and Stout, M.Z., ~~1979~~, Geothermometry, geobarometry, and fluid compositions of metamorphosed calc-silicates and pelites, Mica Creek, British Columbia: American Mineralogist, v. 64, p. 874-885.

Ghent, E.D., Simony, P.S., Mitchell, W., Perry, J., Robbins, D., and Wagner, J., 1977, Structure and metamorphism in southeast Canoe River area, British Columbia: Geological Survey of Canada, Paper 77-1C, p. 13-17.

Ghent, E.D., and Stout, M.Z., 1986, Garnet-hornblende thermometry, $CaMgSi_2O_6$ activity and the minimum pressure limits of metamorphism for garnet amphibolites: Journal of Geology, v. 94, p. 736-743.

Ghent, E.D., Stout, M.Z., and Raeside, R.P., 1983, Plagioclase-clinopyroxene-garnet-quartz equilibria and the geobarometry and geothermometry of garnet amphibolites from Mica Creek, British Columbia: Canadian Journal of Earth Sciences, v. 20, p. 699-706.

Giret, A., Black, R., and Lameyre, J., 1985, Continental and oceanic anorogenic alkaline plutonism (Abstr.): Journal of African Earth Sciences, v. 3, no. 1/2, p. 274.

Gittins, J., and McKie, D., 1980, Alkalic carbonatite magmas: Oldoinyo Lengai and its wider applicability: Lithos, v. 13, p. 213-215.

Glover, J.K., and Price, R.A., 1976, Stratigraphy and structure of the Windermere Supergroup, southern Kootenay Arc, British Columbia: Geological Survey of Canada, Paper 76-1B, p. 21-23.

Greenwood, H.J., Woodsworth, G.J., and Read, P.B., 1985, Metamorphism in the Canadian Cordillera: Geological Society of America, Abstract with Programs, v. 17, no. 6, p. 357.

Grow, J.A., and Sheridan, R.E., 1981, Deep structure and evolution of the

v. 8, no. 6, p. 905.

Heckel, P.H., 1977, Origin of phosphatic black shale facies in Pennsylvanian cyclothems of mid-continent North America: American Association of Petroleum Geologists Bulletin, v. 61, no. 7, p. 1045-1068.

Heinrich, E.Wm., 1966, The Geology of Carbonatites: Rand McNally and Company, 555p.

Henderson, J.R., 1981, Structural analysis of sheath folds with horizontal X-axes, northeast Canada: Journal of Structural Geology, v. 3, p. 203-210.

Hudleston, P.J., 1986, Extracting information from folds in rock: Journal of Geological Education, v. 34, p. 237-245.

Jefferson, C.W., 1978, Stratigraphy and sedimentology, upper Proterozoic Redstone Copper Belt, MacKenzie Mountains, Northwest Territories - a preliminary report: Canadian Department of Indian and Northern Affairs, Mineral Industry Report 1975, p. 157-169.

Jefferson, C.W., 1980, Stratigraphic and sedimentologic history of the late Proterozoic Redstone Copper Belt, MacKenzie Mountains, N.W.T.: Geological Association of Canada, Program with Abstracts, p. 64.

Jefferson, C.W., 1986, Stratigraphy, tectonic and sedimentologic setting of deposits in the Redstone copper belt, MacKenzie Mountains, Northwest Canada: Geological Association of Canada, Program with Abstracts, v. 11, p. 86.

Jeguzo, P., 1980, The south Armorican shear zone: Journal of Structural Geology, v. 2, p. 39-47.

Johannes, W., 1983, On the origin of layered migmatites, in, Atherton, M.P., and Gribble, C.D., eds., Migmatites, Melting and Metamorphism: Shiva Publishing Ltd., Cheshire, U.K., p. 234-248.

Johnson, H.D., 1978, Shallow Siliciclastic Seas, in, Reading, H.G., ed., Sedimentary Environments and Facies: Elsevier, New York, p. 207-258.

Johnson, R.W., 1963, Some time relations of movement and metamorphism in the Scottish highlands: Geologie En Mijnbouw, v. 5, p. 121-142.

Kanasewich, E.R., Claws, R.M., and McCloughan, C.H., 1969, A burried Precambrian rift in western Canada: Tectonophysics, v. 8, p. 513-527.

Keller, J., 1981, Carbonatitic volcanism in the Kaiserstuhl alkaline complex: evidence for highly fluid carbonatitic melts at the earth's surface: Journal of Volcanology and Geothermal Research, v. 9, p. 423-431.

Keller, J., 1985, Tertiary alkaline volcanism of SW Germany: Rhinegraben, Kaiserstuhl, Hegau, Urach (Ab[illegible]): Journal of the Geological Society

of London, v. 142, p. 703.

King, B.C., 1970, Vulcanicity and rift tectonics in East Africa, in, Clifford, T.N., and Gass, I.G., eds., African Magmatism and Tectonics: Oliver and Boyd, Edinburgh, p. 263-283.

Knitter, C.C., 1979, Metamorphism and structure of the Soards Creek area, British Columbia: unpublished M. Sc. thesis, University of Calgary, Alberta, Canada.

Kretz, R., 1983, Symbols for rock-forming minerals: American Mineralogist, v. 68, p. 277-279.

Leatherbarrow, R.W., 1981, Metamorphism of pelitic rocks from northern Selkirk Mountains, southeastrn British Columbia: unpublished Ph. D. thesis, Carleton University, Ottawa, Ontario, Canada, 218p.

Leatherbarrow, R.W., and Brown, R.L., 1978, Metamorphism of the northern Selkirk Mountains, British Columbia; Geological survey of Canada, Paper 78-1A, p. 81-82.

Le Bas, M.J., 1981, Carbonatite magmas: Mineralogical Magazine, v. 44, p. 133-140.

Le Bas, M.J., 1985, Nephelinites and carbonitites (Abstr.): Journal of the Geological Society of London, v. 142, p. 704.

Le Bas, M.J., 1986, Diversification of carbonatite: Geological Association of Canada, Program with Abstracts, v. 11, p. 94.

Le Bas, M.J., and Aspden, J.A., 1981, The comparability of carbonatite fluid inclusions in ijolites and natrocarbonatite lava: Bulletin Volcanologique, v. 44, p. 427-438.

Le Bas, M.J., and Dixon, J.A., 1965, A new Carbonatite in the Legetet Hills, Kenya: Nature, v. 207, p. 68.

Le Bas, M.J., and Handley, C.D., 1979, Variation in apatite composition in ijolitic and carbonatitic igneous rocks: Nature, v. 279, p. 54-56.

LeFournier, J., and Friedman, G.M., 1974, Rate of lateral migration of adjoining sea-marginal sedimentary environments shown by historical records, Authie Bay, France: Geology, v. 2, p. 497-498.

Lewis, T.R., Robinson, P., et al., 1979, Leg 65 drills into young ocean crust: Geotimes, August, p.16-18.

Link, P.K., 1984, Comment on "Subsidence analysis of the Cordilleran miogeocline: Implications for timing of late Proterozoic rifting and amount of extension": Geology, v. 12, p. 699-701.

Lis, M.G., and Price, R.A., 1976, Large-scale block faulting during deposition of the Windermere Supergoup (Hadrynian) in southeastern British Columbia: Geological Survey of Canada, Paper 76-1A, p. 135-136.

Lister, G.S., 1977, Discussion: crossed girdle C-axis fabrics in quartzite plastically deformed by plane strain and progressive simple shear: Tectonophysics, v. 39, p. 51-55.

Lonsdale, P., and Lawver, L.A., 1980, Immature plate boundary zones studied with a submersible in the Gulf of California: Geological Society of America Bulletin, v. 91, p. 555-569.

Mainprice, D., Bouchez, J.-L., Blumenfeld, P., and Tubia, J.M., 1986, Dominant c slip in naturally deformed quartz: Implications for dramatic plastic softening at high temperature: Geology, v. 14, p. 819-822.

Mansy, J.L., and Gabrielse, H., 1978, Stratigraphy, terminology and correlation of upper Proterozoic rocks in Omenica and Cassiar Mountains, north-central British Columbia: Geological Survey of Canada paper 77-19, 17p.

Mariano, A.N., and Roeder, P.L., 1983, Kerimasi: a neglected carbonatite volcano: Journal of Geology, v. 91, p. 449-455.

Martin, A.K., 1984, Propagating rifts: crustal extension during continental rifting: Tectonics, v. 3, no. 6, p. 611-617.

Maxwell, J.C., 1974, Early western margin of the United States, in, Burke, C.A., and Drake, C.L., eds., The Geology of Continental Margins, Springer-Verlag, New York, p. 831-852.

McKie, D., and Frankis, E.J., 1977, Nyerereite: a new volcanic carbonate mineral from Oldoinyo Lengai, Tanzania: Zeitschrift fur Kristallographie, v. 45, p. 73-95.

McMechan, M.E., 1979, Northeastern margin of the Belt-Purcell basin and initiation of the Cordilleran miogeocline, southern Canada and adjacent United States: Geological Association of America, Abstracts with Programs, v. 11, p. 472.

Means, W.D., 1986, Three microstructural exercises for students: Journal of Geological Education, v. 34, p. 224-230.

Meneilly, A.W., and Storey, B.C., 1986, Ductile thrusting within subduction complex rocks on Signy Island, South Orkney Islands: Journal of Structural Geology, v. 8, p. 457-472.

Menzies, M., 1985, Alkaline magmas: a window on the earth's mantle: Journal of the Geological Society of London, v. 142, p. 704-705.

Misch, P., 1969, Paracrystalline microboudinage of zoned grains and other criteria for synkinematic growth of metamorphic minerals: American Journal of Science, v. 267, p. 44-49.

Moller, P., Morteani, G., and Schley, F., 1980, Discussion of REE distribution patterns of carbonatites and alkalic rocks: Lithos, v. 13, p. 171-179.

Monger, J.W.H., and Davis, G.A., 1982, Evolving concepts of the tectonics of the North American Cordillera, in, Leviton, A.E., Rodda, P.U., Yochelson, E.L., and Aldrich, M.L., eds., Frontiers of Geological Exploration of Western North America, the Pacific Division/American Association for the Advancement of Science, San Francisco, p. 215-248.

Morgan, W.J., 1972, Deep mantle convection plumes and plate motion: American Association of Petroleum Geologists Bulletin, v. 56, p. 203-213.

Morris, W.A., and Park, J.K., 1981, Correlation of upper Proterozoic strata in the Cordillera: paleomagnatism of the Tsezotene sills and the Little Dal lavas, in, Campbell, F.H.A., ed., Proterozoic Basins of Canada: Geological Survey of Canada, Paper 81-10, p. 73-78.

Morrison, M.L., 1979, Structure and petrology of the southern portion of the Malton Gneiss, British Columbia: Geological Survey of Canada Paper 79-1B, p. 407-410.

Naruk, S.J., 1986, Strain and displacement across the Pinaleno Mountains shear zone, Arizona, U.S.A.: Journal of Structural Geology, v. 8, p. 35-46.

Ojeda, H.A.O., 1982, Structural framework, stratigraphy, and evolution of Brazilian marginal basins: American Association of Petroleum Geologists Bulletin, v. 66, no. 6, p. 732-749.

Oke, C., and Simony, P.S., 1981, Basement Gneisses of the Hugh Allan Creek area, British Columbia: Geological Survey of Canada, Paper 81-1A, p. 181-184.

Olesen, N.O., 1978, Distinguishing between inter-kinematic and syn-kinematic porphyroblastesis: Geologische Rundschau, v. 67, p. 278-287.

Parrish, R., and Wheeler, J.O., 1983, A U-Pb age from the Kuskanax batholith, southeastern British Columbia: Canadian Journal of Earth Sciences, v. 20, p. 1751-1756.

Pecora, W.T., 1956, Carbonatites: a review: Geological Society of America Bulletin, v. 67, p. 1537-1556.

Pell, J., 1984, Stratigraphy, structure and metamorphism of Hadrynian strata in the southeastern Cariboo Moutains, B.C.: unpublished Ph. D. thesis, University of Calgary, Calgary, Alberta, Canada.

Platt, J.P., and Behrmann, J.H., 1986, Structures and fabrics in a crustal-scale shear zone, Betic Cordillera, SE Spain: Journal of Structural Geology, v. 8, p. 15-33.

Ponce de Lion, M.J., and Choukroune, P., 1980, Shear zones in the Iberian arc: Journal of Structural Geology, v. 2, p. 63-68.

Porter, J.W., Price, R.A., and McCrossan, R.G., 1982, The western Canada sedimentary basin: Philosophical Transcripts of the Royal Society of

London, v. A305, p. 169-192.

Poulton, T.P., and Simony, P.S., 1980, Stratigraphy, sedimentology, and regional correlation of the Horsethief Creek Group (Hadrynian, Late Precambrian) in the northern Purcell and Selkirk Mountains, British Columbia: Canadian Journal of Earth Sciences, v. 17, p. 1708-1724.

Preiss, W.V., Rutland, R.W.R., and Murrell, B., 1980, The Stuart Shelf and Adelaide Geosyncline, in, Hunter, E.R., ed., Precambrian of Southern Hemisphere: Elsevier, Amsterdam, p. 327-360.

Price, R.A., 1964, The Precambrian Purcell system in the Rocky Mountains of southern Alberta and British Columbia: Bulletin Canadian Petroleum Geology, v. 12, Special Issue, p. 399-426.

Price, R.A., and Fermor, P.R., 1981, Three sctions through the southern part of the Rocky Mountain Thrust and Fold Belt: Geological Association of Canada, Program with Abstracts, v. 6, p. A-47.

Price, R.A., and Lis, M.G., 1975, Recurrent displacement on basement-controlled faults across the Cordilleran miogeocline on southern Canada: Geological Association of America, Abstracts with Programs, v. 7, no. 7, p. 1234.

Ramsey, D.M., 1979, Analysis of rotation of folds during progressive deformation: Geological Society of America Bulletin, v. 90, p. 732-738.

Rankin, A.H., and Le Bas, M.J., 1974, Nahcolite (NaHCO3) inclusions in apatites from E. African ijolites and carbonatites: Mineralogical Magazine, v. 39, p. 564-570.

Reesor, J.E., 1965, Valhalla gneiss complex, British Columbia: Geological Survey of Canada, Bulletin 129, 128p.

Reesor, J.E., 1973, Geology of the Lardeau map area, east-half, British Columbia: Geological Survey of Canada, Memoir 369, 129p.

Rhodes, B.P., and Hyndman, D.W., 1984, Kinematics of mylonites in the Priest River "metamorphic core complex," northern Idaho and northeastern Washington: Canadian Journal of Earth Sciences, v. 21, p. 1161-1170.

Ridley, J., 1986, Parallel stretching lineations and fold axes oblique to a shear displacement direction - a model and observations: Journal of Structural Geology, v. 8, p. 647-653.

Roberts, D.G., and Montadert, L., 1979a, Objectives of passive margin drilling, in, Initial Reports of the Deep Sea Drilling Project, v. XLVIII: U.S. Government Printing Office, Washington D.C., p. 5-8.

Roberts, D.G., and Montadert, L., 1979b, Margin paleoenvironments of the northeast Atlantic, in, Initial Reports of the Deep Sea Drilling Project, v. XLVIII: U.S. Government Printing Office, Washington D.C.,

p. 1099-1118.

Roberts, D.G., and Montadert, L., 1979c, Evolution of passive rifted margins - Perspective and retrospective of DSDP Leg 48, in, Initial Reports of the Deep Sea Drilling Project, v. XLVIII: U.S. Government Printing Office, Washington D.C., p. 1143-1153.

Robbins, D.B., 1976, Metamorphism and structure of the Encampment Creek area, British Columbia: unpublished M. Sc. thesis, University of Calgary, Calgary, Alberta, Canada.

Rubie, D.C., and Thompson, A.B., 1984, Kinetics of metamorphic reactions at elevated temperatures and pressures; an appraisal of available experimental data, in, Thompson, A.B., and Rubie, R.C., eds., Metamorphic Reactions: Kinetics, Textures, and Deformation; Advances in Physical Geochemistry, v.4: Springer-Verlag, New York, p. 27-79.

Ru, K., and Pigott, J.D., 1986, Episodic rifting and subsidence in the south China Sea: American Association of Petrolium Geologists, Bulletin, v. 70, p. 1136-1155.

Ryer, T.A., 1977, Patterns of Cretaceous shallow-marine sedimentation, Coalville and Rockport areas, Utah: Geological Society of America Bulletin, v. 88, p. 177-188.

Saleeby, J.B., 1983, Accretionary tectonics of the North American Cordillera: Annual Review of the Earth and Planetary Sciences, v. 15, p. 45-73.

Schlee, J.S., and Jansa, L.F., 1981, The paleoenvironment and development of the eastern North American continental margin: Oceanologica Acta, Proceedings 26th International Geological Congress, Geology of Continental Margins, p. 71-80.

Sevigny, J.H., and Ghent, E.D., 1986, Metamorphism in the northern Adams River area, Northeastern Shuswap Complex, Monashee Mountains, British Columbia: Geological Survey of Canada, Paper 86-1B, p. 693-698.

Shepard, F.P., 1932, Sediments on the continental shelves: Geological Society of America Bulletin, v. 43, p. 1017-1039.

Sibson, R.H., 1977, Fault rocks and fault rock mechanisms: Journal of the Geological Society of London, v. 133, p. 191-213.

Simony, P.S., Morrison, M., McDonough, M., and Oke, C. 1984, Involvment of basement in the thin-skinned Rocky Mountain Thrust belt: Unpublished abstract, Canadian Tectonics Group Meeting, Maniwaki, Quebec, Oct. 1984.

Simony, P.S., and Wind, G., 1970, Structure of the Dogtooth Range and adjacent portions of the Rocky Mountain Trench, in, Wheeler, J.O., ed., Structure of the Southern Canadian Cordillera: Geological Association of Canada, Special Paper no. 6, p. 41-51.

Simpson, C., 1983, Strain and shape variations associated with ductile shear zones: Journal of structural Geology, v. 5, p. 61-72.

Simpson, C., 1985, Movement sense determination in sheared rock: Geological Society of America, Abstracts with Programs, v. 17, no. 7, p. 718.

Simpson, C., 1986, Determination of movement sense in mylonites: Journal of Geological Education, v. 34, p. 246-261.

Sorensen, H., (editor), 1974, The Alkaline Rocks: New York, John Wiley & Sons, 622p.

Stewart, J.H., 1971, Late Precambrian (<750 m.y.) continental separation in western North America - Possible evidence from sedimentary and volcanic rocks: Geological Society of America, Abstracts with Programs, v. 3, p. 201.

Stewart, J.H., McMenamin, M.A.S., Morales-Ramirez, J.M., 1984, Upper Proterozoic and Cambrian rocks in the Caborca Region, Sonora, Mexico - physical stratigraphy, biostratigraphy, paleocurrent studies, and regional relations: U.S. Geological Survey Professional Paper 1309, 36p.

Stewart, J.H., and Poole, F.G., 1974, Lower Paleozoic and uppermost Cordilleran miogeocline, Great Basin, western United States, in, Dickinson, W.R., ed., Tectonics and Sedimentation,: Society of Economic Paleontologists and Mineralogists, Special Publication 22, p. 28-57.

Stewart, J.W., 1970, Precambrian alkaline-ultramafic/carbonatite volcanism at Qagssiarssuk, south Greenland: Bulletin Gronland Geologiske Undersogelse, v. 186, no. 4, 70p.

Strong, D.F., 1979, Proterozoic tectonism of northwestern Gondwanaland: new evidence from eastern Newfoundland: Tectonophysics, v. 54, p. 81-101.

Strong, D.F., O'Brien, S.J., Taylor, S.W., Strong, P.G., and Wilton, D.H., 1978, Aborted proterozoic rifting in eastern Newfoundland: Canadian Journal of Earth Sciences, v. 15, p. 117-131.

Struik, L.C., 1986, Imbricated terranes of the Cariboo gold belt with correlations and implications for tectonics in southeastern British Columbia: Canadian Journal of Earth Sciences, v. 23, p. 1047-1061.

Sykes, L.R., 1978, Intraplate seismicity, reactivation of preexisting zones of weakness, alkaline magmatism, and other tectonism postdating continental fragmentation: Reviews of Geophysics and Space Physics, v. 16, no. 4, p. 621-688.

Takagi, H., 1986, Implications of mylonitic microstructures for the geotectonic evolution of the Median Tectonic Line, central Japan: Journal of Structural Geology, v. 8, p. 3-14.

Takagi, H., and Hara, I., 1979, Relationship between growth of albite

porphyroblasts and deformation in a Sambagawa schist, central Shikoku, Japan: Tectonophysics, v. 58, p. 113-125.

Thompson, A.B., and Rubie, D.C., (eds.), 1984, Metamorphic Reactions: Kinetics, Textures and Deformation, Advances in Physical Geochemistry, v. 4,: Springer-Verlag, New York, 291p.

Tilton, G.R., and Kwon, S.T., 1986, Pb isotope studies of alkalic carbonatite and syenite complexes: Geological Association of Canada, Program with Abstracts, v. 11; p. 137.

Tipper, H.W., Woodsworth, G.J., and Gabrielse, H. (co-ordinators), 1981, Tectonic Assemblage Map of the Canadian Cordillera and ajacent parts of the United States of America: Geological Survey of Canada, Map 1505A.

Toteu, S.F., and Macaudiere, J., 1984, Complex synkinematic and postkinematic garnet porphyroblast growth in polymetamorphic rocks: Journal of Structural Geology, v. 6, p. 669-677.

Treiman, A.H., 1986a, Carbonatite magmas: properties and processes: Geological Association of Canada, Program with Abstracts v. 11, p. 138.

Treiman, A.H., 1986b, A petrogenetic grid for carbonatites: Geological Association of Canada, Program with Abstracts, v. 11, p. 138.

Treiman, R.I., and Schedl, A., 1983, Properties of carbonatite magma and processes in carbonatite magma chambers: Journal of Geology, v. 91, p. 437-447.

Turcotte, D.L., and Emerman, S.H., 1983, Mechanisms of active and passive rifting: Tectonophysics, v. 94, p. 39-50.

Turcotte, D.L., and Oxburgh, E.R., 1973, Mid-plate tectonics: Nature, v. 244, p. 337-339.

Tullis, J., and Yund, R.A., 1985, Dynamic recrystallization of feldspar: a mechanism for ductile shear zone formation: Geology, v. 13, p. 238-241.

Tuttle, O.F., and Gittins, J., (editors), 1966, Carbonatites: Interscience Publishers, John Wiley and Sons, New York, 591p.

Twyman, T.R., and Gittins, J., 1982, Differentiation of carbonatite magmas - evidence for the alkali enrichment and the natrocarbonatite - sovite link: Geological Society of America, Abstracts with Programs, p. 635.

Twyman, T.R., and Gittins, J., 1985, Alkali carbonatite magmas: parental or derivative? Journal of the Geological Society of London, v. 142, p. 706-707.

Vidal, J.-L., Kubin, L., Debat, P., and Soula, J.C., 1980, Deformation and dynamic recrystallization of K-feldspar augen in orthogneiss from

Montagne Noire, Occitania, Southern France: Lithos, v. 13, p. 247-255.

Von Knorring, O., and Du Bois, C.G.B., 1961, Carbonatite lava from Fort Portal area in western Uganda: Nature, v. 192, p. 1064-1065.

Walker, R.G., 1979, Facies model 7. Shallow marine sands, in, Walker, R.G., ed., Facies Models: Geoscience Canada Reprint Series 1, First Edition, p. 75-89.

Wardle, R.J., 1981, Eastern margin of the Labrador Trough: an Aphebian proto-oceanic rift zone: Geological Association of Canada, Program with Abstracts, v. 6, p. A-59.

Wardle, R.J., and Bailey, D.G., 1981, Early Proterozoic sequences in Labrador, in, Campbell, F.A.H., ed., Proterozoic Basins of Canada: Geological Survey of Canada, Paper 81-10, p. 331-359.

Watkinson, D.H., 1970, Experimental studies bearing on the origin of the alkalic rock-carbonatite complex and niobium mineralization at Oka, Quebec: Canadian Mineralogist, v. 10, p. 350-361.

Watts, M.J., and Williams, G.D., 1980, Fault rocks as indicators of progressive shear deformation in the Guingamp region, Brittany: Journal of Structural Geology, v. 1, p. 323-332.

Wernicke, B., and Burchfiel, B.C., 1982, Modes of extensional tectonics: Journal of Structural Geology, v. 4, p. 105-115.

Wheeler, J.O., 1985, Geological belts of the Canadian Cordillera: Geological Society of America, Abstracts with Programs, v. 17, no. 6, p. 418.

White, J.C., and Mawer, C.K., 1986, Extreme ductility of feldspars from a mylonite, Parry Sound, Canada: Journal of Structural Geology, v. 8, p. 133-143.

White, W.H., 1959, Cordilleran tectonics in British Columbia: American Association of Petroleum Geologists Bulletin, v. 43, p. 60-100.

Williams, G.D., 1978, Rotation of contemporaneous folds into the X direction during overthrust processes in Lakesefjord, Finnmark: Tectonophysics, v. 48, p. 29-40.

Winston, D., 1986, An alluvial apron and playa-margin interpretation of Cu- and Ag-bearing sedimentary rocks, middle Proterozoic Belt Supergroup, Montana and Idaho: Geological Association of Canada, Program with Abstracts, v. 11, p. 146.

Winston, D., Woods, M., Jefferson, C.W., Kirkham, R.V., and Donaldson, J.A., 1986, Middle to late Proterozoic (1.8-0.6 Ga) sedimentation, North America: Geological Association of Canada, Program with Abstracts, v. 11, p. 146.

Winston, D., Woods, M., and Byer, G.B., 1984, The case for an intracratonic

Belt-Purcell basin: tectonic, stratigraphic and stable isotope considerations, in, McBane, J.D., and Garrison, P.B., eds., Montana Geological Society 1984 Field Confrence, Northwestern Montana and adjacent Canada, p. 103-118.

Wintsch, R.P., and Knipe, R.J., 1983, Growth of a zoned plagioclase porphyroblast in a mylonite: Geology, v. 11, p. 360-363.

Woolley, A.R., and Jones, G.C., 1985, The Chilwa alkaline igneous province, Malawi: petrochemistry and petrogenesis (Abstr.): Journal of the Geological Society of London, v. 142, p. 707-708.

Wright, L.A., Troxel, B.W., Williams, E.G., Roberts, M.T., and Diehl, P.E., 1974, Precambrian sedimentary environments of the Death Valley region, Eastern California: Geological Society of America, Cordilleran Section, Guidebook: Death Valley Region, California, Nevada, p. 27-35.

Wust, S.L., 1986, Extension deformation with northwest vergence, Pioneer core complex, central Idaho: Geology, v. 14, p. 712-714.

Wyllie, P.J., 1966, Experimental studies of carbonatite problems: the origin and differentiation of carbonatite magmas, in, Tuttle, O.F., and Gittins, J., eds., Carbonatites: Interscience Publishers, John Wiley and Sons, p.311-352.

Wyllie, P.J., and Huang, W.L., 1975, Peridotite, kimberlite, and carbonatite explained in the system CaO-MgO-SiO2-CO2: Geology, v. 3, p. 621-624.

Wyllie, P.J., and Tuttle, O.F., 1960, The system CaO-CO2-H2O and the origin of carbonatites: Journal of Petrology, v. 1, p. 1-16.

Wyllie, P.J., and Tuttle, O.F., 1962, Carbonatitic lavas: Nature, v. 194, p. 1269.

Young, G.M., 1977a, Stratigraphic correlation of upper Proterozoic rocks of northwestern Canada: Canadian Journal of Earth Sciences, v. 14, p. 1771-1787.

Young, G.M., 1977b, Correlation of middle and upper Proterozoic strata of the northern rim of the Atlantic craton: Royal Society of Edinburgh Transactions, v. 70, p. 323-336.

Young, G.M., 1981, The Amundsen embayment, N.W.T.; Relevance to the upper Proterozoic evolution of North America, in, Campbell, F.H.A., ed., Proterozoic Basins of Canada: Geological Survey of Canada, Paper 81-10, p. 203-218.

Young, G.M., Jefferson, C.W., Delaney, G.D., and Yeo, G.M., 1979b, Comment and Reply on "Middle and late Proterozoic evolution of the northern Canadian Cordillera and Shield: Geology, v. 7, p. 329-330.

Young, G.M., Jefferson, C.W., Dalaney, G.D., Yeo, G.M., and Long, D.G.F., 1982, Upper Proterozoic stratigraphy of northwestern Canada and

Precambrian history of the North American Cordillera, in, Reid, R.R., and Williams, G.A., eds., Society of Economic Geologists' Coeur d'Alene Field Conference, Idaho - 1977: Idaho Bureau of Mines and Geology, Bulletin 24, p. 73-96.


ICEFIELD
ICEFIELD
ICEFIELD
38'
37'
500
500
500
500

FIGURE 2

STATION LOCATION MAP

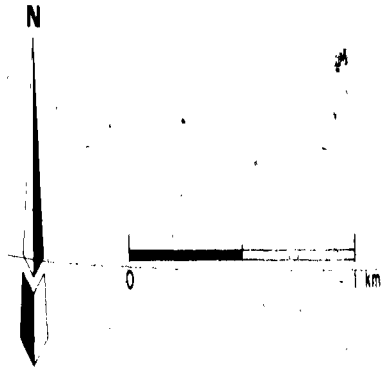

LEGEND

(no) station location and number 1984

(no) station location and number 1985

LEGEND


MD
MD
MD
38
37
8G
10AP
10F
8G
8P
8G
10AP
10F
8G
11P
10AP

FIGURE 4

STRATIGRAPHIC MAP OF THE NORTH END OF THE MONASHEE COMPLEX

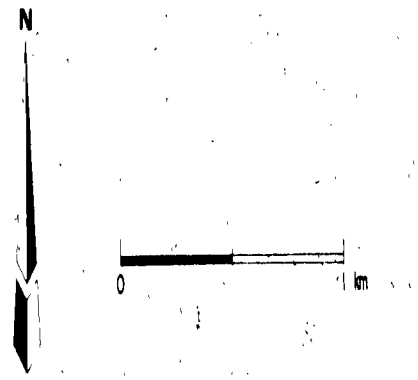

Interlayered

Approximate

Assumed

Fracture zone

Monashee decollement

STRATIGRAPHY

SELKIRK ALLOCHTHON

S4 Dominantly pelitic & semipelitic schists interlayered with Qtz-Fsp gneiss, quartzite and minor amphibolite, pegmatite locally composes ca. 2%

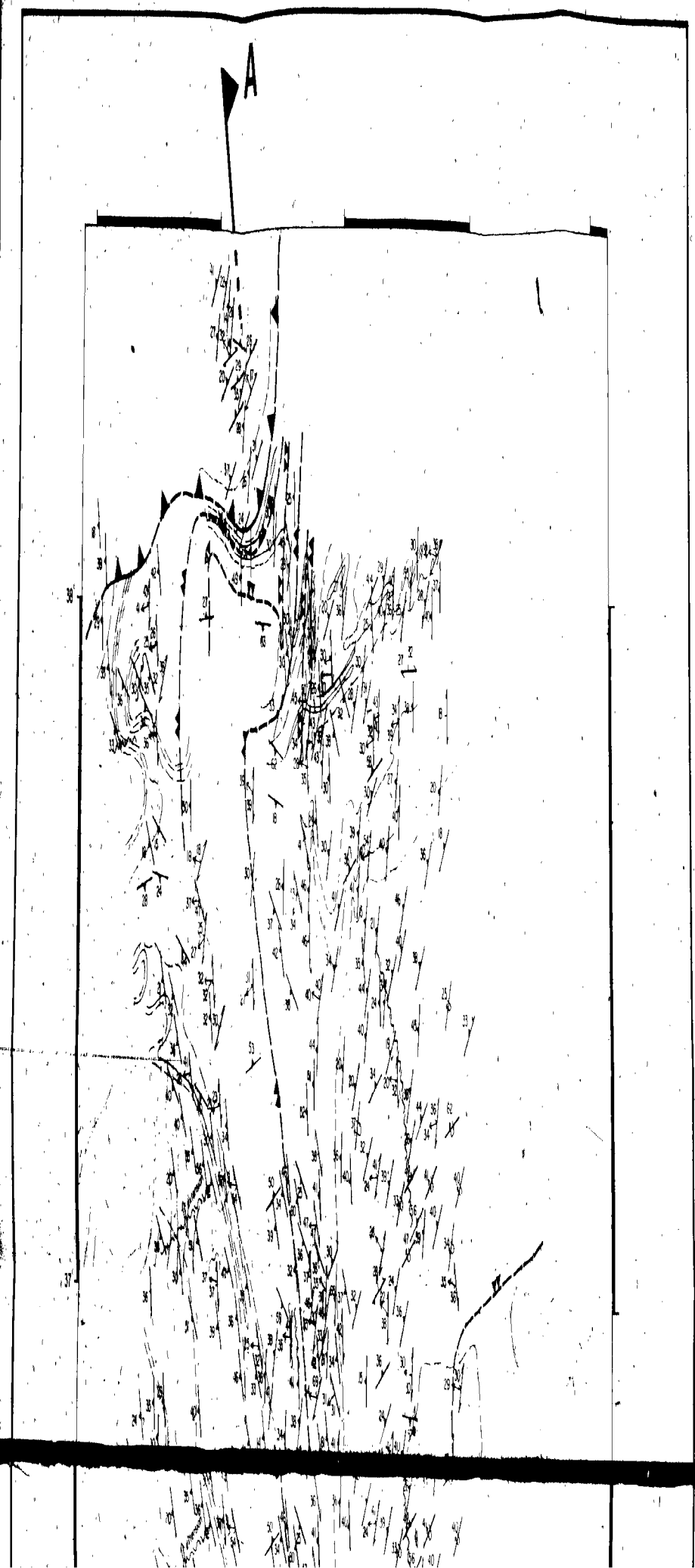
A

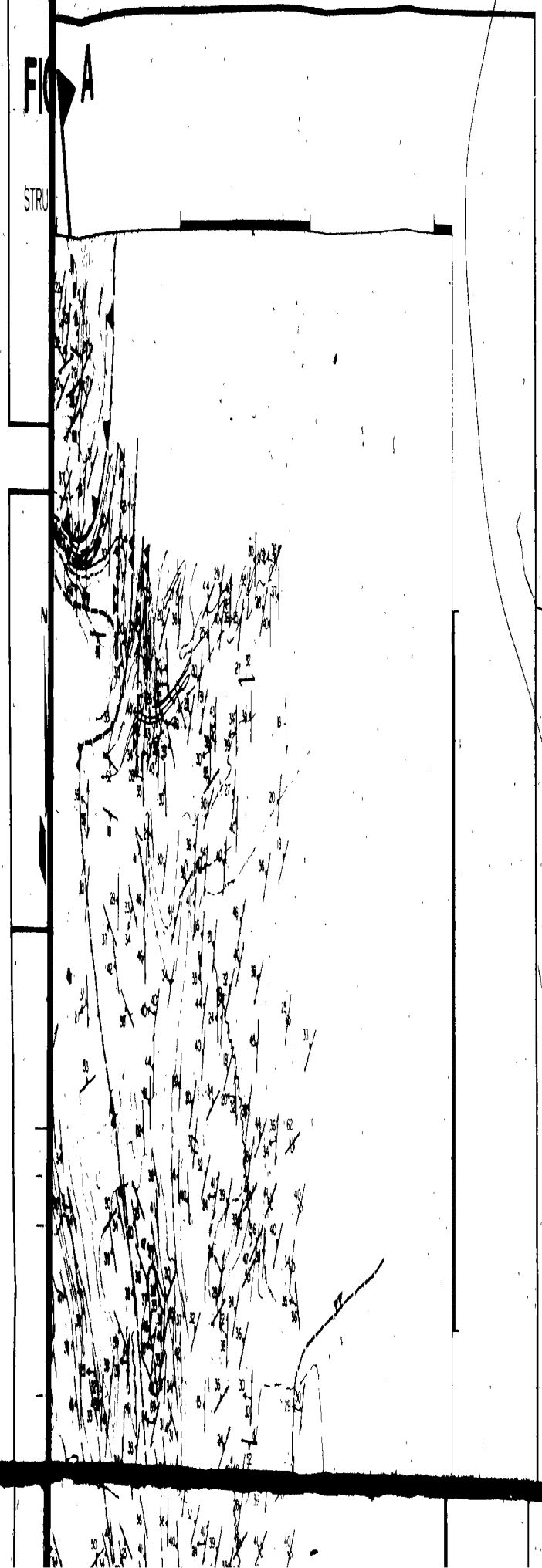
A

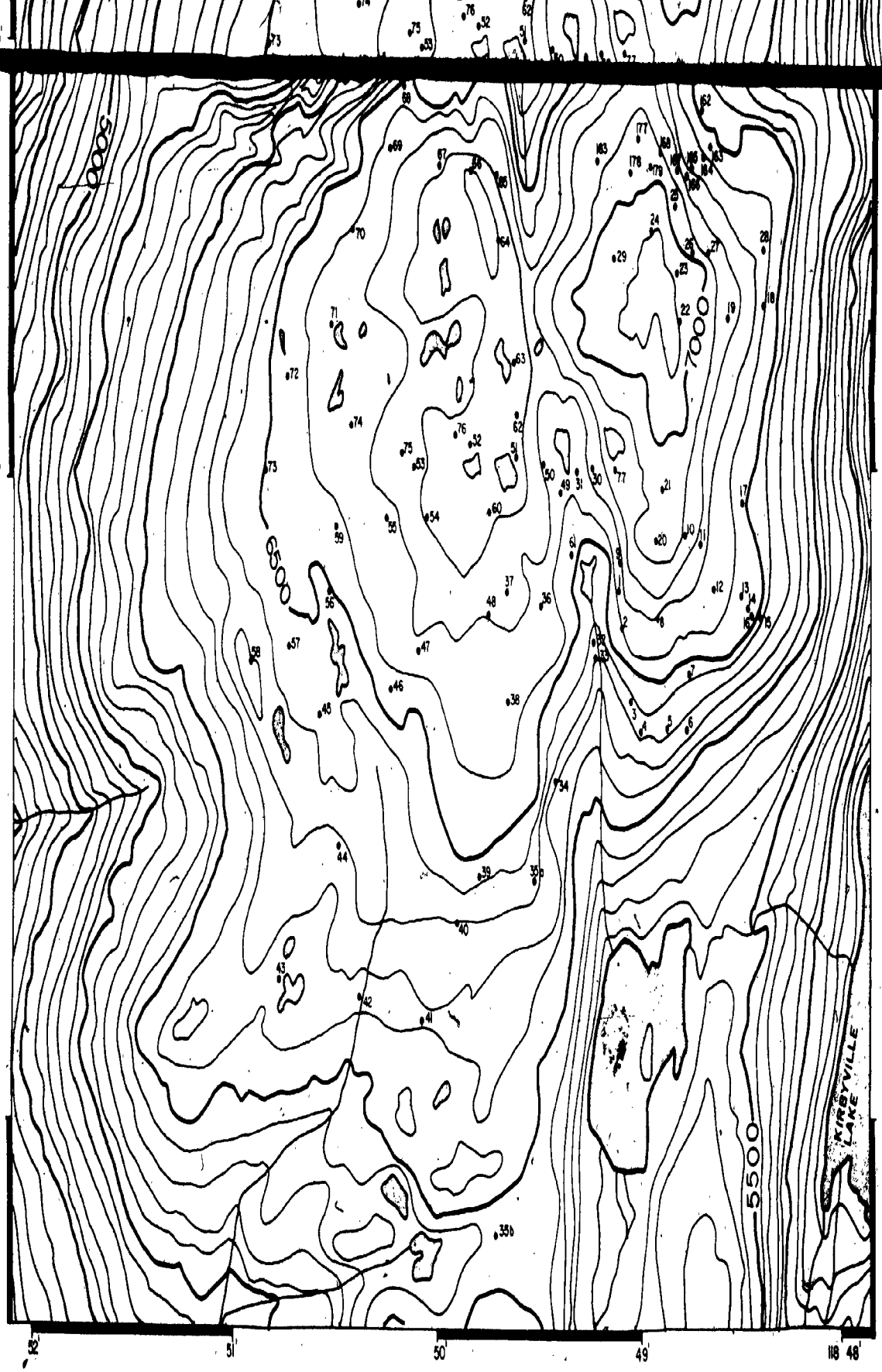

RS/DM 1966


37'
36'
35'
5000
6000
7000

LEGEND

(no) station location and number 1984

(no) station location and number 1985

Contours at 100 ft intervals
Topography from map 82 M/10
Hoskins Creek 1 50000
Surveys and Mapping Branch,
Canadian Energy, Mines & Resources

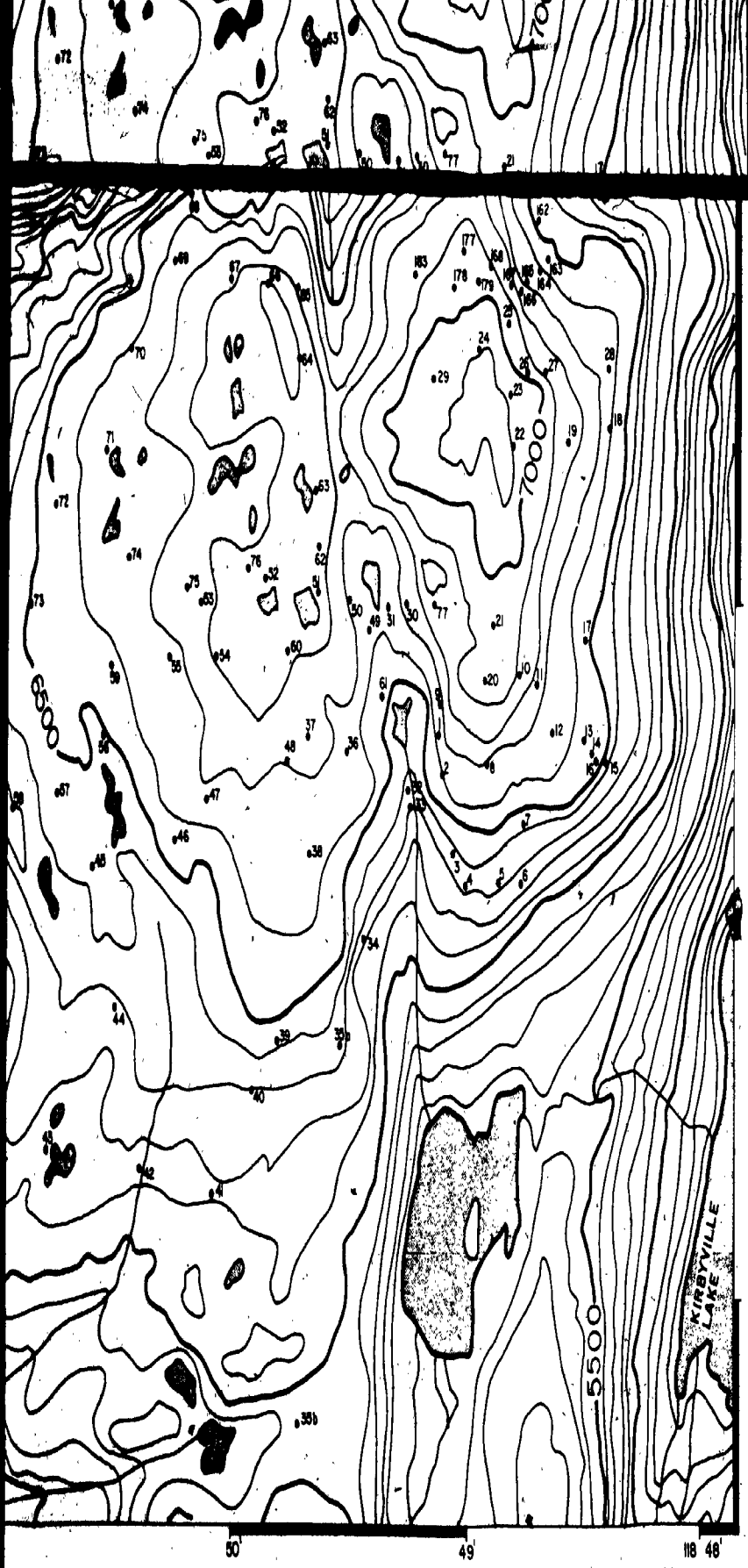

RS/DM 1986

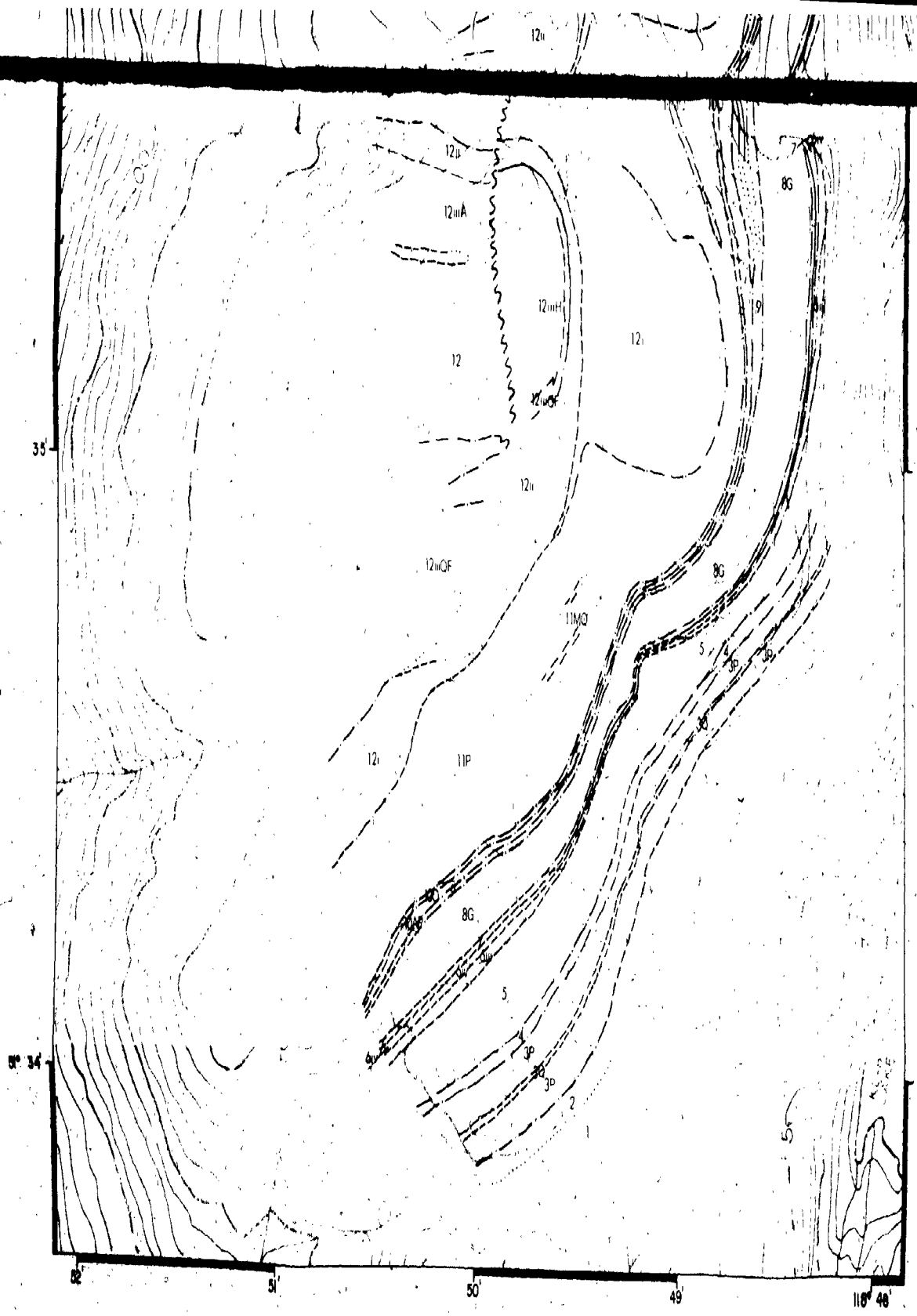
12ii
12iiA
12iiH
12
12i
12iiQF
11MQ
11P
8G
5
3P
2
1
35'
34'
52'
51'
50'
49'
118° 48'

RS/DM 1986


37'
36'
35'
11P
10MQ
10AP
9
8d
10Q
11G
11H
8G
12ii
12iiiA
12iiiH
12i

[illegible] minor amphibolite, [illegible] composes [illegible]

[illegible] Fracture zone

[illegible]

[illegible]

[illegible]

[illegible] - [illegible] and [illegible] interbedded [illegible] Qtz-Fsp gneiss [illegible]

[illegible] Hornblendite, [illegible] gneisses interbedded with minor calcareous [illegible] schist

[illegible] Dominantly pelitic and semipelitic schists interlayered with [illegible] gneiss and [illegible] amphibolite and hornblendite

[illegible] Interbedded impure marble, calc-silicate and quartzite

[illegible] Hornblendite with subordinate Hbl gneiss

[illegible] Flaggy or Hbl-Qtz-Fsp gneiss

[illegible] Amphibolite and Al-deficient pelitic and semi-pelitic schists interlayered with subordinate hornblendite, quartzite, Qtz-Fsp gneiss and metaconglomerate

[illegible] Al-rich [illegible] schists

[illegible] White quartzite

[illegible] Dominantly quartzite with concordant and discordant amphibolite, minor pelitic schists, ultramafic and syenite rocks; interlayered Hbl- & Grt-bearing meta-arkose & subarkose

QF Hbl- & Grt-bearing pink meta-arkose

[illegible] G Amphibolite and flaggy Hbl gneiss interbedded with minor quartzite, various gneisses, carbonate rock and metaconglomerate

[illegible] P Dominantly pelitic and semipelitic schist interlayered with subordinate amphibolite, [illegible]

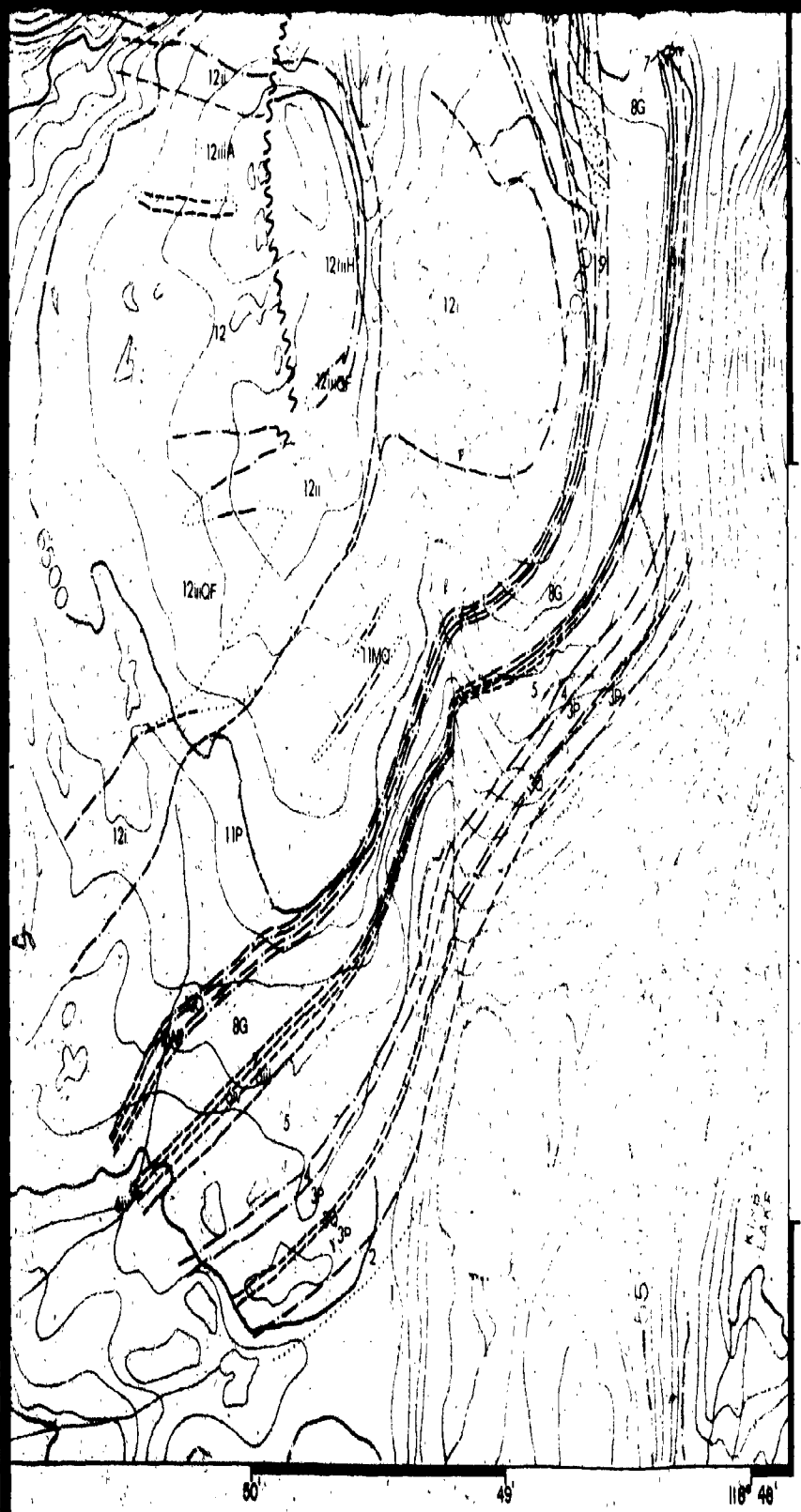

RS/DM 1986

P Dominantly pelitic and semipelitic schist interlayered with subordinate amphibolite, [illegible] and various gneisses

[illegible]

P And-Sil-Ky-Grt-Qtz-Fsp schists

Q White quartzite

Q Dominantly quartzite with subordinate [illegible] amphibolite, minor pelitic schist, ultramafic and syenite rocks; interlayered [illegible] Grt bearing meta-arkose & subarkose

[illegible] Grt-bearing pink meta-arkose

[illegible] Amphibolite and flaggy Hbl gneiss interbedded with minor quartzite, various gneisses, [illegible] rock and metaconglomerate

[illegible] Dominantly pelitic and semipelitic schist interlayered with subordinate amphibolite, [illegible] and various gneisses

[illegible] schist with minor interbedded white [illegible] and calc-silicate at the base, and [illegible] amphibolite at the top

[illegible] quartzite

[illegible] fragmental carbonatite

[illegible] banded [illegible] pure marble

[illegible] banded calc-silicate gneiss

[illegible] gneiss

[illegible] Pelitic schist interlayered with subordinate [illegible] and Qtz-Fsp gneiss

[illegible] Quartzite and feldspathic quartzite with minor pelitic schist partings

[illegible] Pelitic schist with minor interlayered Qtz-Fsp gneiss [illegible] quartzite

[illegible] quartzite

[illegible] Quartzite with pelitic schist partings

Contact not observed; unconformable to the south

CORE GNEISSES

[illegible] Ky-Grt-Ms-Bt schist and Bt-Qtz-Fsp gneiss

INTRUSIVE ROCKS

[illegible] [illegible]yenite intrusive rocks associated with units 6iii marble and 6iv carbonatite

P Pegmatite

NOTE: Lower case roman numerals and arabic numerals imply stratigraphic order. No stratigraphic order is implied for the Selkirk allochthon, or the Monashee decollement which cuts across units 5 to 12, inclusive.

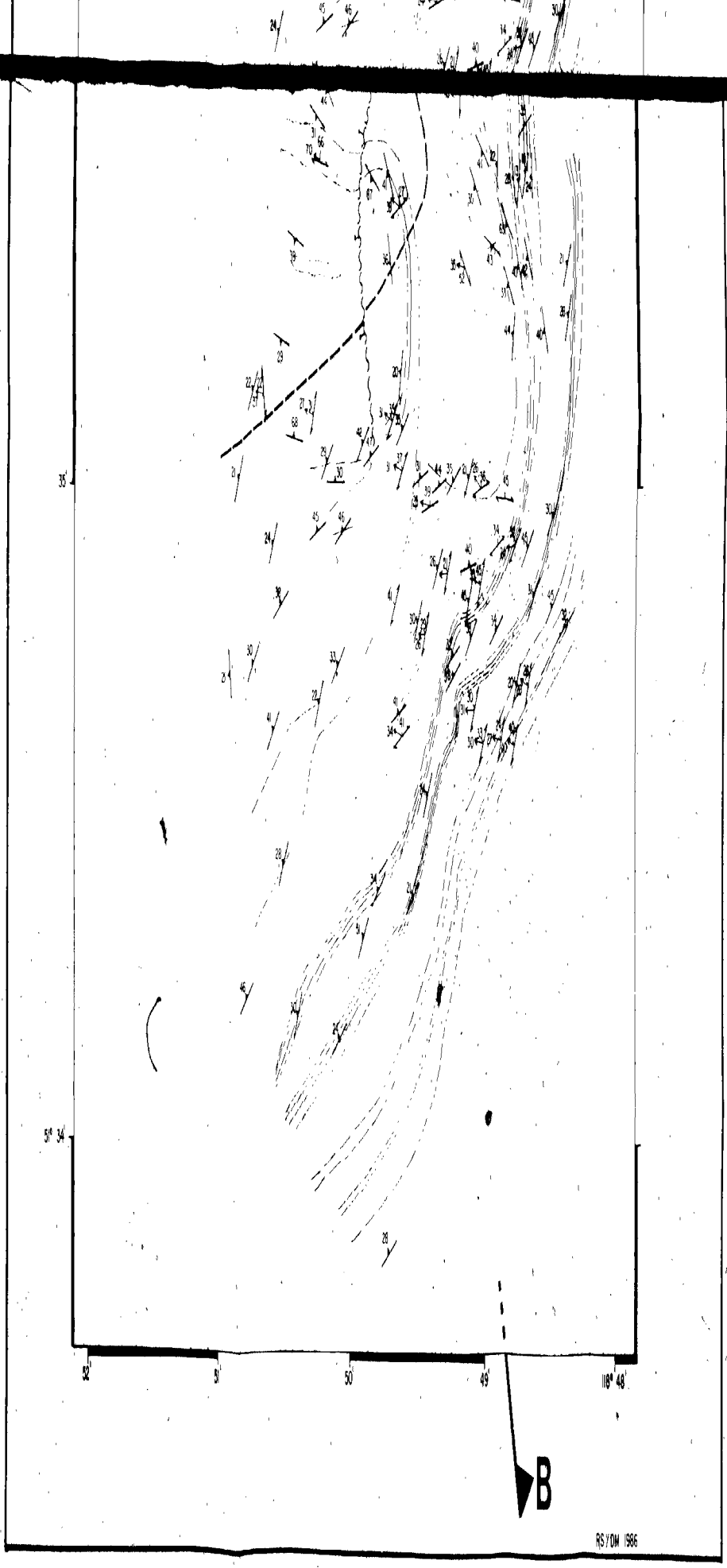
35'
51° 34'
52'
51'
50'
49'
118° 48'
B
RS/DM 1986

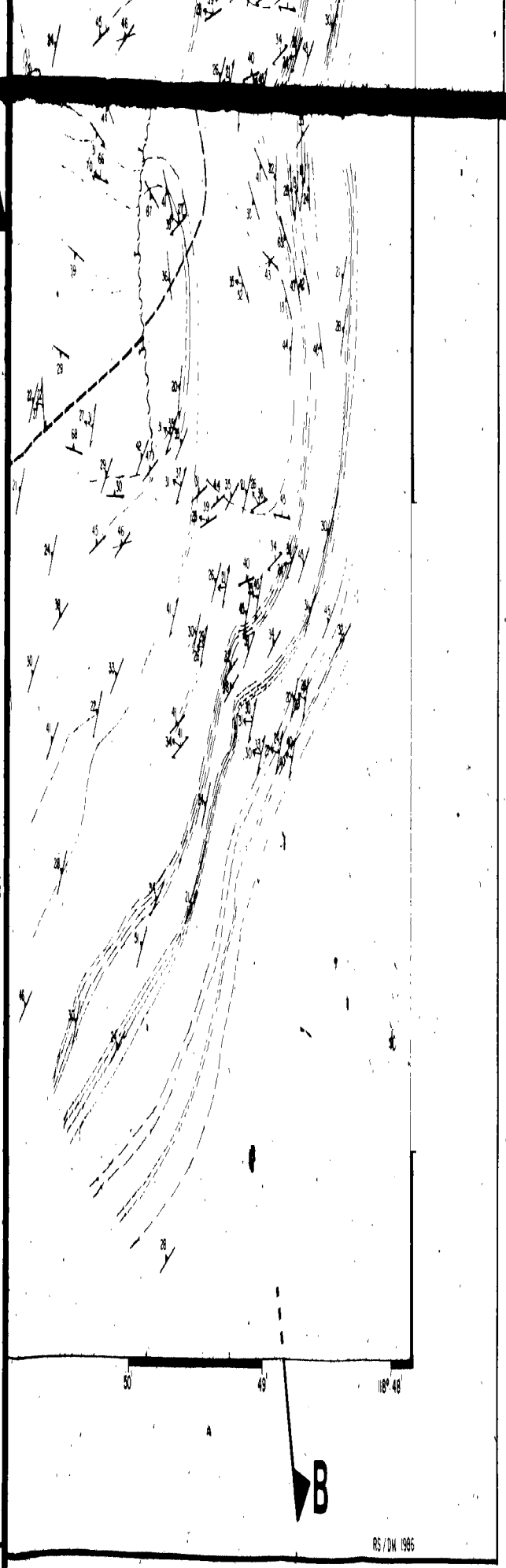
50'
49'
118° 48'
B
RS/DM 1986

37
36
35

4 of/de 4

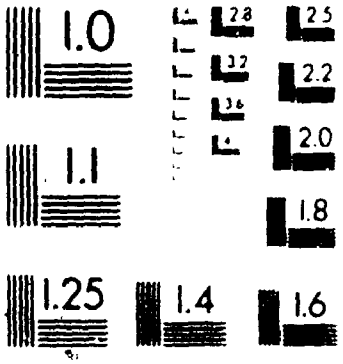

MICROD

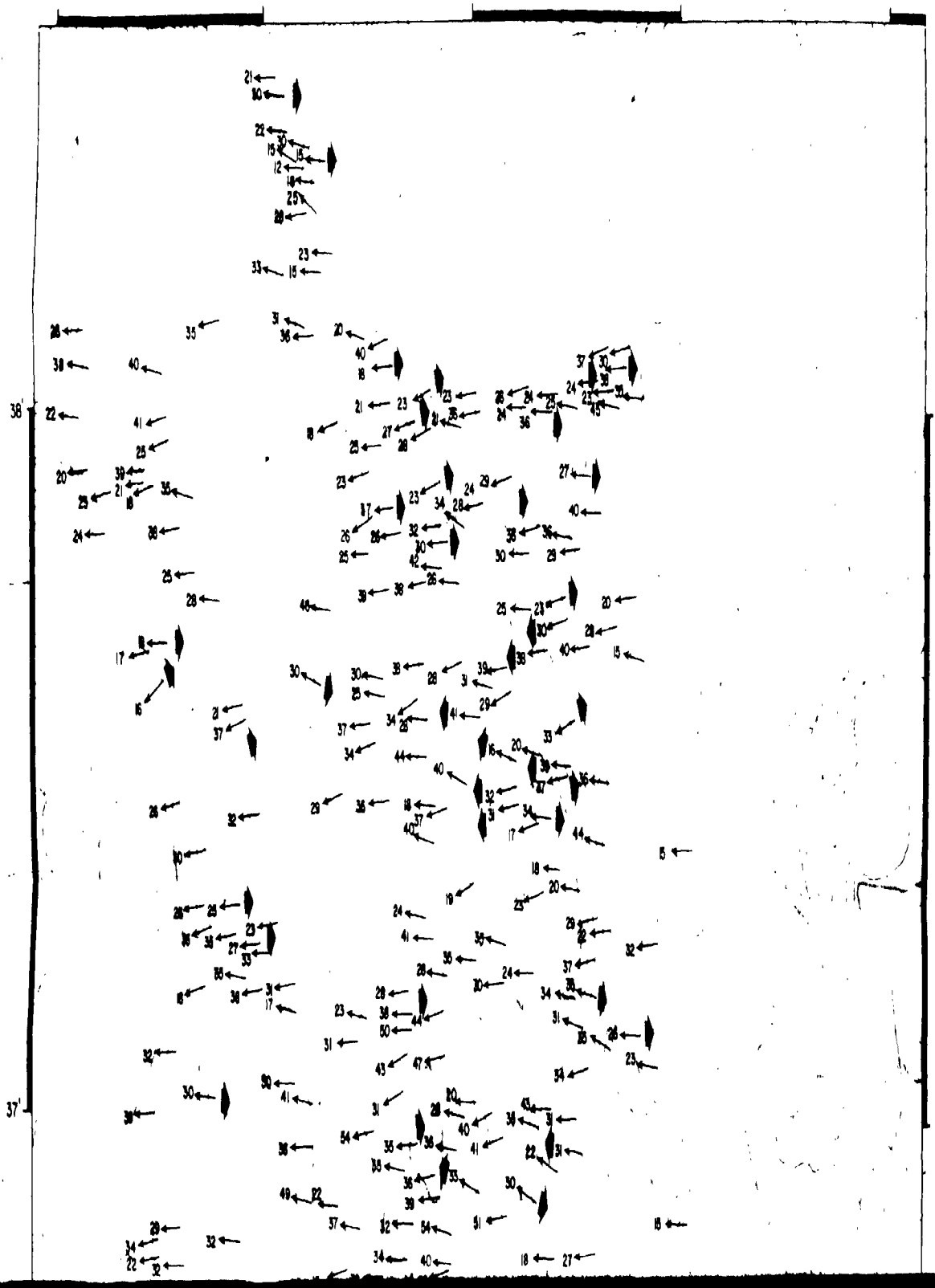

FIGURE 8

STRUCTURAL MAP OF MINERAL STRETCHING LINEATIONS AND SENSE OF SHEAR

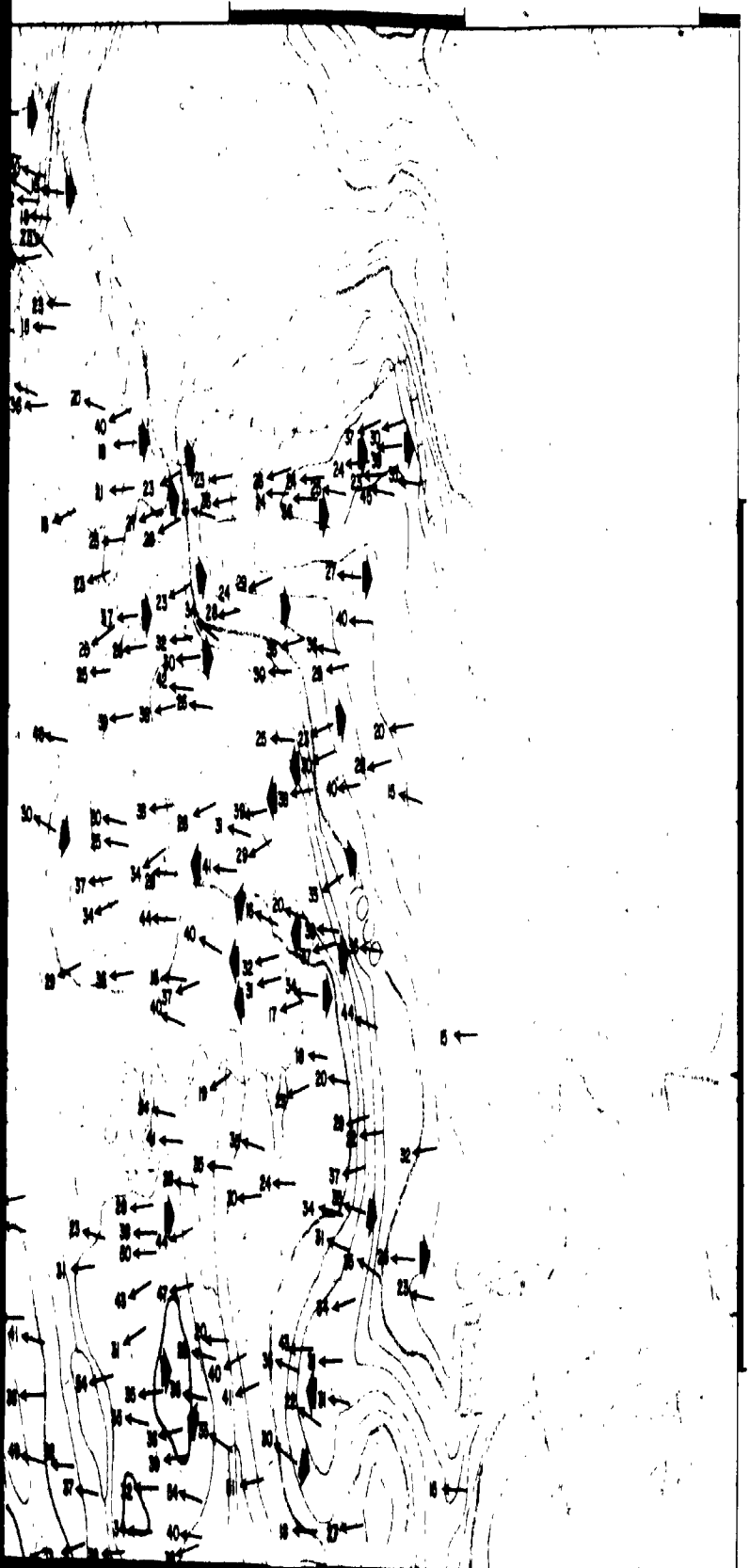

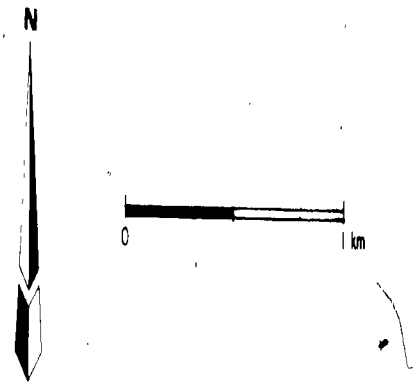

LEGEND

27 ← trend and plunge of mineral stretching lineation

sense of shear:
motion direction of the upper member in the shear couple

LOWER PLATE

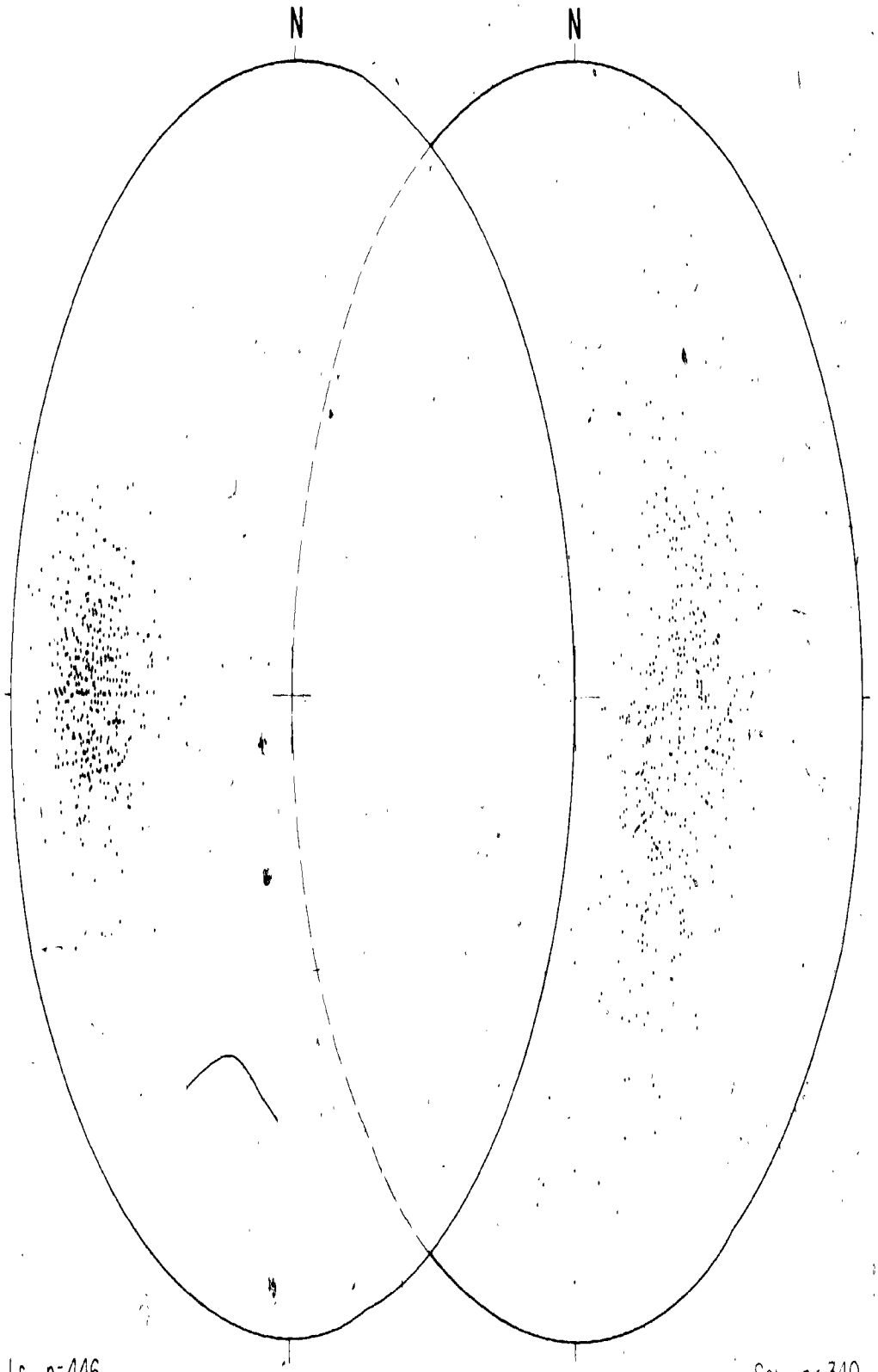

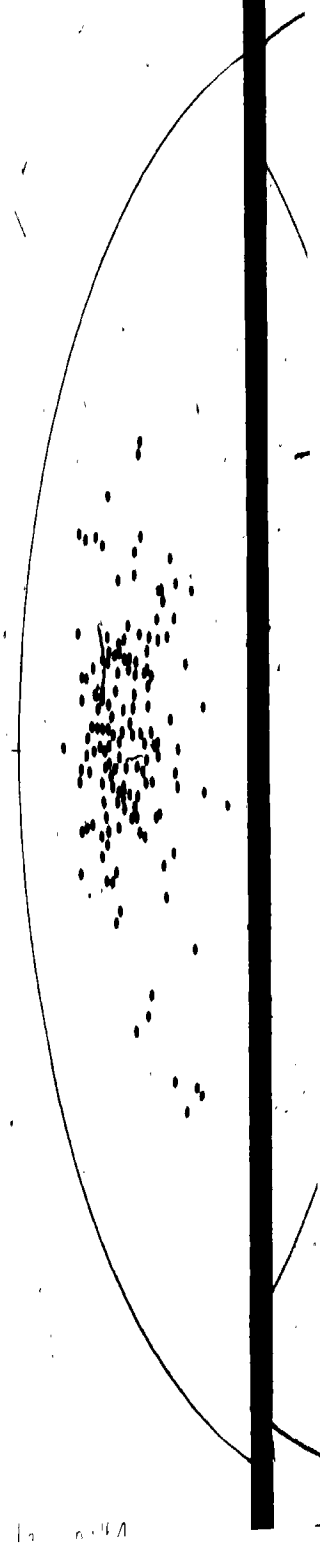

Ls n=446

Sol n=340

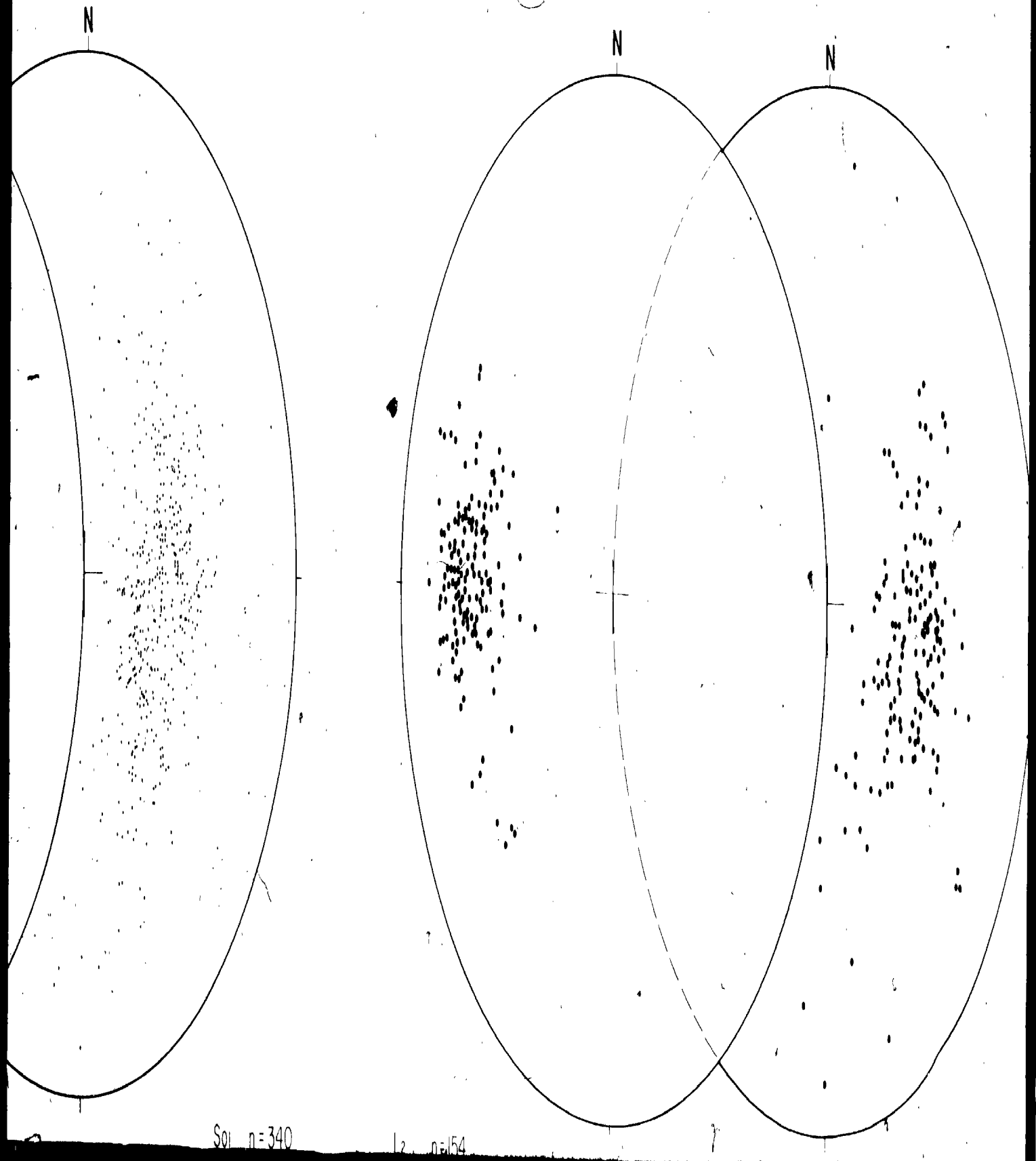
N
N
N
Soi n=340
n=154

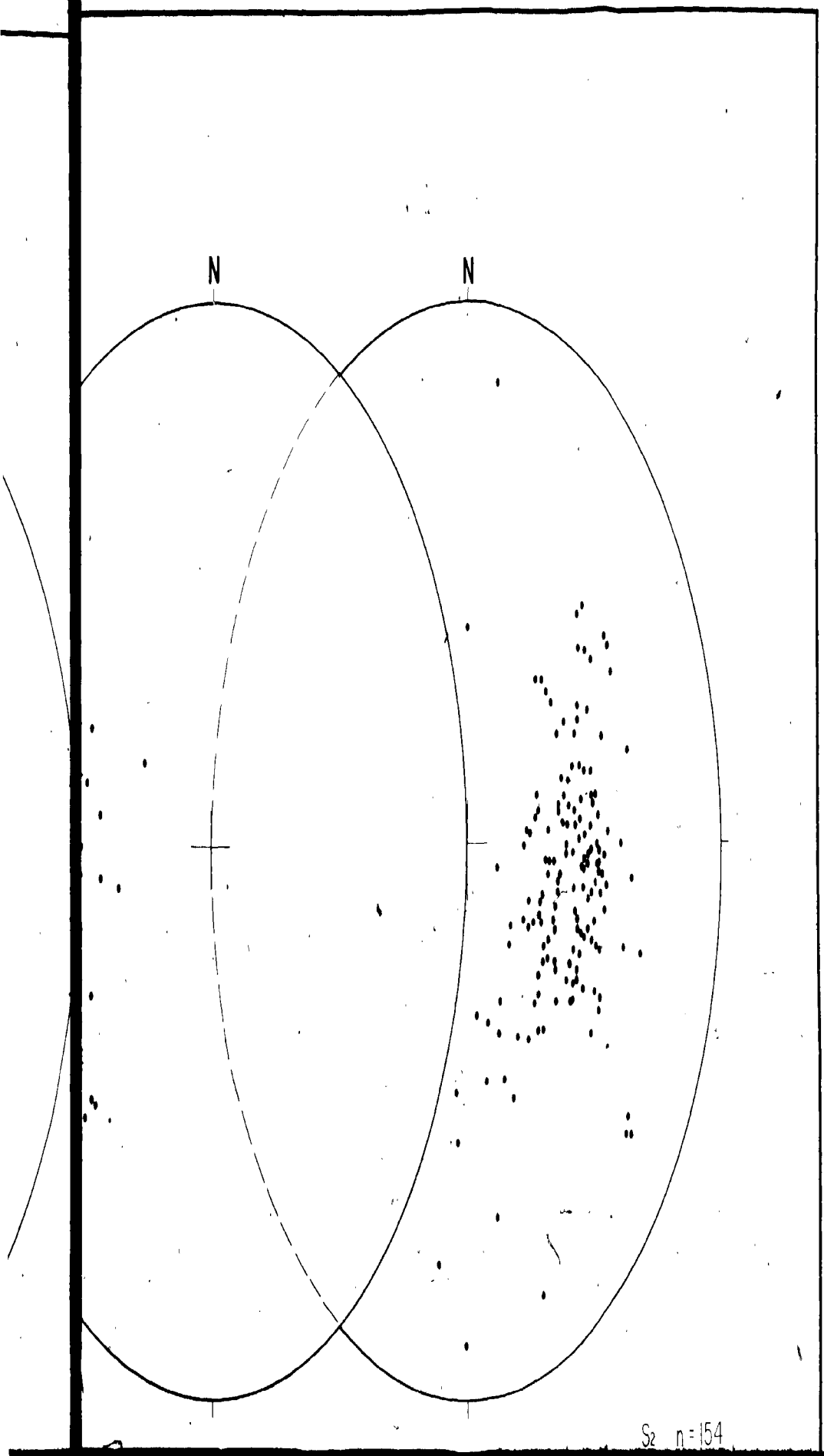

FIGURE 7

EQUAL AREA STEREONET COMPILATION OF PLANAR AND LINEAR FABRIC ELEMENT DATA

LEGEND

Lower Plate

S_{01} = compositional layering

L_s = stretching lineation

S_2 = D_2 axial planes

L_2 = D_2 fold axes

♦ = S_{01} average Subarea A

• = S_{01} average Subarea B

■ = S_{01} average Subarea C

▪ = S_{01} average easterly striking S_{01} from Subarea C

□ = S_{01} average Subarea D

L_s = stretching lineation

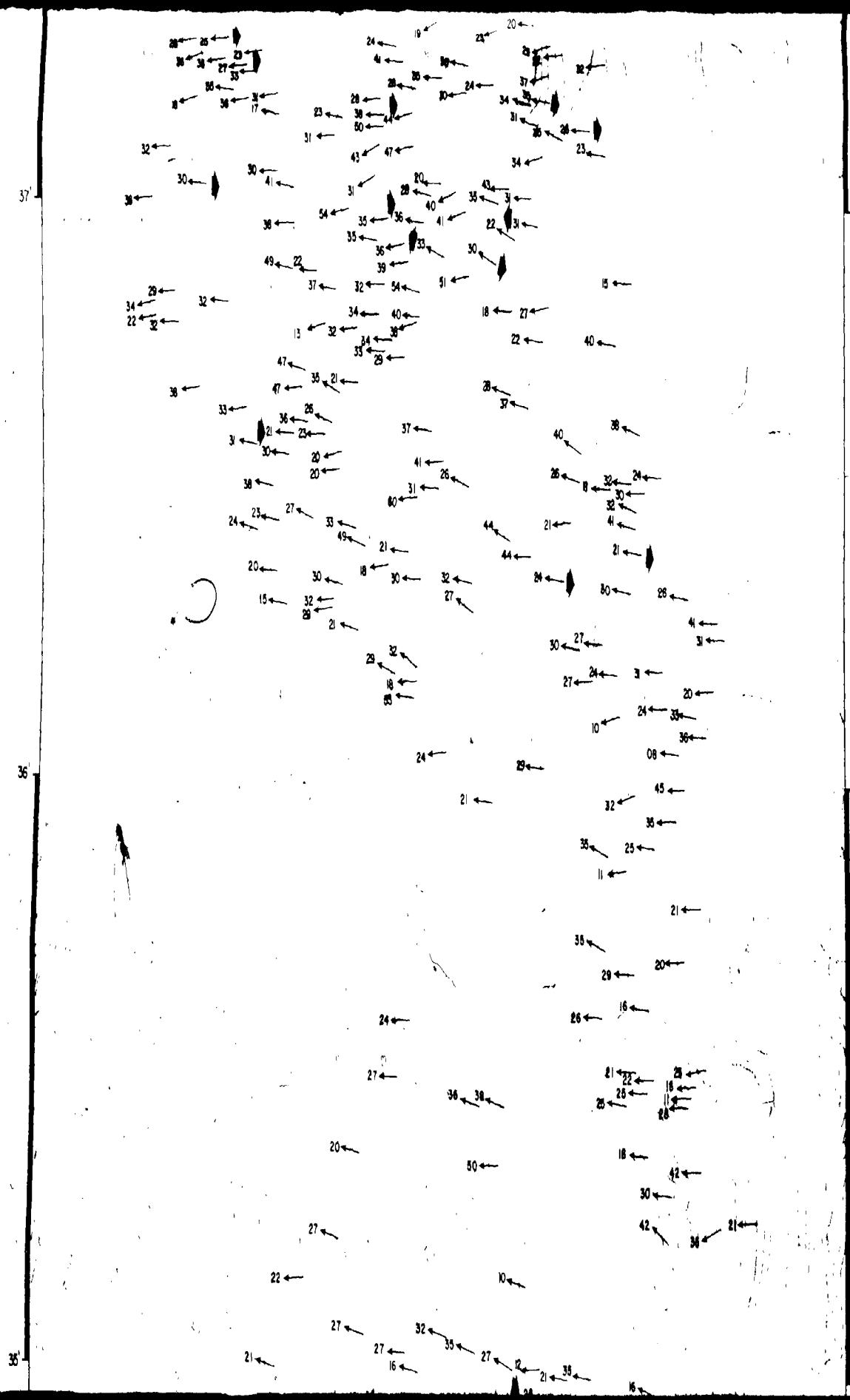

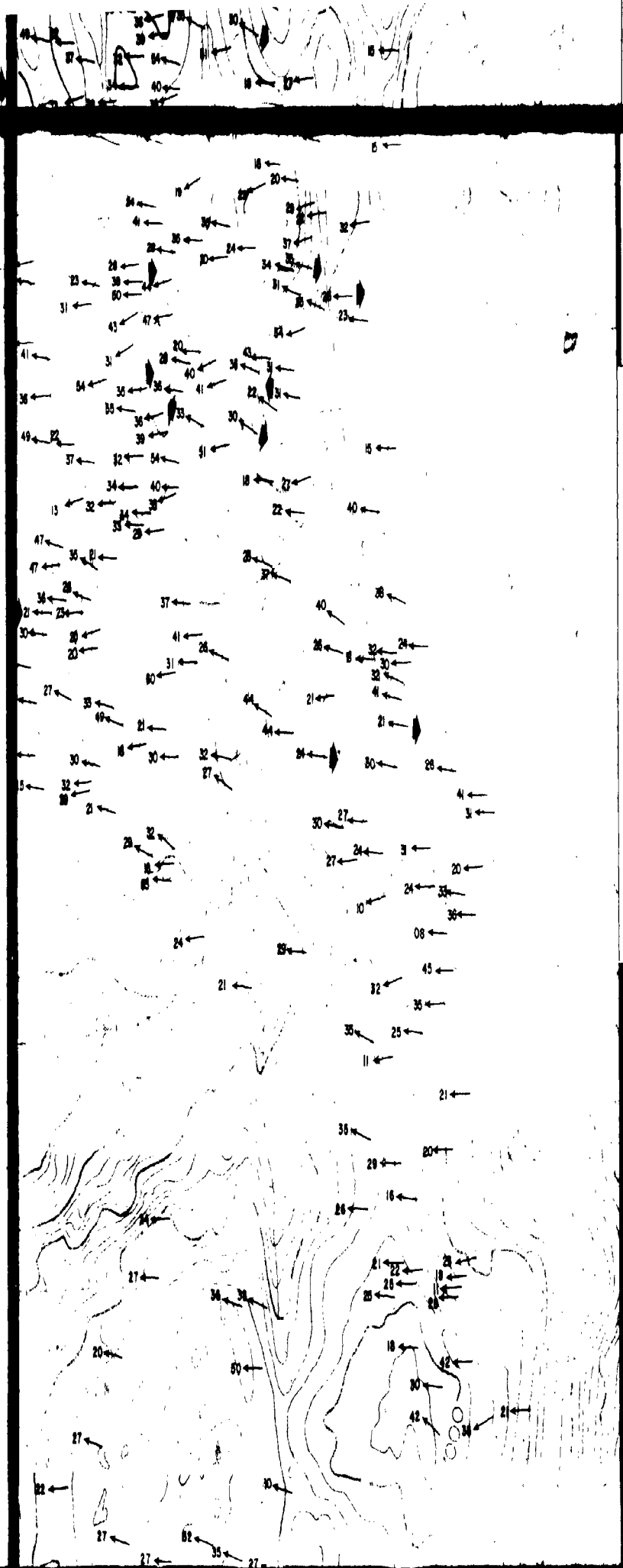

sense of shear:
motion direction of the upper member in the shear couple

LEGEND

27 ← trend and plunge of mineral stretching lineation

sense of shear:
motion direction of the upper member in the shear couple

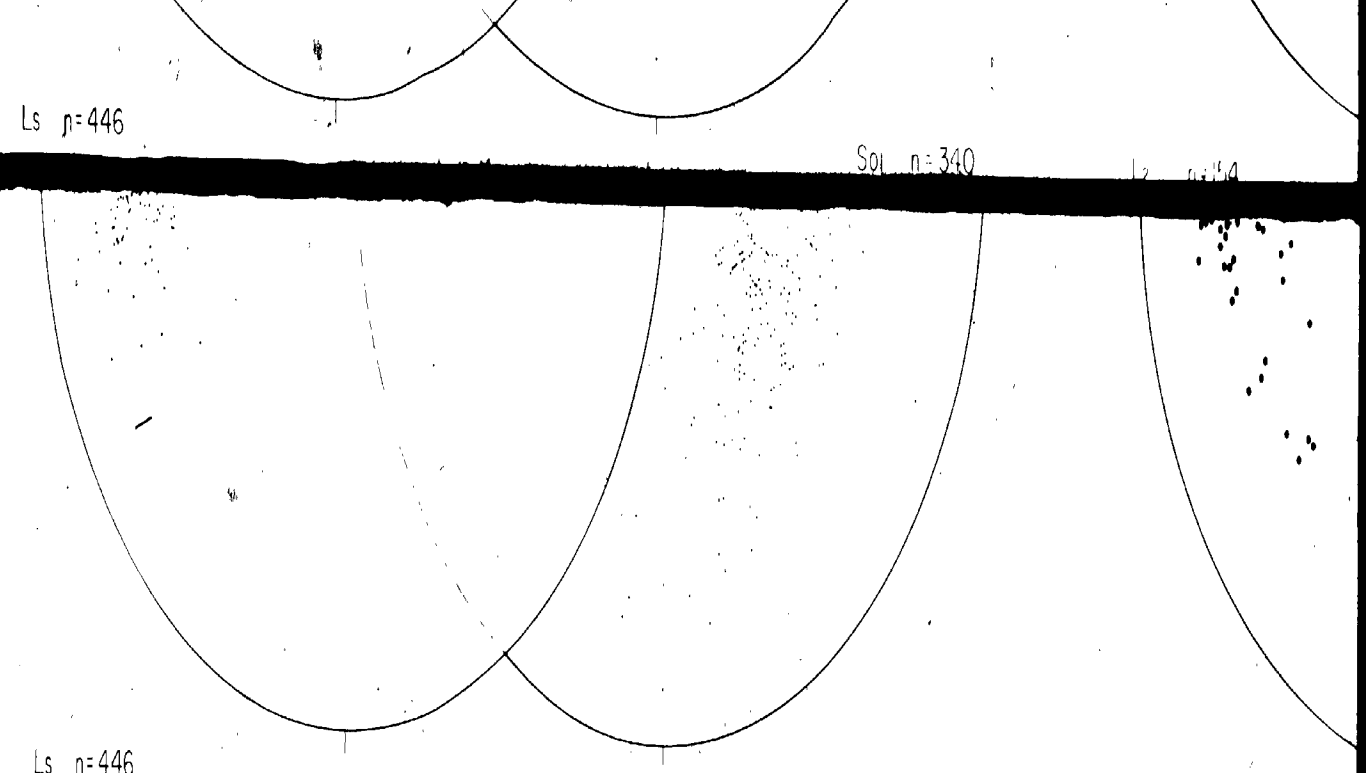
Ls n=446
Soi n=340
L2 n=154

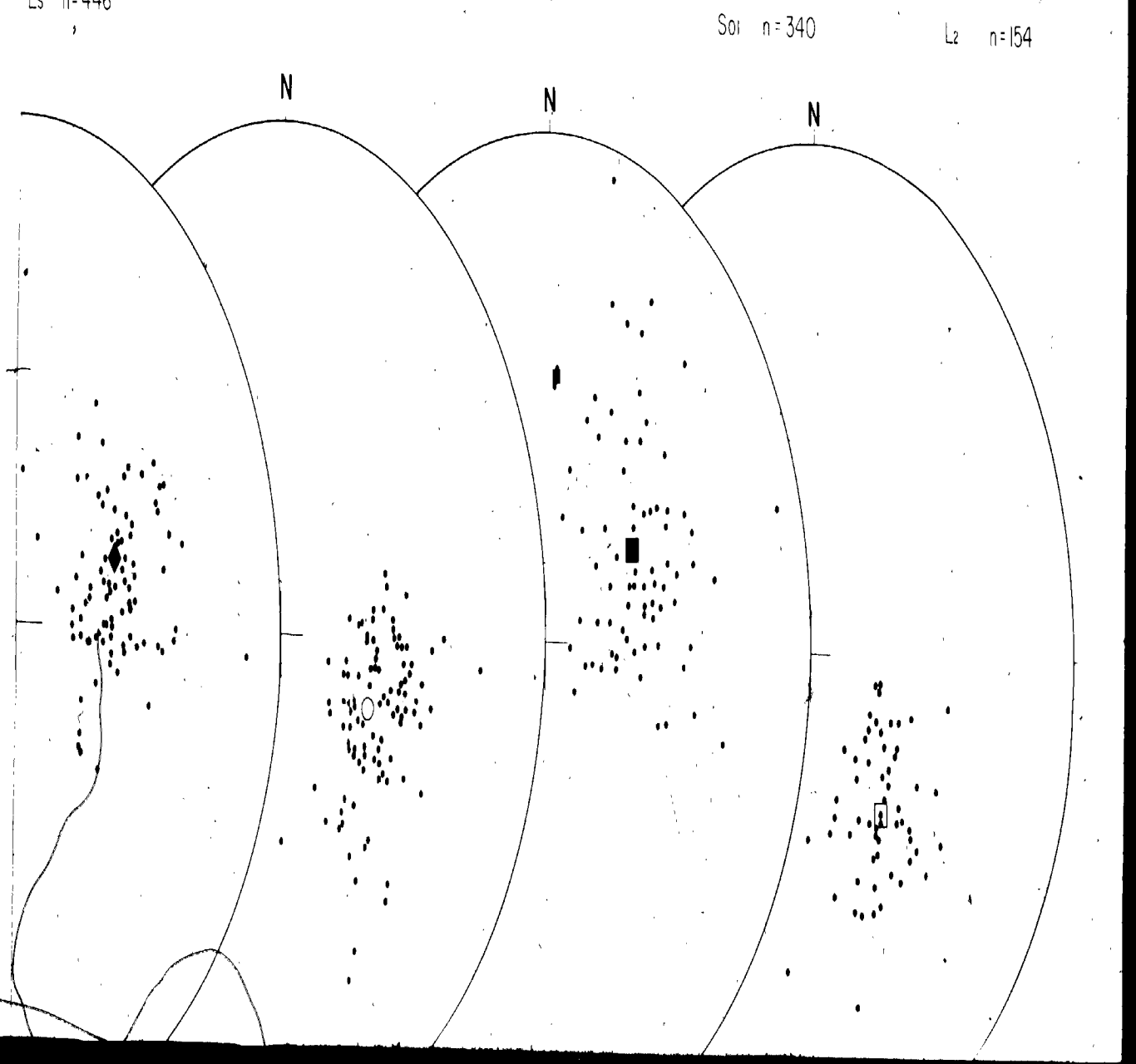
Ls n=446
Soi n=340
L2 n=154
N
N
N
N

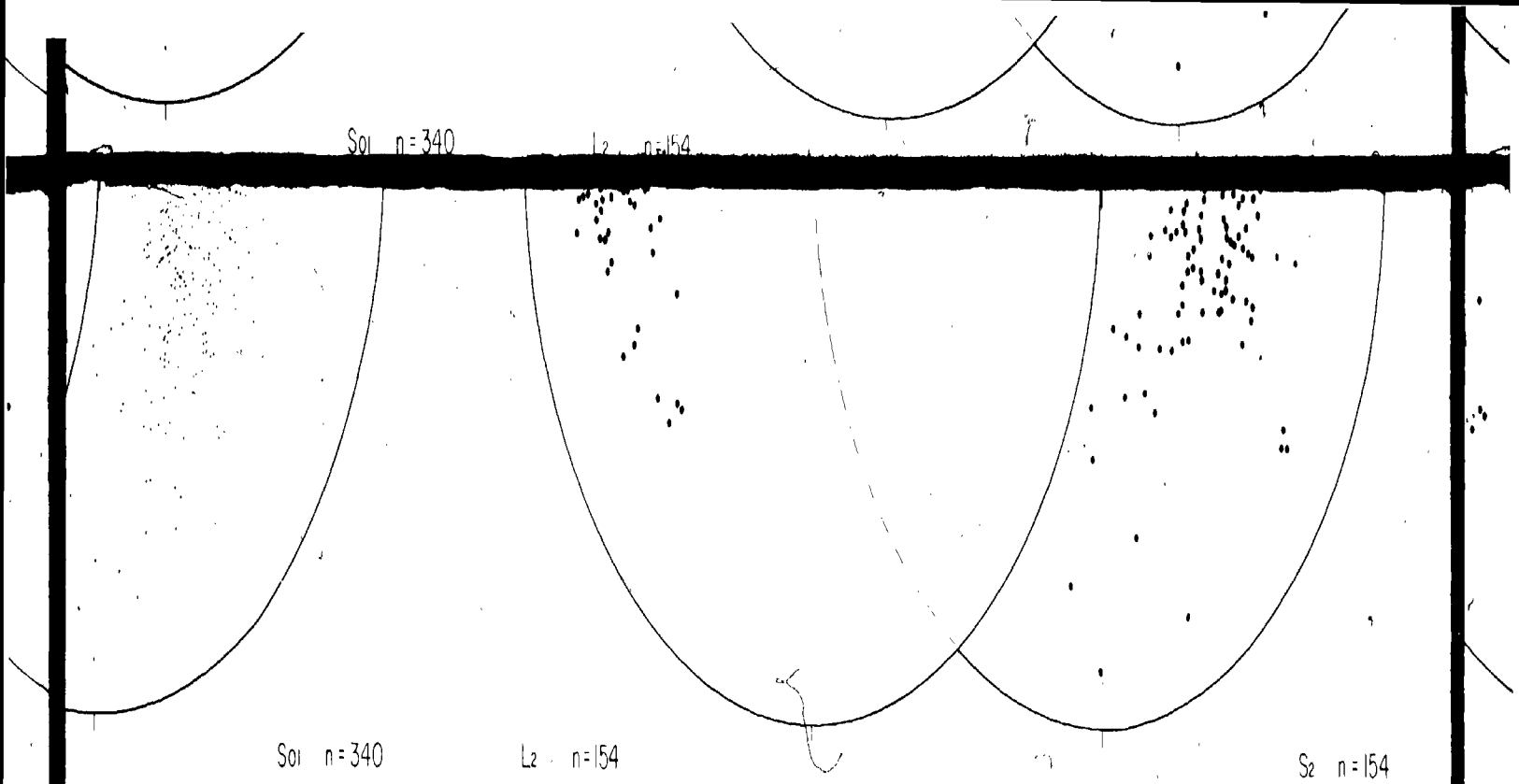
So1 n=340
L2 n=154
So1 n=340
L2 n=154
S2 n=154


N
N

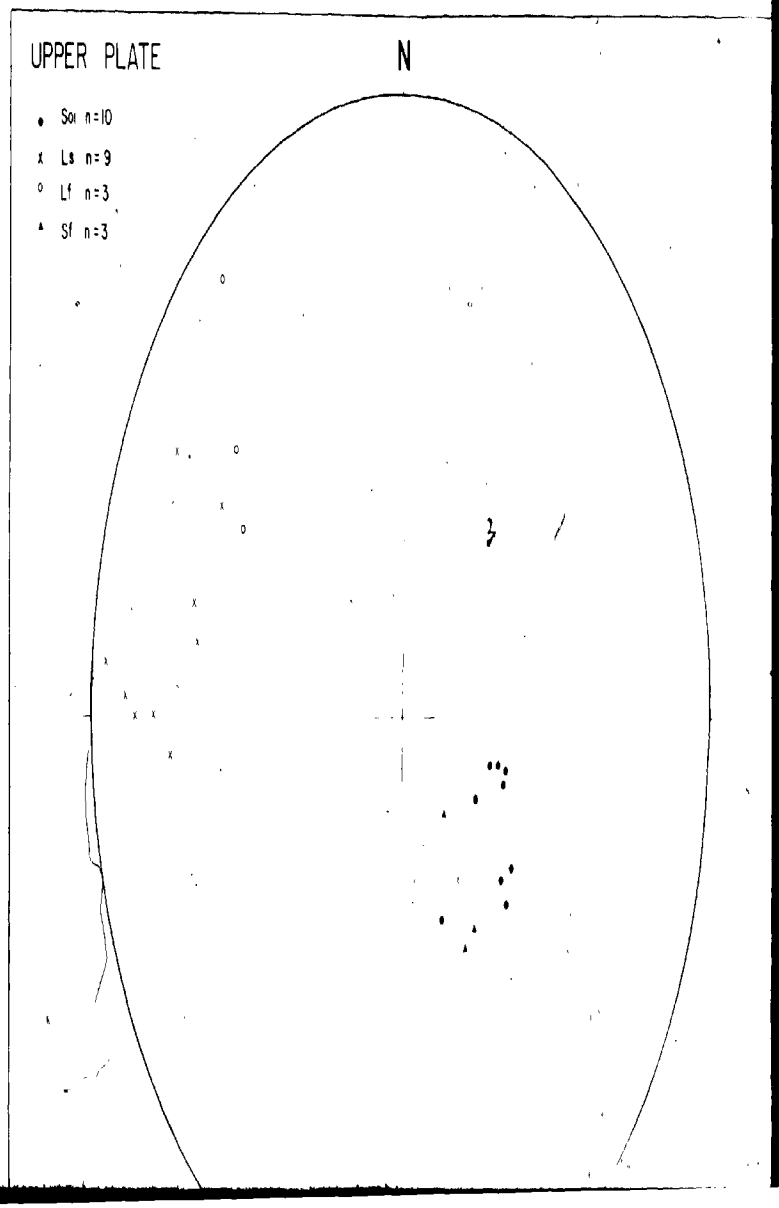
UPPER PLATE
N
So1 n=10
Ls n=9
Lf n=3
Sf n=3

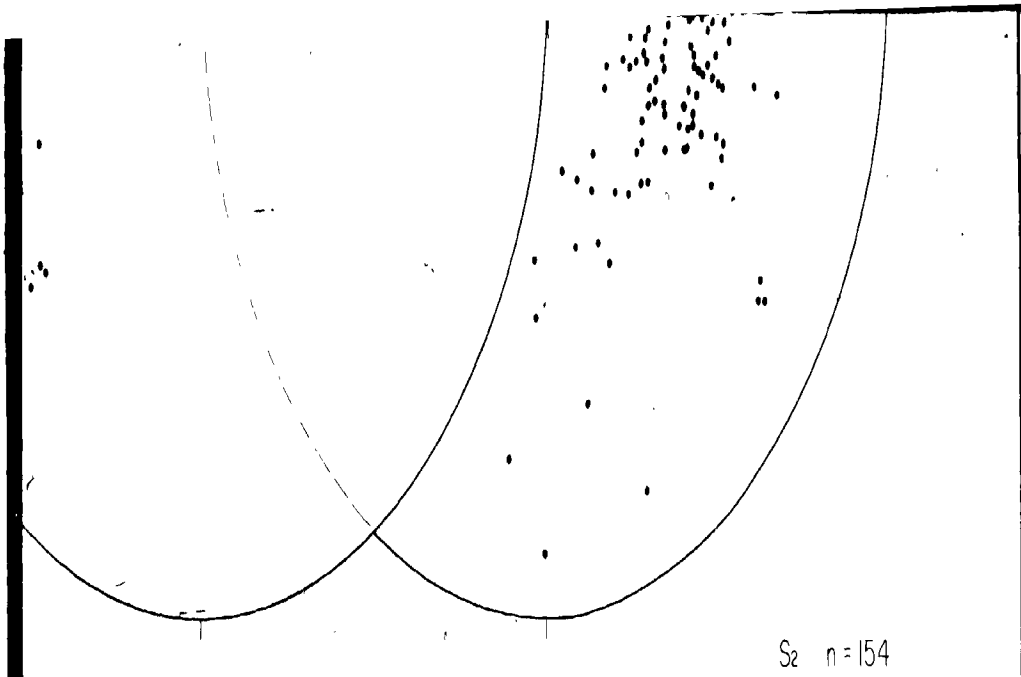

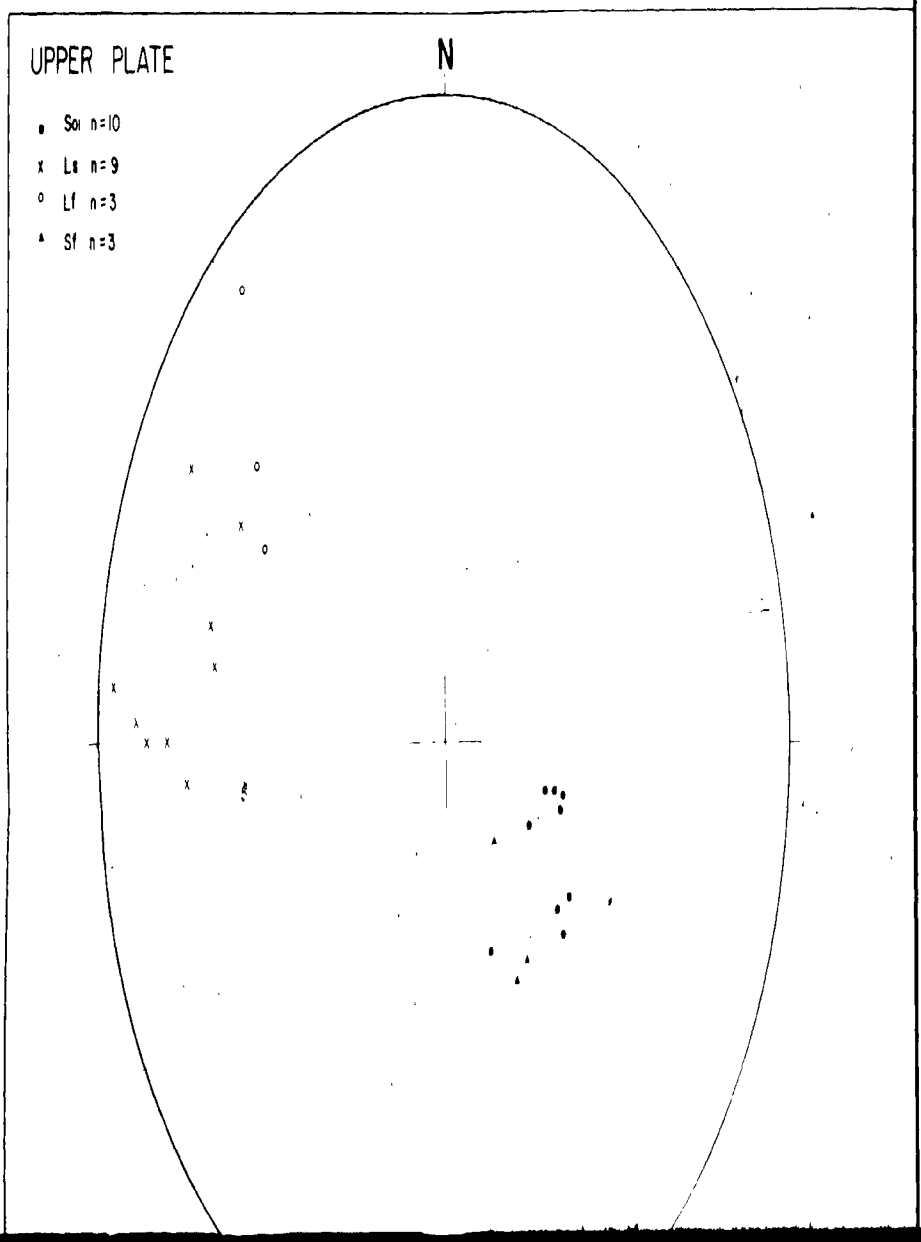

Ls = stretching lineation

S_2 = D_2 axial planes

L_2 = D_2 fold axes

♦ = S_{01} average Subarea A

• = S_{01} average Subarea B

■ = S_{01} average Subarea C

▪ = S_{01} average easterly striking S_{01} from Subarea C

□ = S_{01} average Subarea D

Upper Plate

So = compositional layering

Ls = stretching lineation

Lf = fold axes

Sf = axial plane

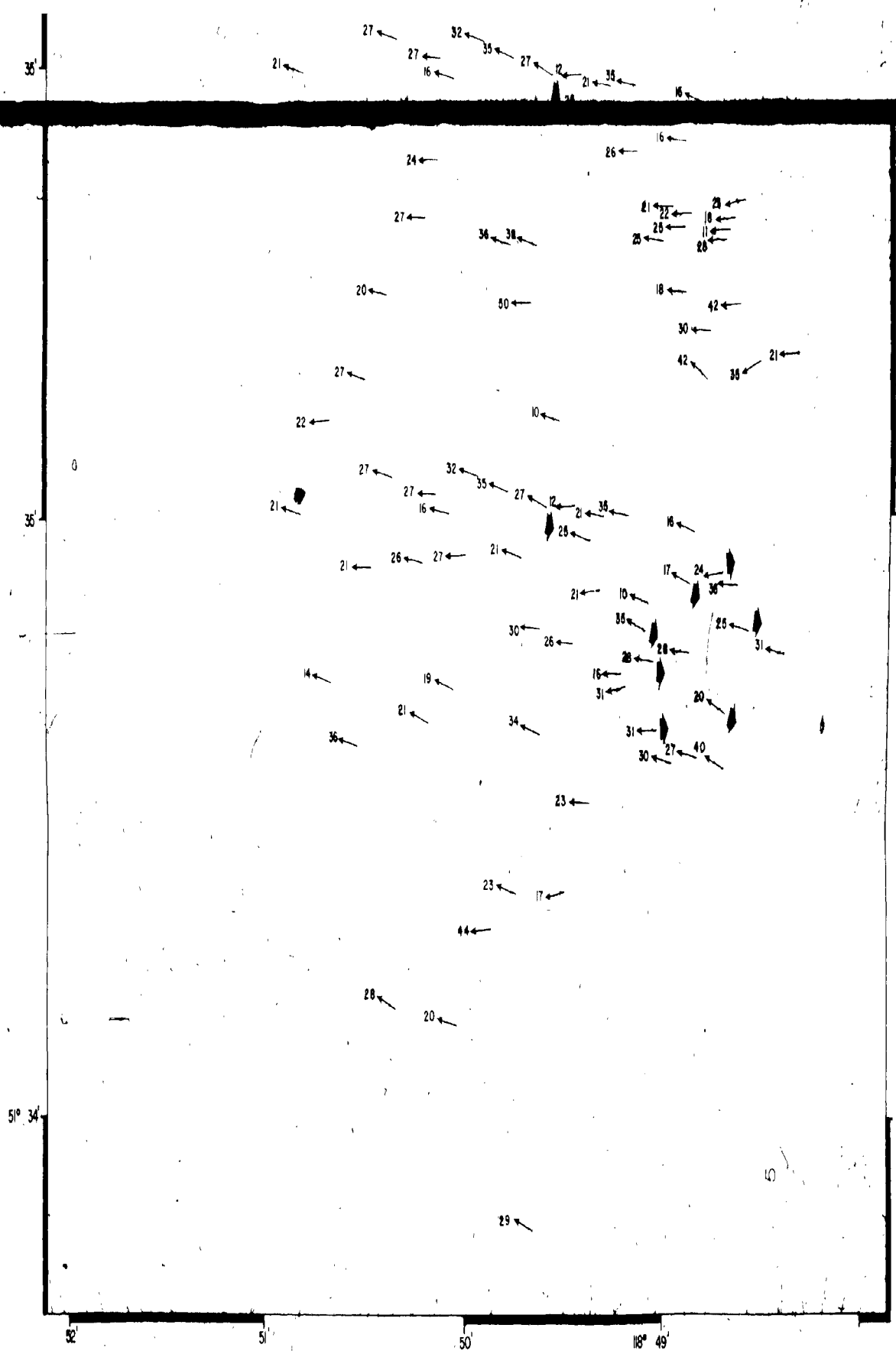

RS/DM 1986

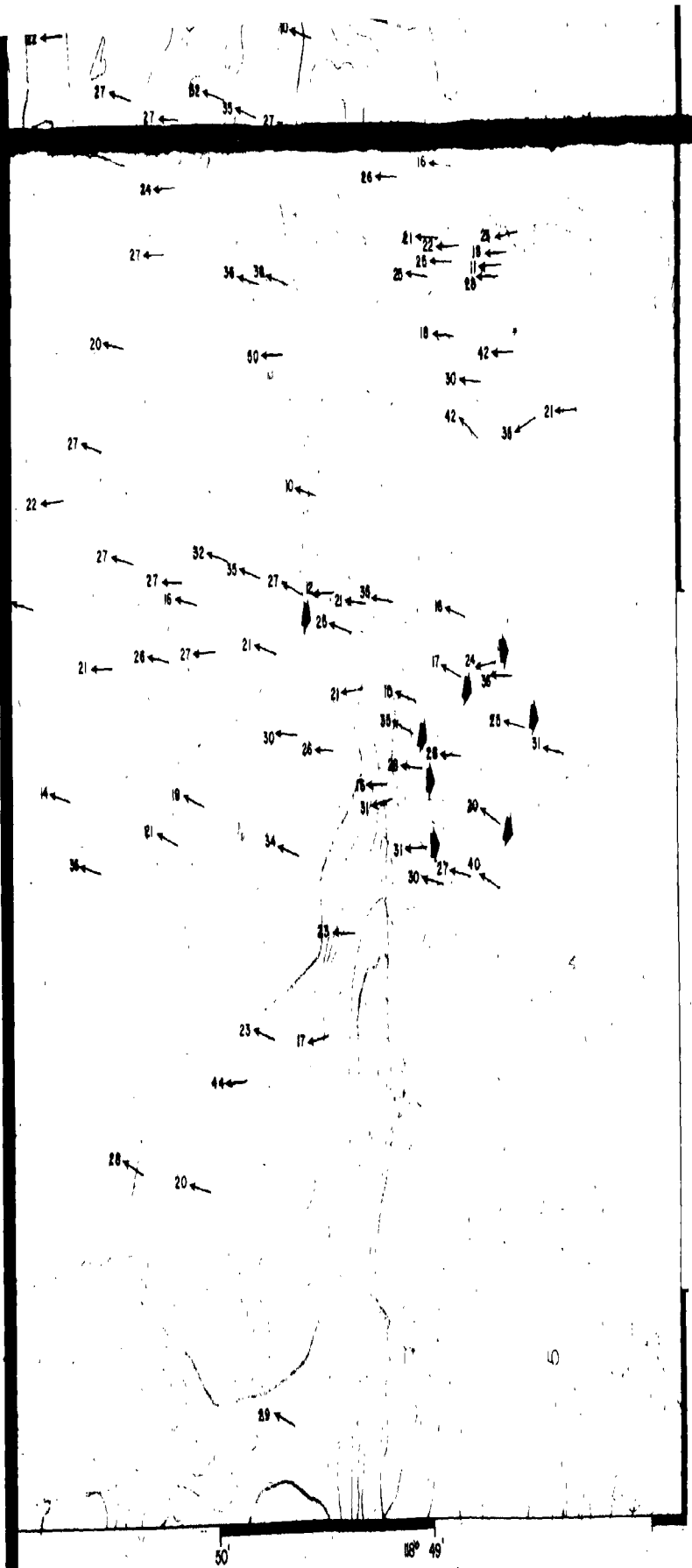

RS/DM 1986

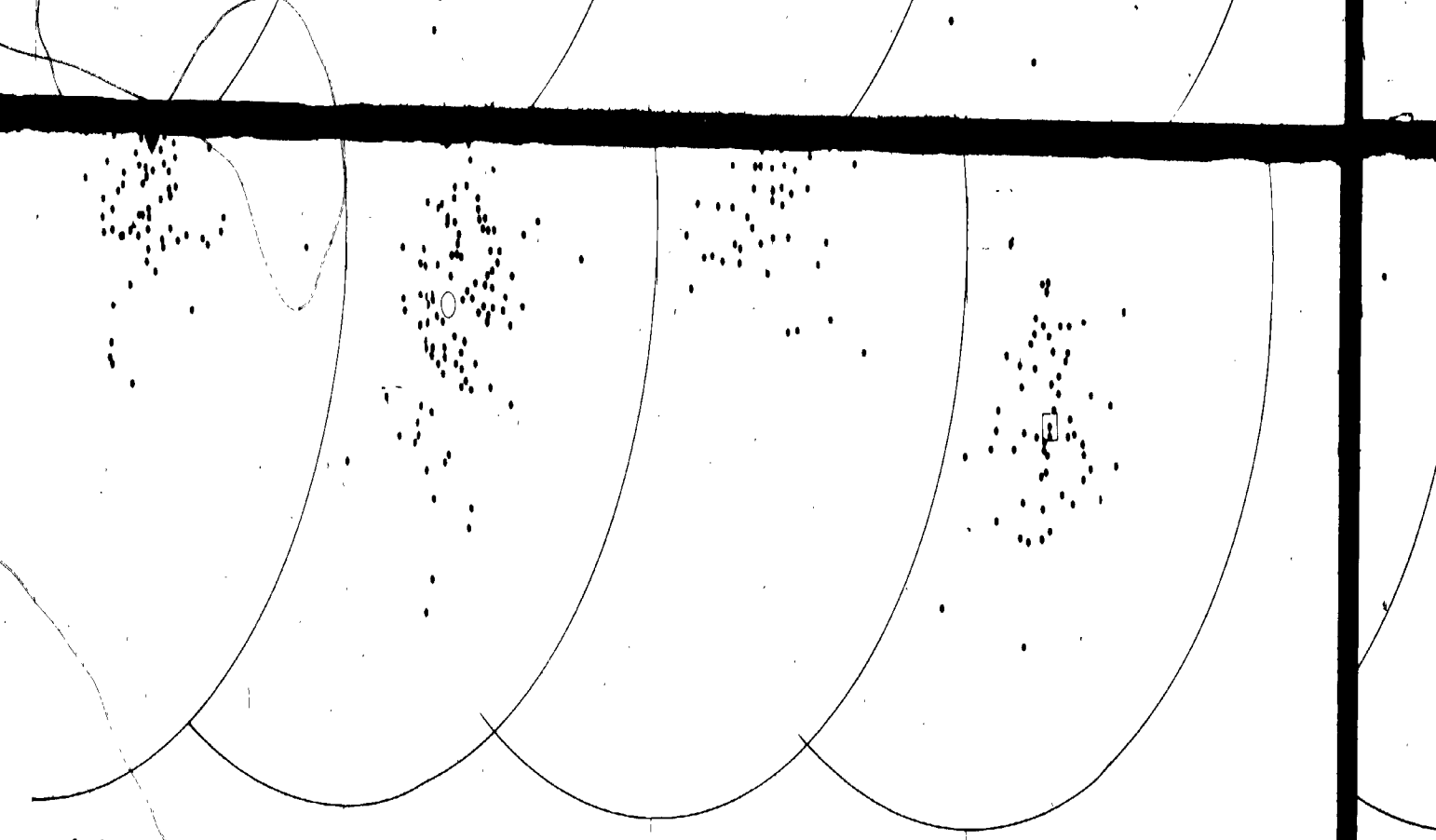

Soi Subarea A
n=83

Soi Subarea B
n=99

Soi Subarea C
n=80

Soi Subarea D
n=55

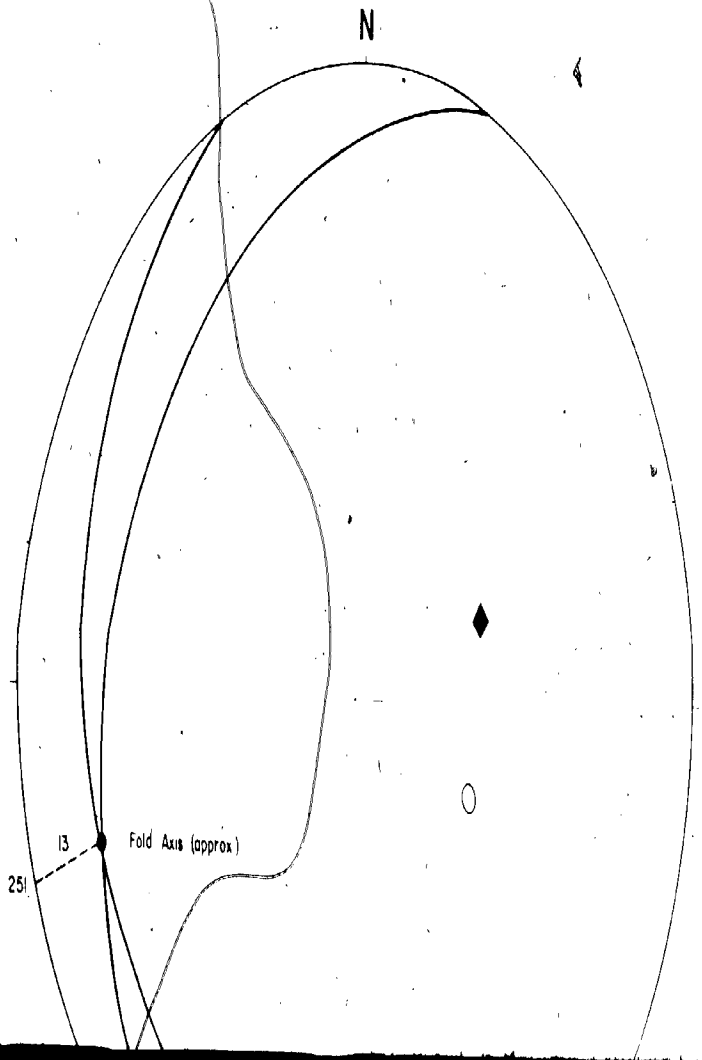

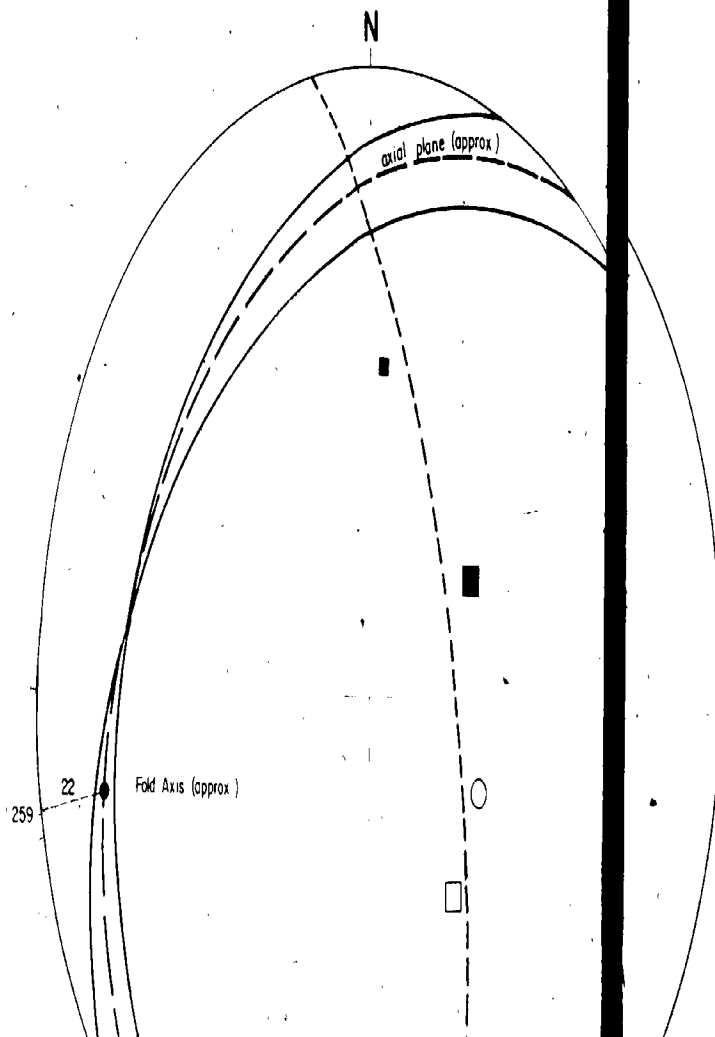

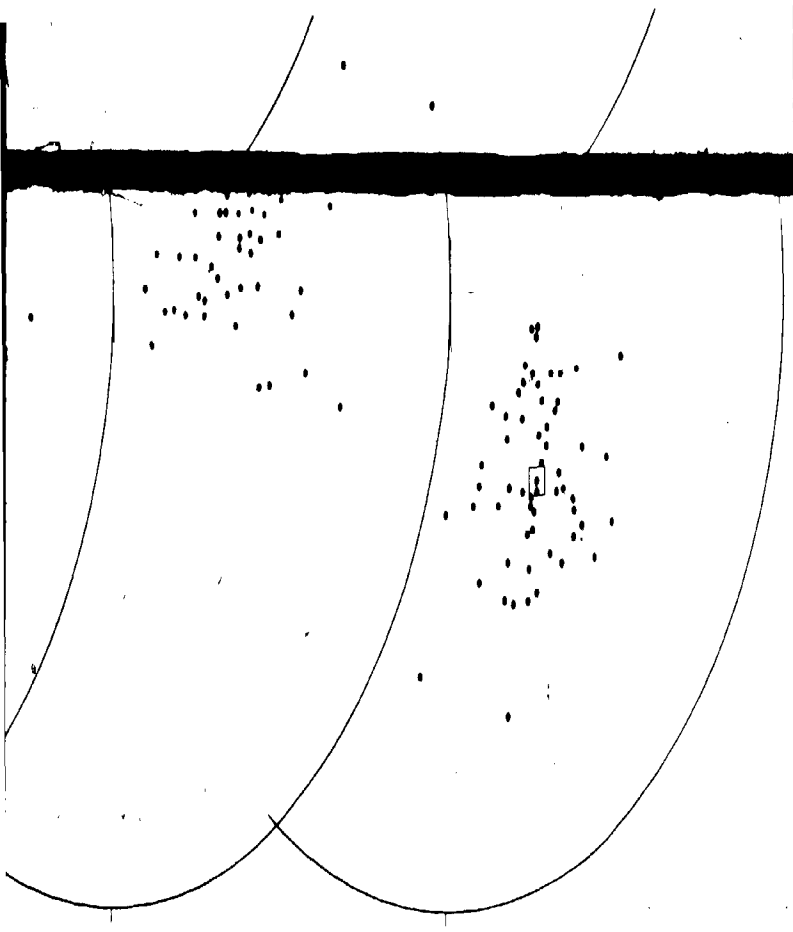

Soi Subarea C
n=80

Soi Subarea D
n=55

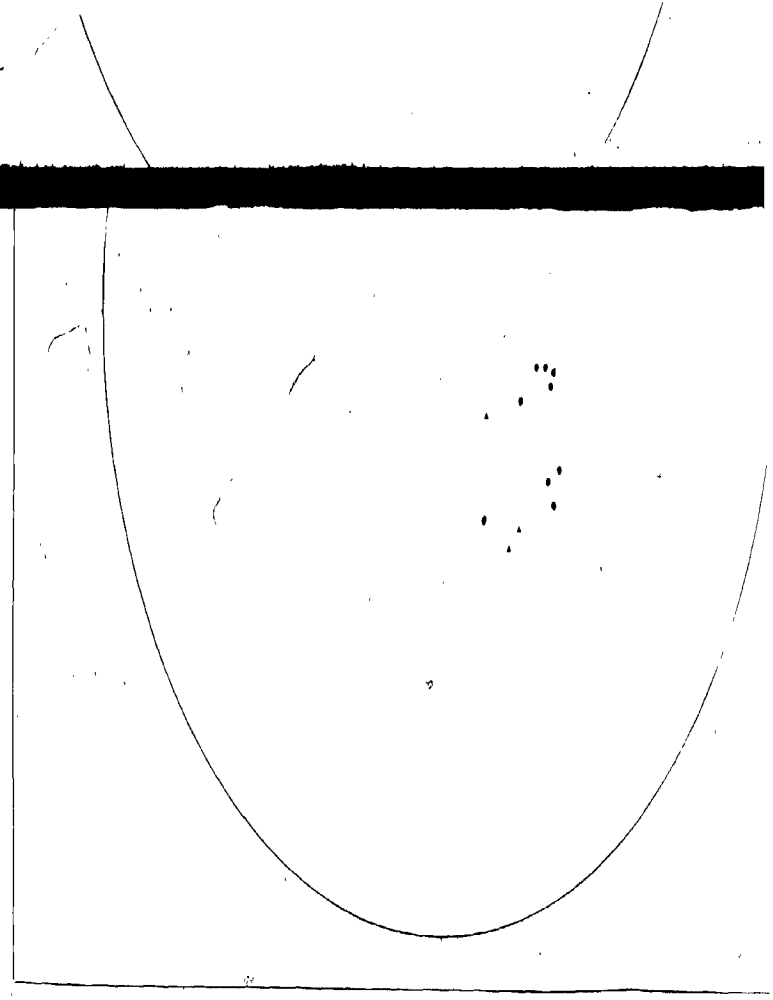

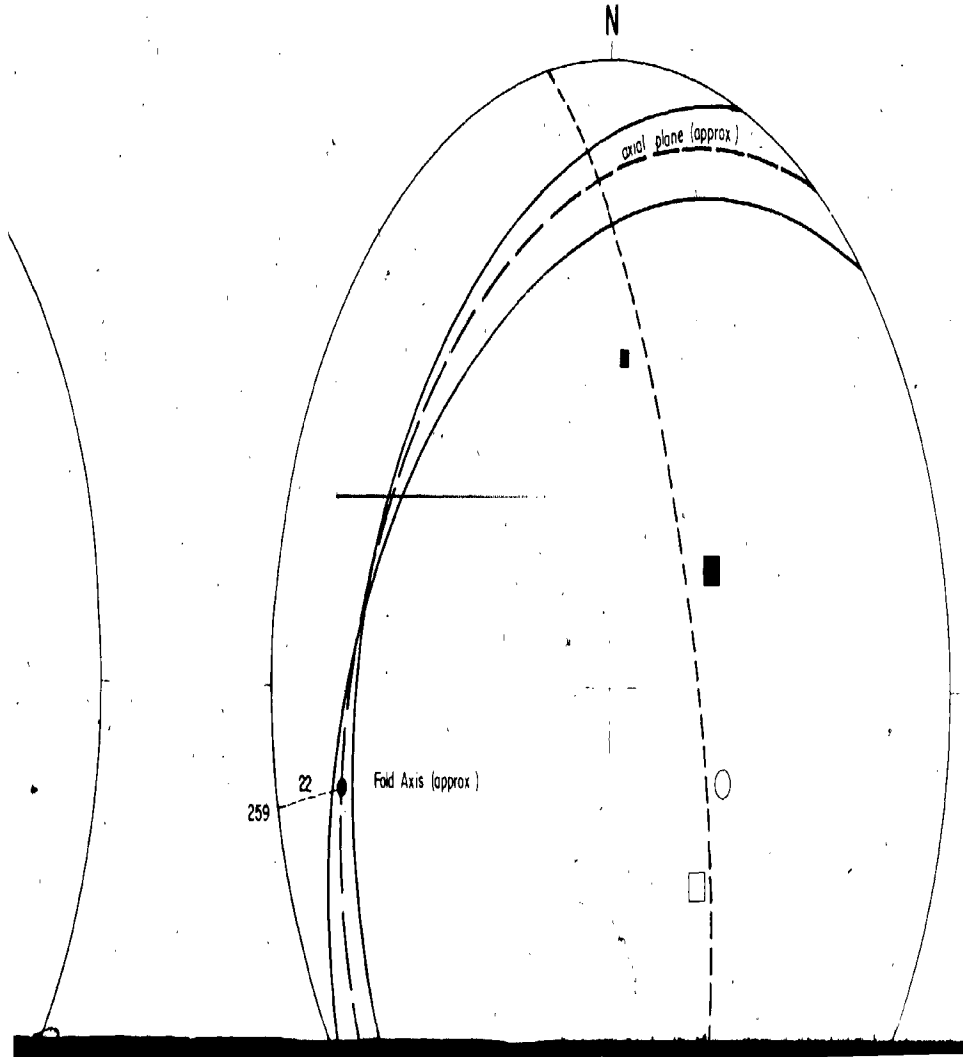

Subarea Location Map

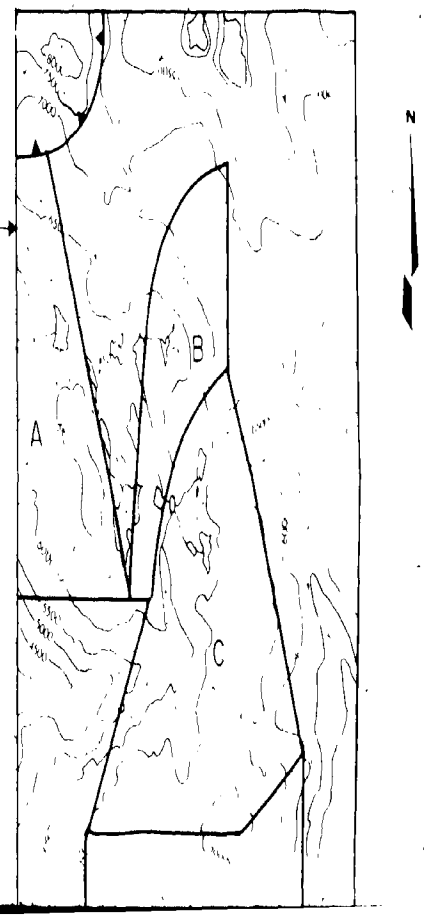

Subarea Location Map

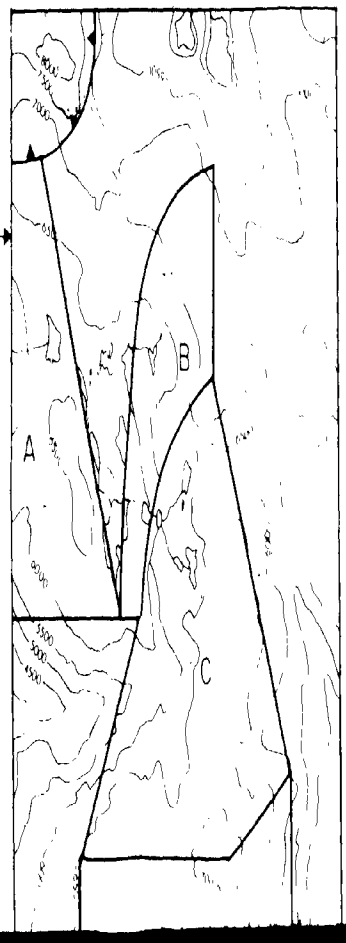

Soil Subarea A
n=83

Soil Subarea B
n=99

Soil Subarea C
n=80

Soil Subarea D
n=55

Soil Subar
n=80

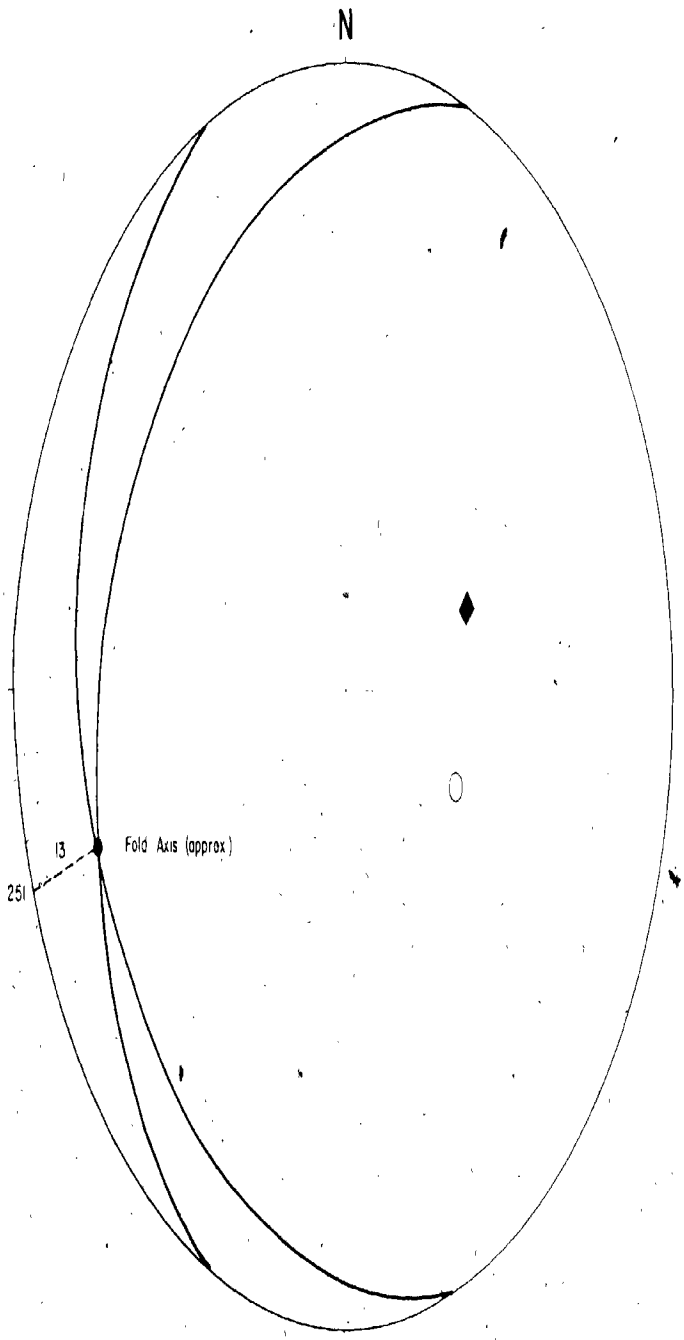

Sibley Creek Anticline

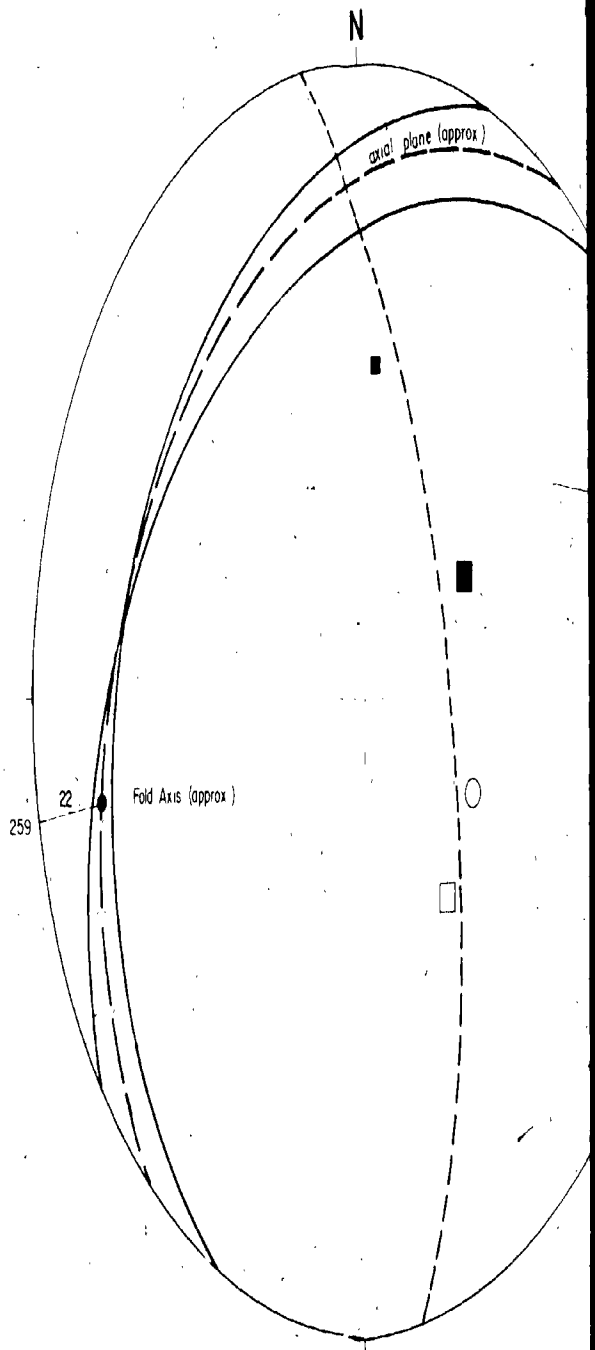

Sibley Creek Syncline

Soi Subarea C
n=80

Soi Subarea D
n=55

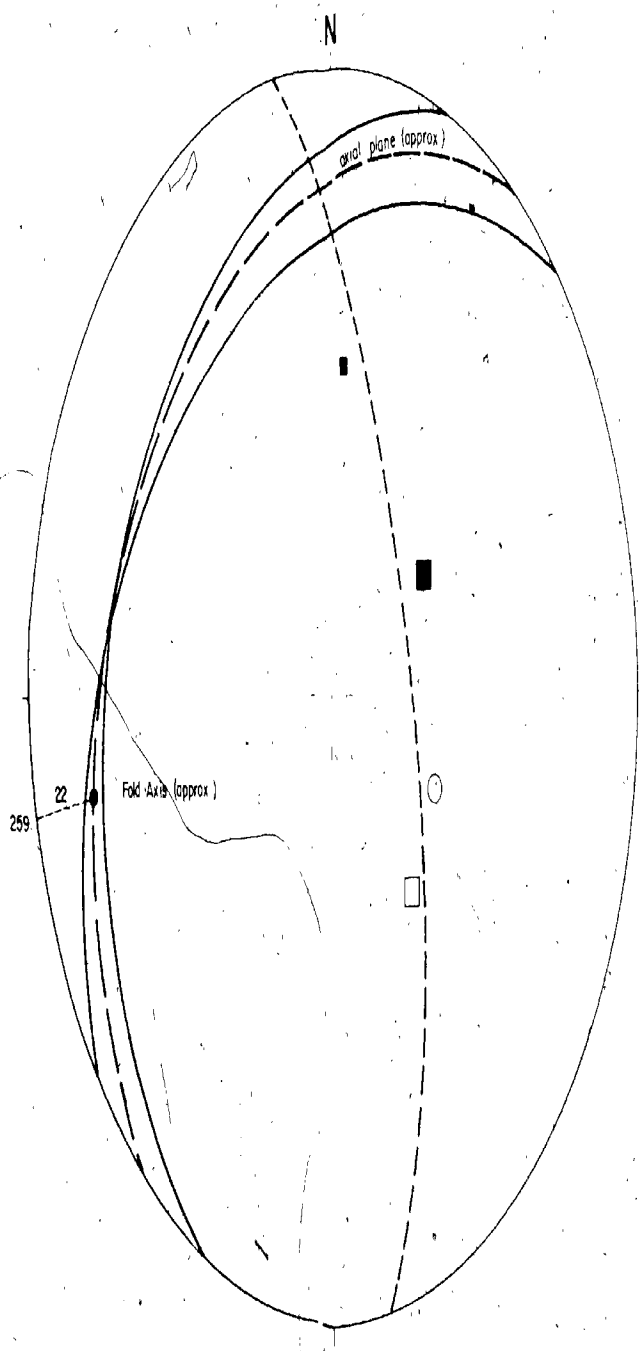

Sibley Creek Syncline

Subarea Location Map

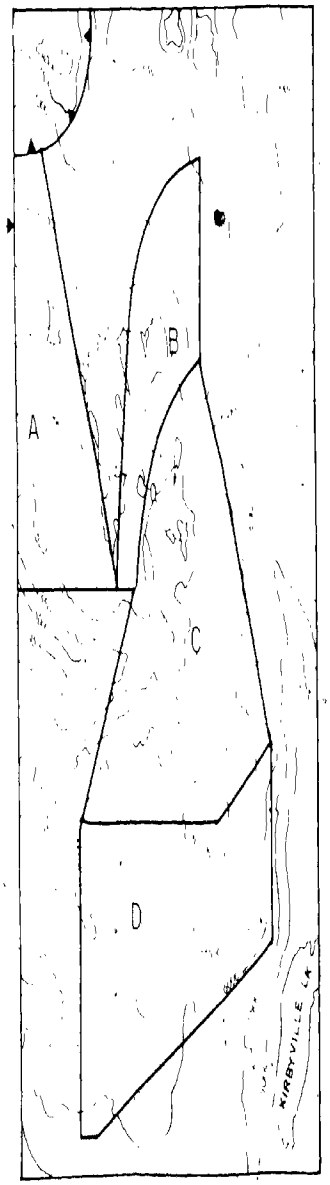

RS/DM 1986

Subarea Location Map

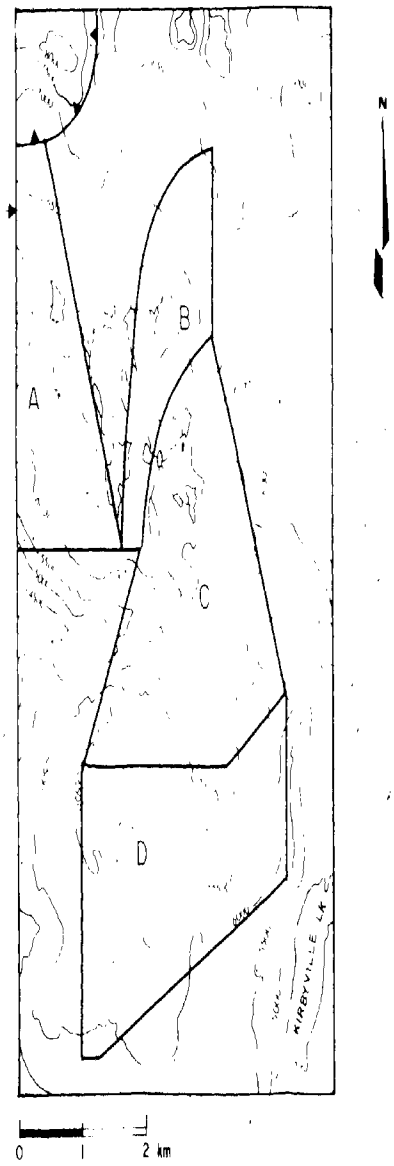

RS/DM 1986

RS/DM 1986

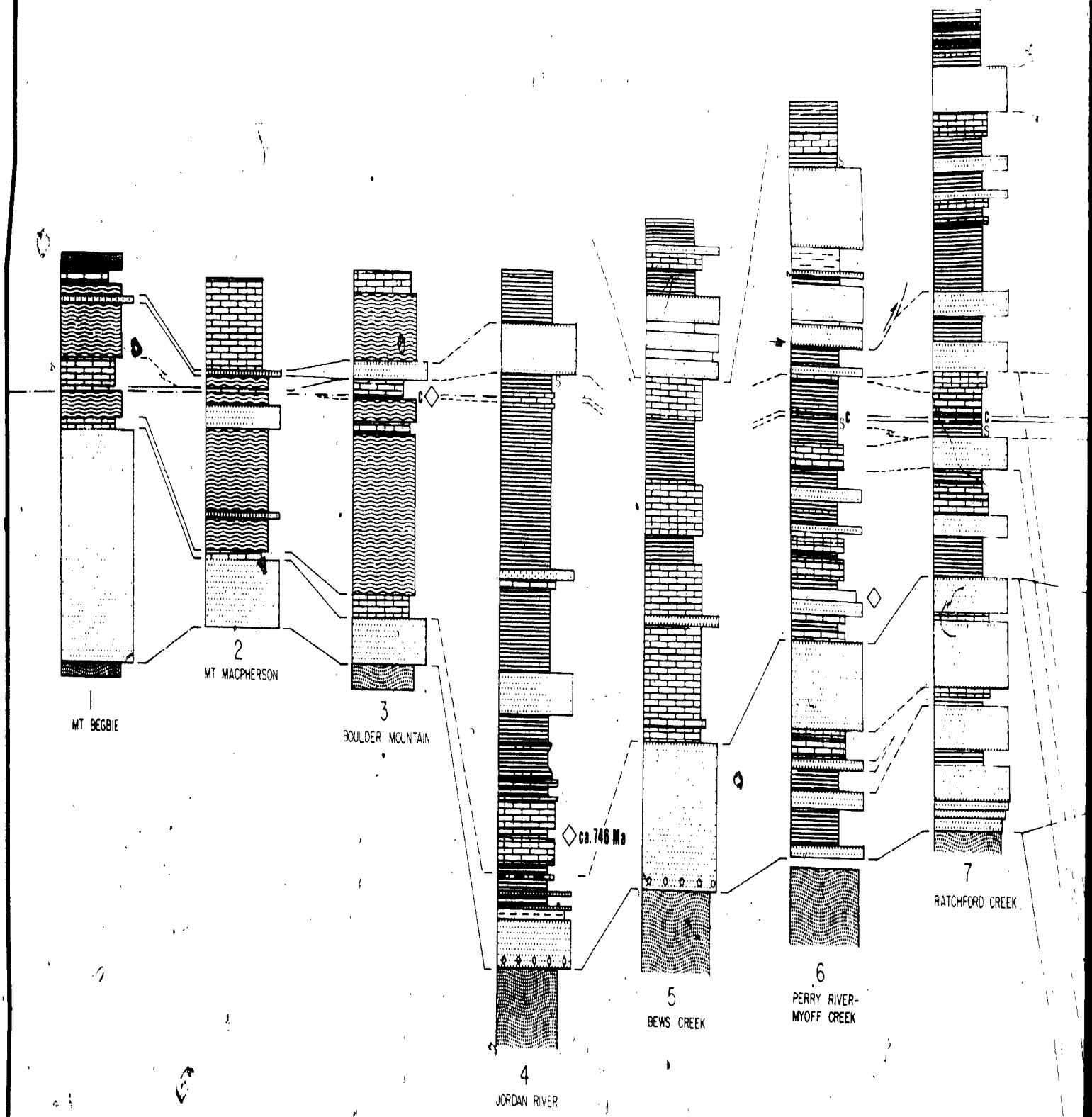

LEGEND

◇ NEPHELINE SYENITE & SYENITE GNEISSES

LOCATION MAP

FIGURE 5

CORRELATION OF MANTLING GNEISS SEQUENCES ABOUT FRENCHMAN CAP DOME AND THOR-ODIN DOMES

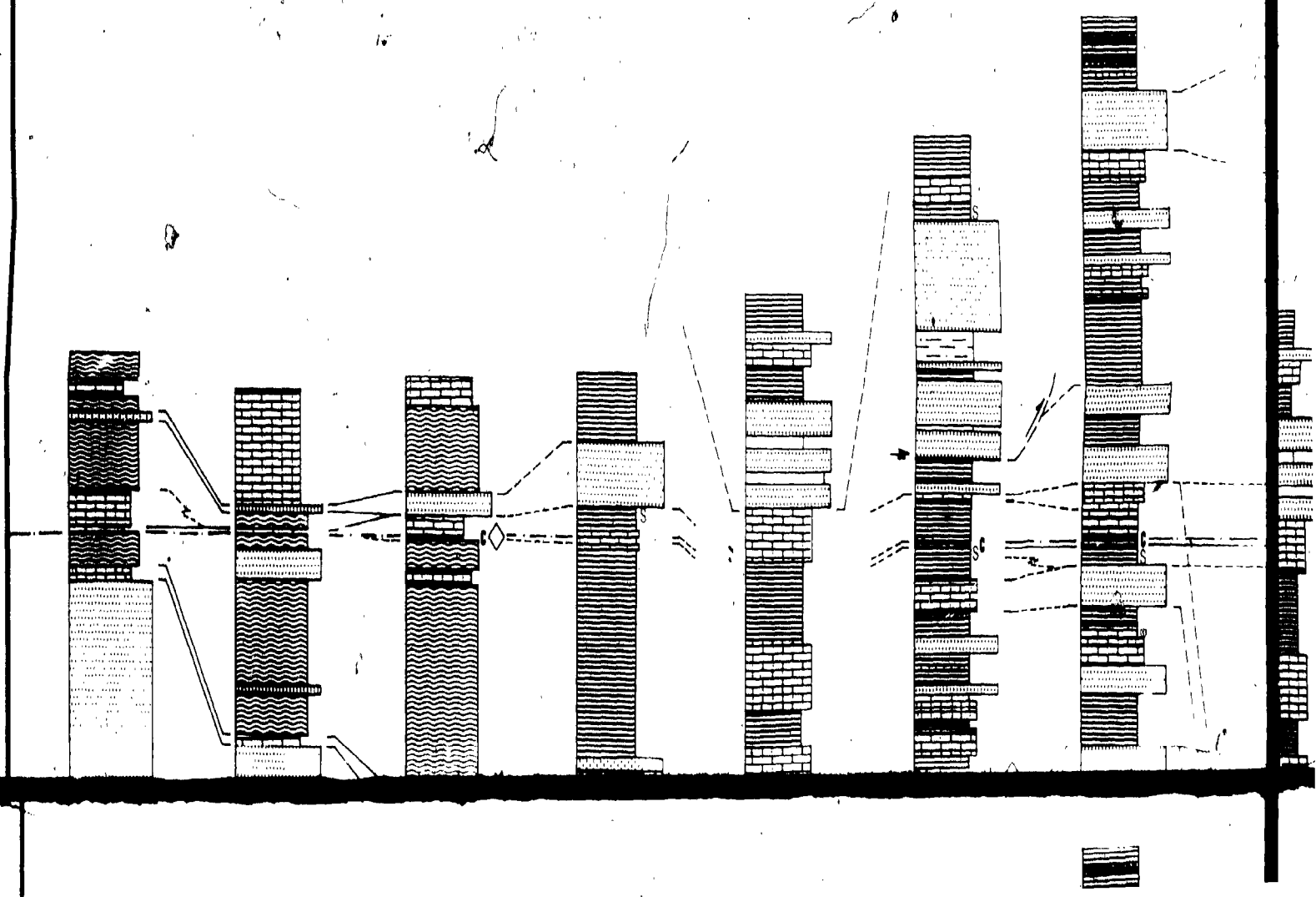

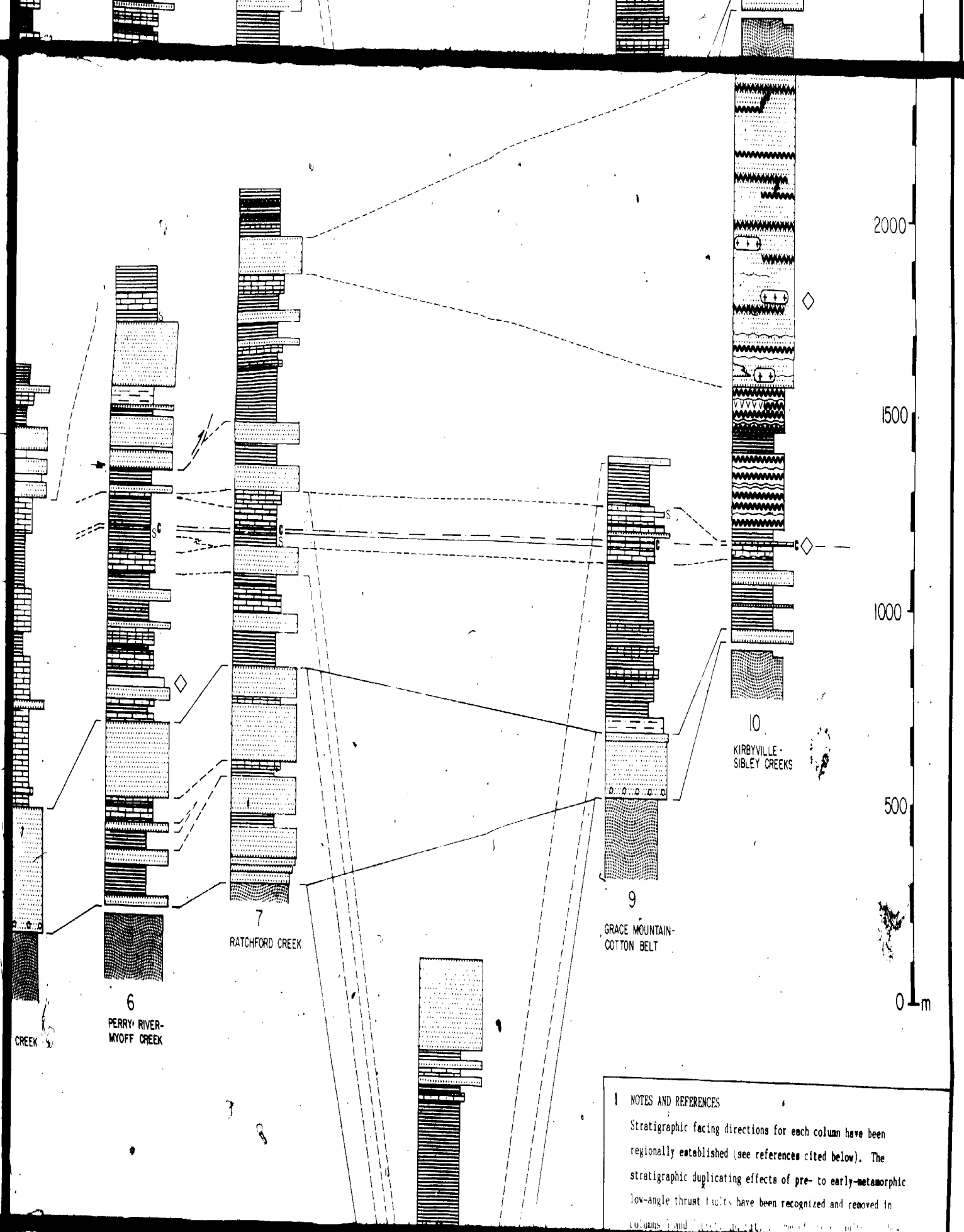

1 NOTES AND REFERENCES

Stratigraphic facing directions for each column have been regionally established (see references cited below). The stratigraphic duplicating effects of pre- to early-metamorphic low-angle thrust faults have been recognized and removed in columns 1 and [illegible]

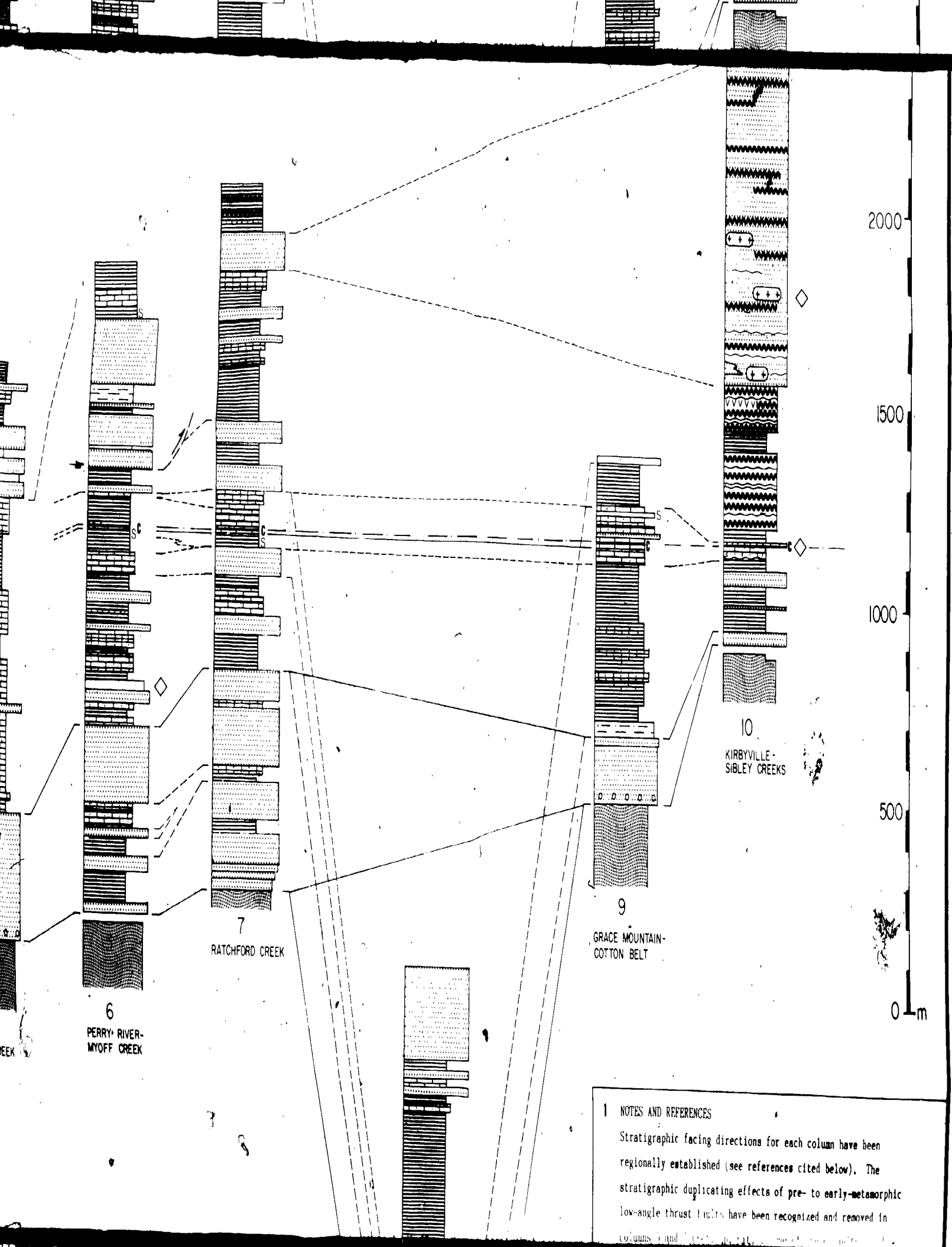

1 NOTES AND REFERENCES

Stratigraphic facing directions for each column have been regionally established (see references cited below). The stratigraphic duplicating effects of pre- to early-metamorphic low-angle thrust faults have been recognized and removed in columns [illegible]

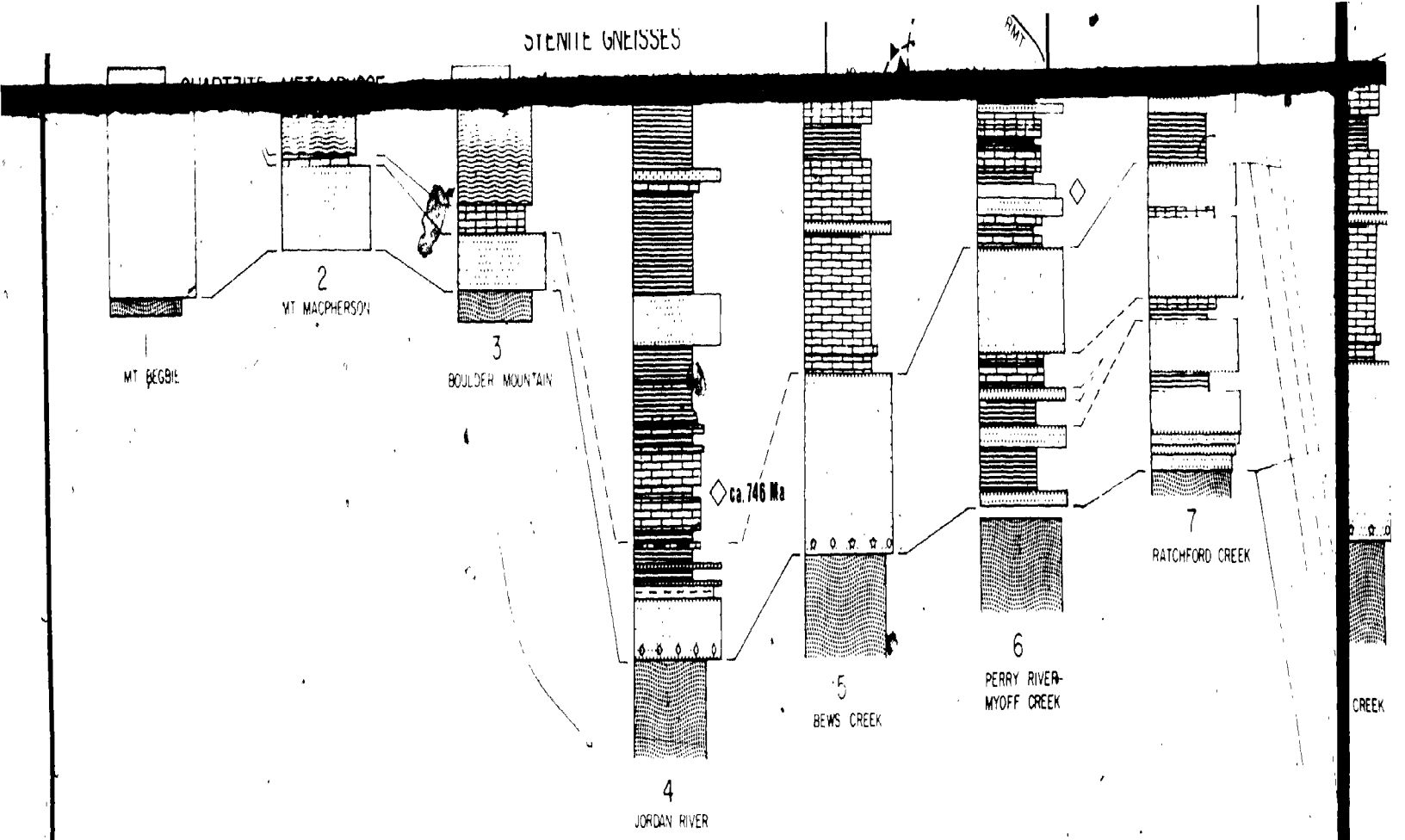

LEGEND

- QUARTZITE, META-ARKOSE METASUBARKOSE
- QUARTZ PEBBLE CONGLOMERATE
- PELITIC SCHIST
- SEMIPELITIC SCHIST
- MARBLE, IMPURE MARBLE
- CALC-SILICATE CALCAREOUS SCHIST
- BIOTITE- & HORNBLENDE-BEARING QUARTZ-FELDSPAR GNEISS
- NEPHELINE SYENITE & SYENITE GNEISSES
- AMPHIBOLITE
- HORNBLENDITE
- VOLCANICLASTIC and/or EPICLASTIC DEPOSIT
- CARBONATITE
- META-ULTRAMAFIC
- SULPHIDE LAYERS
- CORE GNEISSES

LOCATION MAP

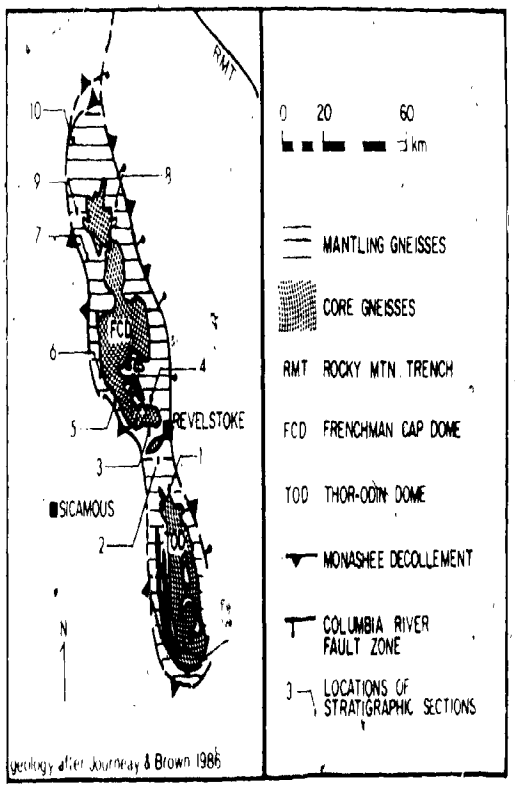

regionally established (see references cited below). The stratigraphic duplicating effects of pre- to early-metamorphic low-angle thrust faults have been recognized and removed in columns 5 and [illegible]

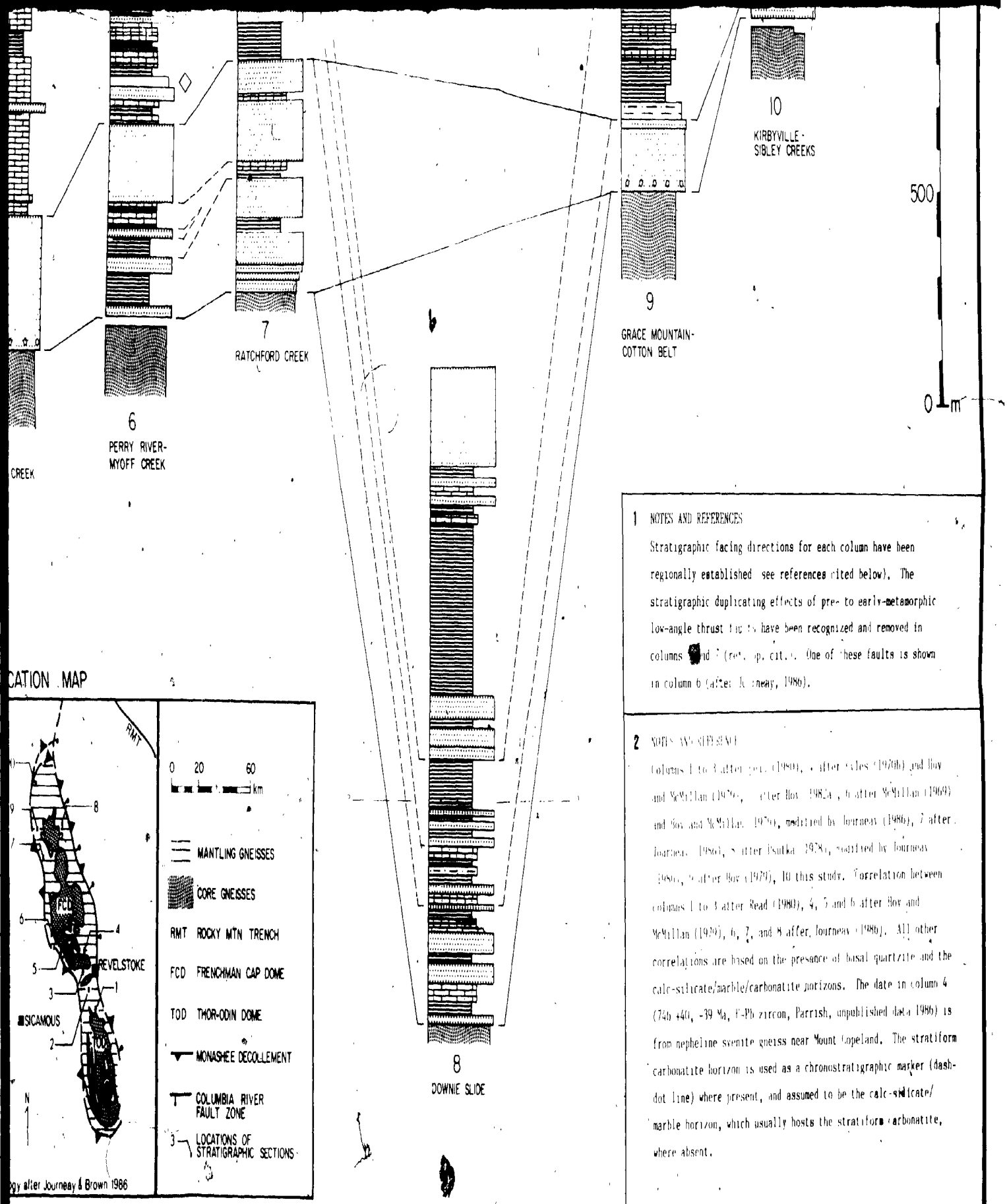

1 NOTES AND REFERENCES

Stratigraphic facing directions for each column have been regionally established (see references cited below). The stratigraphic duplicating effects of pre- to early-metamorphic low-angle thrust faults have been recognized and removed in columns [illegible] and 7 (ref. op. cit.). One of these faults is shown in column 6 (after Journeay, 1986).

2 NOTES AND REFERENCES

Columns 1 to 3 after [illegible] (1980), 4 after Eales (1976b) and Hoy and McMillan (1970), [illegible] after Hoy (1982A), 6 after McMillan (1969) and Hoy and McMillan (1970), modified by Journeay (1986), 7 after Journeay (1986), 8 after Psutka (1978), modified by Journeay (1986), 9 after Hoy (1979), 10 this study. Correlation between columns 1 to 3 after Read (1980), 4, 5 and 6 after Hoy and McMillan (1970), 6, 7, and 8 after Journeay (1986). All other correlations are based on the presence of basal quartzite and the calc-silicate/marble/carbonatite horizons. The date in column 4 (740 ±40, -39 Ma, U-Pb zircon, Parrish, unpublished data 1986) is from nepheline syenite gneiss near Mount Copeland. The stratiform carbonatite horizon is used as a chronostratigraphic marker (dash-dot line) where present, and assumed to be the calc-silicate/marble horizon, which usually hosts the stratiform carbonatite, where absent.

RS/DM 1984

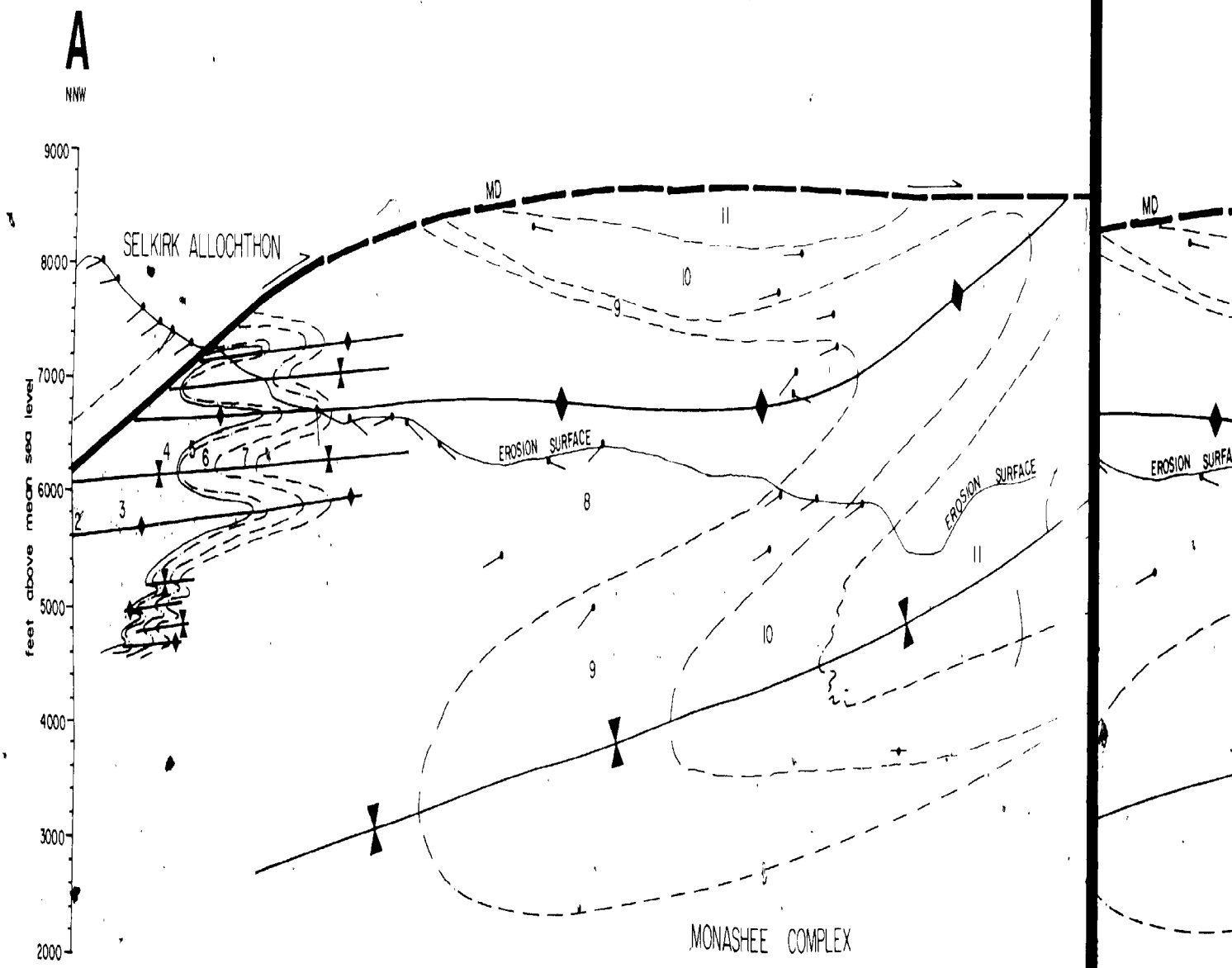
A
NNW
9000
8000
7000
6000
5000
4000
3000
2000
feet above mean sea level
SELKIRK ALLOCHTHON
MD
EROSION SURFACE
MONASHEE COMPLEX
2
3
4
5
6
7
8
9
10
11

NOTES

This cross-section is a best fit between two methods of construction: (1) orthographic projection taking topography into account, and (2) projection of data off the line of section along strike or down-dip, and plotting apparent-dip. The line of section was chosen to be approximately perpendicular to the trend of fold axes to phase I structures which control the map-scale distribution of lithologic units. Truncation of units against the Monashee decollement is based on their observed truncation in the northwest corner of the map area, plus projection of data directly west of the map area (Brown pers. comm. 1986). Note also that the line of section is not perpendicular to the inferred direction of transport of the upper-plate (easterly directed motion). The arrows shown along the trace of the Monashee decollement are only a very small component of this motion.

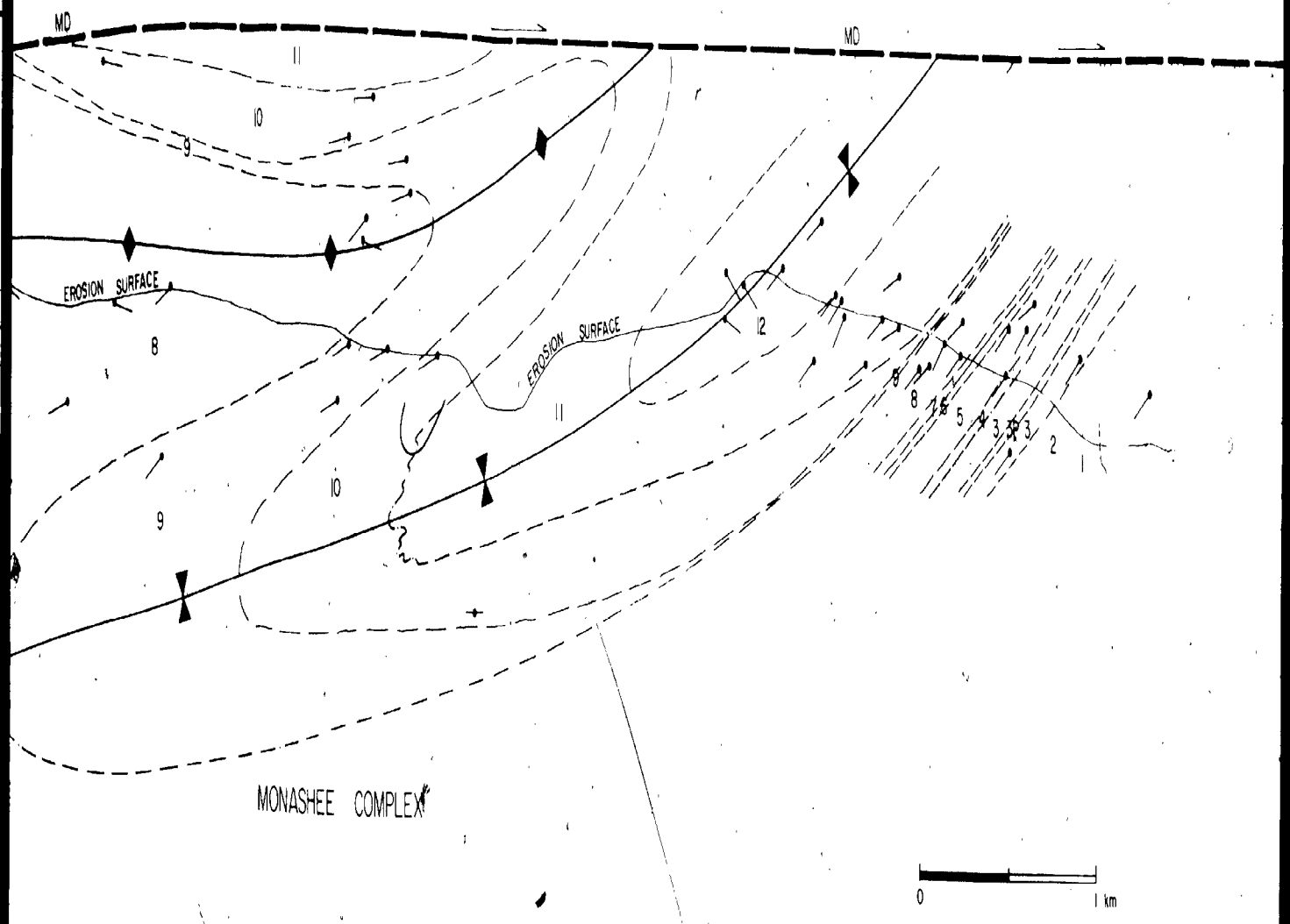

NOTES

This cross-section is a best fit between two methods of construction: (1) orthographic projection taking topography into account, and (2) projection of data off the line of section along strike or down-dip, and plotting apparent-dip. The line of section was chosen to be approximately perpendicular to the trend of fold axes to phase I structures which control the map-scale distribution of lithologic units. Truncation of units against the Monashee decollement is based on their observed truncation in the northwest corner of the map area, plus projection of data directly west of the map area (Brown pers. comm. 1986). Note also that the line of section is not perpendicular to the inferred direction of transport of the upper-plate (easterly directed motion). The arrows shown along the trace of the Monashee decollement are only a very small component of this motion.

FIGURE 9

GENERALIZED UPRIGHT CROSS-SECTION

(See Figure 6 for location)

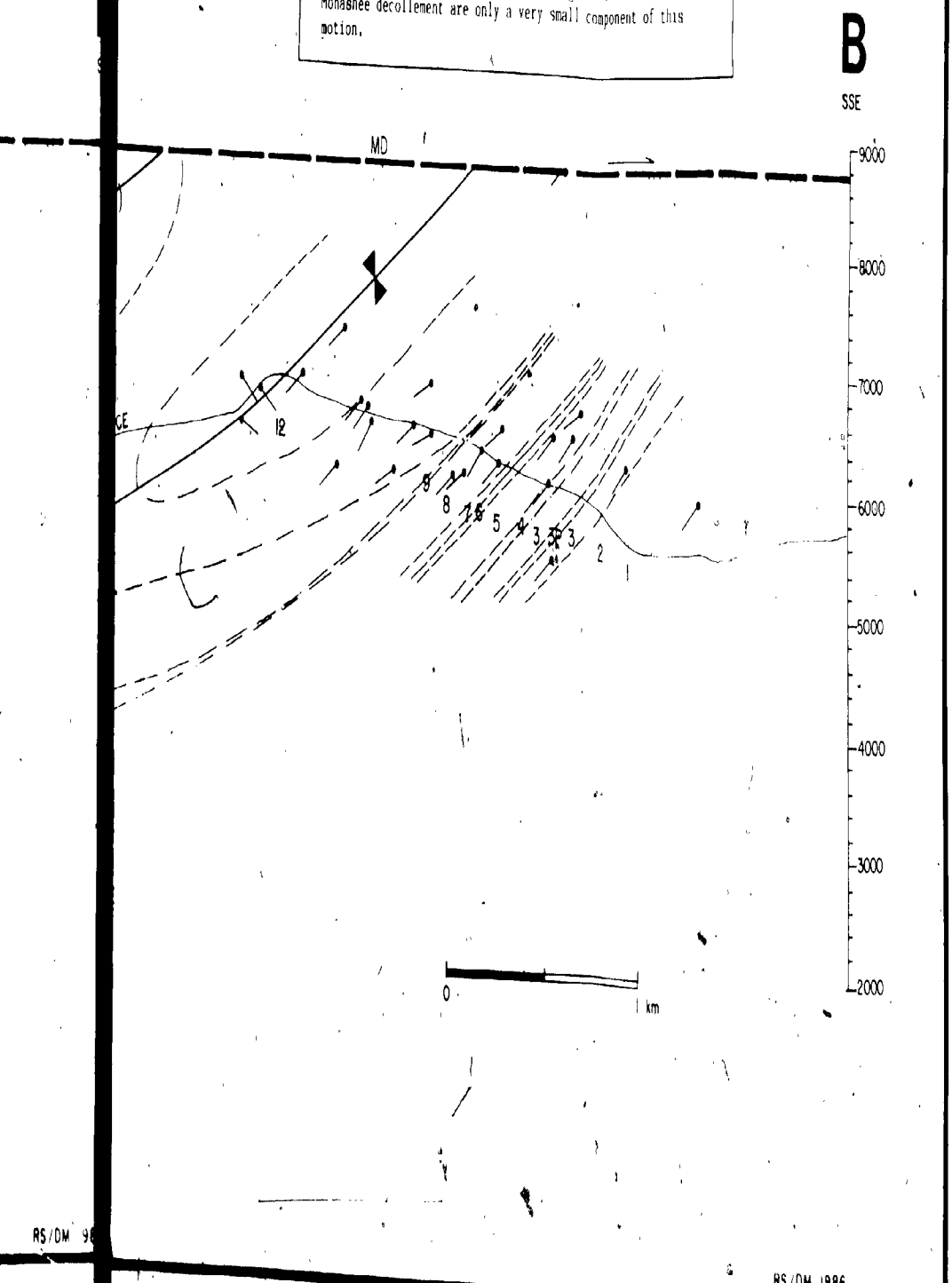

LEGEND

LITHOLOGICAL CONTACTS

- sharp
- interlayered
- approximate
- assumed
- apparent dip of SOI projected into line or on section line, from selected locations

AXIAL SURFACE TRACES

- D_1 anticline
- D_1 syncline

MD — Monashee Decollment (with component of easterly directed overthrusting indicated)

2 — Stratigraphic unit

RS/DM 1986

END

05·01·88

FIN